Investigating the role of human microglia in tau pathogenesis

Maria Kreger Karabova

Sir William Dunn School of Pathology

Lincoln College

University of Oxford

A thesis submitted for the degree of Doctor of Philosophy

Trinity Term 2023

Acknowledgements

''If I have seen further, it is by standing on the shoulders of giants,''
Sir Isaac Newton wrote to his rival Robert Hooke in 1675. Regardless of what he meant; I hope the quote will help convey my appreciation of the many people who have supported me on this journey.

First and foremost, I am indebted to my supervisors, Dr Sally Cowley and Professor William James. They provided me with the most valuable opportunity to keep searching for answers despite all the obstacles in the way. Their guidance, encouragement, and insight taught me two of the most important lessons: to always examine my bias, and that failing is simply a way of eliminating the routes that do not work.

My deepest gratitude extends to Cathy and Jane, the former James lab managers/mums who patiently instilled all the core skills and confidence in me. Much of this thesis would have never happened without the collaborators who kindly donated their knowledge and time to help move the work forward: the protein purification crew: Donatella Di Rienzo, Dr Kourosh Ebhrahimi, Adam Harding, Dr Abul Tarafder, Dr Haitian Fan; the most wonderful, knowledgeable and helpful collaborators from the Vendruscolo lab members: Prof Michele Vendruscolo, Alessia Santambrogio, and Dr Michael A. Metrick; the electron microscopy gurus: Dr Errin Johnson and Dr Charlotte Melia; the flow cytometry masters: Dr Robert Hedley and Vasiliki Tsioligka; and the Wade-Martins lab members: Dr Nora Bengoa-Vergniory and Dr Sarah Pearce. I am also very thankful to the Dunn School department, specifically Dr Anton van der Merwe and Lucinda Risius, for creating an unparalleled, supportive working atmosphere encouraging friendships, collaborations, and the pursuit of scientific excellence. Here, I have found my James lab family, and dearest friends (Emma, Hana, Lachlan, Joana, Juli, Galbha, Cat, Thomas and Aayushi). I will spread the famous Dunn School spirit wherever I go!

A special thank you belongs, firstly, to my husband Dan, my best friend and my rock, to whom I owe my sanity. Thank you for choosing to stand by my side, and for carrying me through the dark times and the good times. Thank you for encouraging me to grow into the person and the scientist I have wanted to become, one day at a time. I am so grateful I could have shared this journey with you and I already cannot wait for all the adventures ahead. Secondly, to Prof Andrew Farmery and Mrs Laura Beck from my years at the Manor Hospital. Their belief in me is the reason why I can sit here, writing these words today. Lastly, to Javi, Alun, Sharat, Sam, Anne H., Ishan, and Hazel – the most special people who have become my family and without whom I genuinely would not have gotten through the past five years.

Above all, I would like to dedicate this work to my Mum and Dad. Thank you for sacrificing your lives so I can pursue the path of my own choosing. Your love, wisdom, support and generosity will stay with me forever, and I hope I can pay it forward one day – hopefully, by helping a few people suffer a little less.

Declaration

All experimental work and downstream analyses were carried out by myself with the following exceptions:

Chapter 5: Characterisation of microglial functional response to tau protein in native and aggregated form

- CRISPR/Cas9 lentiviral vectors for the CRISPR/Cas9-mediated knockdown of LRP1 were prepared by Dr Yixi Chen at the Wellcome Sanger Institute, Cambridge, in collaboration with Dr Sam James Washer, a postdoc in our lab.
- Lentivirus was produced Amy Napier, a PhD student in our lab.
- pSIV3+_Vpx Virus-Like-Particles to aid iPSC-macrophage transduction were prepared by Dr Sam James Washer, a postdoc in our lab.
- Resin-embedding, ultramicrotomy, and negative stain of iPSC-macrophages for negative stain transmission electron microscopy was performed by Dr Errin Johnson, a manager at the Dunn School EM Facility.
- 4R Tau RT-QuIC assay was carried out by Alessia Santambrogio, a PhD student at the Vendruscolo lab, Yusuf Hamied Department of Chemistry, University of Cambridge.

Abstract

In neurodegenerative diseases collectively known as tauopathies, the microtubule-associated tau protein aggregates into insoluble deposits. Tau deposits propagate along synaptically-connected brain regions in a prion-like manner, correlating with disease progression and severity. Genetic studies have recently implicated perturbations in phagolysosomal clearance by microglia, the major brain-resident phagocytes, as a key candidate mechanism driving tau pathology. However, functional studies elucidating the precise mechanisms in a relevant model of human microglia are missing.

In this thesis, I have developed an efficient protocol for purification and *in vitro* aggregation of endotoxin-free, human recombinant tau. I then used an authentic, *in vitro* model of human microglia – induced pluripotent stem cell-derived (iPSC)-macrophages and microglia - to characterise microglial responses to tau at functional level, including tau uptake, degradation, and secretion, as well as prion-like behaviour of the microglia-processed tau. I have identified Low Density Lipoprotein Receptor-Related Protein-1 (LRP1) as major receptor mediating tau entry to microglia. I further found that the internalised soluble tau is readily degraded by microglia but intracellular clearance of aggregated tau is concentration- and incubation-length dependent, and inversely associated with microglial tau release. Tau fibrils processed by microglia retain seeding competency, thus supporting the putative role for microglia in tau prion-like spreading.

In addition, I present novel finding that Leucine-Rich Repeat Kinase 2 (LRRK2), a candidate genetic determinant in the Parkinson's disease (PD) and Progressive Supranuclear Palsy (PSP) tauopathies, influences microglial cargo clearance pathways and tau-specific processing. Specifically, my results show that the PD- and PSP-associated G2019S LRRK2 mutation enhances iPSC-macrophage baseline proteolytic activity, tau uptake, clearance, and possibly prion-like activity of the non-cleared tau species accumulating within the cells.

Collectively, this thesis supports the putative role of microglia in tau pathogenesis and provides further reasoning for investigating microglia-enriched tauopathy risk variants as potential druggable targets.

Table of Contents

Abbreviations

α-syn	α-synuclein
aa	Amino acid
Aβ	Amyloid-beta
AD	Alzheimer's disease
AF-488	Alexa Fluor 488 NHS Ester
AGD	Argyrophilic grain disease
AGM	Aorto-gonado-mesonephros
BMDM	Blood-monocyte-derived-macrophage
BODIPY	Boron-dipyrromethene
BSA	Bovine serum albumin
CNS	Central nervous system
COR	C-terminal of Roc
Cryo-EM	Cryo-electron microscopy
CSF-1	Colony-stimulating factor 1
CV	Column volume
cytD	Cytochalasin D
DAM	Disease-associated microglia
DAPI	4′,6-diamidino-2-phenylindole
DC	Dendritic cells
DIM	Disease inflammatory macrophages
dNTPs	Deoxynucleotide triphosphates
DTT	Dithiothreitol
E	Embryonic day
EB	Embryoid body
ELISA	Enzyme-linked immunosorbent assay

EU	Endotoxin unit
EV	Extracellular vesicle
FTDP-17	Frontotemporal dementia with parkinsonism linked to chromosome 17
gRNA	Guide RNA
HIV-2	Human immunodeficiency virus type 2
HSC	Hematopoietic stem cells
HSPG	Heparan sulfate proteoglycans
hTau	Human tau
IDP	Intrinsically disordered protein
IFNγ	Interferon gamma
IL-1β	Interleukin-1β
IL-34	Interleukin-34
INTG	Intergenic control
iPSC	Induced pluripotent stem cell
IPTG	Isopropyl β-D-1-thiogalactopyranoside
IRF8	Interferon regulatory factor 8
KD	Knockdown
KO	Knockout
LB	Lewy body
LB	Luria-Bertani
LC-MS/MS	Liquid chromatography with tandem mass spectrometry
LCIS	Live Cell Imaging Solution
LDL	Low density lipoprotein
LIC	Ligation independent cloning
LN	Liquid nitrogen
LPS	Lipopolysaccharide
LRP1	Low density lipoprotein receptor-related protein-1

LRRK2	Leucine-rich repeat kinase 2
MAP	Microtubule-associated protein
MBD	Microtubule binding domain
MD2	Myeloid differentiation factor 2
MFI	Mean fluorescence intensity
MGnD	Neurodegenerative microglia
MOI	Multiplicity of infection
MPS	Mononuclear phagocyte system
MTA	Material transfer agreement
Mtb	*Mycobacterium tuberculosis*
MW	Molecular weight
NFT	Neurofibrillary tangle
NO	Nitric oxide
ODDI	Oxford Drug Discovery Institute
P2Y12R	P2Y purinoceptor 12
PAMP	Pathogen-associated molecular pattern
PBS	Phosphate-buffered saline
PBS-T	PBS buffer supplemented with 0.1% Tween® 20
PD	Parkinson's disease
PET	Positron emission tomography
PHF	Paired helical fibril
PMF	Peptide mass fingerprinting
PPR	Pattern recognition receptor
PrP	Prion protein
PSP	Progressive supranuclear palsy
PTM	Posttranslational modification
QC	Quality control

R	Repeat
RAP	Receptor associated protein
RIPA	Radioimmunoprecipitation
Roc	Ras of complex proteins
ROCKi	Y-27632 ROCK inhibitor
ROS	Reactive oxygen species
RT-QuIC	Real time quaking-induced conversion
SAMHD1	SAM Domain and HD domain-containing protein 1
SDS	Sodium dodecyl sulfate
SEC	Size-exclusion chromatography
SEM	Scanning electron microscopy
SENP2	Sentrin-specific protease 2
SH3	Src-homology 3
SHF	Straight helical fibrils
SIV	Simian immunodeficiency virus
sRAP	Synthetic Receptor associated protein
SUMO	Small ubiquitin-like modifier
TB	Terrific Broth
TBS	Tris-buffered saline
TEM	Transmission electron microscopy
TEV	Tobacco Etch Virus
TGFβ1	Transforming growth factor β1
TGN	Trans-Golgi network
TLR	Toll like receptor
TLR4	Toll-like receptor 4
TNF	Tumour necrosis factor
TMEM19	Transmembrane protein 119

VLP	Virus-Like-Particles
Vpx	Virion-associated protein
WB	Western blot
WT	Wild-type
YS	Yolk sac

Chapter 1

Introduction

1.1 The structure and function of tau protein

An effort to identify factors driving microtubule assembly led to a discovery of tau protein in 1975 (Weingarten et al., 1975). Nearly 50 years of research have since significantly advanced our understanding of tau properties, location, and function.

Tau is one of the microtubule-associated proteins (MAPs), encoded by the MAPT gene located on chromosome 17q21.31 (Neve et al., 1986). MAPT comprises of 16 exons. Alternative mRNA splicing of exons 2, 3 and 10 generates six major tau isoforms that differ in the number of N-terminal insertions (N) and the number of sequence repeats (R) in the microtubule-binding domain (MBD) (Figure 1.1). (Goedert et al., 1989). Each repeat is composed of 31 amino acid (aa) stretches, further divided into 18 highly homologous VXSK to PGGG motifs followed by 13 less conserved, intervening residues (Goode & Feinstein, 1994; Himmler et al., 1989; Lee et al., 1988). Additionally, inclusion of the MAPT exon 4a generates a unique, high molecular weight (MW) ‘’big tau’’ isoform, equivalent to the 2N4R isoform extended by an additional 242 residues (Couchie et al., 1992; Goedert et al., 1992). The six main tau isoforms are predominantly localised in the CNS neurons, with a smaller fraction observed in oligodendrocytes (C. Liu & Götz, 2013; LoPresti et al., 1995). ‘’Big tau’’ expression was reported in the peripheral system, specific central nervous system (CNS) regions (i.e., the cerebellum and the visual system), and human myocardium (Fischer, 2023; Luciani et al., 2023).

Tau expression is developmentally regulated. Only the shortest isoform, 0N3R, is present in the human foetal brain whereas the adult brain expresses all six isoforms in equal 3R:4R ratio (Goedert & Jakes, 1990; Kosik et al., 1989; Trabzuni et al., 2012). Tau is initially distributed

evenly throughout the soma and neurites of immature neurons. During maturation, tau becomes increasingly more localised to axons (Kosik & Finch, 1987) as a result of several, isoform-specific sorting mechanisms. These include but may not be limited to selective tau mRNA transport to and translation in axons, selective tau protein degradation in dendrites, preferential tau affinity for axonal over dendritic microtubules, and axon initial segment-mediated barrier against tau diffusion to dendrites (Aronov et al., 2002; Hirokawa et al., 1996; X. Li et al., 2011; C. Liu & Götz, 2013; Morita & Sobue, 2009; Nakata & Hirokawa, 2003). Some studies have reported small amounts of physiological tau is also present in dendrites and nuclei of mature neurons but its role there is yet to be fully understood (reviewed in Antón-Fernández et al., 2023; Hanger et al., 2019).

Tau consists of four functional domains: the N-terminal projection domain, a proline-rich domain, the MBD, and the C-terminal region (Figure 1.1). The MBD is the primary facilitator of tau binding to the microtubules. The MBD repeats, along with ~40 additional, MBD-flanking residues, interact with the α- and β-tubulin microtubule subunits (Kadavath et al., 2015a; Mukrasch et al., 2005a; Sillen et al., 2005). The 4R tau isoform-specific ^{275}KVQIINKK^{280} peptide within the R1-R2 inter-residue binds tubulin with the highest affinity (Goode & Feinstein, 1994), underlying the mechanism by which 3R vs 4R tau isoforms differentially modulate microtubule dynamics and function (Goedert & Jakes, 1990a). Weaker tau association with microtubules can occur also via the C-terminal (Mukrasch et al., 2009) and can be further enhanced by intramolecular interactions between the MBD and the proline-rich region (Goode et al., 1997). The N-terminal domain projects away from the microtubule (Hirokawa 1988) and does not directly contributing to the tau-microtubule interaction. Instead, the N-terminal regulates the spatial organisation of microtubules on axons (J. Chen et al., 1992) and may also affect tau subcellular localisation (C. Liu & Götz, 2013)

The unusually hydrophilic tau composition confers its natively unfolded character, now confirmed by multiple biophysical methods including nuclear magnetic resonance, small-angle X-ray scattering, and circular dichroism (Jeganathan et al., 2008; Mukrasch et al., 2009;

Schweers et al., 1994; von Bergen et al., 2005). Unlike globular proteins, the highly flexible and dynamic tau forms only very amount of transient secondary structures (Mukrasch et al., 2009; Schweers et al., 1994) and remains in solution even following harsh treatments with heat or acid (Cleveland et al., 1977; Fellous et al., 1977). Despite the natively unfolded character, single-molecule Förster resonance energy transfer revealed tau preference for an S-shaped, paperclip-like global order in solution with long-range association of the N- and C-termini folding over the MBD (Elbaum-Garfinkle & Rhoades, 2012; Jeganathan et al., 2006). In addition, tau interaction with microtubules or other binding partners may induce further, local conformation shifts (Grüning et al., 2014; Kadavath et al., 2015b).

Tau acts as a microtubule stabiliser, promoting the microtubule assembly. By regulating the microtubule dynamics and axonal spacing, tau influences organelle and cargo transport, cytoskeleton rearrangement, and cell polarity. This has been the best-characterised tau function to date (reviewed in Barbier et al., 2019). It is, however, far from the only tau function. *In vivo* and *in vitro* tau knockout (KO) studies revealed tau may additionally be involved in multiple, lesser-understood roles, including regulation of neuronal activity (Ittner et al., 2010; Kimura et al., 2014; Padmanabhan et al., 2019; Pallas-Bazarra et al., 2019; Regan et al., 2015), neurogenesis (Criado-Marrero et al., 2020; Pallas-Bazarra et al., 2016), cognitive behavior (Gonçalves et al., 2020), maintenance of DNA/RNA integrity (Bou Samra et al., 2017; Violet et al., 2014), iron homeostasis (Lei et al., 2012), insulin signalling (Marciniak et al., 2017), metabolism dysfunction (Baeuerle et al., 2019), and pancreatic disorders (Wijesekara et al., 2018). The ubiquity of tau functions stems from the protein's ability to interact with a remarkably diverse pool of binding partners due to tau's flexible, mobile, asymmetrically-charged polypeptide chain, multiple splice variants, functional domains, subcellular localisations, and plethora of posttranslational modifications (PTMs) (reviewed in Wang & Mandelkow, 2016). Tau interactome studies are currently under way helping explain how the individual interactions translate to tau function in health and disease (Kavanagh et al., 2022; Tracy et al., 2022).

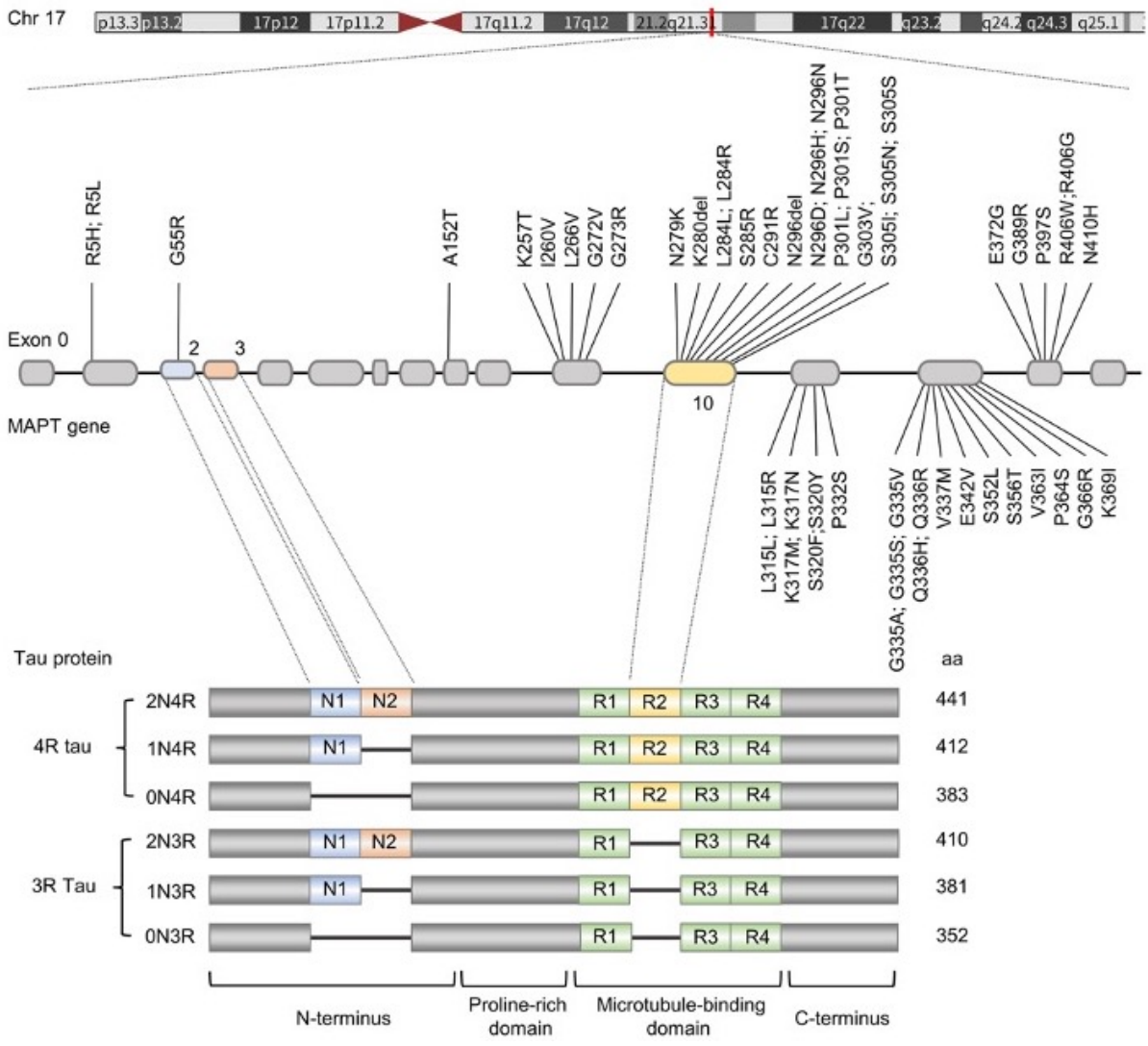

Figure 1.1: MAPT alternative splicing and pathological mutations

Endogenous tau protein, encoded by MAPT on chromosome 17q21.31, is composed of four main domains: N-terminal, C-terminal, proline-rich domain, and microtubule-binding domain. The MAPT gene comprises of 16 exons in humans. Exons 0 and 14 are the untranslated regions of the gene, exons 1, 4, 5, 7, 9, 11, 12, and 13 are constitutively expressed. Alternative splicing of exons 2, 3 and 10 produces six major tau isoforms found in the human brain. Adapted from Y. Zhang et al., 2022.

1.2 Tau pathology in tauopathies

The accumulation of tau fibrillar deposits in neurons and glia is associated with neurodegenerative diseases collectively known as tauopathies. Tau relevance in tauopathies was first recognised in 1986 following the identification of hyperphosphorylated an aggregated form of tau in the paired helical and straight fibrils (PHFs, SFs) extracted from the Alzheimer's disease (AD) brains (Grundke-Iqbal, Iqbal, Quinlan, et al., 1986; Grundke-Iqbal, Iqbal, Tung, et al., 1986; Iqbal et al., 1974; KIDD, 1963; Stelzmann et al., 1995). Currently, over 26 tauopathies have been described (Table 1.1) (Sexton et al., 2022). Clinical presentation varies greatly between the diseases, due to a multitude of comorbidities, genetic, epigenetic, and environmental factors, as well as lack of diagnostic standardization (Figure 1.2) (reviewed in Götz et al., 2019; Y. Zhang et al., 2022). But tau aggregation remains the unifying pathological hallmark. Depending on tau pathology appearing as dominant or additional feature to other protein aggregates (i.e., amyloid-beta or alpha-synuclein), tauopathies are broadly classified as primary or secondary. Based on the tau aggregate isoform composition, tauopathies can be further divided into 3R, the 4R, or the 3R/4R mixed type (Table 1.1) (Zhang et al., 2022).

Tau fibrillar core is composed of MBD residues assembled into β-sheets typical of amyloid fibrils. The highly ordered core is surrounded by disordered N- and C-termini forming the ''fuzzy coat'' (Figure 1.3) (Goedert et al., 1988; Wischik, Novak, Edwards, et al., 1988; Wischik, Novak, Thøgersen, et al., 1988). Major advancements in cryo-electron microscopy (cryo-EM) recently enabled solving the atomic structure of tau aggregates (Figure 1.4A). Intriguingly, tau adopts a disease-unique filament fold in each tauopathy examined thus far (i.e., the extent of the MBD residues involved or the number of protofilaments formed) (Figure 1.4B) (Falcon, Zhang, Murzin, et al., 2018; Falcon, Zhang, Schweighauser, et al., 2018; Falcon et al., 2019; Fitzpatrick et al., 2017; Y. Shi et al., 2021; W. Zhang et al., 2020).

3R	3R/4R	4R
Pick's disease (PiD)	Alzheimer's disease (AD)	Argyrophilic grain disease (AGD)
Familial frontotemporal dementia and parkinsonism (FTDP) – some mutations (G272V, Q336R)	Amyotrophic lateral sclerosis/parkinsonism-dementia complex	Aging-related tau astrogliopathy (ARTAG)
	Anti-IgLON5-related tauopathy	Corticobasal degeneration (CBD)
	Chronic traumatic encephalopathy (CTE)	Guadeloupean parkinsonism
	Diffuse neurofibrillary tangles with calcification	Globular Glial Tauopathy (GGT)
	Down's syndrome	Huntington's disease
	Familial British dementia	Progressive supranuclear palsy (PSP)
	Familial Danish dementia	Familial FTDP – some mutations (P301S, all intronic mutations)
	Gerstmann-Sträussler-Scheinker disease	Parkinson's disease (some mutations)
	Niemann-Pick disease, type C	
	Non-Guamanian motor neuron disease with neurofibrillary tangles	
	Postencephalitic parkinsonism	
	SLC9A6-related parkinsonism	
	Tangle-only dementia (TD)	
	Familial FTDP – some mutations (V337M, R406W)	

Table 1.1: Classification of known tauopathies based on tau isoform composition in tau inclusions

Disease	Tauopathy type	Tau 3R/4R ratio	Pathology	Phenotype
Pick's disease	Primary	3:1	Pick bodies, neuropil threads, ramified astrocytes	Speech problems, aphasia, memory loss, behavioral abnormalities
Frontotemporal dementia with parkinsonism-17	Primary	1:2	Neurofibrillary tangles, neuronal loss, astrogliosis	Cognitive impairment, motor symptoms, bradykinesia, speech problems, behavioral abnormalities
Argyrophilic grain disease	Primary	1:2	Argyrophilic grains, oligodendritic coiled bodies, neuronal pretangles	Very slow-progressing mild cognitive impairment, personality changes
Corticobasal degeneration	Primary	1:2	Ballooned neurons, pretangles, atrocytic plaques, neuritic threads	Stiffness, rigidity, motor symptoms, speech and comprehension impairment, memory loss
Progressive supranuclear palsy	Primary	1:3-4	Neurofibrillary tangles, glial inclusions, tufted astrocytes	Loss of balance and coordination, muscle stiffness, speech, vision and swallowing problems, memory loss
Alzheimer's disease	Secondary	1:1	Neurofibrillary tangles, neuropil threads, amyloid plaqeus	Cognitive impairment, loss of orientation and executive functions, behavioral abnormalities, sleep disturbances
Down's syndrome	Secondary	1:1	Neurofibrillary tangles, neuropil threads, amyloid plaqeus	Progressive cognitive impairment, hypotonia, hearing and visual problems, heart and thyroid disorders
Parkinson's disease	Secondary	unknown	Neurofibrillary tangles, neuropil threads, Lewy bodies	Tremor, rigidity, akinesia, postural instability, anosmia, cognitive impairment, sleep disturbances

Figure 1.2: Diverse neuropathological characteristic of the most common tauopathies

Adapted from *Götz et al., 2019.*

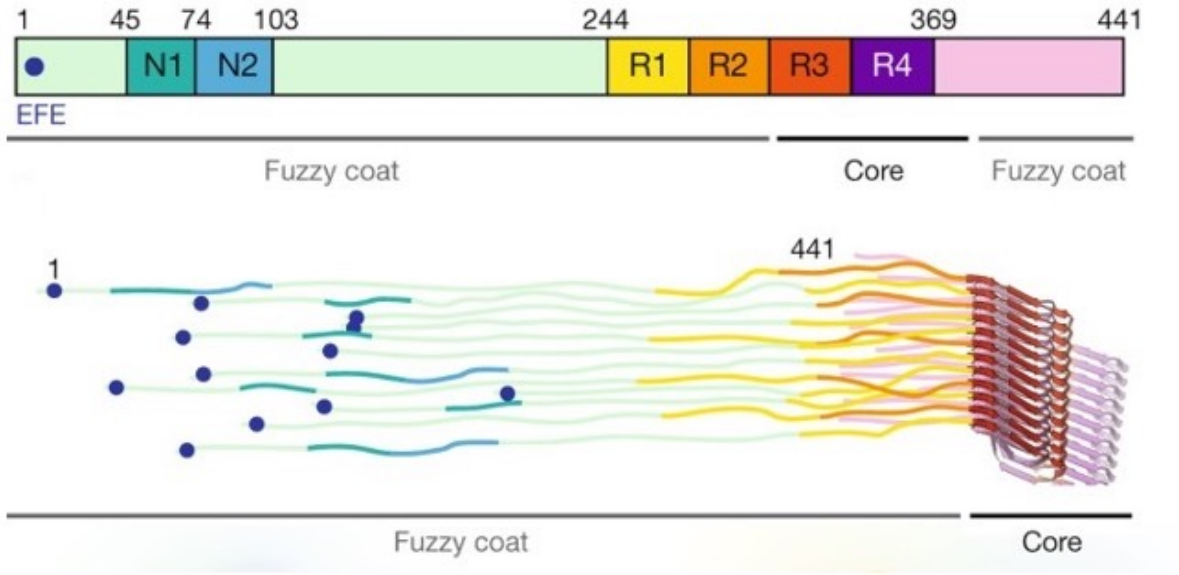

Figure 1.3: Schematic illustration of 2N4R tau domains in an ordered assembly *The ordered core composed of β–sheet strands is surrounded by highly dynamic fuzzy coat formed by the N- and C-termini. Adapted from Fitzpatrick et al., 2017.*

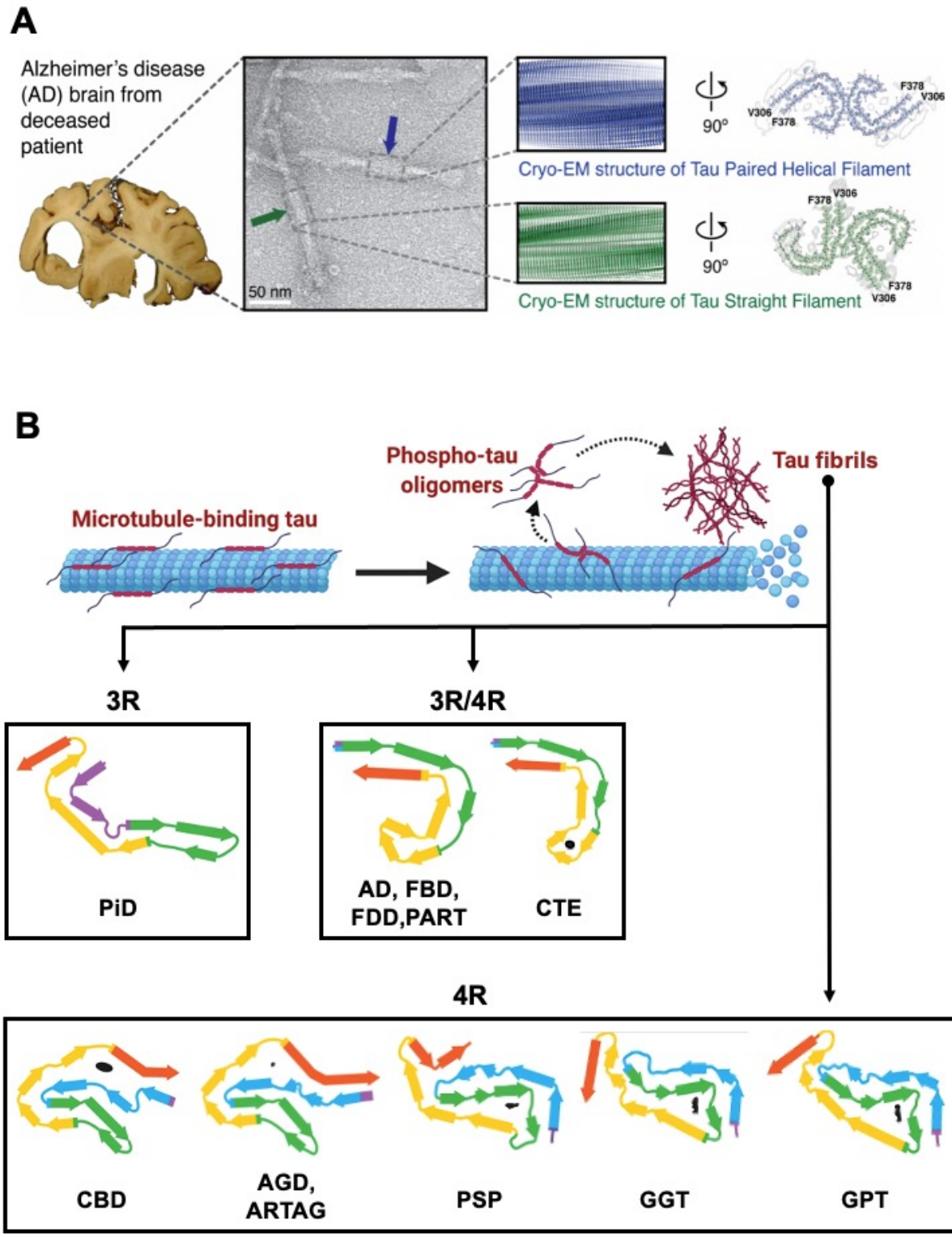

Figure legend on the next page.

Figure 1.4: Structure of tauopathy-associated tau fibrils isolated from diseased, post-mortem brains

(A.) Negative stain transmission electron micrographs and the first, atomic-resolution structure of paired and straight helical tau fibrils extracted from AD brain and solved by cryo-EM. Adapted from Fitzpatrick et al., 2017. (B.) Schematic illustration of the various tau filament folds in tauopathies. MBD region R1 is depicted in purple, R2 in blue, R3 in green, R4 in yellow, and the C-terminal is in red. Adapted from Shi et al., 2021.

Tau ability to form ordered assemblies is unusual, given its natively unfolded structure. The entire tau polypeptide chain is composed of only two short hydrophobic motifs, VQIINK and VQIVYK in R2 and R3, respectively (von Bergen et al., 2000). The two motifs are, however, sufficient and necessary for tau aggregation (Khlistunova et al., 2006; Sawaya et al., 2007; von Bergen et al., 2000). Molecular mechanisms driving the tau β-sheet formation are unclear. Several, potentially contributing factors have been identified. Firstly, tau pathogenic mutations are associated with the fibril formation. Over 80 different mutations have been discovered in the human MAPT, linked to the familial form of frontotemporal dementia with parkinsonism linked to chromosome 17 (FTDP-17), as well as other tauopathies (Alzforum, n.d.; Hutton et al., 1998; Poorkaj et al., 1998; Spillantini et al., 1998). The silent mutations tend to affect alternative splicing, and with that the 4R to 3R isoform expression ratio. The imbalance changes tau affinity for microtubules, and increases tau propensity for hyperphosphorylation and aggregation (Hong, 1998; M. Lu & Kosik, 2001). The missense mutations alter tau sequence in or near MBD. Some of the missense mutations (Δ280, P301L) were shown to accelerate tau self-aggregation by directly strengthening the β-sheet structure formed by the MBD hexapeptide motifs (Barghorn et al., 2000; Khlistunova et al., 2006).

Tau fibrils, however, feature also in sporadic tauopathies with no tau mutations present. Other factors may therefore instigate tau aggregation. For example, truncated tau species containing

MBD residues show higher aggregation propensity, possibly due to the loss of aggregation-protective paperclip formation facilitated by the N- and C-termini. Tau truncation relevance for aggregation *in vivo* was confirmed following the identification of $tau_{151-391}$ in PHFs isolated from AD brains (Wischik, Novak, Thøgersen, et al., 1988; Zilka et al., 2006). In addition, protease-mediated cleavage of full-length tau to aggregation-prone tau_{1-421} (de Calignon et al., 2010) and tau_{1-368} (Zhang et al., 2014) was observed in AD brains as well as rodent models of tauopathies.

Binding of polyanionic cofactors to the positively-charged tau domains can also accelerate tau aggregation. The property has been heavily exploited to form synthetic tau fibrils *in vitro* using heparin, nucleic acids, acidic lipid micelles or peptides, or carboxylated microbeads (Chirita et al., 2005; Friedhoff et al., 1998; Goedert et al., 1996a; Kampers et al., 1996; Pérez et al., 2002; D. M. Wilson & Binder, 1997. Cofactors inducing tau aggregation *in vivo* are currently unknown, though several candidates have been proposed, including RNA (Lester et al., 2021), immunophilin and 14-3-3 proteins (Giustiniani et al., 2014).

Finally, phosphorylation, the most commonly occurring form of tau PTM, is often considered the principal mechanism driving tau aggregation. This is because tau aggregates extracted from the brains of tauopathy patients and rodent models are invariably hyperphosphorylated (8 phosphates compared with two phosphates per molecule in a healthy adult brain tau) (Kanemaru et al., 1992; Köpke et al., 1993). Moreover, the extracted, hyperphosphorylated tau shows capacity to self-assemble *in vitro* (Alonso et al., 2001). It is, however, often overlooked that not all instances of tau hyperphosphorylation lead to an aggregate formation (Arendt et al., 2003; Planel et al., 2007). In addition, tau phosphorylation at certain residues can actually mitigate tau aggregation (Schneider et al., 1999). Importantly, other forms of tau PTMS are becoming increasingly recognised in relation to tau fibrillization and pathology (Wesseling et al., 2020a) including acetylation, glycosylation, deamidation, isomerisation, nitration, methylation, ubiquitylation and sumoylation (reviewed in Wang & Mandelkow, 2016). It is therefore likely that tau phosphorylation plays an important integrative but not an exclusive role in tau PHF assembly.

Tau aggregates may be involved in the development of pathology. The introduction of pro-aggregant or anti-aggregant tau mutations in tauopathy mouse models was sufficient to either accelerate or abrogate tau deposit formation and disease-associated behavioural symptoms (Eckermann et al., 2007; Mocanu et al., 2008). But precisely how tau deposits may instigate the pathology is still a matter of debate. Tau loss and gain of function, as well as aggregation-induced subcellular mislocalisation have been proposed (reviewed in Wang & Mandelkow, 2016). As the various tau folds correlate closely with the particular tauopathy symptoms, it is possible that biochemically distinct tau strains may possess different pathobiological properties, driving the clinical heterogeneity. A new, structure-based tauopathy classification system has been proposed based on this hypothesis (Y. Shi et al., 2021), shifting the current research focus to the investigation of tau structure-function relationship. It is important to note, however, that the insoluble tau neurofibrillary tangles (NFTs) may not be neither necessary nor sufficient to induce pathology in tauopathies. Tau transgene suppression rescued cognitive deficits and neuronal loss observed in an inducible mouse model of tauopathy despite the continued accumulation of NFTs (Santacruz et al., 2005). Accumulating evidence suggests that tau oligomeric species formed in the early stages of aggregation can elicit the tauopathy-associated pathology and NFTs may, instead, play a protective role in sequestering the neurotoxic tau oligomers (reviewed in Niewiadomska et al., 2021). The topic is under intense investigation.

1.3 Prion-like tau propagation

Tau pathology progresses through neuroanatomically-connected brain regions in a predictable spatiotemporal manner that correlates with the onset and severity of clinical symptoms (Bejanin et al., 2017; Giannakopoulos et al., 2003; Ossenkoppele et al., 2016). The stereotypical propagation has now been observed in a number of tauopathies, including AD (Braak & Braak, 1991), Progressive Supranuclear palsy (PSP) (Verny et al., 1996; Williams et al., 2007), Argyrophilic grain disease (AGD) (Saito et al., 2004), and Pick's disease (Irwin et al., 2016). In AD, tau pathology first appears in the entorhinal cortex (Braak stage I, II) from where it

progresses through the hippocampus (stage III, IV), to the cortex in the final stages V and VI (Figure 1.5) (Arnold et al., 1991; Duyckaerts & Hauw, 1997; Hoenig et al., 2018; Schwarz et al., 2016). Different neuronal circuits are involved in tau propagation in other tauopathies (Figure 1.5).

Cell autonomous mechanisms were initially thought to drive the progression pattern. In this model, tau fibrilization would occur in multiple neurons independently, staged in the sequential order of the brain region's selective vulnerability. Some evidence supports the concept (reviewed in Fu et al., 2018; Rexach & Geschwind, 2020) and proposes a number of plausible underlying mechanisms, including regional differences in energy demands (Yan et al., 2013), myelination (Braak & Braak, 1996), neurotransmitter signalling (Leng et al., 2021), and calcium (Praschberger et al., 2023) and protein homeostasis (Silva et al., 2016; Tsvetkov et al., 2013). However, accumulating data implies that cell independent mechanisms, such as prion-like tau behaviour may also account for the pathology spread.

The prion protein (PrP) is a highly-conserved glycoprotein, abundantly expressed on neuronal surface (Herms et al., 1999; Wulf et al., 2017). The normal, cellular PrP (PrP^{C}) can be converted to a β-sheet-rich PrP^{SC} through nucleated polymerisation (K. M. Pan et al., 1993). In prion diseases, a family of rare and fatal neurodegenerative diseases affecting humans and animals, the abnormal PrP^{SC} transmits between cells, regions, and organisms in an infectious manner, inducing the aggregation - ''seeding'' - of PrP^{C} (Jucker & Walker, 2013; Prusiner, 1982, 1998).

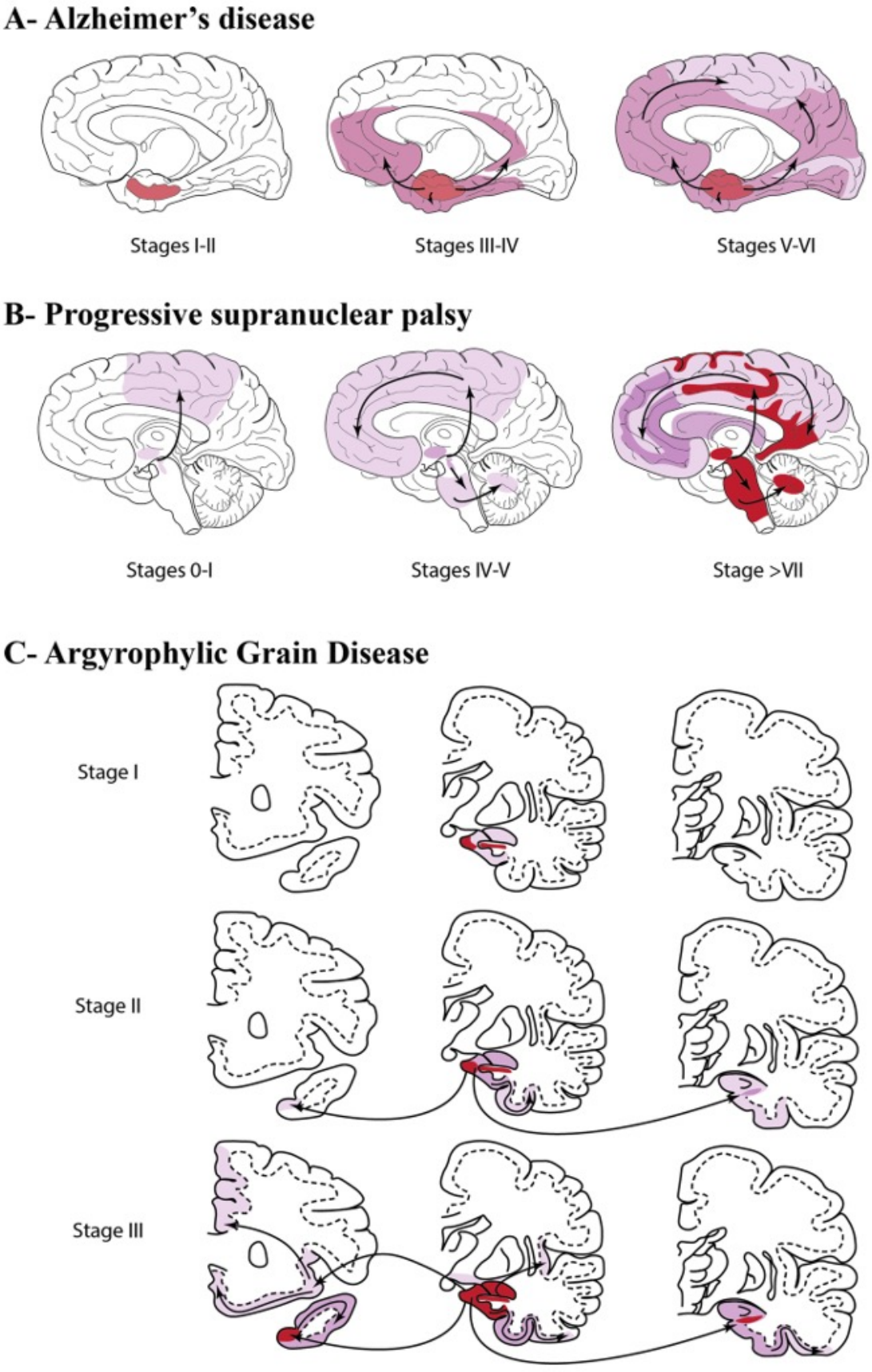

Figure legend on the next page.

Figure 1.5: Stereotypical spatiotemporal propagation of tau pathology in various tauopathies

In AD, tau aggregates propagate from the transentorhinal area (Braak stage I/II) through hippocampus and medial temporal lobe (Braak stage III/IV) to neocortex (Braak stage V/VI). In PSP, tau aggregates progress from the system pallidus to premotor cortex, basal ganglia and dentate nucleus, reaching cerebellum, putamen and all neocortical regions except temporal area in the final stages. In AGD, stage I is characterised by tau deposits in ambient gyrus and hippocampus, progressing to medial temporal lobe in stage II. In stage III, tau pathology reaches frontal lobe and can propagate onto neocortex and brainstem in stage IV (not shown).

The colour intensity (from light purple to purple, and dark red) represents the increasing severity of pathology. Adapted from Dujardin et al., 2019.

Unlike in the prion diseases, there is no recorded evidence of inter-individual tauopathy transmission. However, inter-cellular tau seed propagation was observed *in vivo* and *in vitro*. Seminal study by Clavaguera et al., 2009 showed that inoculation of tau aggregates extracted from transgenic mice expressing human P301S mutant tau into the brain of wild-type (WT) human tau (hTau)-expressing mice induced the WT hTau aggregation and spreading into distant brain regions. The findings have been replicated using various forms of tau aggregates, including synthetic tau fibrils, rodent and human whole-brain lysates, and rodent and human brain-extracted tau aggregates from several tauopathies. In each case, the aggregate injection was sufficient to induce a time-dependent pathology spread in mice transgenic for hTau or even WT mice that do not develop tau pathology (Ahmed et al., 2014; Dai et al., 2017; Gibbons et al., 2017; Iba et al., 2015a, 2015b; Jackson et al., 2016; Kaufman et al., 2016; D. Kim et al., 2015; Narasimhan et al., 2017a; Peeraer et al., 2015; Sanders et al., 2014; Stancu et al., 2015). To exclude the possibility that tau seed simply diffuses from the injection site in lieu of an inter-cellular transfer, several rodent studies restricted tau overexpression promoting deposit

formation in a single brain region. This was achieved using either area-specific promoters (de Calignon et al., 2012; Harris et al., 2012; Liu et al., 2012) or virally-mediated focal expression (Asai et al., 2015; Dujardin et al., 2014; Siman et al., 2013; Wegmann et al., 2015, 2017). Regions neuroanatomically connected to the tau-overexpressing regions developed tau pathology, confirming tau aggregates can propagate between the brain cells *in vivo*. The absence of pathology formation following the injection of tau immunodepleted brain-extract confirmed tau as the causative factor (Clavaguera et al., 2009). Interestingly, an intraperitoneal administration of tau aggregates also resulted in tau deposit formation in the brains of presymptomatic mice, suggesting an extra-cerebral tau transmission route may exist (Clavaguera et al., 2014). These findings are however yet to be replicated.

Notably, the newly formed tau deposits contained endogenously-expressed tau. This supports the hypothesis that exogenous tau inclusions propagate by seeding the endogenous tau monomer. *In vitro* findings align with the *in vivo* studies, showing an efficient cellular uptake of exogenous tau aggregates followed by the endogenous tau aggregation in cell lines, primary rodent neurons, and iPSC-derived neurons (B. Frost et al., 2009; J. L. Guo & Lee, 2011a; Holmes et al., 2014; Kfoury et al., 2012; Manos et al., 2022; Nonaka et al., 2010; Oakley et al., 2021; Santa-Maria et al., 2012; Usenovic et al., 2015; Verheyen et al., 2015; Woerman et al., 2016).

In prion diseases, the infectious PrP^{SC} exists in multiple, distinct conformations underlying the variety of prion disease characteristics (Collinge & Clarke, 2007). Therefore, for tau to fulfil the criteria of prion-like behavior, distinct, stable conformers with varying physicochemical and functional properties would have to exist, stably templating the unique conformation onto naïve, monomeric tau. The matter is still highly debated but support for this hypothesis is steadily growing. Firstly, as discussed in section 1.2, the atomic structure of tau fibrils varies between tauopathies (reviewed in Scheres et al., 2020). Secondly, the tau fibril conformation appears to dictate its seeding capacity. Injections of AGD, PSP, and CBD brain homogenates to human WT tau-expressing mice reproduced pathology characteristic of the respective human disorder

(Clavaguera et al., 2013). The same findings were observed following AD and CBD injections in P301S tau-expressing mice (Boluda et al., 2015). Tau strains generated *in vitro* also induced distinct pathologies in the P301S mice, stably transmissible across three generations (Sanders et al., 2014). Additionally, tau mutations, isoform composition, and post-translational modifications (PTMs) were found to uniquely influence the fibril seeding capacity, correlating with clinical aggressiveness (Dujardin et al., 2018, 2020). Notably, the self-propagating property of misfolded tau has been harnessed to develop cell-based (Holmes et al., 2014) and diagnostic assays to screen for seeding-competent tau in samples (Kraus et al., 2019a; Metrick et al., 2020a; Saijo et al., 2017, 2020a).

1.4 Mechanisms mediating prion-like tau propagation

The mechanisms underlying tau prion-like inter-cellular transmission are currently under intense investigation (reviewed in Brunello et al., 2020). Because of tau toxicity demonstrated *in vitro* (de Calignon et al., 2012) and *in vivo* (Gómez-Ramos et al., 2006; Tian et al., 2013), and the strong association between tau pathology and neuronal loss (Braak & Braak, 1991), tau was long assumed to be passively released from dying neurons (J. L. Guo & Lee, 2011b; Hu et al., 2016). Recent studies, however, clearly demonstrate that tau seed can be actively transferred between synaptically-connected, intact neurons (Calafate et al., 2015; Hallinan et al., 2019; Takeda et al., 2015) in the events preceding neuronal loss (DeVos et al., 2018; Hallinan et al., 2019; Pickett et al., 2017). Furthermore, stimulation of neuronal activity can enhance tau release (Pooler et al., 2013; Wu et al., 2016; Yamada et al., 2014). In line with the findings, tau was found to associate with synaptic vesicles during secretion in an activity-dependent manner (Tracy et al., 2022). *In vivo* propagation of tau pathology between afferently and efferently connected murine neurons (Ahmed et al., 2014) and the complete absence of tau pathology in denervated frontal cortex of an AD patient (Duyckaerts et al., 1997) further support the concept.

However, many additional, diverse, and mutually non-exclusive means of neuronal tau release exist besides the synaptic activity-associated one (Figure 1.6). Free tau is capable of translocating directly across the plasma membrane depending on the interaction with sulphated glycosaminoglycans (Katsinelos et al., 2018). A DnaJC5/Hsc70 chaperone complex-operated pathway can also induce tau release, hinting at a potential intrinsic cellular mechanism for removal of misfolded proteins (Fontaine et al., 2016). Tau can be also released to the extracellular space packaged inside extracellular vesicles (EVs) (Fowler et al., 2023; Miyoshi et al., 2021; Polanco et al., 2021; Saman et al., 2012; Wang et al., 2017) or transferred directly between neurons forming actin-filament-rich tunnelling nanotubes (Abounit et al., 2016; Tardivel et al., 2016). Precisely which of these mechanisms are associated with pathological tau propagation is yet to be elucidated.

Depending on its conformation, the released tau can be internalised from the extracellular space by recipient neurons via bulk-endocytosis (Evans et al., 2018; Wu et al., 2013), LRP1-mediated endocytosis (Rauch et al., 2020), heparan sulfate proteoglycans (HSPGs) (Holmes et al., 2013; Kfoury et al., 2012), or recently implied direct membrane translocation (Figure 1.6) (Dodd et al., 2022). A number of studies demonstrated that the internalised aggregates can induce endolysosomal membrane rupture followed by an escape to the cytosol (Calafate et al., 2016; Falcon, Noad, et al., 2018; Flavin et al., 2017; Polanco et al., 2021), suggesting a route by which intra-neuronal tau seeding may occur.

Importantly, other brain-resident cells besides neurons are capable of internalising the released tau, including astrocytes(Martini-Stoica et al., 2018; Perea et al., 2019) and microglia (Bolós et al., 2016a; W. Luo et al., 2015). Furthermore, a seminal study by Asai et al., 2015 showed that in rodents, cultured microglia can secrete seeding-competent tau in EVs, readily internalised by neurons. The study implied that pathological tau propagation may, in fact, involve multiple cell types and that microglia may play a direct role in prion-like tau transmission. The question of microglial role in tauopathies has instructed the overarching premise of this thesis (Figure 1.7).

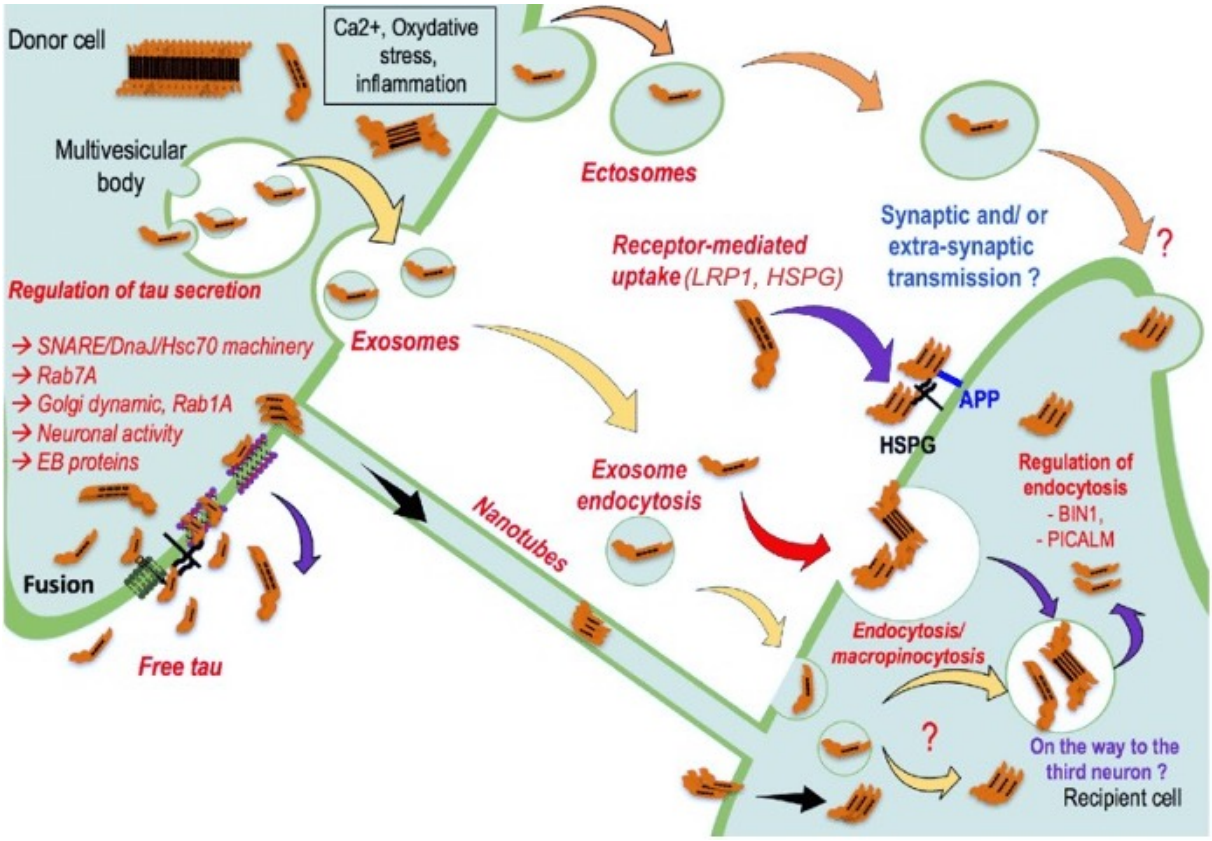

Figure 1.6: Mechanisms of neuronal tau transmission

Donor neurons can release tau (in orange) to the extracellular space via extracellular vesicles, ectosomes, or via free translocation across the membrane. Synaptic activity enhances neuronal release. The majority of extracellular tau is in the free form, not vesicle-bound. Recipient neurons have been demonstrated to internalise tau via LRP1/HSPG receptor-mediated endocytosis, membrane translocation, and extracellular vesicle endocytosis. Direct transfer between donor and recipient neurons can occur via tunnelling nanotubes. Adapted from Colin et al., 2019.

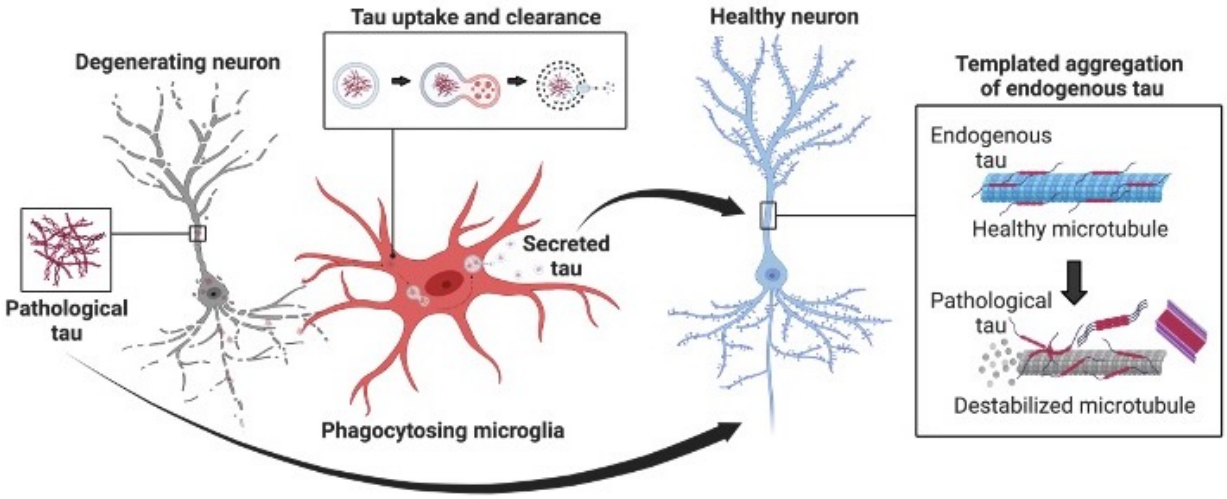

Figure 1.7: The putative role of microglia in tauopathies.

Rodent studies suggest that microglia may be able to internalise tau from extracellular space or contained within degenerating neurons. Microglia were demonstrated to secrete seeding-competent tau in extracellular vesicles, from where it could be internalised by neighbouring neurons (Asai et al., 2015). It is conceivable that this route of tau transmission may contribute to prion-like tau spread in tauopathies but direct evidence from humans is still lacking.

1.5 Microglia – unique, brain-resident macrophages

Microglia, first described by the Spanish neuroscientist Pío del Río-Hortega in 1919 (del Río-Hortega, 1919; Sierra et al., 2019), are the CNS-resident, chief effector cells of the innate immune system (reviewed in Butovsky & Weiner, 2018; Kettenmann et al., 2011; Q. Li & Barres, 2018). Since the proposal of the mononuclear phagocyte system (MPS) in 1969, microglia were grouped together with the peripheral tissue-residing macrophages, dendritic cells, and blood-circulating monocytes based on their apparent morphological (i.e., a single nucleus), and functional similarities (i.e., the ability to phagocytose – recognize, engulf and degrade – foreign material) (van Furth et al., 1972; van Furth & Cohn, 1968). Technological advancements have helped differentiate microglia from other myeloid cells, and provide an important insight into their unique origin, diversity, and role in the brain homeostasis and disease.

Microglia express molecular signatures distinct from the peripheral macrophages (Gautier et al., 2012). In human, these include the P2Y purinoceptor 12 (P2Y12R) and transmembrane protein 119 (TMEM119) (Galatro et al., 2017; Olah et al., 2018a; Satoh et al., 2016; C. Zhu et al., 2017). Microglial origin and renewal throughout the life is also independent of blood monocytes and peripheral tissue-macrophages. Fate-mapping studies in mice demonstrated that microglia originate during primitive haematopoiesis from mesodermal, yolk sac (YS)-derived macrophage progenitors between embryonic day 7 (E7) and E7.5 (Ginhoux et al., 2010; Gomez Perdiguero et al., 2015; Palis et al., 1999). The progenitors begin to colonise the developing brain at E9.5 before the blood-brain barrier is formed and other brain cell types have been differentiated (Alliot et al., 1991, 1999). In contrast, the adult BMDMs and other myeloid cells of hematopoietic lineage originate from the aorto-gonado-mesonephros (AGM) region-derived hematopoietic stem cells (HCSs), populating the foetal liver and bone marrow at E10.5. (Figure 1.8). Microglial development is independent of MYB, a key definitive haematopoiesis transcription factor (Kierdorf et al., 2013; Schulz et al., 2012). Instead, early microglial maturation requires the PU.1 and RUNX1 transcription factors, and the interferon regulatory factor 8 (IRF8). Continued microglial survival and differentiation in the brain relies

on local environment, including the interleukin-34 (IL-34), colony-stimulating factor 1 (CSF-1) and transforming growth factor-β1 (TGFβ1) cytokine signalling (Butovsky et al., 2014; Greter et al., 2012; Wang et al., 2012). The need for environment cues was further demonstrated by a successful differentiation of mature, fully functional microglia from of induced pluripotent stem cell (iPSC)-derived YS macrophages (Haenseler, Sansom, et al., 2017; Takata et al., 2017) and iPSC-microglia with foetal profile (Fattorelli et al., 2021; S. T. Schafer et al., 2023) following *in vitro* neuronal co-culture and *in vivo* brain xenotransplant, respectively.

Importantly, the brain-established, adult microglia rely only on local clonal expansion for self-renewal, without the contribution of peripheral macrophages or monocytes (Askew et al., 2017; Bruttger et al., 2015; Réu et al., 2017; Tay et al., 2017). This was clearly shown by a recent microglial depletion study in which the residual population, and not the HSC-derived progenitors, rapidly repopulated the adult brain (Huang et al., 2018). Peripheral macrophages may be recruited to the brain parenchyma but maintain their own identity and appear to play a distinct role in the brain pathology (Cronk et al., 2018; Silvin et al., 2022). Finally, while much of our understanding of microglial development comes from the rodents, human microglial differentiation has been shown to follow a similar pattern (Monier et al., 2007; Rezaie et al., 2005; Verney et al., 2010).

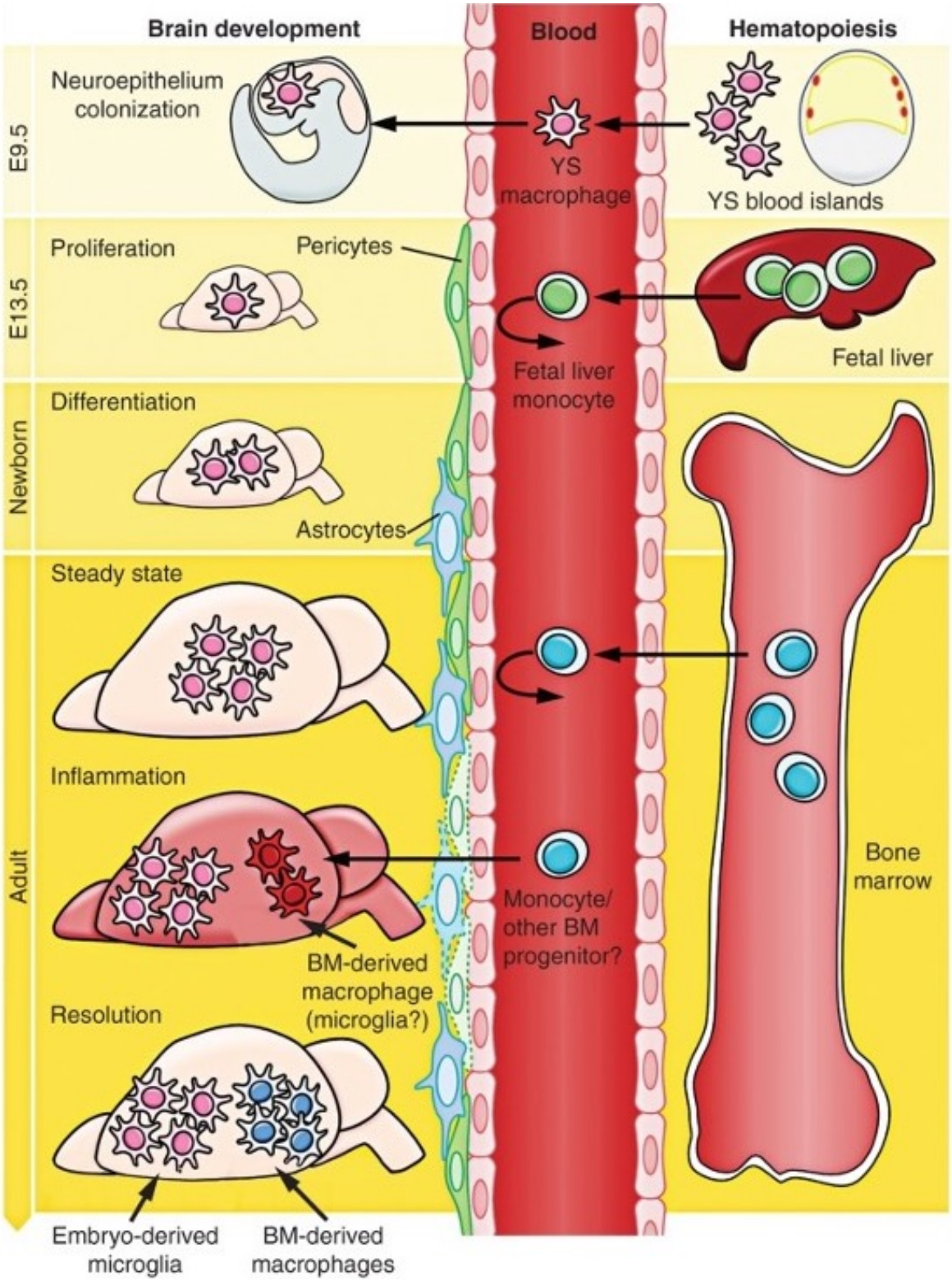

Figure legend on the next page.

Figure 1.8: Microglial ontogeny

Primitive macrophages derived from embryonic YS blood islands colonise developing neuroepithelium at around E9.5, following the onset of blood circulation around E8.5. This primitive wave of haematopoiesis gives rise to embryonic microglia, expanding and colonising the whole CNS. In parallel, the AGM region-derived HSCs colonise the foetal liver and bone marrow during the definitive wave of haematopoiesis, giving rise to adult blood cells. Circulating monocytes can migrate to peripheral tissues, differentiate, and partially or fully replace the peripheral tissue macrophage population. Conversely, microglia locally proliferate to maintain their population throughout the course of life without contribution from the periphery. BMDMs can be recruited to the CNS under certain inflammatory conditions but maintain their own identity. Adapted from Ginhoux et al. 2013.

1.6 Microglial function

According to the current knowledge, microglia perform two essential functions. Firstly, microglia act as sentinels, constantly surveying and interacting with the brain parenchyma using their highly dynamic, ramified processes (Kato et al., 2016; A. Miyamoto et al., 2016; Nimmerjahn et al., 2005; Tremblay et al., 2010; Wake et al., 2009). In the event of a focal injury, microglia can rapidly migrate towards the affected site (Davalos et al., 2005; Haynes et al., 2006; Nimmerjahn et al., 2005). Their sentinel function is enabled by the ‘’sensome’’ - a distinct set of transmembrane proteins and ion channels conserved in all microglial populations across the brain, allowing them to sense and respond to changes in their microenvironment (S. E. Hickman et al., 2013).

The surveillance role thus creates a building block for the second fundamental function of microglia – the phagocytosis. Phagocytosis, from the ancient Greek word ‘’phagein’’ meaning ‘’to devour,’’ is a biological process by which cells recognize, engulf and degrade particles larger than 0.5 μm in diameter (Mukherjee et al., 1997). The process is initiated with a cargo ligand recognition by specific cell-surface receptors. The receptor-ligand binding triggers

activation of signalling pathways inducing cytoskeleton and plasma membrane remodelling in order to seal-off the cargo into a phagosome. Following its internalisation, the phagosome fuses with progressively more acidic, oxidative, and hydrolytic cellular compartments in order to deliver cargo for degradation (Flannagan et al., 2012; Pauwels et al., 2017, Desjardins et al., 1994; Nguyen & Yates, 2021; VIEIRA et al., 2002). While all mammalian cells are capable of phagocytosis, in multicellular organisms with a well-developed immune system, phagocytosis is typically performed by professional phagocytes such as the dendritic cells (DCs), neutrophils, and macrophages (Rabinovitch, 1995). Phagocytosis thus represents a fundamental, evolutionary conserved, intervention mechanisms of the innate immune system to remove material that may threaten the host homeostasis and survival.

Microglia phagocytose a variety of cargo, the nature of which influences their downstream response. By phagocytosing invading pathogens, microglia engage in the first-line tissue defence (reviewed in Rock et al., 2004; Rodríguez et al., 2022). In response to the infectious agents, microglia can initiate the innate inflammatory response similar to the one in the periphery. This includes the secretion of a variety of cytokines, chemokines, degradative enzymes, reactive oxygen species (ROS), and nitric oxide (NO) (Babcock et al., 2003; Boje & Arora, 1992; Cherry et al., 2014; Hartlage-Rübsamen et al., 1999; Kremlev, 2004). Interestingly, microglia were recently shown capable of triggering the adaptive arm of immunity and recruiting T-cells (Ebner et al., 2013), particularly in response to tau pathology (Chen et al., 2023).

Microglia also perform a housekeeping-oriented phagocytosis, subjected to tight regulations in order to mitigate any tissue damage, potentially induced by pro-inflammatory signalling. Specifically, microglia routinely phagocytose dead or senescent brain cells and cell debris (Paolicelli et al., 2011; D. P. Schafer & Stevens, 2013; Sierra et al., 2010). Furthermore, microglia prune excess synaptic connections and axons during development and adulthood, in an activity- and complement-dependent manner (Lui et al., 2016; Marín-Teva et al., 2004; Peri & Nüsslein-Volhard, 2008; D. P. Schafer et al., 2012; Stevens et al., 2007; Vasek et al., 2016),

and control the differentiation and number of oligodendrocytes and their progenitors (Hagemeyer et al., 2017; McNamara et al., 2023; Wlodarczyk et al., 2017). In doing so, microglia importantly regulate several aspects of brain remodelling, including neurogenesis, synaptic plasticity, neuronal myelination, and circuit formation. In addition to the phagocytosis, microglia can contribute to brain tissue remodelling by secretion of multiple growth factors, thus providing direct neurotrophic support, preventing neuronal damage (Kettenmann et al., 2013; Parkhurst et al., 2013; S.-H. Shi et al., 2003), and enhancing neuronal differentiation in the steady-state (Schmidt et al., 2021) and following an injury (Batchelor et al., 1999).

1.7 Microglial phenotypes in tauopathies

As discussed in the previous section, microglia crucially regulate brain homeostasis by engaging in constant, tightly-regulated, dynamic immunosurveillance and neuronal circuit remodelling (Figure 1.9). Dysregulation of microglial function is currently thought to contribute to the pathology observed in tauopathies (reviewed in Chen & Holtzman, 2022; Heneka, 2019; Salter & Stevens, 2017).

Depending on the type of stimuli encountered, microglia were long-assumed to respond with, much like the peripheral macrophages, one of two types of transient signalling: proinflammatory (i.e., the classical M1 activation state) or anti-inflammatory (i.e., the alternative M2 activation state) (Block et al., 2007; Cherry et al., 2014; Gordon, 2002; Mantovani et al., 2005; Martinez & Gordon, 2014). Microglial dysregulation towards chronic proinflammatory, neurotoxic, phenotype was initially thought to contribute to the neuropathology in tauopathies. Post-mortem tissue analyses (Imamura et al., 2003; Minett et al., 2016; Parachikova et al., 2007; Perez-Nievas et al., 2013) as well as positron emission tomography (PET) studies of living subjects have correlated proinflammatory microglial phenotype with pathological tau deposition and cognitive deficits in tauopathies (Cagnin et al., 2001, 2006; Crotti et al., 2014; Dani et al., 2018; Gerhard et al., 2004, 2006a; Pascoal et al., 2021; Terada et al., 2019). The findings led to the formulation of the ‘’chronic neuroinflammation’’ hypothesis, suggesting that an excessive and

persistent microglial production of proinflammatory mediators promotes the apparent neuronal loss in tauopathies. Early RNA-sequencing studies supported the hypothesis, demonstrating microglial transition from homeostatic (Butovsky et al., 2014) towards neurodegeneration-associated signature in a number of diseases. The signature is typically referred to as the ‘’disease-associated microglia’’ (DAM) or ‘’neurodegenerative microglia’’ (MGnD), and is characterised by a downregulation of immune-surveillance pathways, and simultaneous upregulation of stress-related, phagocytosis, and inflammatory pathways (Boche & Gordon, 2022; Del-Aguila et al., 2019; Friedman et al., 2018; Holtman et al., 2015; Keren-Shaul et al., 2017; Krasemann et al., 2017; Marschallinger et al., 2020a; Mathys et al., 2019; Prater et al., 2023; Sobue et al., 2021; Srinivasan et al., 2020a). Notably, the signature, particularly the expression of genes related to tumour necrosis factor (TNF) and interleukin-1β (IL-1β) production, coincides with the appearance of NFTs in the 4-month-old P301L mouse model of tauopathy (H. Wang et al., 2018). Consistent with the transcriptomics data, functional studies showed that aberrant microglial phagocytosis or release of inflammatory molecules may result in synapse and neuronal loss (reviewed in Butler et al., 2021).

Recent evidence, however, portrays a more complex situation than previously assumed. Firstly, microglia were shown to take on and continuously transition between an extraordinary repertoire of phenotypes in health and disease, determined by the individual genetic make-up (Efthymiou & Goate, 2017; Sala Frigerio et al., 2019), sex (Kodama et al., 2020; Sala Frigerio et al., 2019; Villa et al., 2018), age (Olah et al., 2018b; Srinivasan et al., 2020b), brain region (Grabert et al., 2016; Q. Li et al., 2019), environment (Bennett et al., 2018; Gosselin et al., 2017), stage of disease (Keren-Shaul et al., 2017; Marschallinger et al., 2020b), and - relevant to this thesis - tau protein conformation (J. E. Rexach et al., 2020). Owing to the results, the simplistic view of ‘’’toxic proinflammatory or protective antiinflammatory’’ microglia is being replaced with a novel framework recognising that microglia exist on a continual phenotypic spectrum in response to the environment cues (Paolicelli et al., 2022).

Secondly, the concept of neurotoxic DAM has been called into question. An integrative analysis of multiple single-cell RNA-sequencing datasets combined with fate-mapping revealed that DAM can actually be deconvoluted to two ontogenetically and functionally-distinct populations: the *bona fide* DAM and disease inflammatory macrophages (DIM). The bona fide DAM share signatures with embryonic-like and highly-proliferative, white matter-associated microglia promoting myelination, thus may engage in a tissue and myelin repair in a protective manner. In contrast, DIM comprise of BMDMs infiltrating and progressively accumulating in the brain with age and neurodegeneration burden. DIM, not *bona fide* DAM signature is associated with detrimental, proinflammatory effect in tauopathies (Silvin et al., 2022). In support of the DAM protective phenotype, high expression of DAM markers in the neocortex of individuals from Swedish BioFINDER-2 study correlated with less severe AD-related changes, including lower cognitive decline, and amyloid-beta (Ab) and tau deposition (Pereira et al., 2022). In addition, the late stages of tauopathies appear to feature hypofunctional, degenerative microglia in the vicinity of high phospho-tau-bearing neurons, with weak, dystrophic processes, fragmented cytoplasm (Sanchez-Mejias et al., 2016; Streit et al., 2009; van Olst et al., 2020) and immunosuppressive gene expression signature (J. E. Rexach et al., 2020).

Altogether, the data suggests that loss of microglial protective function instead of, or in addition to, potentially detrimental proinflammatory phenotype, may contribute to the pathology in tauopathies.

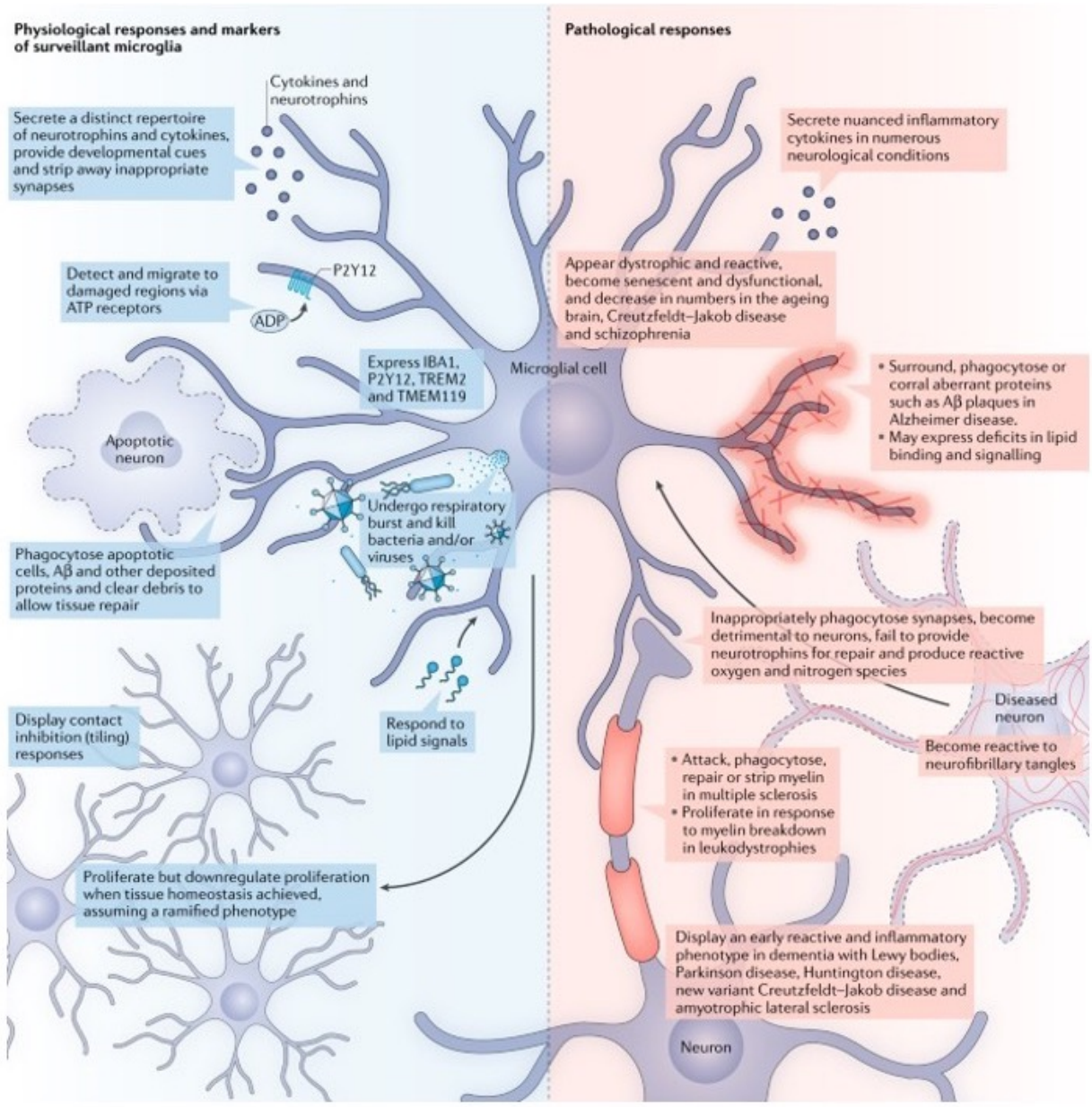

Figure 1.9: Microglial activity in health and disease

Microglia crucially contribute to healthy CNS physiology in a number of ways. They act as phagocytic sentinels during development and in adulthood, surveying the environment, pruning synapses, clearing debris and pathogens, and providing trophic support. In tauopathies and other neurodegenerative diseases, microglia become reactive, proliferate, and engage in chronic proinflammatory signalling and aberrant phagocytosis. Towards the late disease stages, microglia appear dystrophic, senescent, and dysfunctional. Adapted from Pocock et al., 2018.

1.8 The emerging role of microglia in tau pathology

Numerous studies have now consistently documented the perturbations of microglial homeostatic phenotype in tauopathies. How these phenotypic changes relate to the initiation and propagation of tau pathology is unclear. Among the many unanswered questions, two stand out: can microglia drive tau aggregation and propagation? If so, what are the underlying molecular mechanisms?

Some evidence suggests that microglia can, indeed, initiate tau pathology. Aberrant microglial activation and synapse loss precedes NFT formation in the P301S mouse model of familial, early-onset frontotemporal dementia (Yoshiyama et al., 2007). Adoptive transfer of microglia purified from transgenic mice engineered to exhibit accelerated hTau pathology is sufficient to induce tau hyperphosphorylation in WT mice that do not normally develop tau aggregates (Maphis et al., 2015). A recent PET analysis of individuals across the aging and AD spectrum agrees with the rodent findings. The study showed that the spatiotemporal pattern of human microglial activation follows the stereotypical tau propagation trajectory. Importantly, the tau propagation depended on microglia and was potentiated by a synergistic effect between microglial activation and Aβ burden (Pascoal et al., 2021).

Functional studies have recently attempted to obtain mechanistic insight into how microglia may drive tau pathology. Incubation of cultured rodent microglia with truncated recombinant tau instigated microglial pro-inflammatory cytokine production (Kovac et al., 2011). The proinflammatory microglial activation, in turn, induced tau production and release from cultured neuroblastoma cells (M. Lee et al., 2015), and tau hyperphosphorylation in murine neurons *in vitro* and *in vivo* via IL-1β-mediated regulation of tau kinases and phosphatases (Bhaskar et al., 2010; Y. Li et al., 2003). In addition, the exposure to exogenous tau *in vitro* promoted microglial phagocytosis of living neurons (Butler et al., 2021; Pampuscenko et al., 2020). Experimental ablation of microgliosis using a variety of strategies *in vivo*, including the suppression of microglial IL-1β secretion (Ising et al., 2019) and systemic treatments with

immunosuppressant Tacrolimus (Yoshiyama et al., 2007), broad-spectrum antibiotic minocycline (Noble et al., 2009), or the IL-1 receptor blocking antibody (Kitazawa et al., 2011), significantly reduced tau phosphorylation and aggregation, and in some cases also rescued cognitive deficits.

Collectively, the results suggested that microglia may drive neuronal tau production and aggregation via proinflammatory cytokine release and signalling. Accumulating evidence from rodents, however, shows that microglia may also directly contribute to prion-like tau spread across the brain. Specifically, microglia were demonstrated to internalise tau from the extracellular space (Andersson et al., 2019; Asai et al., 2015; Bolós et al., 2016a; Funk et al., 2015a; W. Luo et al., 2015; Majerova et al., 2014; van Olst et al., 2020; Zilkova et al., 2020) or contained within phagocytosed neurons (Sanchez-Mejias et al., 2016). Following tau internalisation, microglia actively secreted seeding-competent tau to the extracellular space (Asai et al., 2015; Clayton et al., 2021; Crotti et al., 2019; Hopp et al., 2018; B. Zhu et al., 2022). In further support of the concept, both the microglia depletion with PLX3397, a CSF1R inhibitor, and inhibition of microglial tau secretion impeded aggregated tau propagation along neuroanatomically-connected regions in two mice models of tauopathy (Asai et al., 2015).

The molecular mechanisms underlying microglia-mediated tau spreading are understudied. Key information is still missing, including the mechanisms of tau uptake, the type of intracellular signalling triggered by tau internalisation, the impact of microglial intracellular environment on tau seeding, microglial capacity to fully degrade tau, and whether a putative lack of tau proteolysis or other mechanisms such as antigen presentation may result in tau secretion by microglia. These are very relevant questions to address as many of the pathways involved in microglial tau processing potentially represent a druggable target.

1.9 Microglial LRRK2 and tau pathology

The importance of investigating microglial tau processing is further emphasized by the outcome of genetic studies and pathway analyses of tauopathy-associated risk-variants. The studies have found that many of the risk variants are highly or exclusively expressed in microglia, or enriched in microglia-specific enhancers, and modulate all aspects of microglial cargo processing, including cargo recognition, engulfment, trafficking between organelles, degradation, and secretion (Figure 1.10). (Andersen et al., 2021; Efthymiou & Goate, 2017; Farrell et al., 2022; Huang et al., 2018; Langston et al., 2022; Nott et al., 2019). Together, the results point out phagolysosomal clearance by microglia as a key candidate mechanism affecting disease susceptibility (reviewed in Podleśny-Drabiniok et al., 2020).

LRRK2 is one of the risk factors associated with the progression of at least two tauopathies, PD and PSP (Herbst et al., 2022) (Table 1.1). Importantly, LRRK2 is highly expressed in myeloid cells (Ahmadi Rastegar & Dzamko, 2020) and has been long-implicated in the regulation of membrane and cargo trafficking (Hur et al., 2019). LRR2K may therefore represent a potential genetic determinant of microglia-mediated tauopathy progression.

LRRK2, also known as dardarin, is a large multidomain, multifunctional protein (Figure 1.11). Autosomal dominant missense mutations in LRRK2 cause familial form of Parkinson's disease (PD) (Paisán-Ruíz et al., 2004; Zimprich et al., 2004), and several variants in the LRRK2 locus are also associated with the development of sporadic PD (Nalls et al., 2014a, 2014b; Simón-Sánchez et al., 2009). PD has been conventionally characterised as α-synucleionopathy. Primary neuropathological features of PD include progressive accumulation of α-synuclein (α-syn) aggregates into intracellular Lewy bodies (LB), and a loss of dopaminergic neurons in the *Substania Nigra pars compacta* of the midbrain (reviewed in Dickson, 2018). However, compelling evidence suggests that PD could be fittingly categorised also as a secondary tauopathy (L. Pan et al., 2021; X. Zhang et al., 2018). Genome-wide association studies (GWAS) studies have repeatedly linked MAPT H1 haplotype with PD risk (Pascale et al.,

2016), and particularly with the risk of developing dementia in PD (Edwards et al., 2010; Nalls et al., 2014b). Tau deposits are frequently observed in PD patients (J. Zhang et al., 2023), often colocalising with α-syn pathology (Arima et al., 1999; Moussaud et al., 2014) and able to interact with α-syn in an aggregation-promoting manner (Dasari et al., 2019; Giasson et al., 2003). Notably, between 21-54% of LRRK2 PD patients never develop LB pathology but some degree of tau pathology has been consistently reported in over 75% of LRRK2 PD patients (Henderson et al., 2019; Kalia et al., 2015; Poulopoulos et al., 2012; X. Zhang et al., 2018). The G2019S LRRK2 mutation is of specific interest to this thesis, as it is the most frequent pathogenic variant in both familial and sporadic form of PD, that is also strongly associated with tau pathology (Henderson et al., 2019; Simpson et al., 2022). In addition to PD, LRRK2 mutations (G2019S and R1441C) and overall expression levels have been recently linked with the progression of PSP – a primary 4R tauopathy (Herbst et al., 2022; Jabbari et al., 2021; Sanchez-Contreras et al., 2017) (Table 1.1).

It is unclear how LRRK2 may drive tau pathology in PD or PSP. Functionally, LRRK2 has been implicated in the regulation of membrane trafficking through phosphorylation of membrane-associated subset of Rab GTPases (Pfeffer, 2017; Steger et al., 2016, 2017). The G2019S LRRK2 mutation, associated with two to eight-fold increase in kinase activity (Anand et al., 2009; Greggio et al., 2006; L. Guo et al., 2007; Luzon-Toro et al., 2007; MacLeod et al., 2006), increases Rab phosphorylation (Steger et al., 2016, 2017) and frequently results in endolysosomal trafficking defects (Henry et al., 2015; Madureira et al., 2020; Manzoni et al., 2013; Obergasteiger et al., 2020; Schapansky et al., 2014; Yadavalli & Ferguson, 2022). In agreement with the inferred LRRK2 function, endogenous neuronal LRRK2 was found to regulate extracellular tau uptake (Evans et al., 2020) and the G1029S mutation to enhance neuronal tau transmission (Nguyen et al., 2018) but not tau pathology induction (Henderson et al., 2021).

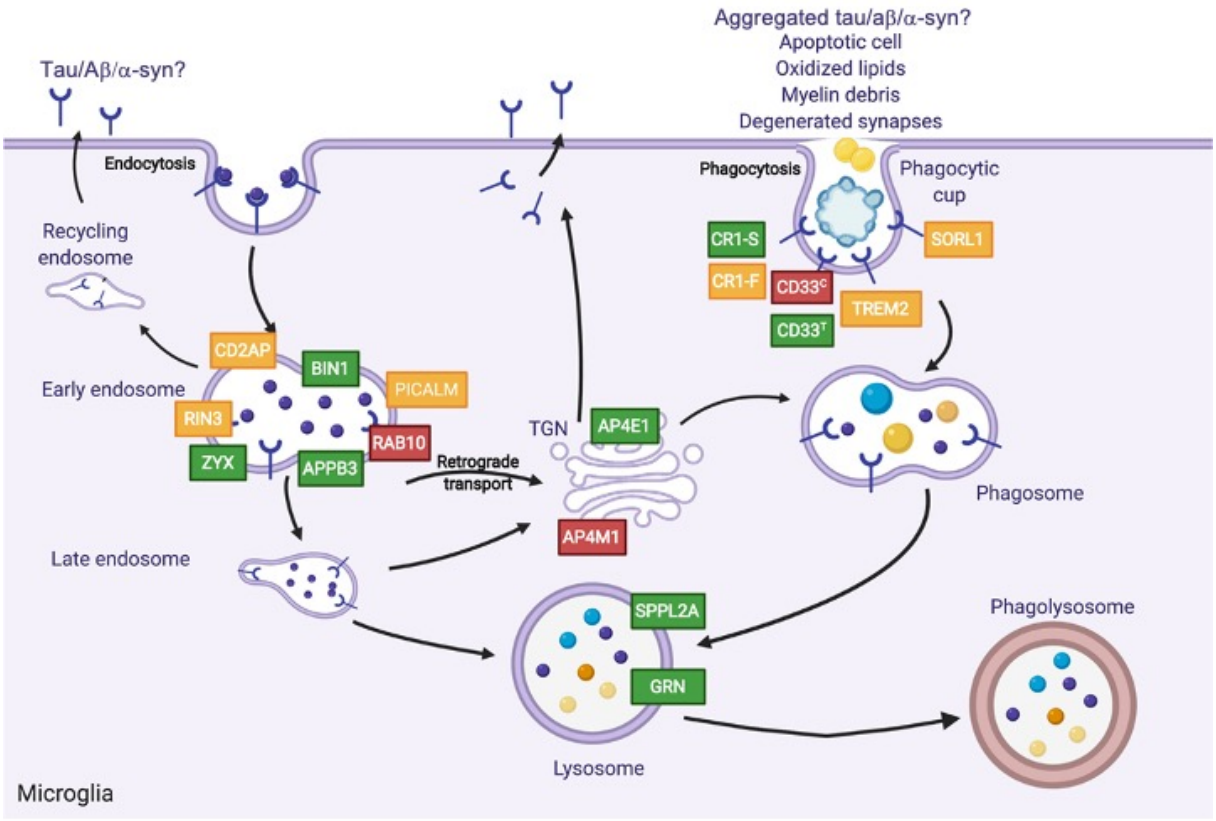

Figure 1.10: Candidate tauopathy-associated risk genes in microglial cargo processing pathways

Microglia constantly survey the environment and internalise smaller, soluble cargo by endocytosis, and large macromolecules (i.e., aggregated proteinopathic seeds, apoptotic bodies, myelin debris, synapses) by phagocytosis. The engulfed material reaches early endosomes or phagosomes that progressively mature and fuse with lysosomes for cargo degradation. The internalised receptors can be sorted to the trans-Golgi network (TGN) via retrograde transport, or recycled back to the plasma membrane. The schematic illustrates AD-specific risk genes. Risk-associated decrease in gene expression is highlighted in green, increase in red, and unknown expression effect in gold. Adapted from Podleśny-Drabiniok et al., 2020.

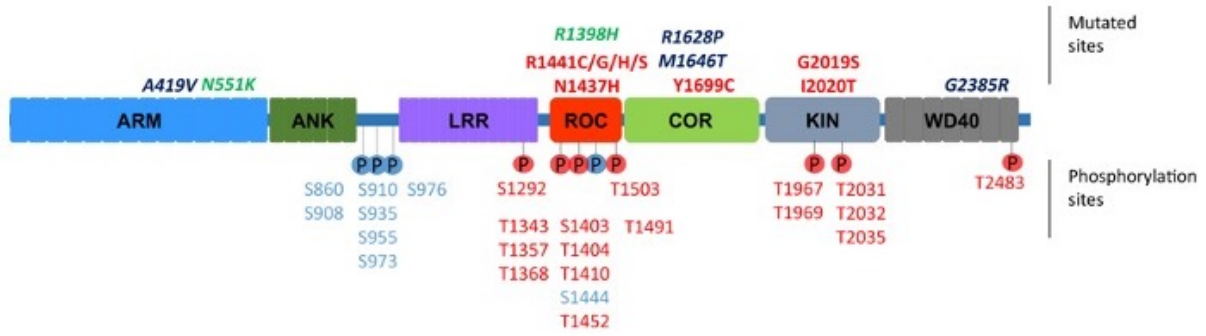

Figure 1.11: LRRK2 protein structure

The armadillo, ankyrin, and leucine-rich repeat domains at the N-terminal region, together with the WD40 domain at the C-terminal region, are believed to be involved in protein-protein interactions. Two additional, enzymatic domains are embedded in the primary sequence: the Roc-COR (Ras of complex proteins - C-terminal of Roc) bidomain, hydrolysing guanosine triphosphate (GTP), and a kinase domain which serves as a serine/threonine kinase Pathogenic PD-associated mutations (in red), risk factor mutations (in blue) and mutations associated with reduced risk for PD (in green) are outlined above the protein schematic. Auto- (in red) and heterologous phosphorylated sites (in blue) are outlined below the schematic. Adapted from Taymans et al., 2023.

Given the notable LRRK2 expression levels in microglia (Ahmadi Rastegar & Dzamko, 2020; Hakimi et al., 2011; H. Lee et al., 2017; Wallings & Tansey, 2019), I reviewed existing evidence for the role of microglial LRRK2 in tau pathology progression. PSP progression and severity was consistently correlated with microglia activation by PET studies (Alster et al., 2020; Gerhard et al., 2006b; Malpetti et al., 2021). In PD, recent genetic study identified a non-coding LRRK2 variant conferring PD-risk via modulating LRRK2 expression specifically and only in microglia (Langston et al., 2022). Most importantly, LRRK2 has been proposed to regulate phagolysosomal clearance in myeloid cells, albeit the precise mechanisms are unresolved (Bonet-Ponce & Cookson, 2022). Some publications have found that LRRK2 may directly influence phagocytic cargo uptake (K. S. Kim et al., 2018a; Maekawa et al., 2016; Marker et al., 2012), others showed no effect on cargo internalisation (Ahmadi Rastegar & Dzamko, 2020; H. Lee et al., 2020; Schapansky et al., 2014) but demonstrated a potential role in phagosomal maturation instead (Härtlova et al., 2018a; H. Lee et al., 2020). Additionally, two studies described LRRK2 recruitment to damaged or stressed lysosomes, and suggested a Rab GTPase-mediated LRRK2 function in membrane repair and lysosomal exocytosis of non-degraded cargo (Eguchi et al., 2018; Herbst et al., 2020) The contradicting results may reflect methodological differences, including the choice of phagocytic cargo, cell model, and model organism (summarised in Table 1.2 and further discussed in section 1.10 and Chapter 3).

Overall, it is becoming clear that LRRK2 is critically involved in microglial phagolysosomal pathways, but the specific role requires further investigation in relevant human cells. Importantly, the role of microglial LRRK2 in the propagation of tau pathology has never been interrogated.

Publication	LRRK2 genotype/ expression manipulation	Cell model	Organism	Cargo	Findings
Marker et al., 2012	siRNA KO	BV2 line	Mouse	HIV-1 Tat protein	Phagocytosis decrease
Maekawa et al., 2016	KO	Microglia	Mouse	α-syn monomer	Internalisation increase
Kim et al., 2018	KO	BMDM, Microglia	Mouse	Latex beads, *E. coli*	Phagocytosis decrease
Härtlova et al., 2018	KO	BMDM	Human, Mouse	*Mycobacterium tuberculosis*	Enhanced phagosomal maturation
	KO	iPSC-macrophages	Human		
Schapansky et al., 2014	shRNA KO	BV2	Mouse	Polystyrene beads	No effect
Rastegar et al., 2020	G2019S	iPSC-macrophages	Human	Latex beads	No effect
Lee et al., 2020	WT/KO/ G2019S	iPSC-macrophages	Human	Zymosan, *E. coli, S. typhimurium*	LRRK2 recruitment to $LAMP1^{+}$ $Rab9^{+}$ maturing phagosomes, bona fide phosphorylation of Rab8a and Rab10
Kim et al., 2018	G2019S	BMDM	Human	Latex beads, *E. coli*	Phagocytosis increase
		BMDM, microglia	Mouse		

Table 1.2: Summary of published evidence on the role of LRRK2 in phagolysosomal pathways

1.10 *In vitro* modelling of human microglia using iPSCs

So far, I have discussed the evidence for prion-like tau propagation in tauopathies and the putative role of microglial endolysosomal system in the process. The majority of studies investigating the topic have been, however, carried out in rodents. Corroborative evidence using an authentic model of human microglia is yet to be provided.

The lack of human data stems largely from the lack of availability of human brain tissue and technical challenges associated with the extraction of primary human microglia. Primary human microglia can be currently isolated from neurosurgical resection specimen, and from foetal or adult post-mortem brain samples (Mizee et al., 2017; T. I.-H. Park et al., 2022; Popova et al., 2021) (Table 1.3). However, in addition to variable quality and limited yield, primary microglia removed from the brain environment rapidly undergo a major transition away from their homeostatic gene-expression and phenotype (Bohlen et al., 2017; Butovsky et al., 2014; Dachet et al., 2021; Gosselin et al., 2017; Lue et al., 2019).

Primary rodent microglia, immortalised microglia cell lines, or human, blood-monocyte-derived macrophages (BMDMs) are frequently used as an alternative to primary human microglia, but each of these models is associated with important limitations and may thus provide a narrow translational value (Table 1.3). Rodent microglia, the most commonly used microglia model, fail to fully recapitulate human microglial physiology in health and disease (A. M. Smith & Dragunow, 2014). Distinct spatial and temporal gene expression differences between human and rodent microglia have been consistently demonstrated (Geirsdottir et al., 2019; Masuda et al., 2019), particularly in the pathways involving brain parenchyma surveillance and phagocytosis (Abels et al., 2021), inflammatory responses, responses to Aβ plaques (Zhou et al., 2020), as well as general aging (Galatro et al., 2017). In addition, at least one third of the human microglia-expressed, AD-associated risk variants lacks adequate mouse orthologs (Hasselmann & Blurton-Jones, 2020a; Mancuso et al., 2019). The absence of rodent research translation to clinic further illustrates the point. The immortalised microglia cell lines, while cost-

effective through their ability to self-renew, show chromosomal instabilities (C. Dello Russo et al., 2018; He et al., 2023; Luan et al., 2022; Tsuchiya et al., 1980) and alterations in metabolic profile (C. Dello Russo et al., 2018). In addition, their abnormal proliferative capacity makes them unsuitable to model the terminally-differentiated microglia. Lastly, human BMDMs differ from brain-residing microglia in ontogeny as discussed in section 1.5 (i.e., adult, definitive haematopoiesis vs microglia primitive haematopoiesis), as well as their environment-induced responses (Bennett et al., 2018; Ginhoux et al., 2013a), and therefore cannot faithfully reproduce authentic human microglial responses.

The identification of microglial ontogeny (reviewed in Ginhoux et al., 2013b) (section 1.5) together with the development of the human iPSC technology (I.-H. Park et al., 2008; Takahashi et al., 2007; J. Yu et al., 2007) revolutionised modelling of human microglia *in vitro*. The use of microglia differentiated from iPSCs overcomes the majority of issues associated with other microglia models, including the abnormal karyotype, inadequate cell yield, and the lack of cell terminal differentiation. In addition, iPSCs are genetically tractable and retain patient's genetic background, enabling a thorough interrogation of genes of interest, more accurate disease modelling, and a potential development of personalised therapeutic strategies (Penney et al., 2020; Valadez-Barba et al., 2020).

Several iPSC-derived microglia differentiation protocols have been published recently (summarised in Washer et al., 2022), all aiming to recapitulate the sequence of events during embryonic primitive haematopoiesis. The protocols, however, vary greatly in medium composition, produced population purity, and reproducibility among different cell lines and labs (reviewed in Haenseler & Rajendran, 2019; Hasselmann & Blurton-Jones, 2020; Hedegaard et al., 2020; Speicher et al., 2019). Our lab has recently conducted a systemic comparison of the available protocols to identify medium that best recapitulates authentic human microglia *in vitro.* As a result, we have described an optimised, highly scalable method for differentiation of microglia from iPSCs with an improved microglia identity and morphology (Washer et al., 2022). Earlier work from our lab also provided a highly-efficient protocol for differentiation of iPSC-

macrophages – a more straightforward, time- and cost-effective surrogate of iPSC-microglia (Karlsson et al., 2008; Vaughan-Jackson et al., 2021; Wilgenburg et al., 2013). Importantly, both cell models were shown to derive from MYB-independent, RUNX1 and PU.1-dependent precursors, thus faithfully reproducing the hallmarks of primitive haematopoiesis, characteristic of YS-derived peripheral tissue-resident macrophages and microglia (Buchrieser et al., 2017; Vanhee et al., 2015). In addition, both models are pathophysiologically authentic and genetically tractable.

Organism	Source	Phenotype	Advantages	Disadvantages
Primary microglia				
Human	Foetal tissue Post-mortem tissue Brain surgery	Low/absent CD45 and CCR2 expression High expression of mature microglia-enriched genes (P2RY12, TMEM19, TREM2, GPR34, CX3CR1, C1QA, GAS6)	Patient-specific Best *in vivo* microglia correlate when freshly isolated	Post-mortem delay Limited resource Tedious isolation Limited yield and purity Ethical challenges Variable phenotype depending on the isolation
Rodents	Neonatal/adult mice and rats, WT or transgenic	Downregulation of mature microglia markers (P2RY12, TMEM119) Enhanced inflammatory activation Highly proliferative phenotype	Controllable genotype No post-mortem delay Increased availability compared with human primary material	Limited translation to humans due to interspecies differences in the expression of immune function related genes Limited yield Long-term cultures at risk for proliferation of contaminating cells (e.g., pericytes, astrocytes)
Immortalised microglial cell lines				
Human	**HMO6** Embryonic, transformed, *v-myc* oncogene	Lack of response to inflammatory stimuli	Easy maintenance Unlimited availability Homogeneous population	Genetic alteration Prone to dedifferentiation Lack of sensitivity to inflammatory stimuli Chromosomal abnormalities (prone to genetic drift) Metabolic abnormalities Subject to morphology changes
	HμGlia Adult, transformed, SV40 large T antigen	Lack of expression of microglia-enriched genes		
	CHME-5 Embryonic, transformed, SV40 large T antigen	Uncertain origin (rat origin suggested)		
	HMC3 Derived from CHME-5	Lack of expression of microglia-enriched genes		
	C13NJ Derived from CHME-5	Lack of expression of microglia-enriched genes		
	SV40 Embryonic, transformed, SV40 large T antigen	Lack of expression of microglia-enriched genes		
Rodents	**BV2 (mouse)** Neonatal, transformed, *v-raft/v-myc* oncogene	Lack of responses to inflammatory stimuli		
	N9, N11 (mouse) Embryonic, transformed, *v-myc* oncogene	Limited expression of inflammatory mediators		
	EOC (mouse) Neonatal, spontaneously immortalised	Attenuated antigen-presenting (MHCII) gene expression		
	IMG (mouse) Adult, transformed, *v-raft/v-myc* oncogene	Amoeboid morphology		
	HAPI (rat) Neonatal, spontaneously immortalised	Attenuated response to inflammatory stimuli		
Blood monocyte-derived macrophages				
Human	Isolation from peripheral blood	Peripheral tissue macrophage phenotype (low expression of TREM2, TMEM119, P2RY12 compared with adult microglia	Cost-effective protocol compared with iPSC-microglia differentiation	Do not recapitulate microglial ontogeny Limited resource

Table 1.3: In vitro microglia models alternative to those differentiated from iPSCs

1.11 Scope of the work

To summarise the introduction to this thesis, pathogenic tau aggregates have been shown to propagate through neuroanatomically-connected brain regions in a prion-like manner in tauopathies, correlating with the disease progression and severity. Compelling data from rodents suggests that microglia, the brain-resident phagocytes, are central to the pathological process. However, the mechanisms by which microglia may contribute to pathogenic tau transmission are unclear. In addition, direct involvement of human microglia has never been demonstrated.

Here, I address these gaps in our knowledge and investigate the molecular mechanisms surrounding human microglial processing of exogenous native and aggregated tau. Within this broad goal, I focus specifically on microglial tau uptake, degradation, secretion, and on the seeding capacity of tau processed by microglia. Given the emerging role of LRRK2 in the microglial phagolysosomal system, as well as in the development and progression of PD and PSP tauopathies, I additionally interrogate the role of microglial LRRK2 in tau clearance and prion-like transmission.

To model authentic human microglia and examine their responses *in vitro,* I capitalise on the James lab protocols for differentiation of iPSC-macrophages and microglia (section 1.10), and on the access to healthy donor and G2019S LRRK2 PD patient fibroblasts. Isogenic LRRK2 WT and CRISPR/Cas9-induced LRRK2 KO iPSC lines, together with G2019S LRRK2 PD patient-isolated iPSC lines will be used for the differentiation (sections 2.1.1 and 2.2.1). The particular cell type used (i.e., iPSC-macrophages vs microglia) is clearly indicated in the individual experiment descriptions.

The investigation of tau processing by an *in vitro* model of human microglia is described in Chapter 5. The result Chapters 3 and 4 provide an important, preliminary groundwork to Chapter 5 (Figure 1.12). Specifically, the experiments in Chapter 3 are motivated by the lack of consensus on the role of LRRK2 in microglial phagolysosomal pathways. Here, I describe

an assay I have optimised to quantitate baseline phagolysosomal clearance in iPSC-macrophages. Using the assay, I further examine the influence of LRRK2 on baseline phagolysosomal clearance in iPSC-macrophages. The results will be contrasted with the influence of LRRK2 on tau-specific clearance by iPSC-macrophages investigated in Chapter 5. In Chapter 4, I describe the optimised protocol for large-scale production of endotoxin-free, human recombinant 2N4R tau protein in monomeric and *in vitro* aggregated form. In contrast with brain tissue-extracted tau, the recombinant tau has a distinct advantage of readily quantifiable, known composition, and can be reproducibly obtained in high yield and purity. The recombinant preparation is therefore used to interrogate microglial responses to tau protein in Chapter 5.

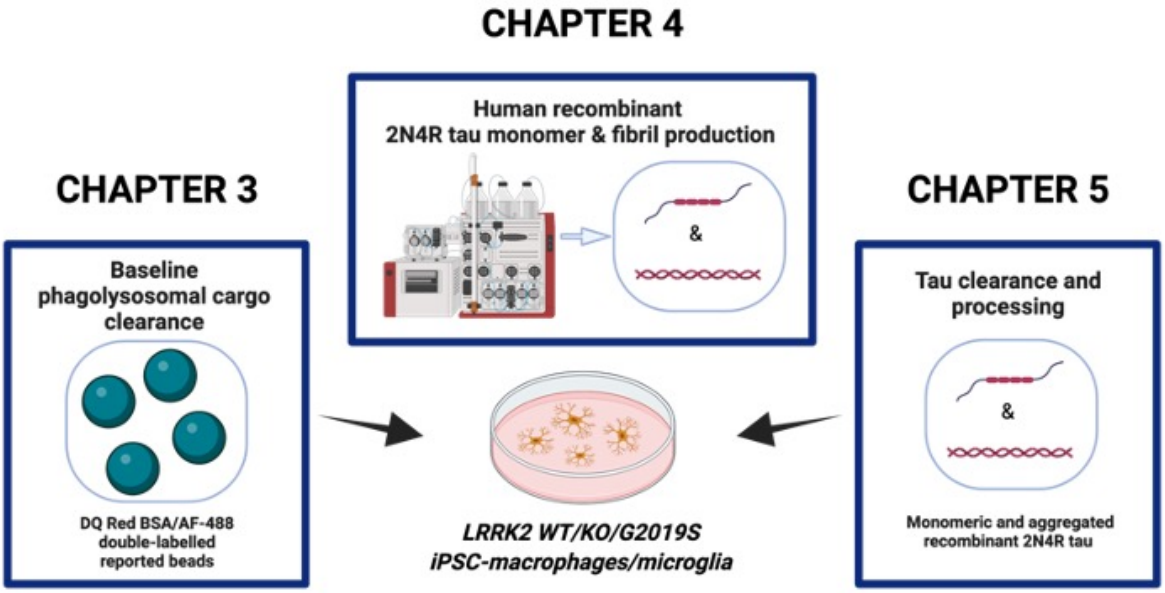

Figure 1.12.: The main aims of individual result chapters

Chapter 2

Materials and Methods

2.1 Cell culture

2.1.1 iPSC lines

KOLF2.1S iPSC line (Washer et al., 2022) was obtained under material transfer agreement (MTA) from the Wellcome Sanger Institute in Cambridge, UK. All other iPSC lines used in this thesis (detailed in Table 2.1) were derived from dermal fibroblasts of G2019S PD patients and disease-free donors recruited through the Oxford Parkinson's Disease Center and StemBANCC projects (Morrison et al., 2015) and have been published previously. Participants gave signed, informed consent for procedures which included mutation screening and derivation of iPSC lines from skin biopsies (Ethics Committee that specifically approved this part of the study: National Health Service, Health Research Authority, NRES Committee South Central, Berkshire, UK, REC 10/H0505/71 and 16/SC/0108).

The iPSC lines (except KOLF2.1S) were derived in the James Martin Stem Cell Facility using non-integrating Sendai viral kit (Cytotune, Life Technologies) for the delivery of Oct3/4, Sox2, Klf4, and cMyc reprogramming factors. Each reprogrammed line passed a quality-control (QC) check for mycoplasma, sterility, viability, Tra-1-60 and Nanog expression, and SNP analysis for genome integrity and tracking on the bulked masterstock deposited in long-term, liquid nitrogen (LN) storage.

To ensure consistency across multiple differentiation rounds, low passage number cell lines from large-scale, SNP-QCed batches were used for all experiments.

Thesis label	Fibroblast ID	iPSC clone ID	Diagnosis	LRRK2 Genotype	Gender	Age of biopsy (years)
●	SF841	SFC841-03-01	Healthy	WT/WT	M	36
●	SF856	SFC856-03-04	Healthy	WT/WT	F	78
●	n/a	KOLF2.1S	Healthy	WT/WT	M	57
○	SF840	SFC840-03-03	Healthy	WT/WT	F	67
●	SF840	SFC840-03-03 D10	CRISPR/Cas9 edited	-/-	F	67
●	SF832	SFC832-03-06	G2019S PD	G2019S/WT	F	77
●	SF833	SFC833-03-05	G2019S PD	G2019S/WT	M	81
●	SF855	SFC855-03-06	G2019S PD	G2019S/WT	M	57

Table 2.1.: iPSC lines used in the thesis

2.1.2 iPSC culture

iPSC lines were thawed from a frozen stock in 37°C water bath, topped up with 9 mL of 1x Phosphate-buffered saline (PBS) (Sigma, D8537-500ML) and centrifuged at 400g (VWR, Rotanta 460R) for 5 minutes at room temperature (RT). Cell pellet was gently resuspended in OXE8 medium (Table 2.2) (Vaughan-Jackson et al., 2021) and the iPSCs were distributed evenly on Geltrex™ (Gibco, A1413302)-coated 6-well plates (Greiner, 657160) to generate a feeder-free iPSC culture. OXE8 medium was supplemented with 10 μM Y-27632 (ROCKi) (Abcam, ab120129) for the first 24 hours of the iPSC growth to aid their survival.

Cells were cultured at 37°C, 5% CO_2, with daily, 100% medium changes. At approximately 80-90% confluency, cells were passaged in clusters using 0.5 mM EDTA (ThermoFisher Scientific, 15575-020) in 1x PBS (Beers et al., 2012) for 5 minutes at 37°C. Passaging was carried out only once before further differentiation to minimise potential karyotype changes.

Medium	Component	Manufacturer	Cat no.	Final concentration
OXE8	Advanced DMEM/F12	ThermoFisher Scientific	12634010	97.4%
	GlutaMAX (100x)	ThermoFisher Scientific	35050-038	1x
	Heparin solution 0.2%	STEMCELL™	07980	100 ng/mL
	Ascorbic Acid-2-phosphate magnesium salt	Sigma	A8960	0.22 mM
	HEPES 1M pH 7.4	ThermoFisher Scientific	15630080	15mM
	FGF-2 basic 145aa	R&D Systems	4114-TC-01M	100 ng/mL
	TGF-β	Peprotech	AF-100-21C	2 ng/mL
	30% human serum albumin (HAS) in water (buffer for FGF-2)	Sigma	A9080-10ML	0.001%

Table 2.2: OXE8 medium composition

2.1.3 iPSC-derived macrophage differentiation

iPSCs were differentiated into macrophages using our previously developed serum- and feeder-free protocol (Wilgenburg et al., 2013) with minor modifications. Specifically, iPSCs were washed with once with 1 mL of TrypIE™ Express Enzyme (Gibco, 12604013), incubated for 5 minutes at 37°C, 5% CO_2, and lifted into a single-cell suspension with 1x PBS. Cells were then counted, centrifuged at 400g for 5 minutes at RT, and resuspended in EB medium supplemented with 10 μM ROCKi at $4x10^6$ cells per 1 mL. EB medium - OXE8 medium supplemented with 50 ng/mL BMP4 (Peprotech, PHC9534), 50 ng/mL VEGF (Peprotech,

PHC9394), and 20 ng/mL SCF (Miltenyi Biotec, 130- 096-695) - was formulated to promote mesodermal lineage and hemogenic endothelium differentiation.

In parallel, Aggrewell TM 800 plates (STEMCELL Technologies, 34815), which iPSCs were to be transferred to in order to encourage embryoid body (EB) formation, were prepared for plating. First, potential bubbles were removed from the Aggrewell microwells by the addition of 500 µL of Anti-Adherence Rinsing solution (STEMCELL Technologies, 07010), followed by centrifugation at 1,200g for 3 minutes at RT. Aggrewells were then washed once with 1x PBS and filled with 1 mL of EB medium supplemented with 10 µM ROCKi. $4x10^6$ cells of iPSCs were transferred to each Aggrewell and the plates were spun gently at 100g for 3 minutes at 4°C with no braking to ensure even distribution of cells across microwells. EBs formed within 24 hours of plating and were cultured for 7 days at 37ºC, 5% CO_2. EBs were fed daily by 75% EB medium change. This was achieved by two consecutive, gentle removals and additions of 1 mL of medium to avoid disturbing the EBs.

At the end of the 7-day maturation, approximately 300 EBs from each Aggrewell were gently lifted with 5 mL serological pipette, passed through 40 µm strainer to remove dead cells and debris, and distributed evenly into two T175 tissue culture flasks (Corning, 431080) filled with 20 mL of XVIVO or OXM precursor medium (Table 2.3). This step initiated the IL-3 directed myeloid differentiation stage. These long-term, precursor ‘’factory’’ cultures were kept at 37ºC, 5% CO_2 for a total period of 12 weeks. Weekly addition of 10 mL medium was performed until the start of precursor production (typically around week 2 from the factory set-up), then increased to 20 mL addition until week 5.

Precursors were harvested for the final iPSC-macrophage differentiation each week between weeks 5 and 12 of the factory lifetime. Each harvest involved up to 50% medium change, with minimum of equal volume of medium replaced to the amount collected. The collected precursors were counted, centrifuged at 400g for 5 minutes, resuspended in XVIVO or OXM macrophage medium (Table 2.3), plated in appropriately sized tissue culture plates, and

cultured for 7 days at 37ºC, 5% CO_2. 50% medium change was performed on day 4. From day 7, the now-terminally differentiated iPSC-macrophages were used for further experiments.

2.1.4 iPSC-derived microglia differentiation

iPSC-microglia were differentiated according to protocol described by Washer et al., 2022 . The protocol follows steps delineated in section 2.1.3 up to the precursor plating. Precursors harvested for iPSC-microglia differentiation were resuspended in ITMG microglia medium (Table 2.3), containing M-CSF, GM-CSF and IL-34 to aid microglia survival and TGFβ1 to promote microglia identity and maturation. The precursors were plated in tissue culture plates, and cultured for 14 days at 37°C, 5% CO_2. 50% medium change was performed on day 4, 7, and day 11. Day 14 terminally differentiated iPSC-microglia were used for further experiments.

2.1.5 Cell count

19 µL of single cell suspension was stained with 1 µL of Solution 13 AO-DAPI (Chemometec, 910-3013) and transferred to A8-slide (Chemometec, 942-0003). Automated quantification of cell number, size, and viability was performed by the NucleoCounter® NC-3000™ (Chemometec).

2.1.6 Resazurin cell viability assay

Resazurin (Sigma, 199303-5G) was used to establish cytotoxic dose of drug compounds, and recombinant human tau monomer and fibrils used in cell assays. The lyophilised powder was dissolved in 1x PBS to make up 10 mg/mL resazurin stock stored at -20°C. Terminally differentiated iPSC-macrophages or microglia, plated in a clear, 96-well tissue culture plate (Corning, 3596) were washed once with 1x PBS, then incubated for an appropriate amount of time with 100 µL of cell medium alone or with tested compound dissolved in cell medium. At the end of the stimulation, resazurin was added directly to all wells in 1:1,000 final dilution. Minimum of three cell-free wells were also filled with 100 µL of 1:1,000 resazurin in cell medium in order to subtract background fluorescence from the final reading. The plate was incubated for 2 hours at 37°C, 5% CO_2, during which viable cells with intact mitochondrial respiratory chain

would reduce the internalised, non-fluorescent blue resazurin to a red fluorescent resorufin (excitation wavelength 530-560 nm, emission wavelength 590 nm). The amount of resorufin produced is proportional to the number of viable cells. Fluorescence was detected on the SpectraMax M5 microplate reader using the SoftMaxPro software v5.

2.1.7 Live cell staining

Cell-permeable fluorescent dyes (Table 2.4) were used to stain cell cytoplasm and organelles for the downstream application of live confocal microscopy. Terminally differentiated iPSC-macrophages or microglia, plated in tissue culture plates, were washed once with 1x PBS and incubated with dyes dissolved to their respective appropriate final concentration in cell medium for 30 minutes at 37^{o}C, 5% CO_2. Uninternalised dye was then removed, and cells were washed with 1x PBS. All downstream assay were carried out with cells protected from direct light.

2.1.8 iPSC-macrophage/microglia treatment

Table 2.5 lists reagents used for iPSC-macrophage/microglia stimulation.

2.1.9 iPSC-macrophage incubation with reporter beads

Reporter bead stock to assay iPSC-macrophage phagolysosomal clearance was prepared as described in section 2.4.1. Prior to incubation with cells, minimum of 50 µL of the stock was washed in 1x PBS (2,000g centrifugation for 2 minutes), then resuspended in cell culture medium and counted with Kova Glasstic 10-chamber slide (Hycor, 87144). The suspension was diluted further in cell culture medium to achieve the desired concentration.

Medium	Component	Manufacturer	Cat no.	Final concentration
XVIVO precursor medium	X-VIVO-15T^{M}	SLS (Lonza)	BE02-060F	97.8%
	GlutaMAX (100x)	ThermoFisher Scientific	35050-038	1x
	2-Mercaptoethanol (1000x)	ThermoFisher Scientific	31350-010	1%
	IL-3	Invitrogen	PHC0033	25 ng/mL
	M-CSF	Invitrogen	PHC9501	50 ng/mL
	Penicillin-Streptomycin (100x)	ThermoFisher Scientific	15140-122	1%
OXM precursor medium	Advanced DMEM/F12	ThermoFisher Scientific	12634010	96.3%
	GlutaMAX (100x)	ThermoFisher Scientific	35050-038	1x
	HEPES 1 M pH 7.4	ThermoFisher Scientific	15630080	15 mM
	Human recombinant Insulin solution	Sigma	19278-5ML	5 µg/mL
	Tropolone	Sigma	T89702-1G	15 µM
	IL-3	Invitrogen	PHC0033	25 ng/mL
	M-CSF	Invitrogen	PHC9501	50 ng/mL
	Penicillin-Streptomycin (100x)	ThermoFisher Scientific	15140-122	1%
XVIVO macrophage medium	X-VIVO-15T^{M}	SLS (Lonza)	BE02-060F	97.9%
	GlutaMAX (100x)	ThermoFisher Scientific	35050-038	1x
	M-CSF	Invitrogen	PHC9501	50 ng/mL
OXM macrophage medium	Advanced DMEM/F12	ThermoFisher Scientific	12634010	96.5%
	GlutaMAX (100x)	ThermoFisher Scientific	35050-038	1x
	Human recombinant Insulin solution	Sigma	19278-5ML	5 µg/mL
	HEPES 1 M pH 7.4	ThermoFisher Scientific	15630080	15 mM
	M-CSF	Invitrogen	PHC9501	50 ng/mL
ITMG microglia medium	Advanced DMEM/F12	ThermoFisher Scientific	12634010	96.2%
	GlutaMAX (100x)	ThermoFisher Scientific	35050-038	1x
	M-CSF	Invitrogen	PHC9501	25 ng/mL
	GM-CSF	Invitrogen	PHC2013	10 ng/mL
	IL-34	Peprotech	200-34	100 ng/mL
	TFGβ1	Peprotech	100-21C	50 ng/mL

Table 2.3: iPSC-macrophage and microglia differentiation media components

Probe	Manufacturer	Cat No.	Exc /Em (nm)	Stains	Final concentration
NucBlue™ Live ReadyProbes™ Reagent	ThermoFisher Scientific	R37605	360/460	DNA	1 drop/3 mL medium
LysoTracker ™ Red DND-99	ThermoFisher Scientific	L7528	577/590	Acidic cellular compartments	50 nM
CellTracker™ Deep Red	ThermoFisher Scientific	C34565	630-650	Protein amine groups	4 µM

Table 2.4: Cell-staining reagents

2.1.10 iPSC-macrophage/microglia incubation with recombinant tau protein

iPSC-macrophages/microglia were incubated with human recombinant 2N4R tau monomer or *in vitro* aggregated synthetic tau fibrils (see section 2.3) to assess their phenotypic and molecular response to tau. Stored aliquots of tau monomer or fibrils were thawed immediately before cell stimulation. Appropriate dilutions were prepared in Protein LoBind® tubes (Eppendorf, 0030108116) and mixed by thorough but gentle pipetting. This was particularly important for tau fibril preparations to ensure even dispersion in the solution. Tau monomer or fibrils were then added as 10x of the required final concentration directly to the cell medium covering adherent cells, in an effort to prevent protein adsorption to the tissue culture plastic. Plates were agitated side-to-side to aid even tau distribution before returning to the incubator for a required amount of time. 2.5% TrypIE™ incubation for 1 minute (Michel et al., 2014) followed by 1x PBS wash was used to remove uninternalised tau at the end of tau incubation, prior to further assays. All labware that came into contact with tau monomer or fibrils was soaked overnight in 1% sodium dodecyl sulfate (SDS) (Sigma, 436143) solution according to the lab COSHH assessment to ensure safe removal and disassembly from the surface (Fenyi et al., 2018).

Reagent	Manufacturer	Cat No.	Mode of action	Incubation length	Final concentration
Cytochalasin D	Cayman Chemical Company	11330	Actin polymerization inhibitor	45 minutes	10 μM
E64d	Abcam	Ab144048-1mg	Cathepsin B/H/L inhibitor	2/24 hours	50 μM
IFNγ	Gibco	#PHC4031	Cytokine	72 hours	100 ng/mL
IL-4	Gibco	#PHC0044	Cytokine	16 hours	50 ng/mL
Leupeptin	Enzo Life Sciences	ALX-260-009-M005	Broad protease inhibitor	2/24 hours	50 μM
LPS	Invivogen	#tlrl-eklps	TLR-4 agonist	16 hours	100 ng/mL
Pepstatin A	Enzo Life Sciences	ALX-260-085-M005	Aspartyl protease inhibitor	2/24 hours	50 μM
MG-132	Sigma	474791	26S proteasome inhibitor	24 hours	25 μM
Mli-2	Tocris Bioscience	5756	LRRK2 kinase inhibitor	2 hours	100 nM
sRAP	Ximbio	153996	LRP1 antagonist	2 hours	5-500 nM

Table 2.5: iPSC-macrophages and microglia treatment list

2.2 Genome engineering

2.2.1 CRISPR/Cas9-edited iPSC line

One CRISPR/Cas9-edited, homozygous LRRK2 KO iPSC line was used in this thesis (table 2.1). The line was previously generated in our lab by Dr Sally Cowley, using a double nickase strategy to target exon 3 with a pair of guide RNAs (Ran et al., 2013). Line expansion, validation and characterisation of genotype following differentiation into iPSC-macrophages/microglia was performed by Dr Heyne Lee (H. Lee et al., 2020).

2.2.2 CRISPR/Cas9-mediated knockdown (KD) in iPSC-macrophages

A lentivirus-mediated CRISPR/Cas9 editing strategy was used to manipulate the levels of LRP1 (Gene ID: 4035) directly in iPSC-macrophages, omitting the need to create an edited iPSC line. The method was optimised by Dr Sam James Washer.

2.2.2.1 Plasmid preparation

Three LRP1 CRISPR/Cas9 lentiviral vectors were prepared to knockdown LRP1. The guide RNAs (gRNA) sequences targeted exon 12, 13, and 38 of LRP1 (Table 2.6, Figure 5.5A). In addition, eight intergenic control (INTG) CRISPR/Cas9 lentivectors, predicted not to affect LRP1 or other protein-coding sequences, were prepared as a negative control of DNA damage response. Golden Gate Assembly (Engler et al., 2008, 2009) via *BsmB*I was used to clone gRNA oligos into pLentiCRISPRv3 backbone, a novel version of pLentiCRISPRv2 (Addgene, #52961) with a modified gRNA scaffold. The backbone details are yet to be published.

The plasmids were transformed into chemically competent Stbl3™ *E. coli* (ThermoFisher Scientific, C737303) for amplification. 100 ng of plasmid DNA was added to 50 µL of cells and incubated on ice for 30 minutes. Cells were then heat-shocked at 42°C for 30 seconds, followed by 5-minute incubation on ice. 450 µL of Invitrogen™ S.O.C. Medium (ThermoFisher Scientific, 15544-034) at RT was added, and the mixture was incubated at 37°C for 30 minutes with orbital shaking at 180rpm. 50 µL of cells was spread on Luria-Bertani (LB) agar plates containing 100 µg/mL ampicillin and incubated overnight at 37°C. Selected clones were further grown

overnight in LB broth supplemented with 100 µg/mL ampicillin (Sigma, A9518-25G) at 37°C with 180rpm shaking, for plasmid isolation using EndoFree® Plasmid Maxi Prep Kits (QIAGEN, 12362). Plasmid sequence was validated through Source BioScience (Sanger Sequencing, Cambridge, UK) and stored at -20°C.

gRNA design, plasmid cloning, and maxi-prep was carried out by Dr Yixi Chen at the Wellcome Sanger Institute, Cambridge, in collaboration with Dr Sam James Washer.

Target	gRNA #	Sequence
LRP1	1	GTCTCGATGCGGTCGTAGA
LRP1	2	TCTGTACTGGACGGACGAT
LRP1	3	GCCGAGACCGCTCAATACG
INTG	1	TTGGGCAGAATGTCTGCCC
INTG	2	AAGCTCCTCACCATGCCCA
INTG	3	CAGTTGCCTAACAGGAGCA
INTG	4	ACCAAGGGTTACCAAGAAG
INTG	5	CACCTCCCAGTGTCTTGAA
INTG	6	CAGAGGTCAACCTTGACCC
INTG	7	CTTATTAGGGATCAAGGGT
INTG	8	CTAGATCTAGGGTGTGTTG

Table 2.6: LRP1- and INTG-gRNA sequences

2.2.2.2 Production of lentivirus

The LRP1 gRNA and INTG gRNA lentiviral production using HEK293T cells was carried out by Amy Napier, a James lab PhD student. 24 hours prior to transfection, two T175 flasks per lentivirus to be made were seeded with $11x10^6$ HEK293T each, in 30 mL HEK293T medium (DMEM/F12 (Gibco, 11320-0330 supplemented with 10% FBS (Sigma, F9665-500ML), and GlutaMAX (Gibco, 35050-061)) to achieve 70-80% confluency on the day of transfection. JetPRIME® Buffer was mixed with 100 µL of JetPRIME® transfection reagent (Polyplus, 101000046), 5.5 µg of psPAX2 lentiviral packaging plasmid DNA, 4.4 µg of pMD2.G lentiviral envelope plasmid DNA, and total of 9 µg of gRNA plasmid DNA (3 µg per each LRP1 gRNA plasmid or 1.1 µg per each INTG gRNA plasmid) to a 2 mL total reaction volume. The transfection mixture was vortexed for 15 seconds and incubated at RT for 15 minutes before

adding 1 mL directly to each flask, mixing gently with the cell medium. Cells were incubated at 37°C, 5% CO_2 for 24 hours before complete medium change. Supernatant containing lentivirus was collected at 48- and 72-hour timepoint, pooled, spun at 2,000g for 5 minutes to remove any floating cells and cell debris, and passed through a 0.45 µm filter (Starlab, E4780-1456). Virus was concentrated by ultracentrifugation (SW-32Ti rotor) in 38.5 mL Open-Top Thinwall Ultra-Clear Tubes (Beckman Coulter, 344058) at 100,000g for 2 hours at 4°C. Pellets were resuspended in ice-cold, sterile-filtered, 1.5% bovine serum albumin (BSA) (Merck, A9418-50G) in 1x PBS, aliquoted, and stored at -80°C.

2.2.2.3 Quantification of viral titer and iPSC-macrophage transduction

The CRISPR/Cas9 lentiviruses were titrated on iPSC-macrophages. $3.3x10^4$ iPSC-macrophage precursors were seeded on 96-well tissue culture plate in iPSC-macrophage differentiation medium supplemented with 4 ug/mL of polybrene (Sigma, TR-1003-G) to increase binding between the cell membrane and lentivirus envelope. Immediately after plating, cells were double-transduced simultaneously with 1:400 dilution of virion-associated protein (Vpx) packaged in Virus-Like-Particles (VLP) and a total of five, 2-fold serial dilutions of LRP1 or INTG gRNA lentivirus. The human immunodeficiency virus type 2 (HIV-2)- and simian immunodeficiency virus (SIV)-encoded accessory protein Vpx was used to counteract the cytoplasmic nucleotide depletion by SAM Domain and HD domain-containing protein 1 (SAMHD1) (Goujon et al., 2006; Hofmann et al., 2012; Lahouassa et al., 2012; Nègre et al., 2000) thus improving lentiviral transduction efficiency in SAMHD1-expressing myeloid cells such as monocytes and macrophages (Bobadilla et al., 2013; Moyes et al., 2017). Vpx VLP was prepared and titrated by Dr Sam Washer from a pSIV3+_Vpx plasmid (Figure 2.1) generously gifted by the Cosset lab at Inserm, France. Each transduction reaction was run in triplicate. Cells were incubated at 37°C, 5% CO_2. Medium was replaced with standard iPSC-macrophage medium 24 hours later. Puromycin was added to the wells at 3 µg/mL 72 hours post transfection. Puromycin selection, indicative of successful lentiviral integration, was assessed by resazurin cell viability assay (described in 2.1.6).

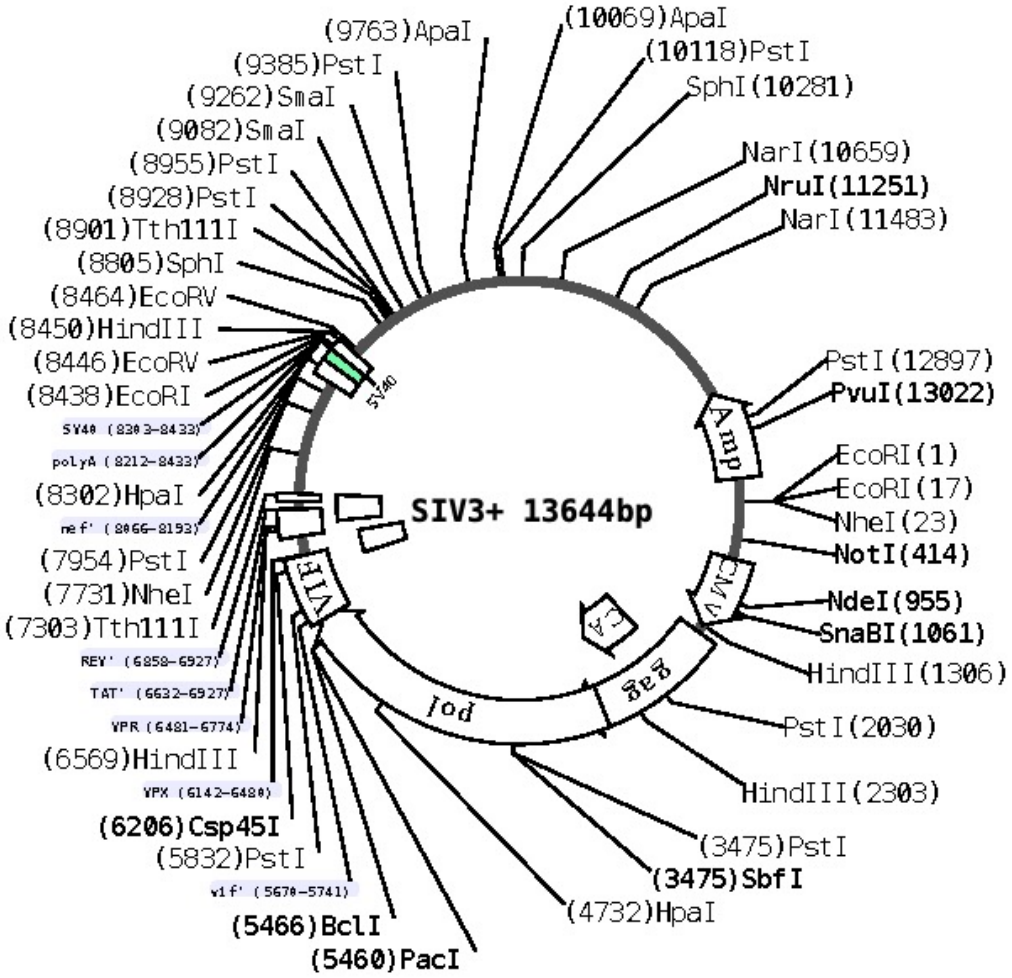

Figure 2.1: SIV3+_Vpx plasmid map including all accessory genes

Map generated with DNADynamo DNA Sequence Analysis Software.

2.3 Human recombinant 2N4R tau protein production

2.3.1 Plasmids and cloning

A glycerol stock of Mach1 $T1^R$ Chemically Competent *E. coli* (ThermoFisher Scientific, C862003) transformed with pNIC28-Bsa4_6xHis-tag_TauWT 2N4R vector (Figure 2.2) was a kind gift from Donatella Di Rienzo at the Oxford Drug Discovery Institute (ODDI). The plasmid had been created by ligation-independent cloning (LIC) of the human 2N4R tau (aa1-441) (Uniprot P10636-8) coding sequence into the BsaI restriction site of the pNIC28-Bsa4 expression backbone (Addgene #26103), downstream of 22-aa N-terminal fusion of poly-histidine (6xHis) tag and Tobacco Etch Virus (TEV) protease-recognition sequence (ENLYFQG). A single colony from the glycerol stock was inoculated into 10 mL of selective LB broth containing 50 µg/mL kanamycin (ThermoFisher Scientific, 11815024) and grown overnight at 37°C with 180rpm orbital shaking for amplification. Plasmid was purified using the QIAprep Spin Miniprep Kit (QIAGEN, 27104), eluted in ddH_2O, and stored at -20°C.

In order to optimise tau purification, tau protein sequence from the pNIC28-Bsa4_6xHis-tag_TauWT 2N4R vector was subcloned into SUMO-GFP_TB004_pETM11SUMO3_sense backbone with Gibson assembly (Gibson et al., 2009). The SUMO-GFP_TB004_pETM11SUMO3_sense plasmid (Figure 2.3) was a generous gift from the Bharat lab at the Sir William Dunn School of Pathology. The plasmid features N-terminal fusion of 6xHis_SUMO3 tag demonstrated to enhance protein expression, solubility, and yield during affinity chromatography purification (Malakhov et al., 2004) (see section 4.2.4). PCR reaction for Phusion® High-Fidelity DNA Polymerase (New England Biolabs, M0530AA) was used to amplify tau sequence and the entire SUMO plasmid sequence except the EGFP region that was to be deleted. Primer design and binding is described in Table 2.7 /Figure 2.4. Template DNA was then digested with 4U DpnI in CutSmart® Buffer (New England Biolabs, R0176S) at 37°C for 30 minutes followed by 15-minute heat deactivation at 65°C. The products were analysed in 1.5% agarose gel, extracted with QIAquick® Gel Extraction Kit (QIAGEN, 28704), and purified with Monarch® PCR & DNA Cleanup Kit (NEB, T1030L). The purified fragments

were assembled in a Gibson Assembly reaction with NEBuilder HiFi DNA Assembly Master Mix (New England Biolabs, E2621L) for 15 minutes at 50°C. The assembled SUMO_TauWT 2N4R_pETM11SUMO3_sense plasmid (Figure 2.5) was transformed into Stbl3™ *E. coli,* then grown on warm LB agar supplemented with 30 µg/mL kanamycin at 37°C overnight. Single colonies were selected and returned to liquid culture overnight for amplification. Plasmids were isolated as described above and sequenced using T7 forward and reverse primers. Plasmids with confirmed correct sequence were further transformed into standard BL21(DE3) *E. coli* for tau protein expression and purification.

DNA concentration was determined by the NanoDrop™ 2000/2000c Spectrophotomer (ThermoFisher Scientific, ND-2000). DNA sequencing was performed externally by Source BioScience (Sanger Sequencing, Cambridge, UK). SnapGene Viewer v6.2.1 and SnapGene v6.2 were used to analyse plasmid sequences and alignments.

Target	Primer	5'(overlap/spacer/ANNEAL)3'	Length (bp)	GC%	Tm (°C)
Tau	F	tccagcaacagaccggtggaATGGCTGAGCCCCGCCA	38	66	76
	R	tggtgctcgagtgcggccgcTCACAAACCCTGCTTGGC	41	66	78
pSUMO backbone	F	GCGGCCGCACTCGAGCAC	18	78	65
	R	TCCACCGGTCTGTTGCTGGAAC	22	59	63

Table 2.7: Tau fragment and SUMO plasmid primer pair for Gibson assembly

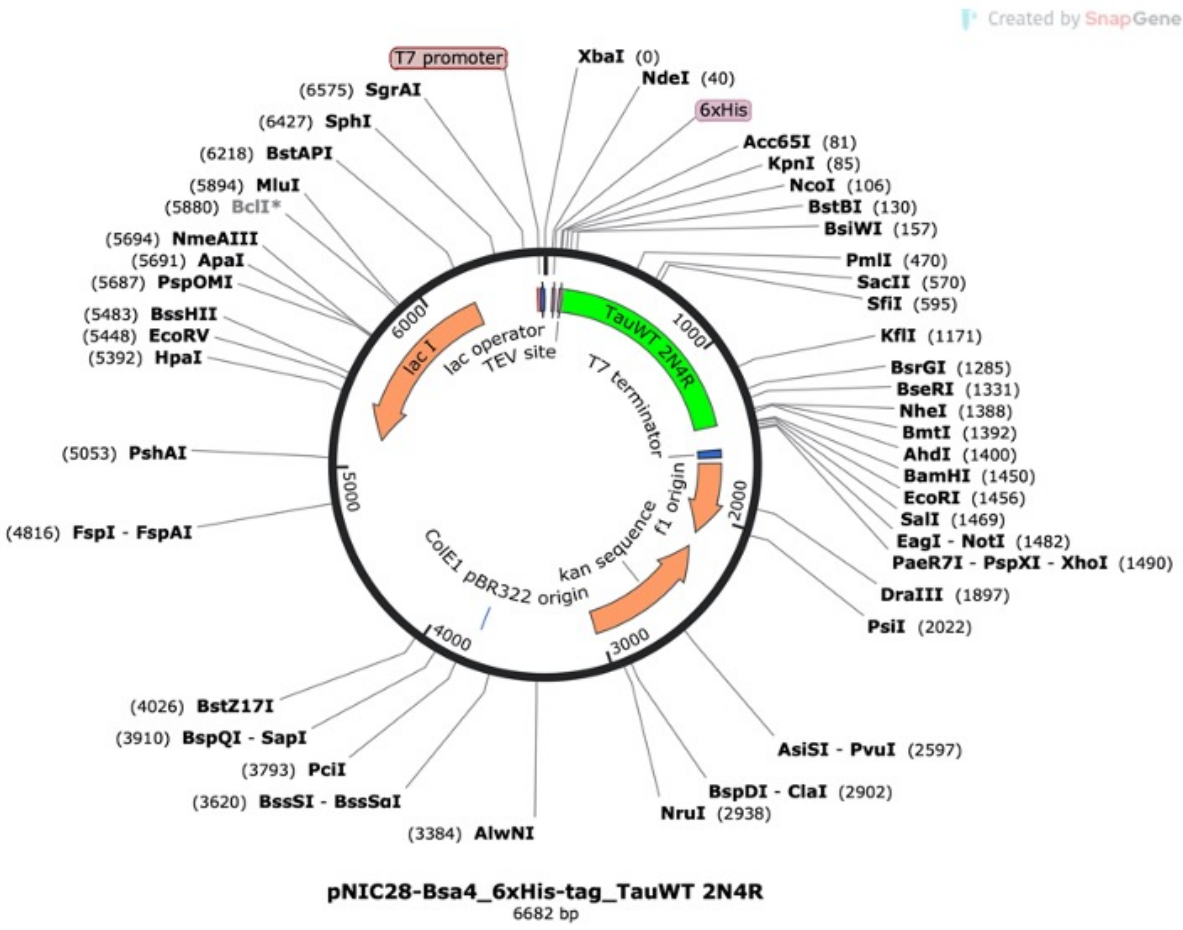

Figure 2.2: pNIC28-Bsa4_6xHis-tag_TauWT 2N4R plasmid map featuring 6xHis tag, donated by Donatella Di Rienzo at the Oxford Drug Discovery Institute

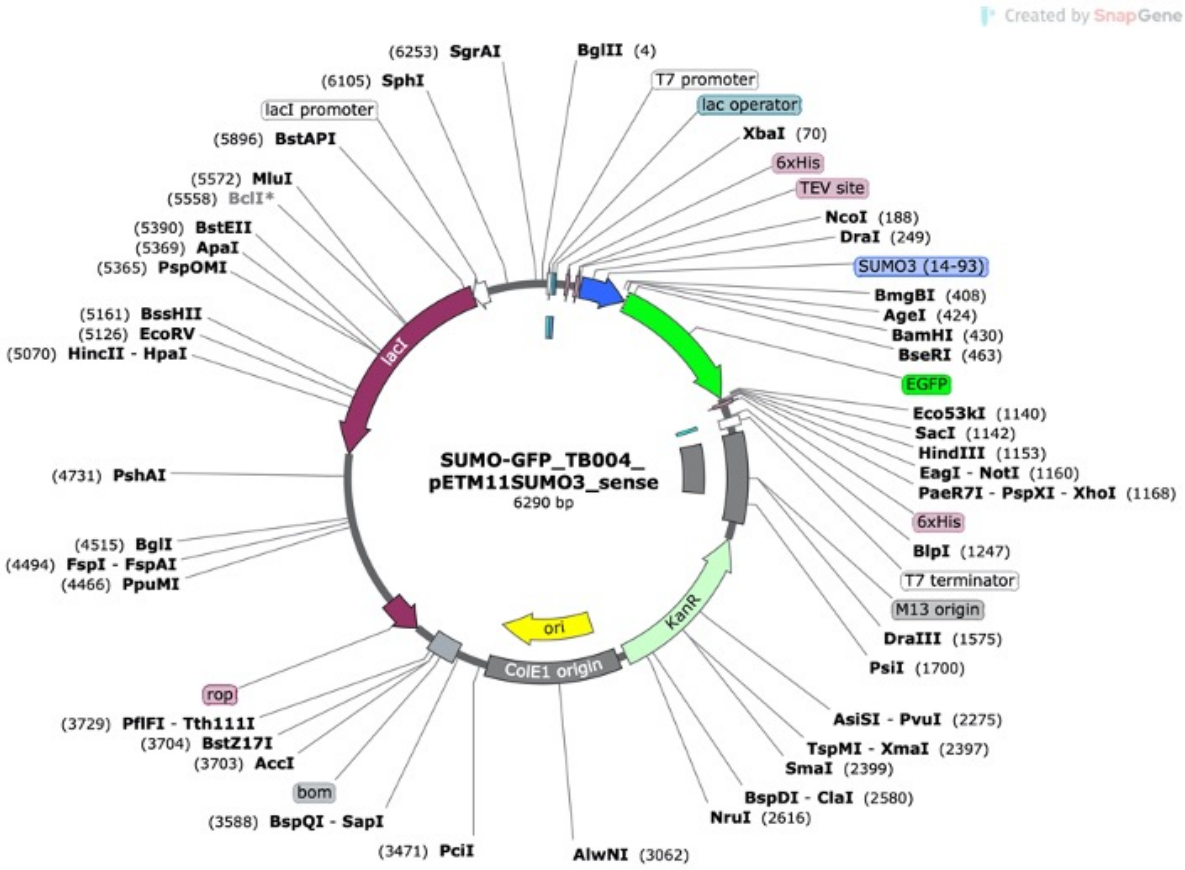

Figure 2.3: SUMO-GFP_TB004_pETM11SUMO3_sense plasmid map featuring 6xHis_SUMO tag, donated by Bharat lab at the University of Oxford

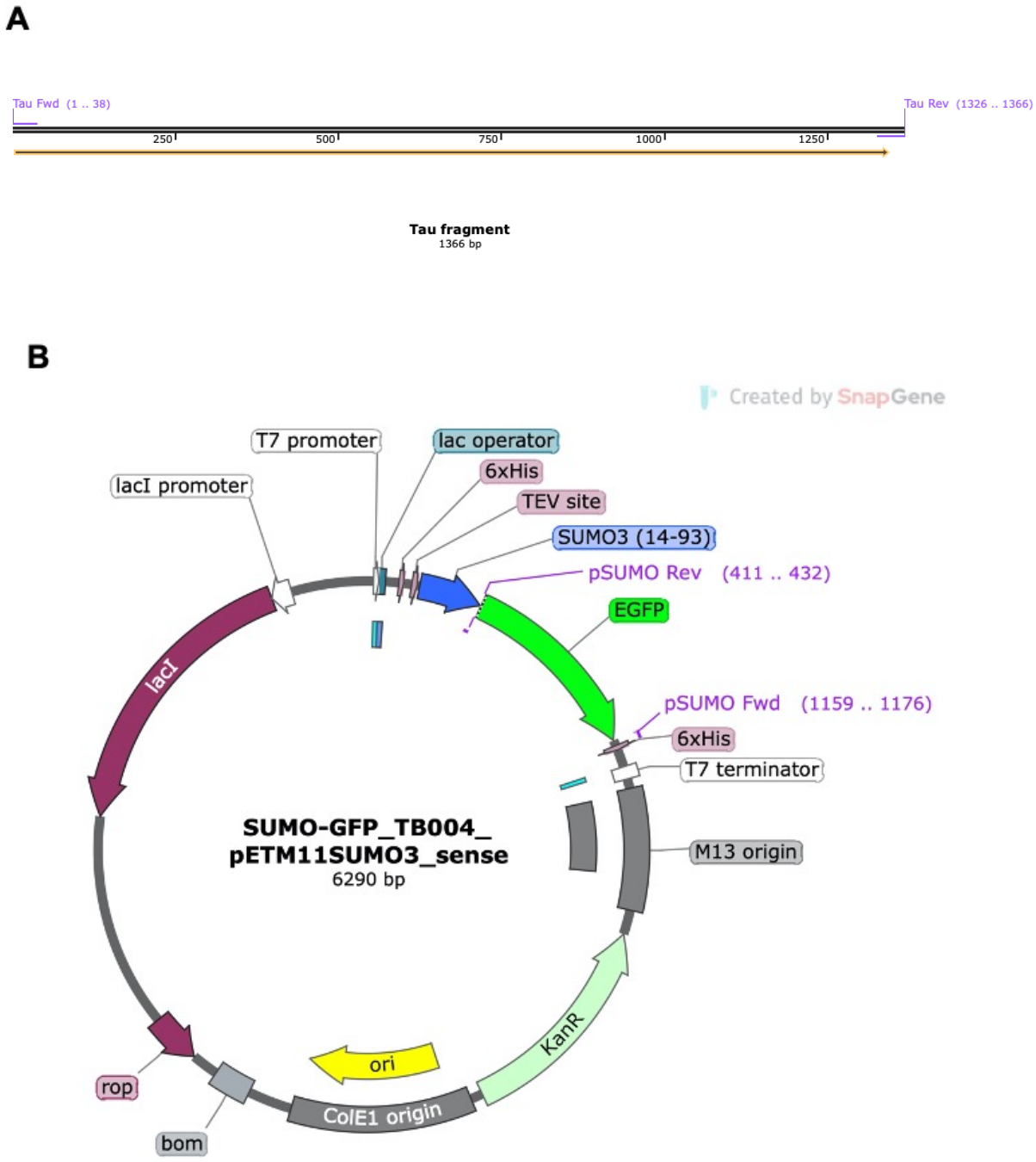

Figure 2.4: Primer binding diagram to (A.) TauWT_2N4R fragment and (B.) SUMO-GFP_TB004_pETM11SUMO3_sense plasmid

.

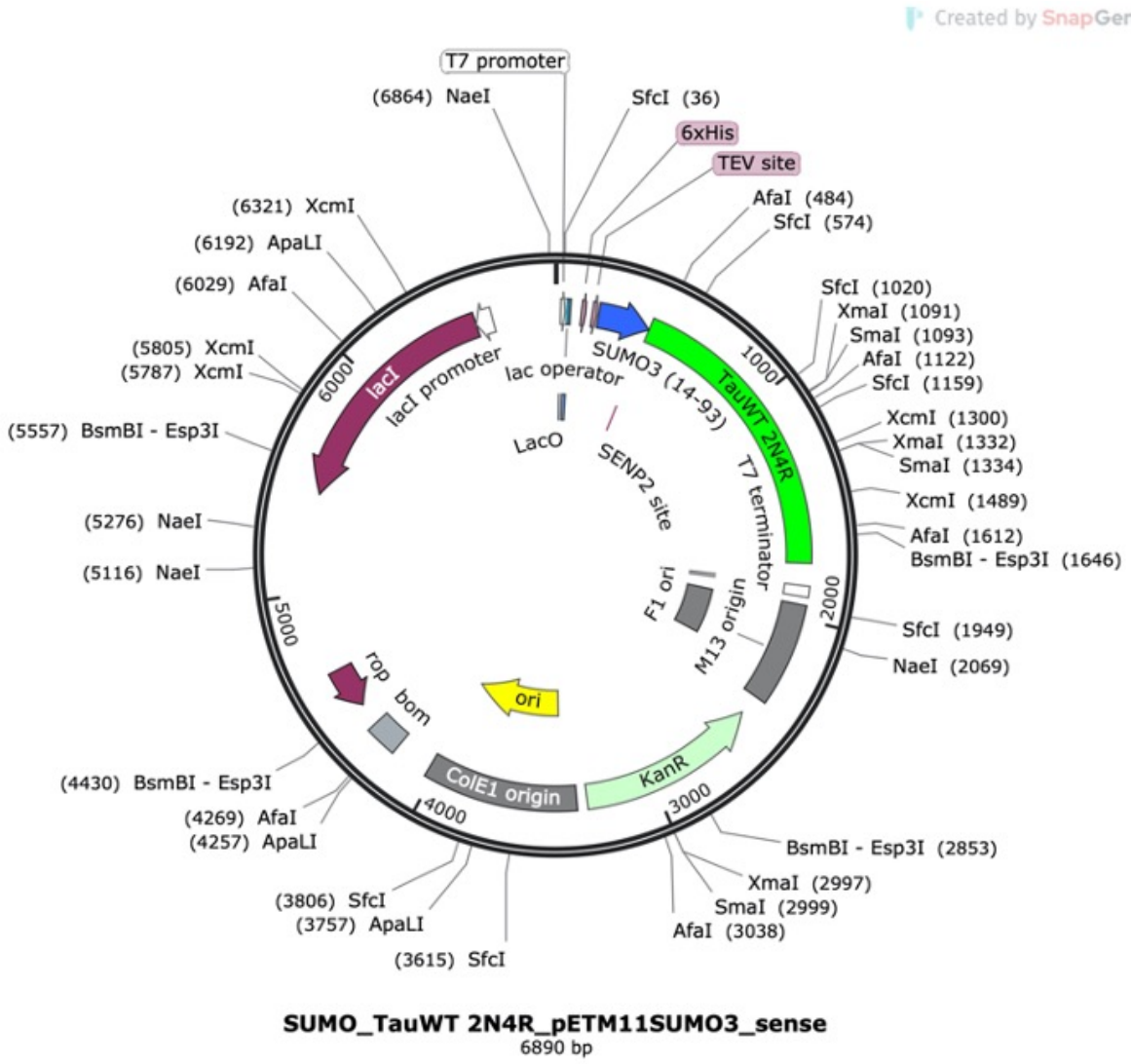

Figure 2.5: SUMO_TauWT 2N4R_pETM11SUMO3_sense plasmid created by subcloning TauWT_2N4R fragment into SUMO-GFP_TB004_pETM11SUMO3_sense backbone using Gibson assembly

2.3.2 Bacterial transformation

Transformation of the chemically competent Stbl3™ *E. coli* or BL21(DE3) *E. coli* (a gift from the Bharat lab) was carried out as per protocol described in section 2.2.2.1. 50 µL of the heat-shock transformed cells was plated on pre-warmed LB agar plates supplemented with 30 µg/mL kanamycin and incubated overnight at 37°C. Single colonies formed overnight were then used to inoculate 10 mL LB broth supplemented with 50 µg/mL kanamycin and grown overnight at 37°C with 180rpm agitation. 800 µL of the overnight culture was mixed with 200 µL of 80% glycerol (Sigma, G5516-1L) to prepare glycerol stocks of the transformed cells to be stored at -80°C.

The electrocompetent ClearColi™ BL21(DE3) cells (Lucigen, 60810-1) were transformed by electroporation. Protocol was based on the manufacturer's recommendations with modifications. 25 µL of cells, thawed on ice, was mixed with 50 ng of plasmid DNA and 25 µL glycerol, and transferred to a pre-chilled electroporation cuvette (VWR, 732-2268, 2mm gap), taking care not to introduce bubbles to prevent arcing. Cells were electroporated using Gene Pulser II electroporator (BioRad) set to 2.4 kV, 25 µF, 750 Ω. 975 µL Expression Recovery Medium (provided with the cells) was added to the cells and the mixture was incubated at 37°C for 1 hour with 250rpm orbital shaking. 50 µL of the cells was then spread onto pre-warmed LB Miller agar plate containing 50 µg/mL kanamycin and grown for 36 hours at 37°C with 350rpm agitation. Glycerol stock of transformed cells was prepared from single colonies as described above.

2.3.3 Tau protein expression and purification

Starter cultures were prepared by inoculating 40 mL of standard LB broth with 50 µg/mL kanamycin or LB Miller broth with 50 µg/mL kanamycin and 0.2 g glucose (Sigma, G8270), with a single colony from glycerol stocks of transformed BL21(DE3) or ClearColi cells, respectively. Cultures were grown overnight at 37°C with 180rpm agitation for BL21(DE3) or 250rpm for ClearColi. Each overnight culture was further inoculated to 1 L of Terrific Broth (TB) broth supplemented with 50 µg/mL kanamycin and 1x TB salts and returned to the shaking incubator

at 37 °C with 200rpm agitation. At OD_{600} = 0.5-0.7, the cells were induced with 0.5 mM isopropyl β-D-1-thiogalactopyranoside (IPTG) (Sigma, 15502-5G) and left to grow overnight at 25°C with 200rpm agitation, unless stated otherwise. Cell pellets were harvest the next morning by centrifugation at 5,000g for 30 minutes at 4°C using the Beckman Coulter Avanti JXN-26 centrifuge with a JLA-8.1000 rotor. Pellets were resuspended in 25 mL ice-cold lysis buffer per 1 L of pelleted culture and stored at -80°C until required.

ÄKTA Pure 25M was used for all purification described in this thesis. The buffer composition is described in Table 2.8. As all purification steps were carried out at 4°C, buffer pH was adjusted at 4°C, and buffers were kept at 4°C following sterile-filtering and thorough degassing. If columns were re-used multiple times, a column cleaning procedure (1-hour soak with 1 M NaOH followed by 10 column volumes (CV) ddH_2O and 10 CV buffer A1 or buffer C washes) would precede sample application. Eluted protein fractions were analysed with SDS-PAGE gel electrophoresis. 25 µL samples composed of 5-15 µL eluate mixed with NuPAGE™ 4x LDS sample buffer (Invitrogen, NP0007) and ddH_2O were boiled at 70°C for 10 minutes. Samples were loaded on Novex™ WedgeWell™ 8-16%, Tris-Glycine pre-cast mini gels (Invitrogen, XP08165BOX), along with 5 µL of Precision Plus Protein Dual Colo Standards (Bio-Rad, 1610374), and ran in Novex™ Tris-Glycine SDS Running Buffer (Invitrogen, LC2675) at 200 V for 45 minutes. 1-hour RT gel incubation with SimplyBlue™ Safe Stain (ThermoFisher Scientific, LC6060) was used to detect protein.

On the day of the purification, bacteria cells were thawed, lysed using EmulsiFlex-C5 French Press homogeniser (Avestin) operating at 15 kpsi, and centrifuged at 4,500g for 1 hour. An additional step of 10-minute direct heating in 70°C water bath, followed by 4,500g centrifugation for 1 hour, was used for the large-scale purification of SUMO-tagged tau. Pellets were discarded and supernatant passed through a 0.45 µm cut-off filter. All centrifugation was carried out at 4°C and samples were kept on ice throughout the entire purification procedure except during the cell heating step.

The crude extract was applied to HisTrap column (Cytiva Life Sciences, 17-5248-02) pre-equilibrated with 5 column volumes (CV) of buffer A1. The column was washed with 20 CV buffer A1 for purification from ClearColi or with 50 CV buffer A2 followed by 20 CV buffer A1 for purification from BL21(DE3). Protein was eluted with linear gradient of buffer B. Overnight dialysis at 4°C in SnakeSkin^{M} Dialysis Tubing (ThermoFisher Scientific, 3.5K MWCO, 60835) in the presence of TEV or Sentrin-specific protease 2 (SENP2) proteases (1:100 protease:protein ratio), against 4 L of dialysis buffer was used to remove imidazole and cleave the 6xHis-TEV or 6xHis-SUMO tags. TEV and SENP2 proteases, purified in-house from *E. coli,* were generous gifts from the Fodor and the Bharat lab, respectively. The dialysed, cleaved product was re-applied to the HisTrap column, endotoxin-decontaminated with 1 M NaOH (1 hour contact time) and equilibrated as described above, to isolate the tag-less tau. Selected fractions were pooled and purified further using the CaptoS column (Cytiva Life Sciences, 17-5441-23), pre- equilibrated with 5 column volumes (CV) of buffer C. The column was washed with 6 CV of buffer C and eluted with linear gradient of buffer D. Purest tau-containing fractions were concentrated to 2 mL using 10K MWCO Pierce Protein concentrator (ThermoFisher Scientific, 88528) and filtered through a 0.22 µm cut-off filter (Starlab, E4780-1226). Residual endotoxin was removed from the final product using PierceT^{M} High-Capacity Endotoxin Removal Spin Column (ThermoFisher Scientific, 88275), as per manufacturer's instructions. Endotoxin levels in preparations were quantified with Pierce^{TM} Limulus Amebocyte Lysate (LAL) Chromogenic Endotoxin Quantitation Kit (ThermoFisher Scientific, A39553) based on the agglutination of the haemolymph of a horseshoe crab (Limulus polyphemus) in the presence of endotoxins (L. Chen & Mozier, 2013).

Buffer	Component	Manufacturer	Cat no.	Final concentration
Lysis (pH 7.6)	HEPES	Sigma	H33575	25 mM
	NaCl	Sigma	S9888	150 mM
	Imidazole	Sigma	I2399	10 mM
	Bond Breaker ™ TCEP	Invitrogen	77720	1 mM
	DNase I	Invitrogen	18047-019	1.68 U/mL
	Halt Protease and Phosphatase Inhibitor Cocktail, EDTA-free (100x)	ThermoFisher Scientific	78441	1x
HisTrap A1 (pH 7.6)	HEPES	Sigma	H33575	25 mM
	NaCl	Sigma	S9888	150 mM
	Imidazole	Sigma	I2399	10 mM
	Bond Breaker ™ TCEP	Invitrogen	77720	1 mM
	Pierce™ Protease Inhibitor XL Capsules, EDTA-free	ThermoFisher Scientific	A37989	1:500
HisTrap A2 (pH 7.6)	HEPES	Sigma	H33575	25 mM
	NaCl	Sigma	S9888	150 mM
	Imidazole	Sigma	I2399	10 mM
	Bond Breaker ™ TCEP	Invitrogen	77720	1 mM
	Triton™X-114	Sigma	648468	0.1%
HisTrap B (pH 7.6)	HEPES	Sigma	H33575	25 mM
	NaCl	Sigma	S9888	150 mM
	Imidazole	Sigma	I2399	500 mM
	Bond Breaker ™ TCEP	Invitrogen	77720	1 mM
	Pierce™ Protease Inhibitor XL Capsules, EDTA-free	ThermoFisher Scientific	A37989	1:500
Dialysis (pH 7.6)	HEPES	Sigma	H33575	25 mM
	NaCl	Sigma	S9888	100 mM
	BME	Sigma	97622	5 mM
HisTrap Rebind A (pH 7.1)	HEPES	Sigma	H33575	25 mM
	NaCl	Sigma	S9888	100 mM
	Imidazole	Sigma	I2399	10 mM
	BME	Sigma	97622	5 mM
HisTrap Rebind B (pH 7.1)	HEPES	Sigma	H33575	25 mM
	NaCl	Sigma	S9888	100 mM
	Imidazole	Sigma	I2399	500 mM
	BME	Sigma	97622	5 mM
CIEX C (pH 7.1)	HEPES	Sigma	H33575	25 mM
	NaCl	Sigma	S9888	100 mM
	BME	Sigma	97622	5 mM
CIEX D (pH 7.1)	HEPES	Sigma	H33575	25 mM
	NaCl	Sigma	S9888	1 M
	BME	Sigma	97622	5 mM

Table 2.8: Buffer composition used for the purification of 2N4R recombinant tau

Protein concentration was estimated using Pierce™ BCA Protein Assay Kit (ThermoFisher Scientific, 23225). Protein purity was determined by liquid chromatography with tandem mass spectrometry (LC-MS/MS) for trypsin-digested in-gel protein as well as LC/MS for intact protein characterisation, carried out externally by the Centre for Medicines Discovery at the University of Oxford. Following the mass spectrometry verification, purified tau was aliquoted, flash-frozen in LN, and stored at -80°C until required.

2.3.4 *In vitro* synthetic tau fibril assembly

Aggregation of unlabelled, purified recombinant tau monomer was induced by heparin at 4:1 tau:heparin molar ratio as previously described (Fichou, Oberholtzer, et al., 2019; Goedert et al., 1996b; von Bergen et al., 2005). 500 µL aliquot of 28 µM tau in Protein LoBind® tube was thawed and incubated with sterile filtered, 7 µM heparin (Sigma Aldrich, H3393, average molecular weight of 18kDa) and 2 mM DTT (Sigma Aldrich, 43816) for 11 days at 37°C with orbital shaking at 250rpm. The formation of fibrils was assessed by negative stain electron microscopy (section 2.4.5) and Thioflavin T assay (section 2.3.5). Protein concentration was determined by Pierce™ BCA Protein Assay Kit. Fibrils were aliquoted to Protein LoBind® tubes and stored at -80°C.

2.3.5 Thioflavin T (ThT) assay

ThT assay was used to verify the presence of β-sheets in tau fibril preparation (Biancalana & Koide, 2010; Krebs et al., 2005).100 uL reactions were prepared in black, clear-bottom 96-well PhenoPlate™ (PerkinElmer, 6055300) by mixing 28 µM tau monomer, 7 µM heparin, and 25 µM ThT (Sigma, T3516-5G) in 1x PBS, pH 7.2. The sealed plate was incubated at 37°C with 250rpm agitation for 11 days. ThT fluorescence readings (excitation wavelength 440 nm/emission wavelength 510 nm) were taken at regular intervals using SpectraMax M5 microplate reader. Background fluorescence of 1x PBS buffer only was subtracted from all values at corresponding timepoints.

2.3.6 Labelling of purified recombinant tau

Monomeric and aggregated tau were labelled with DyLight 488 NHS Ester (ThermoFisher Scientific, 53024, Excitation wavelength 493nm, Emission wavelength 518nm) according to the manufacturer's protocol with minor modifications. Thawed, 500 µL aliquots of tau monomer (1.3 mg/mL) and tau fibrils (1 mg/mL) were mixed with 50 µg of DyLight 488 desiccated dye in Protein LoBind® tubes and left incubating in the dark with end-to-end mixing, either overnight at 4°C for the monomer or for 2 hours at RT for the fibrils. Non-incorporated dye was removed from the monomer preparation using the spin columns provided in the kit. Overnight dialysis in D-Tube™ Dialyzer Midi (Sigma, 71507-3, MWCO 6-8kDa) against 4 L of 25 mM HEPES (Sigma, H3375-500G), pH 7.1 at 4°C was used to remove non-reacted dye from the fibril preparation. Protein concentration was determined by Pierce™ BCA Protein Assay Kit. Samples were aliquoted to Protein LoBind® tubes and stored at -80°C.

2.4 General methods

2.4.1 Generation of double-labelled reporter beads

DQ Red BSA and Alexa Fluor 488 double-labelled reporter beads were used to assess phagolysosomal clearance by iPSC-macrophages (see section 2.1.9). To prepare the beads, 50 µg/mL of 3 µm, carboxy-modified silica beads (Kisker Biotech, PSI-3.0COOH) were transferred to 1.5 mL Protein LoBind Eppendorf to minimize bead loss between washes, spun to remove the storage solution, and washed twice with 1 mL of 1x PBS, using benchtop centrifuge at 2,000g for 2 minutes. The beads were next treated with 25 mg/mL of heterobifunctional crosslinker cyanamide (Sigma, 187364-5G), freshly dissolved in 1x PBS, for 30 minutes at RT with end-to-end mixing. Excess cyanamide was removed by washing the beads twice with coupling buffer (0.1 M sodium tetraborate (Sigma, 221732-100g) in ddH_2O, pH 8.0). Bead-conjugated cyanamide served as a substrate for subsequent covalent attachment of 1 mg DQ Red BSA (ThermoFisher Scientific, D12051) resuspended in 500 µL coupling buffer. The DQ Red BSA bead solution was left to react overnight at 4°C with constant, gentle end-to-end mixing. The next day, the beads were washed twice with 250 mM glycine

quenching buffer (250 mM glycine (Sigma, 50046) in 1x PBS, pH 7.2) to remove excess DQ Red BSA and to quench unreacted cyanamide, and two more times with coupling buffer, prior to incubation with 50 µg/mL of Alexa Fluor 488 NHS Ester (AF-488) (ThermoFisher Scientific, A20000) in coupling buffer for 60 minutes at RT with agitation. This step ensured sufficient labelling of the amine-reactive green-fluorescent dye to the bead-cyanamide-DQ Red BSA complex. Finally, the beads were washed three more times with quenching buffer to remove excess fluor and quench any unreacted BSA, and resuspended in 1 mL 1x PBS with 0.02% sodium azide (Sigma, 71289) to inhibit microbial growth during long-term storage at 4°C.

All buffers and reagents were sterile-filtered and the protocol was carried out in laminar flow cabinet to prevent contamination. LAL assay was used prior to bead incubation with cells to determine potential microbial contamination.

2.4.2 Flow cytometry

Cells differentiated on 24-well tissue culture plate (Corning, 3524) and treated according to experimental design were lifted by 10-minute incubation with StemPro™ Accutase™ (Gibco, A1110501) at 37ºC, 5% CO_2. Lifted cells in suspension were transferred to a 96-well V-bottom plate (ThermoFisher Scientific, 611V96 and 642000) and kept at 4°C or on ice throughout all steps, unless stated otherwise. All centrifugation was carried out at 400g for 5 minutes.

For live-cell flow cytometry analyses of phagolysosomal proteolysis (Figures 3.3, 3.4, 3.5 F, 3.6) and tau internalisation (Figures 5.3, 5.4, 5.6), cells were spun, washed with 1x PBS, spun again, and resuspended in 40 µL/well of ice-cold Invitrogen™ Live Cell Imaging Solution (LCIS) (ThermoFisher Scientific, A14291DJ) in preparation for acquisition.

For cell surface marker staining, cells were lifted into ice-cold 1x PBS, counted, spun, and resuspended in ice-cold FACS buffer (1x PBS supplemented with 1% FBS, 10 µg/mL human-IgG (Sigma, I8640-100MG), and 0.01% sodium azide) before being transferred into a 96-well V-bottom plate at 100,000 cells/well. Non-specific Fc-receptor interactions were blocked by 30-

minute incubation in FACS buffer. Cells were then spun again and stained with primary antibodies diluted in FACS buffer (Table 2.9) directly without fixation for 1 hour in the dark. If using fluorescent primary antibodies, isotype controls conjugated to the same fluorophore, obtained from the same company, were used at the same dilution. If using non-fluorescent primary antibodies, isotype control was achieved by staining with secondary antibody only. Whenever secondary antibody incubation was necessary, cells were washed once with 1x FACS buffer following primary antibody incubation, then stained with secondary antibodies diluted in FACS buffer (Table 2.10) for 30 minutes in the dark. After staining, cells were washed once with FACS buffer and fixed by resuspension in 2% PFA (ThermoFisher Scientific, J61899.AP) in FACS buffer.

The protocol steps for total marker staining were identical to those used for surface marker staining, with the following exception. Cell fixation was carried out with 2% PFA in FACS buffer for 10 minutes at RT immediately after transfer to a 96-well V-bottom plate. Cells were then washed once with FACS buffer, and permeabilised with 0.1% Triton-X100 (Sigma, T8787) in 1x PBS for 10 minutes at RT, before blocking and staining.

Forward scatter (FSC-H), side-scatter (SSC-A), and fluorescence measurements were obtained by passing single-cell suspension through Cytoflex LX (Beckman Coulter) flow cytometer. Minimum of 20,000 events was recorded per condition. Laser settings and gating strategy are described in detail in individual results chapters. Acquired data was analysed using the FlowJo™ v10 software.

Target	Clone	Species	Isotype	Fluorochrome	Manufacturer	Cat no	FACS	ICC	WB
CD14	MEM-18	Mouse	IgG1	FITC	Immunotools	21270143	1:50		
CD45	MEM-28	Mouse	IgG1	FITC	Immunotools	21270453X2	1:50		
CD16	LNK16	Mouse	IgG1	PE	Immunotools	21279164	1:50		
CD86	IT2.2	Mouse	IgG2bk	PE	Bio-legend	305405	1:50		
CD11b	ICRF44	Mouse	IgG1k	APC	Bio-legend	301310	1:50		
IgG1	PPV06	Mouse	-	FITC	Immunotools	21335013	1;25		
IgG1	11711	Mouse	-	PE	R&D	IC002P	1:50		
IgG2bk	MPC-11	Mouse	-	PE	Bio-legend	400311	1:50		
IgG1k	MOPC-21	Mouse	-	APC	Bio-legend	400120	1:50		
LAMP-1	D2D11	Rabbit	IgG	-	Cell Signaling	9091		1:200	
LRP1	EPR3724	Rabbit	IgG	-	Abcam	ab92544	1:100	1:200	
LRP1	5A6	Mouse	IgG2b	-	Calbiochem	438192		1:200	
LRP1		Rabbit	IgG	-	Cell Signaling	64099			1:500
LRRK2	N241A/34	Mouse	IgG2b	-	NeuroMab	75-253		1:1,000	
Rab8a (pT72)	MJF-R20	Rabbit	IgG	-	Abcam	ab230260		1:250	
Rab10 (pT73)	MJF-R21-22-5	Rabbit	IgG	-	Abcam	ab241060		1:250	
Tau	Tau-12	Mouse	IgG1k	-	Sigma	MAB2241		1:200	1:250
Vinculin	V284	Mouse	IgG1	-	Bio-Rad	MCA465GA			1:2,000
ITGαV		Rabbit	IgG	-	Proteintech	27096-1-AB			1:250

Table 2.9: List of primary antibodies

Target	Species	Fluorochrome	Manufacturer	Cat no	FACS	ICC	WB
Rabbit IgG	goat	IRDye® 800	Licor	926-3221			1:2,000
Mouse IgG	donkey	IRDye® 680	Licor	926-68072			1:2,000
Rabbit IgG (H+L)	donkey	Alexa Fluor 488	Invitrogen	A21206	1:500	1:500	
Rabbit IgG (H+L)	donkey	Alexa Fluor 568	Invitrogen	A10042	1:500	1:500	
Rabbit IgG (H+L)	donkey	Alexa Fluor 647	Invitrogen	A31573	1:500	1:500	
Mouse IgG (H+L)	donkey	Alexa Fluor 647	Invitrogen	A31571	1:500	1:500	

Table 2.10: List of secondary antibodies

2.4.3 Immunocytochemistry

Cells were fixed with 2% PFA in 1x PBS for 10 minutes at RT. Cells were then washed once with 1x PBS, permeabilized with 0.1% Triton-X100 for 10 minutes at RT, washed again with 1x PBS, and blocked with 10% donkey serum (Bio-Rad, C06SB) in blocking buffer (PBS supplemented with 5% BSA (Sigma, A7906-100G) and 0.01% sodium azide) for 1 hour at RT. Blocking buffer was replaced with primary antibodies against targeted antigens (Table 2.9), diluted in blocking buffer for an overnight incubation at 4°C with shaking. After two, 10-minute 1x PBS washes to remove unbound antibodies, cells were incubated in the dark with secondary antibodies (Table 2.10) diluted in blocking buffer for 1 hour at RT with shaking. Secondary antibodies were replaced with 1:2,000 4′,6-diamidino-2-phenylindole (DAPI) stain (Abcam, ab228954) in 1x PBS for 10 minutes at RT. Finally, cells were washed twice with 1x PBS, 15 minutes each, then stored at 4°C in 1x PBS, parafilmed and protected from light.

2.4.4 Light and fluorescence microscopy

Cells were differentiated in black, 96-well ibiTreat µ-plates (ibidi, IB-89626) for all fluorescence microscopy readouts.

20x, 2D images of live or fixed iPSC-macrophages/microglia were captured with EVOS FL Auto fluorescent microscope (ThermoFisher Scientific) and analysed with ImageJ v1.53 freeware.

Minimum of 3 random fields per well were used for analysis. Mean fluorescence intensity was defined as integrated density normalised to the cell number per each thresholded image.

63x, Z-stack (0.5 – 8 µm, 0.5 µm apart) images were acquired with the automated spinning disk confocal Opera Phenix High Content Screening System (Perkin Elmer, 63x objective, water lens). Subsequent image analysis was performed with Columbus Image Data Storage and Analysis System (CambridgeSoft). Minimum of 15 randomised fields per well were captured and used for analysis.

2.4.5 Transmission electron microscopy (TEM)

The formation of *in vitro* aggregated recombinant tau fibrils was assessed by negative stain TEM (see section 2.3.4). Tau monomer and fibril preparation were diluted 1:20 in 25 mM HEPES, pH 7.1. 10 µL of each sample was applied to freshly glow-discharged (Pelco EasiGlow) 300-mesh carbon-coated copper grids (TAAB Laboratories, C267) for 2 minutes. After removing excess sample with filter paper, grids were washed once with ddH_2O, negative-stained with 2% uranyl acetate (Agar Scientific, R1260A) for 20 seconds, and air-dried.

TEM was also used to analyse the uptake of tau fibrils by iPSC-macrophages. Cells were differentiated on a glass coverslip inserted into 24-well tissue culture plate. Following an overnight incubation with vehicle or 2.5 µg/mL of tau fibrils, cells were prepared for image capture by Dr Errin Johnson at the Dunn School EM Facility. Briefly, cells were fixed with pre-warmed 2.5% glutaraldehyde (Agar Scientific, R1020) and 2% PFA in 0.1 M PIPES buffer (Sigma, P6757) pH 7.2, for 1 hour at RT. After five washes with 0.1 M PIPES buffer, cells were incubated with 50 mM glycine (Sigma, G7126) in 0.1 M PIPES for 15 minutes at RT, then washed once with 0.1 M PIPES again. Secondary fixation was carried out with 1% osmium tetroxide (TAAB Laboratories, O001/1) + 1.5% potassium ferrocyanide (Acros Organics, 223111000) in 0.1 M PIPES at 4°C for 1 hour. Samples were washed 5 times with ddH_2O, stained with 0.5% uranyl acetate overnight at 4°C in the dark, then washed again with ddH_2O, 10 minutes each, protected from light. Consecutive, 10-minute long, ice cold ethanol

incubations (30%, 50%, 70%, 80%, 90% and 95%) on ice were used to dehydrate the samples. Final 20-minute incubation in 100% dry ethanol was repeated twice. After epoxy resin infiltration (Agar Scientific, Agar 100-Hard epoxy resin, AGR1140), coverslips were removed from the wells, inverted onto Beem capsules (Agar Scientific, Type 00, AGG360-1) filled with fresh 100% resin and blocks were polymerised for 24 hours at 60°C. Ultrathin (90 nm) sections of the resin-embedded cells were obtained with a Diatome diamond knife on a Leica UC7 ultramicrotome. Individual sections were mounted onto 200-mesh carbon-coated copper grids, stained with Reynold's lead citrate (Reynolds, 1963) for 5 minutes at RT, washed with five droplets of degassed ddH_2O, and air-dried.

All images were acquired using a Gatan OneView camera on a FEI Tecnai T12 transmission electron microscope operated at 120 kV.

2.4.6 Scanning electron microscopy (SEM)

SEM was used to visualise the surface of iPSC-macrophages following tau fibril incubation. Similar to the TEM protocol, iPSC-macrophages were differentiated on coverslips inserted to 24-well tissue culture plates, then incubated overnight with vehicle or 2.5 µg/mL of tau fibrils. Primary fixative of 2.5% glutaraldehyde in 0.1 M PIPES, pH 7.2 was added for 1 hour at RT for crosslinking. Cells were rinsed three times with 0.1 M PIPES, then fixed with 1% osmium tetroxide in 0.1 M PIPES for 1 hour at 4°C. After three washes with ddH_2O, samples were dehydrated in an increasingly more concentrated ethanol (50% - 70% - 90% - 95%) for 5 minutes each, then three times in 100 % ethanol for 10 minutes each. Cells were then chemically dried using Hexamethyldisilazane (HMDS, 440191 Sigma) as follows: 1:1 100% ethanol:HMDS for 3 mins, followed by two consecutive 2-minute incubations with pure HMDS, after which the HMDS was removed, and the samples were left to dry overnight. Samples were sputter coated with ~15 nm of gold using a Quorum Technologies Q150R ES coating unit. Images were captured with Zeiss Sigma 300 Field Emission Gun Scanning Electron Microscope (FEG-SEM).

2.4.7 Western blot (WB)

Levels of total and cell-surface proteins of interest in cell lysates were analysed with WB. iPSC-macrophages were differentiated in 6-well tissue culture plates at $1.5x10^6$ cells/well density.

For total protein extraction, cells were washed once with ice-cold 1x PBS, then lysed directly with 100 µL/well of ice-cold Radioimmunoprecipitation (RIPA) buffer (Cell Signalling, (ThermoFisher Scientific, 89901) supplemented with cOmplete™ ULTRA Tablets, Mini, EDTA-free, EASYpack Protease Inhibitor Cocktail (Roche, 5892791001) and Pierce™ Phosphatase Inhibitor Mini Tablets (ThermoFisher Scientific, A32957). Cell lysates were scraped into tubes (NovasBio, MCT-175-C) and centrifuged at 21,000g for 30 minutes at 4°C. Cleared lysates were snap-frozen in LN and stored at -80°C for further use.

Cell surface proteins were extracted using Pierce™ Cell Surface Biotinylation and Isolation Kit (ThermoFisher Scientific, A44390). The manufacturer's protocol was adapted as follows. Adherent cells were washed once with BupH™ Phosphate Buffered Saline at RT and biotinylated with 2 mL of 1x EZ-Link™ Sulfo-NHS-SS-Biotin for 10 minutes at RT. After two washes with ice-cold BupH™ Tris Buffered Saline (TBS), cells were scraped into 1 mL of TBS, transferred to Eppendorfs, and centrifuged at 500g for 5 minutes at 4°C. Supernatants were discarded. Cell pellets were lysed on ice for 30 minutes with 200 µL of kit-provided Lysis buffer supplemented with Halt Protease and Phosphatase Inhibitor Cocktail, EDTA-free (100x) (ThermoFisher Scientific, 78441), then centrifuged at 21,000g for 5 minutes at 4°C. Biotinylated proteins in the clarified supernatant were captured by 1-hour RT incubation with NeutrAvidin™ Agarose in 1:1 ratio. The captured protein-resin complex was washed four times before final protein elution with 50 µL of Elution buffer supplemented with 10 mM Dithithreitol (DTT). Eluted protein samples were snap-frozen in LN and stored at -80°C until required.

After thawing, protein concentration in all samples was determined with Pierce™ BCA Protein Assay Kit and normalised by dilution with ddH_2O. Samples were mixed with NuPAGE™ 4x LDS sample buffer and NuPAGE™ 10x Sample Reducing Agent (Invitrogen, NP0009), unless

eluted in buffer supplemented with DTT. Samples were then heated at 70°C for 10 min. 25 µL of sample containing minimum of 10-50 µg of protein was loaded onto Novex™ WedgeWell™ 8-16%, Tris-Glycine pre-cast mini gels, along with 5 µL of Precision Plus Protein Dual Color Standards, and ran in Novex™ Tris-Glycine SDS Running Buffer at 180V for 45 minutes.

Following the electrophoresis, gels were rinsed with ddH_2O and 1x Trans-Blot Turbo Transfer Buffer (Bio-Rad, #10026938) before semi-dry protein transfer to a Low-Fluorescence PVDF transfer membrane (ThermoFisher Scientific, 22860) using the Mixed Molecular Weight (1.3 A, 25 V, 7 minutes) pre-programmed settings on Trans-Blot Turbo transfer machine (Bio-Rad). Membranes were blocked with iBind™ Flex blocking solution (ThermoFisher Scientific, SLF1020) for 1 hour at RT and probed with relevant, iBind™ Flex-diluted primary antibodies (Table 2.9) overnight at 4°C. After three washes with 1x PBS buffer supplemented with 0.1% Tween® 20 (PBS-T) (Sigma, P7949-500ML) membranes were further stained with relevant, LI-COR fluorophore-conjugated secondary antibodies (Table 2.10) diluted in iBind™ Flex supplemented with 1:200 10% SDS. Unbound antibody was removed with six 1x PBS-T washes. Blots were visualised using the Odyssey Sa Infrared Imaging System (LI-COR Biosciences). Image Studio Lite open-source software v5.2 was used for densitometric analysis.

2.4.8 Enzyme-linked immunosorbent assay (ELISA)

Levels of intracellular tau and tau released to conditioned medium by iPSC-macrophages were quantified using Invitrogen™ Tau (Total) Human ELISA kit (ThermoFisher Scientific, KHB0041). Cytokine secretion by iPSC-macrophages was quantified using Human Uncoated TNF-α and IL-6 ELISA Kits (ThermoFisher Scientific, 88-7346-88, 88-7066-88). Protocols were used as per manufacturer's instructions.

Total protein was extracted from iPSC-macrophages at baseline or following tau treatment using protocol described in section 2.4.7. Protein concentration was quantified with Pierce™ BCA Protein Assay Kit. Samples were snap-frozen in LN and stored at -80°C until required.

Collected conditioned medium for tau or cytokine quantification was centrifuged at 400g for 5 minutes at 4°C to remove any floating cells and cell debris, aliquoted to 96-well V-bottom plates, parafilmed, and stored at -80°C until required.

After thawing, sample dilution was optimised to 1:100 for tau quantification in cell lysates, 1:10 for tau quantification in supernatants, and 1:10 and 1:100 for cytokine quantification in supernatants. Absorbance (450 nm) was measured using the SpectraMax M5 microplate reader. Background reading was subtracted from all values. Tau or cytokine concentration in samples was calculated by interpolation from standard curve (sigmoidal, 4PL, X is concentration) in GraphPad Prism v9.0. Values above and below the range of the standard curve were excluded. If multiple dilutions of a sample were assessed, values presented are an average of the dilutions.

2.4.9 4R tau real time quaking-induced conversion (RT-QuIC)

Modified version of the 4R tau RT-QuIC seed amplification assay (Metrick et al., 2020b; Saijo et al., 2020b) was used to determine seeding capacity of soluble and insoluble intracellular tau and tau secreted to conditioned medium by iPSC-macrophages.

iPSC-macrophages were differentiated in 6-well tissue culture plates and treated overnight with 2.5 µg/mL of tau monomer, tau fibrils, or vehicle. 2.5% TryplE™ incubation for 1 minute (Michel et al., 2014) followed by 1x PBS wash was used to remove uninternalised tau. Cells were left to process internalised tau in standard, tau-free, iPSC-macrophage differentiation medium at 37°C, 5% CO_2. After 24 hours, conditioned medium and cell lysates were collected. Medium was spun at 400g for 5 minutes at 4°C to remove floating cells and cell debris, then aliquoted, frozen on dry-ice, and stored at -80°C until further processing. The amount of tau in supernatants was quantified with Invitrogen™ Tau (Total) ELISA. Cells were lysed with 100 µL of ice-cold Triton lysis buffer (1% Triton-X100 in 50 mM Tris (Sigma, T1503-500G), 150 mM NaCl, pH 7.6) supplemented with EASYpack Protease Inhibitor Cocktail and Pierce™ Phosphatase Inhibitor Mini Tablets. Cell lysates were collected by scraping, then centrifuged

at 21,000g for 30 minutes at 4°C. Supernatants containing total cell protein including soluble tau (the Triton fraction) were transferred to Eppendorfs. Pellets containing insoluble tau were solubilised in SDS lysis buffer (1% SDS in 50mM Tris, 150mM NaCl, pH 7.6) supplemented with EASYpack Protease Inhibitor Cocktail and Pierce™ Phosphatase Inhibitor Mini Tablets to form the SDS fraction (Michel et al., 2014). Protein concentration in both fractions was quantified with Pierce™ BCA Protein Assay Kit and normalised by dilution with ddH_2O. Samples were snap-frozen in LN, then stored at -80°C.

Medium and cell lysate aliquots were shipped on dry ice for RT-QuIC analysis by Alessia Santambrogio at the Yusuf Hamied Department of Chemistry, University of Cambridge.

K11 tau (tau residues 244-394) was used as tau seeding substrate (see section 5.) One aliquot of lyophilized K11 purified from *E. coli* was dissolved in 1 mL of 8 M GuHCl prior to size-exclusion chromatography (SEC) separation on Superdex 75 10/300 column equilibrated in 20 mM sodium phosphate, 200 mM NaCl, pH 7.4. 50 µL/well total volume reactions were prepared in a 384-well optical BTM Polybase Black plate (Thermo Scientific, 242764) by adding the individual samples-to-be-examined (i.e., the Triton/SDS cell lysate fractions and the conditioned medium) in respective 1:10,000 and 1;100 final dilutions to the reaction buffer. The reaction buffer comprised of 4 µM K11 tau monomer, 10 µM ThT, 500 mM Na_2SO_4, and 40 mM HEPES buffer at pH 7.4. Reactions were transferred to a 384-well Nunc microplate (non-treated polymer base #242764) covered with aluminium sealing cover to prevent evaporation and subjected to rounds of 60 s shaking (500 rpm, orbital) and 60 s rest with periodic ThT readings every 15 min at 37 °C in a BMG FluoStar Omega lite microplate reader.

1.12 Statistical analysis

All statistical analyses were performed in GraphPad Prism v9.0 (GraphPad Software Inc.) using one-way ANOVA, two-way ANOVA or Student's *t*-test, with Tukey's, Dunnett's or Šídák's multiple comparison tests, as appropriate. Specific methods used are detailed in individual results chapters. Data is presented as mean ± standard deviation (SD), unless stated otherwise. Significance was defined as $*P \leq 0.05$, $**P \leq 0.01$, $***P \leq 0.001$, $****P \leq 0.0001$. n.s. = not significant.

Chapter 3

The influence of LRRK2 on phagolysosomal pathways in microglia

3.1 Introduction

Protein coding mutations in LRRK2 and noncoding variations increasing LRRK2 expression levels have been linked with the risk and progression of PD and PSP (Herbst et al., 2022; Jabbari et al., 2021; Nalls et al., 2014a; Zimprich et al., 2004). Emerging evidence suggests that the risk may be mediated specifically by perturbed phagolysosomal clearance of cargo, including aggregated tau, by microglia (Langston et al., 2022; Podleśny-Drabiniok et al., 2020). LRRK2 is highly expressed in microglia and has been proposed to modulate membrane trafficking events (Bonet-Ponce & Cookson, 2022; H. Lee et al., 2017) but its precise role in the microglial phagolysosomal pathways is unclear. As discussed in the section 1.9., published studies offer contradicting evidence, reflecting the lack of assay standardisation (summarised in Table 1.2, reviewed in Russo et al., 2022).

The methodological differences are likely to affect the results in a number of ways. Firstly, the majority of studies have used rodent microglia which fail to recapitulate the unique cell-state and gene-expression heterogeneity of human microglia in health and disease (see section 1.10) (Geirsdottir et al., 2019; Gosselin et al., 2017; Mancuso et al., 2019; Masuda et al., 2019). Investigations in human microglia or an authentic microglial model are lacking.

Secondly, commercially available media formulations used to culture macrophages and microglia *in vitro* may contain undisclosed components, likely to influence cellular metabolism and phenotype. XVIVO, the medium used previously in our lab to differentiate iPSC-macrophages, and utilised in several studies investigating LRRK2, was recently shown to

contain anti-inflammatories, anti-infectives, cell-permeable cryoprotectants, and excessive glucose concentration (Vaughan-Jackson et al., 2021). Given that phagocytosis is a highly energy-demanding mechanism, results from studies using XVIVO or other proprietary medium should be interpreted with care.

The choice of readout analysis, too, has to be considered. Recent technological advancements in microscopy now allow for high temporal and sub-cellular resolution of phagocytosis. However, a microscopy readout can produce erroneous results, in the absence of sophisticated image analysis software and quantity of analysed samples sufficient for robust statistical analysis.

Finally, the majority of studies investigating microglial LRRK2 focus on the initial part of phagocytosis, the act of cargo internalisation. Phagolysosomal cargo degradation is generally studied separately, if at all, offering a limited insight into the increasingly more recognised kinetic coupling of the two processes (Frankenberg et al., 2008; Wong et al., 2017a; Y. Yu et al., 2022). Successful degradation of internalised cargo was recently found necessary for continuous phagocytosis of the exogenous cargo (Wong et al., 2017b). Investigating the uptake-clearance dynamics may therefore be particularly relevant in the context of sustained presence of neuronal debris and aggregated, pathogenic proteins in neurodegenerative diseases.

Altogether, the current state of art highlights the need for a reliable method assessing phagolysosomal clearance in human microglia. With a robust method in place, we can begin addressing the specific role of microglial LRRK2 in the process and contrast the baseline responses with responses specific to tau protein (i.e., the main aim of Chapter 5).

Considering this need, I focused on the following aims within this chapter:
1. Development of a high-throughput assay for quantitation of phagolysosomal proteolysis in an authentic, *in vitro* model of human microglia (sections 3.2.1, 3.2.2).

2. Utilising the assay to examine the influence of LRRK2 on the microglial baseline phagocytic and degradative capacity (section 3.2.3).

3.2 Results

3.2.1 Set up and optimisation of quantitative, *in vitro* phagolysosomal proteolysis assay

The first aim of this chapter was to establish a dependable method for visualizing and quantitating real-time phagocytic uptake and bulk phagolysosomal proteolytic activity in relevant *in vitro* model of human microglia. The assay development stage was carried out using iPSC-macrophages as faster and cost-effective iPSC-microglia surrogate.

To measure the intracellular proteolytic activity, I relied on a previously described DQ^{TM} BSA fluorescent reporter. DQ^{TM} BSA is a BSA molecule conjugated to boron-dipyrromethene (BODIPY) dyes, either the green fluorescent BODIPY-FL (DQ Green BSA) or the red fluorescent BODIPY TR-X (DQ Red BSA), at degree of substitution so high that it results in intramolecular fluorescence self-quenching. Following DQ BSA internalization, cellular proteases within acidic compartments hydrolyse the DQ BSA probe to albumin fragments bound to individual fluorophores. The probe proteolysis thus effectively relieves the fluorescence self-quenching and produces a strong, measurable fluorescent signal (Figure 3.1A).

I first used a cell-free approach to verify the use of DQ BSA for monitoring proteolysis. 50 µg/mL of DQ Red BSA dissolved in x1 PBS was incubated in a standard, 96-well, flat-bottom plate in presence or absence of 50% TrypLE at 37°C for 24 hours. TrypLE was used as a highly pure and specific recombinant substitute for trypsin. Fluorescence was measured every 10 minutes using SpectraMax M5 plate reader at 550 nm excitation and 620 nm emission wavelengths. Intact DQ Red BSA displayed very low levels of background fluorescence while DQ Red BSA fragments generated by TrypLE proteolysis resulted in a ten-fold increase in

fluorescence that saturated over time (Figure 3.1B). DQ Red BSA peak fluorescence intensity following 3-hour TrypLE digest remained unchanged regardless of the buffer pH (Figure 3.1C). TrypLE works at optimum across the examined pH range, therefore we can be reasonably confident that the observed stability of DQ Red BSA signal reflects the manufacturer's claim that DQ Red BSA allows for a detection of proteolytic activity within acidic intracellular compartments.

Next, I aimed to validate the use of DQ Red BSA for studying proteolysis within cells *in vitro.* iPSC-macrophages from healthy controls were differentiated as per standard XVIVO differentiation protocol (section 2.1.3). Cells were stained with a nuclear NucBlue live cell stain (section 2.1.7), and pulsed for 30 minutes with 10 µg/mL DQ Red BSA dissolved in medium. Uninternalized DQ Red BSA was washed off with two changes of 1x PBS and replaced by XVIVO macrophage medium with or without the addition of 50 µM each of broad-spectrum protease inhibitors, leupeptin, pepstatin A and E64d. The cells were placed in a temperature and humidity–controlled stage of the EVOS FL Auto microscope maintained at 37°C and 5% CO_2. Images were captured every 4 hours over the course of 24 hours for live, time-lapse visualization of DQ Red BSA hydrolysis *in vitro*. Representative pictures are shown in Figure 3.1D. Image analysis revealed an increase of DQ Red BSA fluorescent signal over time indicating a successful DQ Red BSA internalization and hydrolysis by iPSC-macrophages. The presence of protease inhibitors in cell culture medium significantly decreased the DQ Red BSA proteolysis (Figure 3.1E). The individual protease inhibitor concentration selected for the assay (50 µM) did not affect cell viability (Figure 3.1F) as determined by a resazurin cell viability assay (section 2.1.6).

At the end of the time-course, the iPSC-macrophages were fixed and immunocytochemistry was undertaken for the lysosomal LAMP-1 marker (section 2.4.3). Figure 3.1G depicts representative confocal images of red DQ Red BSA fluorescence colocalising with the green-fluorescent LAMP-1 lysosome marker. Columbus image analysis indicated 70.4% of LAMP-

1 positive DQ Red BSA puncta, decreased to 51.7% in presence of protease inhibitors (Figure 3.1H).

iPSC-macrophages are likely to take up DQ Red BSA in solution by bulk fluid-phase uptake mechanisms, notably by macropinocytosis. Macropinocytosis involves constitutive, non-specific internalisation of fluids and small soluble material from the extracellular space. It is, therefore, distinct from phagocytosis, a process of engulfing particles larger than 0.5 μm in diameter by professional phagocytes, including macrophages and microglia (Mukherjee et al., 1997; Rabinovitch, 1995).

The experiments thus far validated DQ Red BSA as a suitable tool for tracking intracellular proteolysis following a fluid-phase uptake. The main aim of this chapter was, however, quantifying proteolysis occurring specifically within phagosomes and phagolysosomes of iPSC-macrophages. To achieve that, I utilised reporter beads; a simple phagocytic cargo widely used in the field to investigate basic mechanisms of phagocytosis in myeloid cells. The beads were created according to a published protocol by step-wise, double-labelling of 3 μm carboxylated silica beads with AF-488 fluorophore to track bead internalisation, and the DQ Red BSA for simultaneous indication of hydrolysis of the BSA conjugated to the phagocytosed beads (Figure 3.2A, section 2.4.1) (Yates & Russell, 2008).

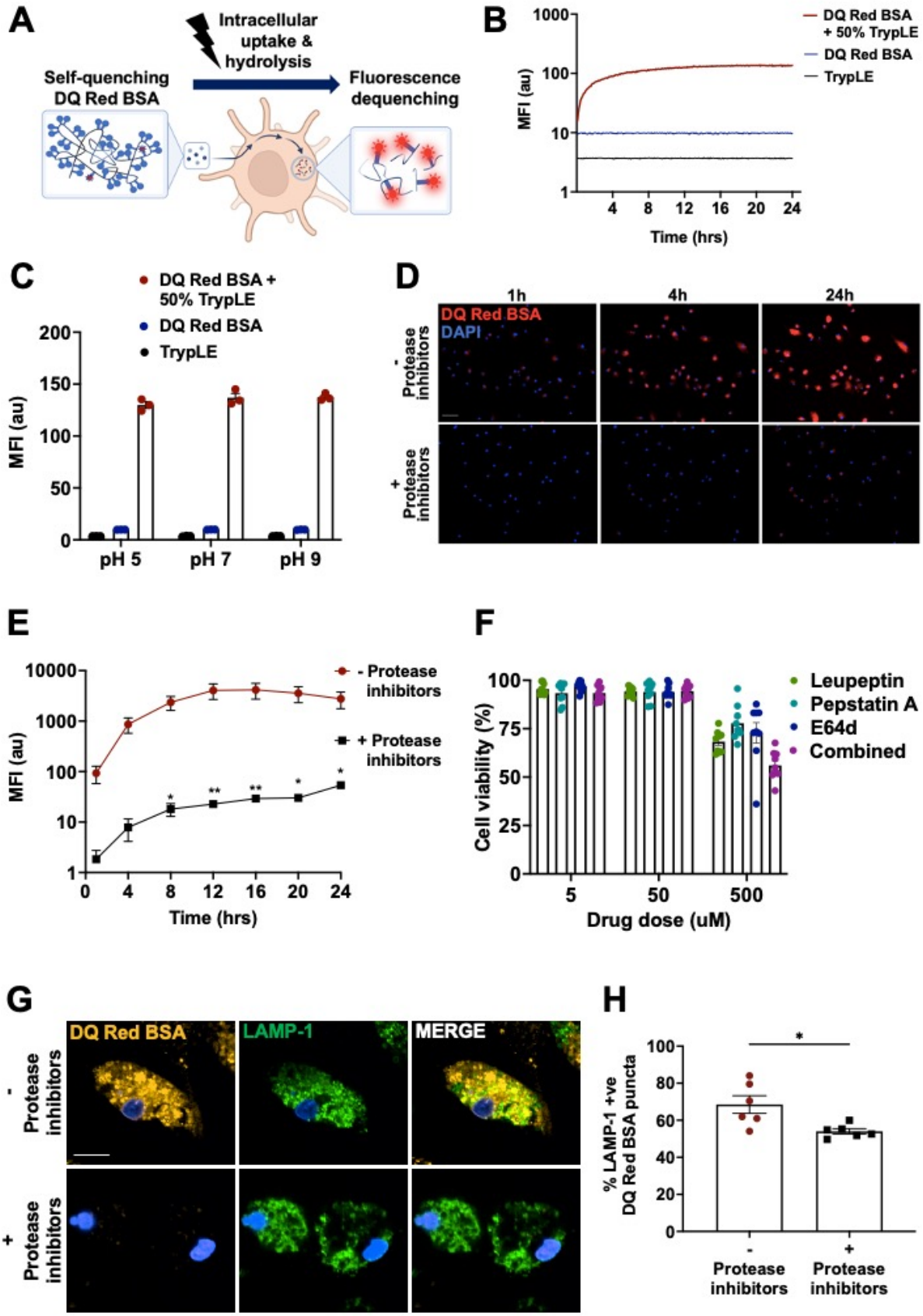

Figure legend on the next page.

Figure 3.1: Characterization of DQ Red BSA fluorogenic substrate as degradation probe for use in iPSC-macrophages

*(A.) Schematic of DQ Red BSA processing in cells. (B.) DQ Red BSA hydrolysis with 50% TrypLE (cell-free). (C.) DQ Red BSA hydrolysis with TrypLE is independent of the buffer pH (cell-free). n=3 technical replicates. (D.) 30-minute DQ Red BSA pulse in iPSC-macrophages, followed by 24-hour chase visualized by live-cell fluorescence microscopy. Scale bar = 20 µm. (E.) Quantification of D. Protease inhibitors significantly reduce DQ Red BSA degradation by iPSC-macrophages. Two-way ANOVA with Šídák multiple comparison corrections. n=1 in 3 cell lines, mean ± SD, * p<0.05, ** p<0.01. (F.) Resazurin cell viability assay in iPSC-macrophages (n=3) after 24-hour incubation with protease inhibitors. (G.) Hydrolysed DQ Red BSA signal colocalizes with lysosomal LAMP-1 marker in iPSC-macrophages. Scale bar =10 µm. (H.) % LAMP-1 positive hydrolysed DQ Red BSA spots in iPSC-macrophages. n=2 in 3 cell lines, mean ± SD, Welch's t-test, * p<0.05. MFI = mean fluorescence intensity*

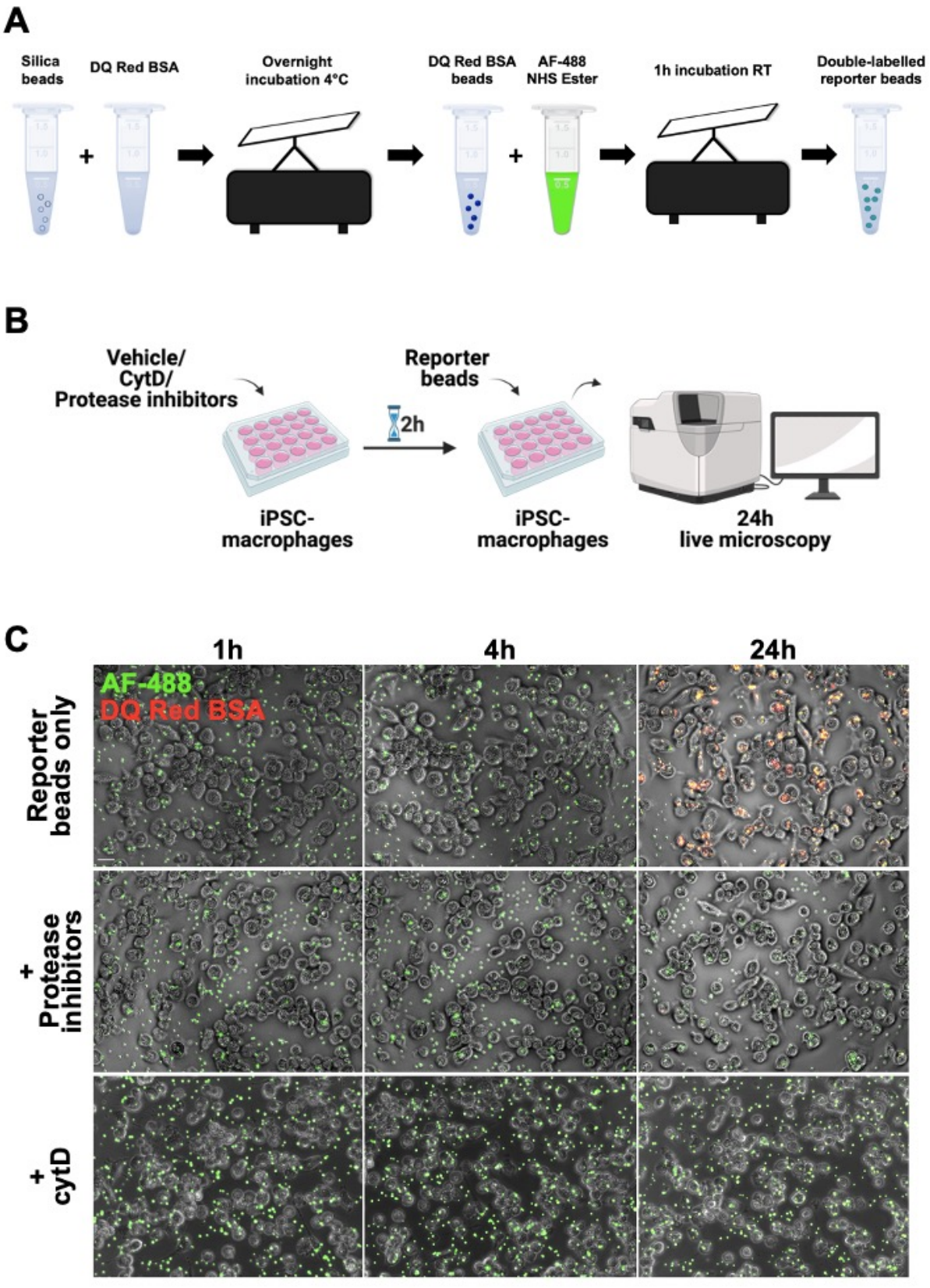

Figure legend on the next page.

Figure 3.2: Production of double-labelled reporter beads as phagocytic cargo for iPSC-macrophages

(A.) Schematic of reporter bead production protocol. (B.) Experiment workflow. (C.) 24-hour live-cell, time-lapse fluorescence microscopy showing that iPSC-macrophages effectively phagocyte the beads and degrade the attached DQ Red BSA label over time. Scale bar = 20 μm

The following proof of principle experiment was designed to test the efficacy of this approach (Figure 3.2B). Healthy donor derived iPSC-macrophages were pre-treated with either vehicle, 10 μM cytochalasin D (cytD), or 50 μM each of broad protease inhibitors, leupeptin, pepstatin A and E64d at 37°C. CytD is an actin polymerization inhibitor that blocks actin-remodelling-requiring modes of uptake, including almost 90% of phagocytosis (Kapetanovic et al., 2007) and as such was selected as a negative control of bead uptake. Protease inhibitors were selected as a negative control of DQ Red BSA hydrolysis.

Following the preincubation, reporter beads were added directly to the cell culture in 1:2 cell:bead ratio. Live bead uptake and DQ Red BSA label hydrolysis was visualized over the course of 24 hours using the EVOS FL Auto fluorescence microscope. Representative images captured at the 1-, 4- and 24-hour timepoints are shown in Figure 3.2C. Image observation analysis showed an intracellular increase of the green-fluorescent AF-488 signal, reduced in presence of cytD, indicative of a phagocytic bead uptake by iPSC macrophages. Similarly, intracellular increase in the red fluorescent signal beads was observed over time in the cells, colocalizing with the green-fluorescent beads, unless pre-treated with protease inhibitors, implying that iPSC-macrophages effectively hydrolysed the DQ Red BSA label conjugated to the phagocytosed bead cargo. Thus, the results validated the use of the reporter beads for monitoring the phagolysosomal proteolysis in iPSC-macrophages.

In the next step, I aimed to supplement the visual observations generated by microscopy with a robust and quantifiable flow cytometry readout. iPSC-macrophages from three healthy donors were treated as in the previous experiment. Cells were harvested at 1-, 4-, and 24-hour incubation timepoints, resuspended in ice-cold LCIS to prevent any further internalization or degradation, and analysed live with Cytoflex LX flow cytometer (section 2.4.2). The following laser settings were used for the two bead-conjugated fluorophores:

For AF-488: 488 nm laser, 525/40 nm detection channel
For DQ Red BSA: 561 nm laser, 610/20 nm detection channel

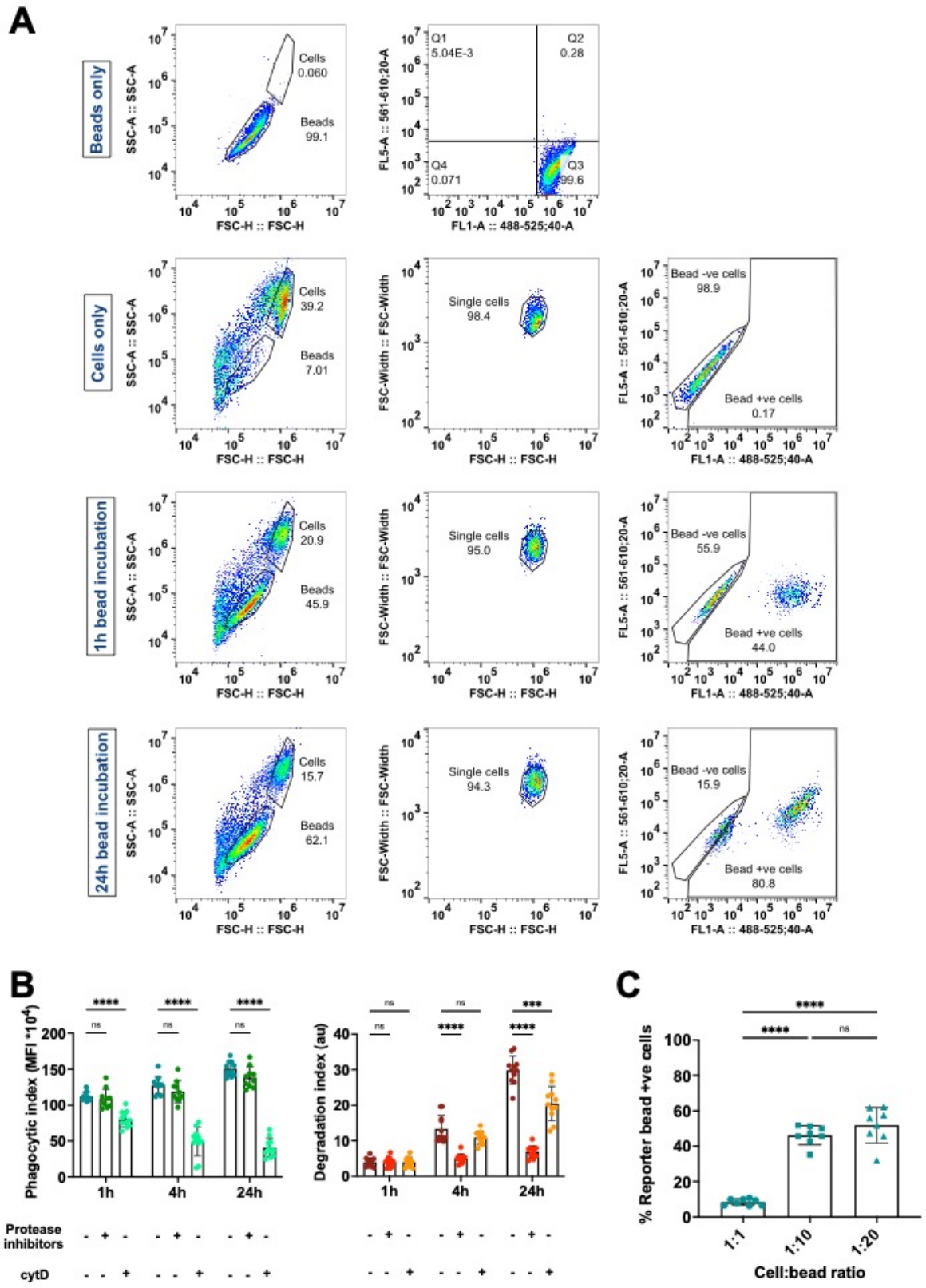

Figure legend on the next page.

Figure 3.3: Flow cytometry quantification of phagolysosomal proteolysis assay in iPSC-macrophages

*(A.) Flow cytometry gating strategy. (B.) Flow cytometry analysis of phagocytic and degradation index in control iPSC-macrophages incubated with reporter beads at 1:2 cell:bead ratio in the presence or absence of cytD and protease inhibitors. n=4 in 3 independent cell lines, mean±SD. Significance was calculated with two-way ANOVA, Dunnett's multiple comparison test. *** p<0.001, **** p<0.0001. Phagocytic index represents the geometric mean fluorescence intensity of internalized beads. Degradation index represents the geometric mean fluorescence intensity of hydrolysed DQ Red BSA, relative to phagocytic index. (C.) Optimisation of phagocytic cell:bead ratio following 4-hour reporter bead incubation. n=2 in 4 independent cell lines. One-way ANOVA with Tukey's multiple comparisons test. **** p<0.0001.*

Figure 3.3A describes the selected gating strategy in detail. Reporter beads were analysed first to adjust the laser power settings due to the brightness of the AF-488 signal (Figure 3.3A, ‘’Beads only’’ row). In agreement with Figure 3.1B results, intact DQ Red BSA label attached to the beads displayed low levels of background fluorescence. Untreated control samples were analysed next to identify the single cell population based on the forward scatter height and width, and the bead negative population due to natural iPSC-macrophage autofluorescence detectable with both the 488 and 561 nm lasers (Figure 3.3A, ‘’Cells only’’ row). Finally, bead-treated sample analysis allowed for gating on bead-positive macrophage population (Figure 3.3A, ‘’1h and 24h bead incubation’’ rows).

Results from four independent biological replicates are summarised in Figure 3.3B. The phagocytic index, defined as geometric mean of the 488-fluorescence intensity in the bead positive population, did not increase significantly between 1- and 4- and or between 1- and 24-hour timepoint. This indicates that iPSC-macrophages internalized the majority of the beads within the first few hours of incubation. Presence of protease inhibitors in the cell culture medium did not negatively affect the bead uptake. CytD pre-treatment significantly decreased bead internalization across all timepoints, confirming phagocytosis to be the most likely mode of bead uptake. The degradation index, indicative of the macrophage proteolytic activity generating fluorescent DQ Red BSA degradation products, was determined as the geometric mean ratio of the 561- to the 488- fluorescence intensity in the bead positive population. Protease inhibition significantly decreased the DQ Red BSA label hydrolysis at 4- and 24-hour timepoints. These findings were consistent with the qualitative observations from the live fluorescence microscopy. Interestingly, cells pre-treated with cytD hydrolysed significantly less DQ Red BSA probe relative to the number of internalized beads compared to the non-treated cells at 24-hour timepoint, possibly hinting at the cellular mechanisms coupling phagocytosis and degradation.

Finally, to optimise the rate of bead uptake and the number of internalized beads per cell, I incubated iPSC-macrophages with reporter beads at 1:1, 1:10, and 1:20 cell:bead ratio. At 4-hour incubation timepoint, cells were harvested and analysed with flow cytometry. I observed significant increase in percentage of bead-positive cells in the 10-fold bead:cell ratio compared with the equal bead:cell ratio condition. Incubating cells with 20-times more beads did not increase the percentage of bead positive cells any further than the 10-fold ratio, therefore, 1:10 cell:bead ratio was chosen for all future experiments (Figure 3.3C).

Collectively, these results validate the use of DQ Red BSA- and AF-488- double-labelled bead cargo for monitoring phagocytic and degradative capacity of iPSC-macrophages *in vitro,* and describe an optimised protocol for a quick, robust and reliable assay quantification.

3.2.2 Validating the use of new, defined-formula, iPSC-macrophage culture medium for studying phagolysosomal proteolysis

Parallel with establishing the phagolysosomal proteolysis assay, our lab published a novel protocol for differentiating iPSC-macrophages using a serum-free, defined, open-source culture medium with physiological levels of glucose, termed OXM. Culturing iPSC-macrophages in OXM, compared with the previously used, proprietary XVIVO medium, improved terminal macrophage differentiation and morphology, as well as polarization capacity and responsiveness upon inflammatory stimuli (Vaughan-Jackson et al., 2021). Considering the chapter aim of investigating phagocytic clearance in an authentic and relevant cell type, I sought out to examine potential differences in XVIVO vs OXM-differentiated macrophages utilizing the above-described phagolysosomal proteolysis assay.

The experiment schematic is outlined in Figure 3.4A. Four independent macrophage differentiations from healthy donor-derived iPSC were set up: two following the standard XVIVO differentiation protocol, and two using the OXM differentiation protocol (section 2.1.3). The apparent morphological differences between the terminally differentiated macrophages were in line with the published observations (Vaughan-Jackson et al., 2021). Specifically,

OXM-cultured macrophages were more flattened out and adherent, and contained multiple projections compared with the rounded, large, XVIVO-produced macrophages (Figure 3.4A). Prior to the phagolysosomal proteolysis assay, half of the cultured macrophages were pre-stimulated with 100 ng/mL of interferon gamma (IFNγ) for 72 hours to induce proinflammatory phenotype as described previously (H. Lee et al., 2020). Both protocols yielded equally phagocytically competent macrophages under basal conditions. However, IFNγ treatment significantly reduced bead phagocytosis in OXM-differentiated macrophages compared to XVIVO-macrophages across all timepoints. Furthermore, two-way ANOVA analysis of the degradation index showed an increased phagolysosomal proteolysis in OXM-cultured macrophages in both basal and proinflammatory state (Figure 3.4B).

IFNγ is an important immunomodulator, affecting multiple macrophage effector functions, including phagocytosis, intracellular pathogen clearance, antigen processing, as well as cytokine secretion (reviewed in Schroder et al., 2004). The limited responsiveness of XVIVO-differentiated macrophages to IFNγ stimulation shown in Figure 3.4B, therefore, highlighted the benefits of shifting from XVIVO to OXM macrophage differentiation protocol in order to maximise the assay's physiological relevance.

The OXM differentiation protocol, however, produces significantly lower macrophage precursor yield (Vaughan-Jackson et al., 2021). This outcome would have consequently prevented me from conducting any large-scale experiments. To overcome the limitation, I investigated whether combining the two differentiation protocols into a hybrid method could recapitulate the OXM-induced, faithful *in vitro* representation of human macrophages in quantities yielded using the XVIVO medium.

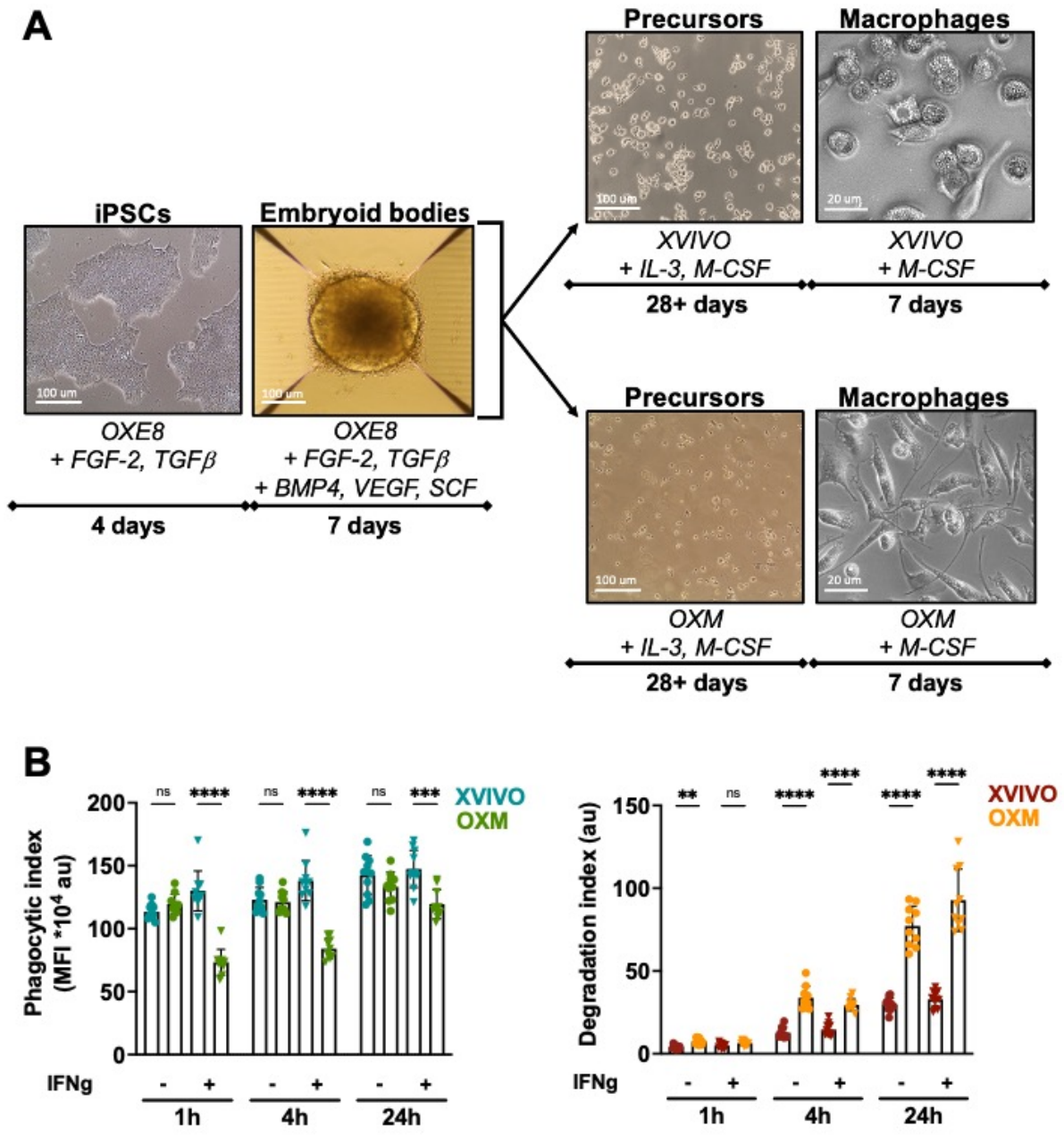

Figure 3.4: XVIVO- and OXM-differentiated iPSC-macrophages differ in phagocytic uptake and proteolysis

*(A.) Schematic of iPSC-macrophage differentiation using XVIVO vs OXM-based culture medium. (B.) Flow cytometry analysis of reporter bead phagocytosis and DQ Red BSA label proteolysis by XVIVO vs OXM-cultured iPSC-macrophages at baseline and following IFNγ stimulation. Results are shown from 4 experiments in 3 control cell lines across two differentiations per medium, mean±SD. Significance was calculated with two-way ANOVA, Šídák multiple comparison test. ** p<0.01, *** p<0.001, **** p<0.0001.*

The experiment design is outlined in Figure 3.5A. The aim was to compare morphology and phenotype of iPSC-macrophages produced by standard XVIVO differentiation protocol, the new OXM differentiation protocol, and a hybrid protocol whereby macrophage precursors are generated in XVIVO medium, followed by macrophage differentiation in OXM medium.

Morphologically, differentiated hybrid macrophages resembled OXM macrophages with multiple processes, and flattened, adherent cell bodies (Figure 3.5B). Next, I measured the baseline surface CD marker expression using flow cytometry. The selection of analysed markers was based on the previously identified significant differences between XVIVO vs OXM macrophages (Vaughan-Jackson et al., 2021). The following laser settings were used for the different fluorophores in this experiment:

For FITC: 488 nm laser, 525/40 nm detection channel
For PE: 561 nm laser, 585/42 nm detection channel
For APC: 638 nm laser, 660/10 nm detection channel

All macrophages regardless of the differentiation protocol expressed the same levels of the key markers of macrophage lineage, the lipopolysaccharide (LPS) co-receptor CD14 and the pan-leukocyte marker CD45 (Figure 3.5C). Previous findings identified significantly higher levels of Fc gamma receptor III, CD16, and significantly lower amount of β2-integrin receptor, CD11b, and its costimulatory receptor, CD86, in OXM macrophages compared with XVIVO-cultured macrophages (Vaughan-Jackson et al., 2021). The findings were recapitulated in this experiment. Furthermore, the difference in CD16, CD11b, and CD86 expression between XVIVO- and hybrid-cultured macrophages closely mimicked the differences between XVIVO vs OXM macrophages, suggesting that XVIVO precursors readily adopt the OXM macrophage surface marker phenotype upon OXM macrophage medium stimulation (Figure 3.5C).

To test whether hybrid macrophages also resemble the OXM-differentiated cells in polarization capacity, I assessed the surface markers of polarization after stimulation. Cells were activated

towards classically defined ''M1'' phenotype with LPS and IFNγ, or towards alternative ''M2'' state with IL-4 overnight as previously described (Wilgenburg et al., 2013). Following the stimulation, cells were immunostained for polarization surface markers CD11b and CD86 (Mosser, 2003; Rőszer, 2015). Activation did not alter the surface CD45 expression in macrophages produced with any of the three methods. However, both surface CD11b and CD86 expression increased significantly in classically activated macrophages produced using the OXM as well the hybrid protocol (Figure 3.5D).

Supernatants from the same experiment were also collected to supplement the data on macrophage polarization capacity with a functional cytokine secretion readout (section 2.4.8). In line with the previous report, XVIVO macrophages secreted constitutive low levels of TNF-α at resting condition, unlike the OXM or hybrid-protocol differentiated cells (Figure 3.5E). XVIVO macrophages also secreted significantly higher levels of TNF-α and IL-6 following the LPS/IFNγ activation compared with the OXM and hybrid macrophages. However, the mean fold change in TNF-α secretion in activated vs resting state was higher in OXM and hybrid cells (10,000 and 3,460 respectively) than in XVIVO cells (1,593), indicating a blunted sensitivity of the XVIVO cells to classical activation.

Finally, I used the phagolysosomal proteolysis assay to examine whether the process of differentiating iPSC-macrophages with the hybrid protocol generates just as sensitive model of *in vitro* phagocytosis and phagolysosomal degradation as the OXM protocol. The hybrid protocol-differentiated macrophages showed no significant difference in phagocytic nor degradation index compared to the OXM protocol-differentiated cells, suggesting further similarities in the overall macrophage phenotype (Figure 3.5F).

Overall, the results showed that differentiating iPSC to macrophages using the hybrid protocol produces OXM-protocol-like macrophages while simultaneously overcoming the OXM protocol precursor yield barrier. The hybrid protocol was therefore used to differentiate iPSC-macrophages in all further experiments.

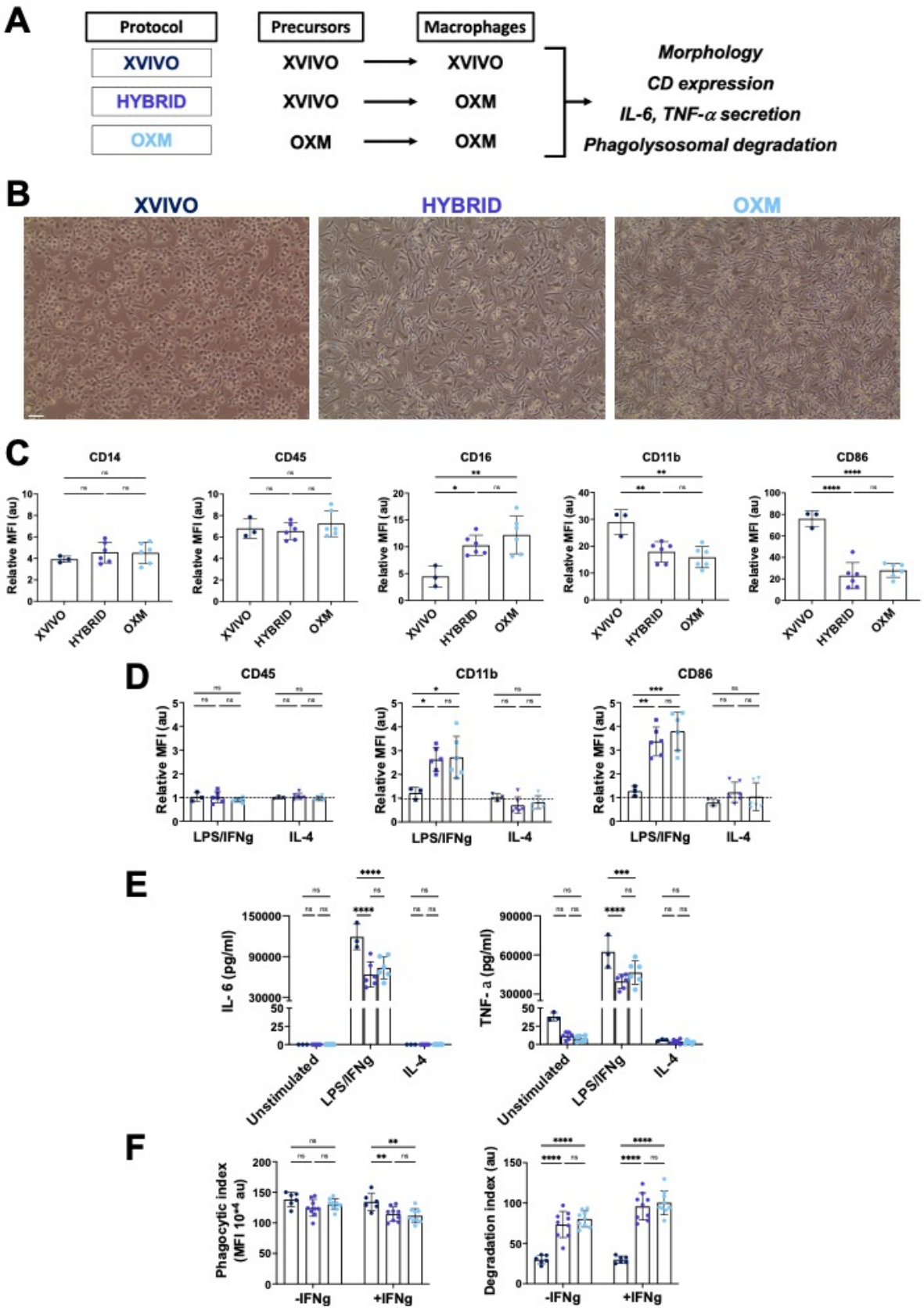

Figure legend on the next page.

Figure 3.5: XVIVO macrophage precursors differentiated in OXM macrophage medium readily take on the OXM-protocol phenotype

(A.) Workflow diagram. (B.) iPSC-macrophage morphology. Scale bar = 50 µm. (C.) Baseline surface expression of CD14, CD45, CD16, CD11b and CD86 on unstimulated macrophages measured by flow cytometry. Data is shown as geometric MFI normalized to the isotype control. One-way ANOVA, Šídák multiple comparison test. (D.) Flow cytometry-measured surface expression of CD45, CD11b and CD86 on LPS/IFNγ and IL-4 stimulated cells relative to the unstimulated cell expression. One-way ANOVA, Šídák multiple comparison test. (E.) IL-6 and TNF-a secretion from unstimulated, LPS/IFNγ, or IL-4 stimulated cells. Two-way ANOVA with Bonferroni multiple comparisons test. (F.) Phagolysosomal proteolysis assay in unstimulated or IFNγ-stimulated macrophages. Two-way ANOVA with Bonferroni multiple comparisons test.

C-E. XVIVO: n=1 in 3 control cell lines, HYBRID and OXM: n=2 in 3 control cell lines. F. n=2 in 3 control cell lines.

*All data is displayed as mean±SD, *p<0.05, ** p<0.01, *** p<0.001, **** p<0.0001.*

3.2.3 Investigation of the influence of LRRK2 on phagolysosomal proteolysis in iPSC-macrophages

Having optimised the method for quantification of phagolysosomal degradation in a more authentic model of human microglia, I next investigating the influence of the LRRK2 protein on the process.

Healthy control iPSC lines (LRRK2 WT), CRISPR/Cas9-edited LRRK2 KO line, and LRRK2 G2019S PD patient-derived lines (see sections 2.1.1 and 2.2.1 for details) were differentiated to iPSC-macrophages. Cells were treated as described in Figure 3.6A. 72-hour IFNγ pre-stimulation was selected to upregulate endogenous LRRK2 protein levels and its kinase activity in our cell model, as per previous findings (H. Lee et al., 2020) (Figure 7.1A). LRRK2 kinase activity was modulated using Mli-2, a potent and highly selective LRRK2 kinase inhibitor (Fell et al., 2015; Härtlova et al., 2018b; Scott et al., 2017) (Figure 7.1B).

Compared with LRRK2 WT, G2019S iPSC-macrophages internalised significantly fewer beads following both short (4-hour) and long-term (24-hour) incubation (Figures 3.6B and D). However, LRRK2 KO cells showed no difference in phagocytic index at neither timepoint, suggesting LRRK2 may not be involved in the process. Furthermore, if LRRK2 kinase activity negatively regulated bead internalisation, I would have expected to see a reduced number of beads in IFNγ-stimulated LRRK2 WT cells and a phenotype rescue following Mli-2 – induced LRRK2 kinase inhibition. Phagocytic index was indeed significantly decreased in IFNγ-stimulated LRRK2 WT cells at both timepoints but Mli-2 treatment did not restore the levels to baseline (Figures 3.6C and E). Neither IFNγ nor Mli-2 stimulation, alone or combined, had an effect on bead internalisation in LRRK2 KO and G2019S iPSC-macrophages.

Next, G2019S macrophages showed significantly increased BSA hydrolysis per bead taken up at both timepoints, compared with the LRRK2 WT (Figures 3.6B and D). The opposite was true in LRRK2 KO cells at the 4-hour timepoint (50.6% reduction). The degradation index was 25.5% lower in LRRK2 KO cells also at 24 hours but the difference did not reach statistical

significance. Increased degradation index, similar to the G2019S phenotype, was also observed in WT cells in response to IFNγ-induced LRRK2 upregulation and the effect was reversed by Mli-2 treatment at 24-hour timepoint (Figures 3.6C and E). LRRK2 upregulation in G2019S cells showed an upward trend in degradative capacity but did not reach significance. Most interestingly, Mli-2 LRRK2 inhibition significantly decreased the levels of BSA hydrolysis in G2019S macrophages back down to the levels observed in WT cells.

Altogether, the results did not identify a clear effect of LRRK2 kinase activity phagocytosis in iPSC-macrophages but suggested an involvement in regulation of phagolysosomal proteolytic activity in a temporal manner.

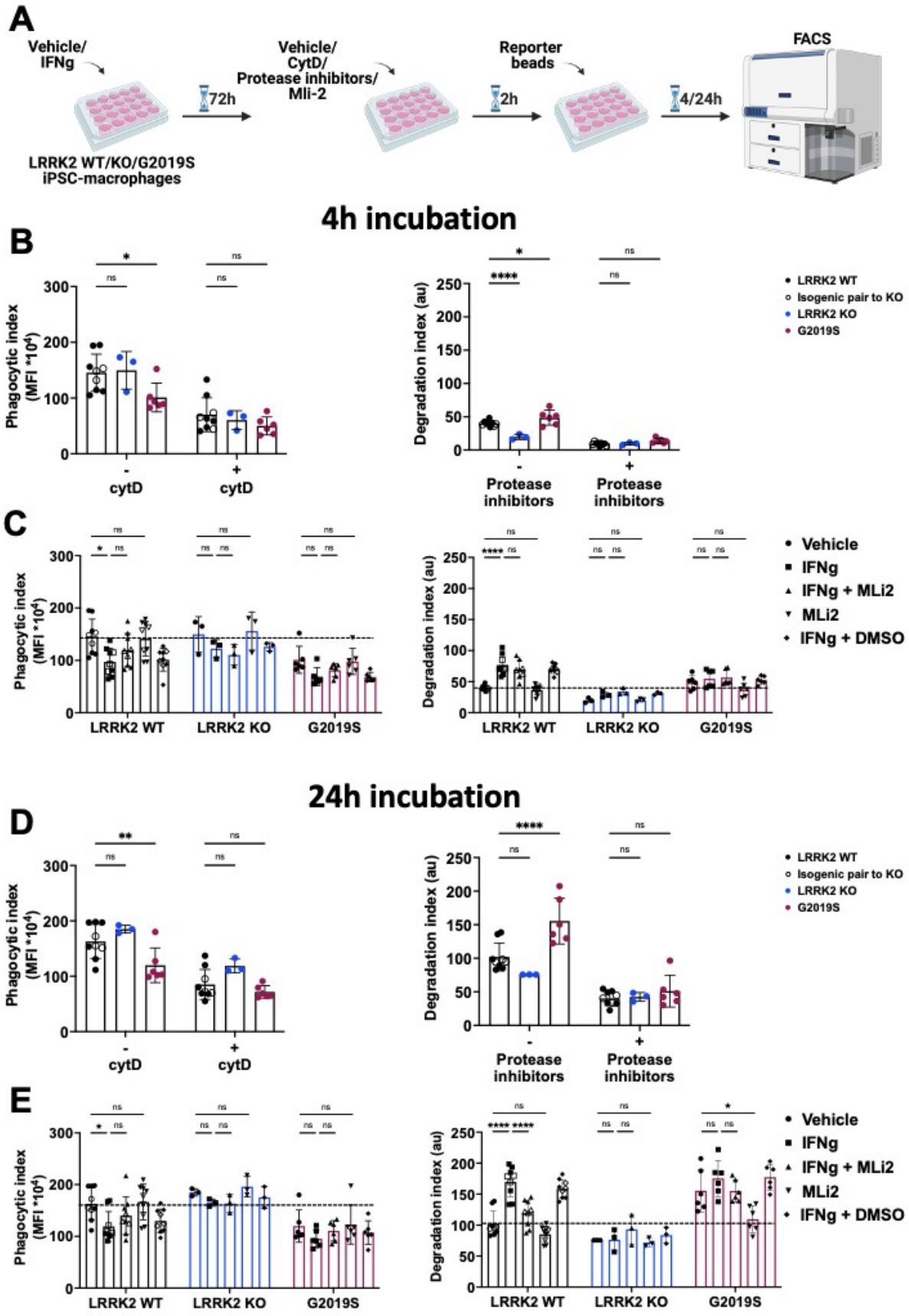

Figure legend on the next page.

Figure 3.6: LRRK2 influences phagolysosomal proteolysis in iPSC-macrophages

(A.) Workflow diagram. (B-C.) 4-hour and (D-E.) 24-hour phagolysosomal proteolysis assay iPSC-macrophages derived from healthy control lines (LRRK2 WT), CRISPR/Cas9 induced LRRK2 KO line (LRRK2 KO), and G2019S LRRK2 patient lines.

Open symbols represent values for LRRK2 WT cell line isogenic to the LRRK2 KO. MFI is expressed as relative to the individual cell line autofluorescence. Two-way ANOVA with Dunnett's multiple comparisons test for A. and C. Two-way ANOVA with Tukey's multiple comparison test for B. and D.

*n=3 in x3 LRRK2 WT, x1 LRRK2 KO, and x2 LRRK2 G2019S cell lines. All data is displayed as mean±SD, *p<0.05, ** p<0.01, **** p<0.0001.*

3.3 Discussion

This chapter describes an optimised protocol for quantitation of phagolysosomal clearance in iPSC-macrophages, a simple, preliminary *in vitro* model of human microglia. The assay was successfully applied to investigate the influence of LRRK2 on phagolysosomal pathways. The results identified a potential relationship between LRRK2 and proteolytic activity inside the phagolysosomes of iPSC-macrophages.

DQ Red BSA fluorescent probe was selected as a practical tool to measure intracellular proteolytic cleavage. The initial set of results (Figure 3.1) validated the use of DQ Red BSA for the stated purpose in agreement with published literature (Filipello et al., 2023; L. S. Frost et al., 2017; Gray et al., 2016; Marwaha & Sharma, 2017). Beads were chosen as phagocytic cargo to be conjugated with the DQ Red BSA probe. Beads of various sizes and material (i.e., silica, polystyrene, latex) have long been utilised in the field as a simple yet functional phagocytic substrate (Aderem & Underhill, 1999; Champion et al., 2008; Desjardins & Griffiths, 2003; Podinovskaia et al., 2013; Tabata & Ikada, 1988). In addition, the non-degradable beads can be viewed as an approximation to the proteolysis-resistant tau fibrils (Quinn et al., 2018), thus creating an opportunity to study basic cellular responses to non-digestible material.

3 µm silica beads were conjugated with AF-488 and DQ Red BSA fluorescent dyes, allowing for a convenient, simultaneous tracking of cargo internalisation and proteolytic degradation. This particular combination of bead labelling was first described by the group of David G Russell (Yates & Russell, 2008) and has since been widely utilised to understand the responses of peripheral innate immune system (Cheung et al., 2017; Fabrik et al., 2023; Pei et al., 2014; Podinovskaia et al., 2013; Podinovskaia & Russell, 2015; Tan & Russell, 2015; Tram et al., 2019). Here, I build on this work and demonstrate the AF-488/DQ Red BSA reporter beads can also be adapted to understand the basics of phagolysosomal proteolysis in iPSC-macrophages, serving as a simple *in vitro* model of brain-resident, human microglia. Live flow-cytometry was selected as a readout to provide a real-time, semi-automated, and

robust data analysis, and to eliminate the operator-bias and low-throughput typically associated with microscopy.

The use of phagocytic cargo reporting simultaneously on its uptake and degradation enables investigation into the potential coupling of the two events. Recent studies have begun to shed light into the tight regulations and bridging of the processes. For example, defective phagocytosis associated with the loss of TREM2 receptor in Nasu-Hakola disease was shown to attenuate lysosomal acidification, and led to an accumulation of undigested material within multivesicular bodies in iPSC-microglia (Filipello et al., 2023). Conversely, defective lysosomal degradation of *E. coli* in RAW 264.7 macrophages compromised further phagocytosis of bacteria and downstream NFκB signalling activation (Wong et al., 2017b).

In my set of results, inhibition of phagocytosis via cytD-induced actin depolymerisation significantly decreased intracellular proteolytic activity (Figure 3.3B). This observation adds to the previously observed coupling of degradation to intracellular transport. Inhibition of actin rearrangement was found to prevent phagolysosomal fusion, and with that the subsequent acidification necessary for cargo degradation (Guérin & de Chastellier, 2000; Kjeken et al., 2004; Lancaster et al., 2021). Furthermore, in macrophages exposed to overwhelming, non-degradable phagocytic load, transient F-actin networks assembled on immature phagosomes, actively preventing contact between early phagosomes and endolysosomes (Liebl & Griffiths, 2009). This evidence highlights the crucial role of healthy actin dynamics on the effector function of the innate immune system. It is also an important phenomenon to consider with regards to the specific role of LRRK2 in cargo processing, given its association with microtubules and potential control of actin rearrangement (Civiero et al., 2018; B. Kim et al., 2022; K. S. Kim et al., 2018b; Leschziner & Reck-Peterson, 2021; Snead et al., 2022).

Among the limitations of the phagolysosomal proteolysis assay described in this chapter is the lack of extracellular fluorescence quenching. The otherwise routinely used trypan blue exclusion could not be performed. As observed previously, upon binding to the BSA protein on

the reporter beads, trypan blue exhibiting strong spectral overlap with DQ Red BSA (Mosiman et al., 1997). It is therefore possible that the green fluorescence detected by flow cytometry accounted both for internalised beads as well as beads merely bound to the plasma membrane. Nevertheless, the assay provides an efficient tool to study the intracellular pathways associated with cargo phagocytosis and clearance *in vitro*.

Using the phagolysosomal proteolysis assay, I further demonstrate how the selected microglial model may impact the overall study outcome. In this chapter, iPSC-macrophages recapitulating the microglial MYB-independent ontogeny were used as a simple *in vitro* model of human microglia (Buchrieser et al., 2017; Karlsson et al., 2008; Wilgenburg et al., 2013) The differentiation protocol was developed in our lab using commercial, proprietary XVIVO medium, later replaced with an open-source OXM medium to maximise both physiological relevance and medium-composition transparency (Vaughan-Jackson et al., 2021). Compared with OXM-differentiated iPSC-macrophages, the XVIVO-macrophages had elevated levels of classical M1 (proinflammatory) markers and displayed relative insensitivity to LPS/IFNγ stimulation (Vaughan-Jackson et al., 2021). In agreement with these findings, IFNγ stimulation of XVIVO-macrophages did not significantly change their phagocytic or degradative phenotype (Figure 3.4B) In contrast, the IFNγ-stimulated OXM-macrophages appeared less phagocytic but hydrolysed more BSA per bead taken up.

IFNγ is a fundamental modulator of innate and adaptive immune system responses, exerting antiviral, antimicrobial and antitumor effects. Relatively little is known about microglial responses to IFNγ stimulation (reviewed in Kann et al., 2022). In murine microglia, IFNγ seems to increase their proteolytic enzyme secretion and oxidative burst activity (M. E. Smith et al., 1998), while decreasing myelin phagocytosis (Shen et al., 2021). Upregulation of genes involved in antigen presentation was recorded in human foetal microglia stimulated with IFNγ (Rock et al., 2005). Importantly, PD pathology is distinctly associated with an increase in IFNγ levels (Chakrabarty et al., 2011; Kustrimovic et al., 2018; Liscovitch & French, 2014; Mogi et

al., 2007; Mount et al., 2007). As LRRK2 is also one of the genes induced by IFNγ (H. Lee et al., 2020; Panagiotakopoulou et al., 2020), it was important to select for a *in vitro* cell model responsive to IFNγ stimulation. I therefore sought to switch exclusively to the OXM-macrophage differentiation protocol.

OXM-differentiation protocol yields significantly poorer number of macrophage precursors harvestable for an experimental use, probably due to increased cell adherence (Vaughan-Jackson et al., 2021). To overcome this technical limitation, I describe a novel hybrid protocol combining XVIVO-precursor culture with a terminal macrophage differentiation in the OXM medium (Figure 3.5). I show that the terminal, 7-day differentiation in OXM macrophage medium is sufficient for the hybrid macrophages to readily adopt the OXM phenotype, including OXM-like morphology, relevant phagocytic and proteolytic responses to reporter beads, cytokine secretion, and polarization capacity. The hybrid protocol allowed for continued modelling accuracy and sufficient number of cells for downstream applications, and was therefore used for all further experimental work involving iPSC-macrophages.

Finally, the phagolysosomal proteolysis assay was utilised to study the influence of LRRK2 on cargo uptake and proteolysis in iPSC-macrophages. Neither CRISPR/Cas9-induced LRRK2 KO nor pharmacological inhibition of LRRK2 in WT cells significantly impacted bead phagocytosis at 4- or 24-hour timepoint. The patient-derived G2019S iPSC-macrophages were overall less phagocytic compared with LRRK2 WT but the phenotype was not rescued by LRRK2 kinase inhibition (Figure 3.6). These results partially agree with a recent observation by Ahmadi Rastegar et al., 2022. In this study, 3-hour phagocytosis of latex beads by iPSC-macrophages produced the same outcome. However, by 16-hour timepoint, the LRRK2 KO macrophages have internalised less beads and the phagocytic uptake of G2019S cells matched that of the WT. The authors did not examine the influence of pharmacological LRRK2 inhibition on phagocytosis. It should be noted that the flow cytometry readout used in this chapter allowed for a significantly higher statistical power, analysing a minimum of 10,000 cells

per condition compared with the 250 cells assessed on average by the image-based approach in Ahmadi Rastegar et al., 2022. Compelling evidence by two studies using our lab's earlier protocol for XVIVO-differentiated iPSC-macrophages suggested LRRK2 may not be involved in the act of cargo engulfment at all (Härtlova et al., 2018c; H. Lee et al., 2020). Phagocytic uptake of beads and zymosan particles remained unaltered in both LRRK2 KO cells and LRRK2 WT cells treated with LRRKK2 kinase inhibitors. Instead, LRRK2 appeared to negatively regulate phagosome maturation upon *Mycobacterium tuberculosis* (Mtb) treatment. LRRK2 inhibition significantly increased phagosomal maturation and intra-phagolysosomal proteolytic activity, ultimately limiting Mtb replication (Härtlova et al., 2018c). In agreement with the idea that LRRK2 regulates later stages of phagocytosis, Lee et al., 2020 showed LRRK2 kinase activity-dependent recruitment of Rab8a and Rab10 GTPases to maturing phagosomes.

My results further showed increased hydrolysis of bead-conjugated DQ Red BSA label per bead taken up by G2019S iPSC-macrophages. LRRK2 WT iPSC-macrophages pre-treated with IFNγ to express high levels of LRRK2 (H. Lee et al., 2020) were more proteolytically active compared to the untreated ones, phenocopying the increased LRRK2 kinase activity in the G2019S genotype. Inhibition of LRRK2 kinase activity with Mli-2 reduced the degradation index at 24-hour timepoint in both G2019S and IFNγ-treated LRRK2 WT cells. Consistently, genetic deletion of LRRK2 led to significantly reduced proteolysis. Interestingly, the effect was only apparent at 4-hour but not at 24-hour timepoint (Figure 3.6). Overall, the results point towards a strong positive association between LRRK2 kinase activity and proteolytic degradation in phagolysosomes of IPSC-macrophages. However, these findings are in direct contrast with published literature. Proteomics analysis of isolated late phagosomes loaded with latex beads revealed a strong enrichment for genes associated with proteolytic activity in LRRK2 KO BMDMs compared to WT (Härtlova et al., 2018c). Moreover, LRRK2 KO BMDMs showed greater association of Mtb with hydrolytically-active lysosomes, as measured by LAMP-1 colocalization, and cathepsin L and D activity. Yadavalli & Ferguson, 2022 used fluid-phase

DQ BSA uptake to investigate degradation in iPSC-macrophages and microglia. Similar to Hartlova, their results indicated a negative modulation of proteolytic activity by LRRK2 in both cell types via inhibition of TFE3 transcription factor.

Overall, the inconsistencies between experimental approaches and contradictory evidence have prevented consensus in the literature on the role of LRRK2 in microglial phagocytosis and phagolysosomal proteolysis. The results presented in this chapter fit better with the proposed model of LRRK2 as a modulator of later phagocytosis stages, such as phagosomal transport, maturation, and cargo degradation. However, it is becoming increasingly evident that LRRK2 may play varying roles in specific cell type and with respect to specific stimuli. In addition, the molecular mechanisms surrounding LRRK2's involvement in cargo processing are yet to be elucidated. A focused, systematic comparison is needed in the future to help resolve these questions.

Chapter 4

Production of endotoxin-free, human recombinant 2N4R tau protein in native and aggregated form

4.1 Introduction

In the previous chapter, I completed the assessment of iPSC-macrophage baseline capacity to clear a simple phagocytic cargo. The work served as an important stepping stone to compare these findings with microglial processing of tau as a tauopathy-specific cargo.

The objective of characterising microglial response to tau required an exploratory approach with relatively high sample-throughput experiments and an extensive protocol optimisation. A need emerged for large volume of tau preparations, in native and aggregated form. Human post-mortem brains remain a precious and scarce resource to extract tau from. I, therefore, opted to utilise human recombinant tau instead, as purification of synthetic proteins offers the distinct advantage of generating high yields of pure material. Importantly, the biophysical and biochemical properties of recombinant tau have been reported to closely mimic those of native, human tau (Goedert & Jakes, 1990b).To that effect, recombinant tau has been widely utilised in the field as a substrate of choice for studies investigating its behaviour and function under physiological conditions and in disease. In addition, the composition of recombinant preparations is largely reproducible and readily quantifiable, compared with brain tissue-extracted tau preparations. The recombinant preparation can therefore provide insight into fundamental cellular responses to tau protein itself, before assessing physiologically complex, tauopathy-associated deposits composed of post-translationally modified, fibrillised tau,

aggregated with other co-factors (Arakhamia et al., 2021; Fichou et al., 2018; Fichou, Oberholtzer, et al., 2019).

The 4R tau isoforms are the predominant tau isoforms observed in tauopathy-associated aggregates (Arendt et al., 2016; Waheed et al., 2023; Zhong et al., 2012). The 4R isoforms have been also specifically associated with PD and PSP, relevant to the interest of this thesis (Flament et al., 1991; Henderson et al., 2019; Nakano et al., 2020; Poorkaj et al., 2010). For that reason, the 2N4R full-length tau isoform was chosen for recombinant production and subsequent investigation of microglial responses to tau.

To date, several protocols have been published describing the expression and purification of tau protein from *E. coli* (Barghorn et al., n.d.; Bugiani et al., 1999; Combs et al., 2017; Csokova et al., 2004; Ferrari & Rüdiger, 2018a; Goedert & Jakes, 1990b; Hasegawa et al., 1998; Karikari et al., 2017, 2020; Tepper et al., 2014). Such preparations are, however, likely to contain significant levels of residual bacterial endotoxin. Endotoxin is a type of LPS, forming a major outer-membrane component on all gram-negative bacteria, including *E. coli.* The 10-20 kDa large endotoxin monomers are composed of an outermost, bacteria strain-specific O-antigen glycan, a conserved oligosaccharide core, and Lipid A inserted in the bacterial membrane (reviewed in Raetz & Whitfield, 2002) (Figure 4.1A). Biochemically, endotoxins present as extremely heat-stable, partially phosphorylated, amphipathic molecules carrying an overall negative charge in solution. Owing to their amphipathic nature, endotoxins can assemble into supra-molecular aggregates of various sizes (up to 1,000 kDa) and shapes (Hirayama & Sakata, 2002; Petsch, 2000). During recombinant purification process from *E. coli*, endotoxin monomers are released into the solution following bacteria lysis and can stably bind protein to be purified via hydrophobic and electrostatic interactions (Berlec & Štrukelj, 2013; R. Chen, 2012). As the full length 2N4R tau protein has an overall positive charge (Mandelkow & Mandelkow, 2012), a strong binding to negatively charged bacterial endotoxin during purification process is likely (Petsch et al., 1998).

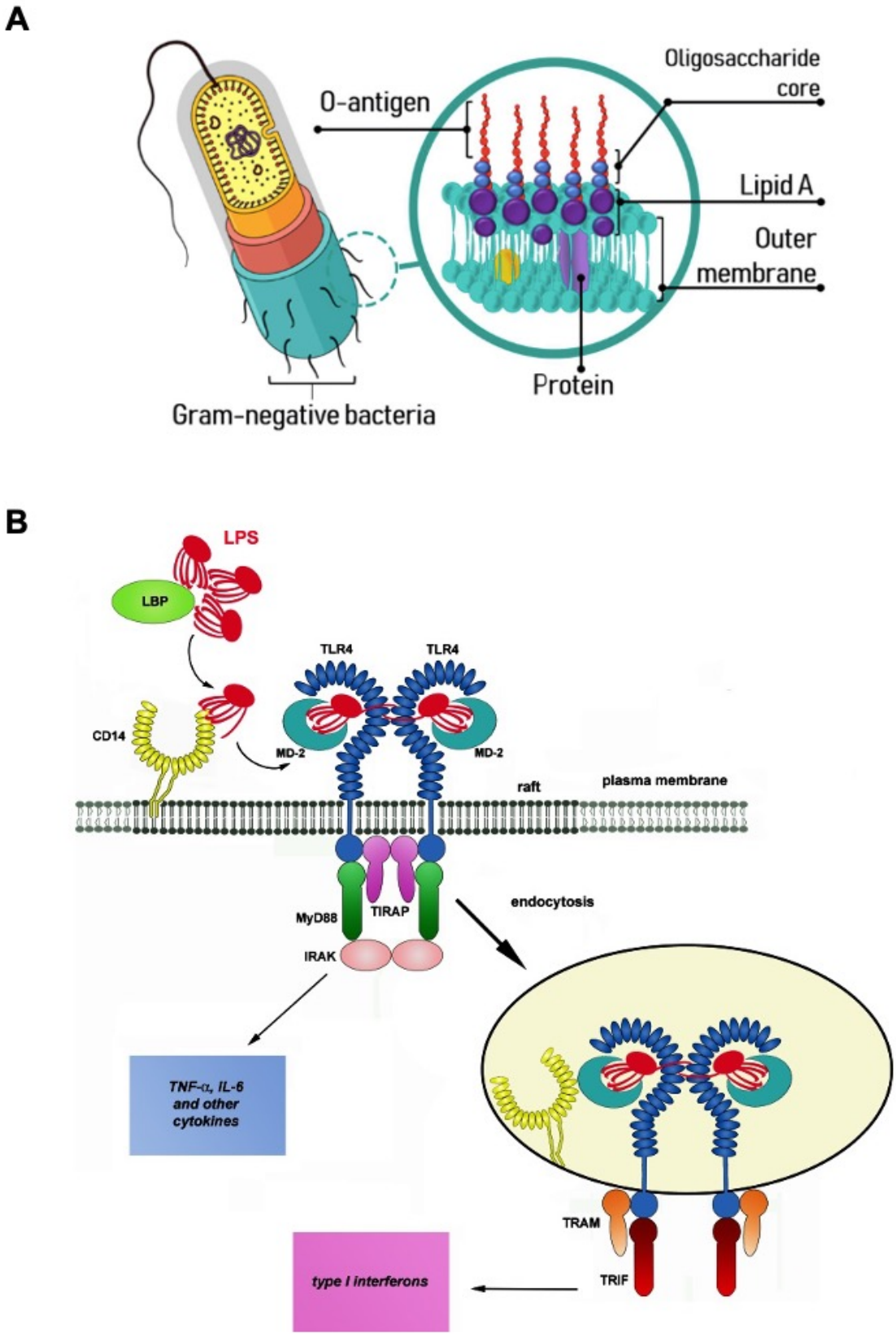

Figure legend on the next page.

Figure 4.1: LPS structure and inflammatory response orchestrated upon LPS-TLR4 activation.

(A.) LPS is a large, amphipathic component of the outer membrane of gram-negative bacteria. LPS comprises of hydrophobic Lipid A, a core oligosaccharide, and a distal polysaccharide known as O-antigen. The well-conserved Lipid A mediates LPS biological activity. Adapted from Marcano et al., 2021. (B.) Proinflammatory response induced upon activation of TLR4 by LPS. CD14 facilitates LPS transfer to TLR4/MD2 receptor complex. Dimerisation of the receptor complex triggers signalling pathways leading to the production of proinflammatory cytokines. Adapted from Plociennikowska et al., 2014.

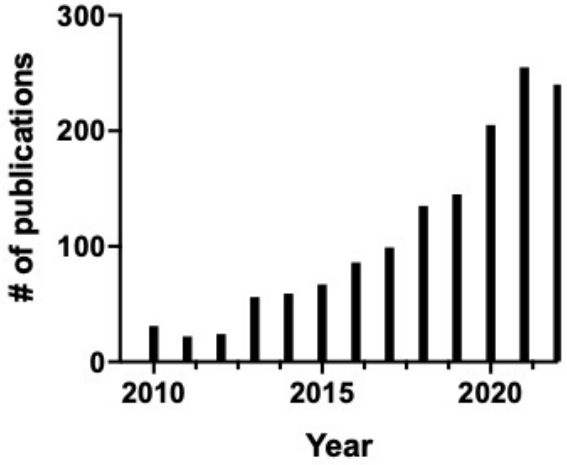

Figure 4.2: Number of publications examining the relationship between microglia and tau protein between years 2010 – 2022. Data generated by PubMed database using ‘’(microglia) AND (tau)’’ search.

Endotoxin contamination in purified tau preparation does not represent a major limitation for publications utilising cell-free approach or those applying recombinant tau to cell types of non-myeloid origin (i.e., neurons). However, near complete elimination of endotoxin is required for studies investigating microglial response to tau. This is because the cells of the innate immune system, including microglia, orchestrate a strong inflammatory response upon endotoxin stimulation, as part of the immune system's ability to detect and destroy pathogens (Akira et al., 2006; Kawai & Akira, 2010; D. Li & Wu, 2021). The response is mediated by cell-surface pattern recognition receptors (PRRs) recognising structural motifs characteristic of pathogen-associated molecular patterns (PAMPs). Myeloid cells recognise the 6-acyl chain of Lipid A synthesized by *E. coli* via the main PRR complex of CD14/toll-like receptor 4 (TLR4) / myeloid differentiation factor 2 (MD2) (Lu et al., 2008; Maeshima & Fernandez, 2013; Park & Lee, 2013; Yamamoto & Akira, 2009). The glycolipid-anchored plasma membrane glycoprotein CD14 binds and transfers LPS to the TLR4/MD2 complex. The LPS-TLR4 activation promotes MD2-dependent TLR4 internalisation and triggers the p38(MAPK)-STAT3 and NF-κB signal transduction pathways leading to a secretion of pro-inflammatory cytokines, including TNF-α, IL-6, and IL-1β. (Bode et al., 2012; T. Liu et al., 2017) (Figure 4.1B). CD14 is highly expressed by myeloid cells, making microglia exquisitely sensitive to LPS stimulation (Janova et al., 2016; Vasudevan et al., 2022). As little as 0.1 ng/mL, equivalent to 1 endotoxin units/mL (EU/mL) induces TNF-α proinflammatory cytokine production in microglia (Kim & Li, 2013). In the event of endotoxin entering a bloodstream of a host organism, the immune system's inflammatory response can culminate in fever, intravascular coagulation, and ultimately sepsis and death (Beutler & Rietschel, 2003; M. Wilson et al., 2001).

The interest in microglial processing of tau protein has grown over the last decade, evident by the steady increase in number of publications (data generated by PubMed database using ''(microglia) AND (tau)'' search) (Figure 4.2). Amongst the published studies, several incubated *in vitro* microglia cultures with recombinant tau (summarised in Table 4.1). Surprisingly, only one study out of the 14 found, provided demonstrable evidence of using endotoxin-free tau

preparation. Four studies tested their preparations for the level of endotoxin but not all disclosed the results. Those that did, indicated endotoxin contamination higher than generally acceptable (i.e., ≤ 0.01 EU/mL, Haenseler, Zambon, et al., 2017; S. Liu et al., 2012) to avoid triggering the TLR4 response (i.e., <1 EU/mL in Wang et al., 2022, and between 14-95 EU/mL in Pampuscenko et al., 2020, 2021). Pampuscenko et al attempted to control for the endotoxin contamination using polymixin B, an antibiotic binding and neutralising LPS.

Altogether, the evidence shown in studies that have failed to report and/or address the endotoxin contamination is hard to interpret. It is yet to be determined whether the observed effects were tau-specific or due to the endotoxin inflammagen co-presented with tau.

The main focus of the work described in this chapter was therefore to address these methodological limitations and generate high yield of endotoxin-free, recombinant tau preparation as a pre-requisite for examining authentic microglial response to the tau protein.

Publication	Recombinant tau source	Endotoxin removal methods used	Endotoxin detection test	Test results provided
Asai et al., 2015	rPeptide (T-1001-1), *E. coli* purification	N	N	N
Zhu et al., 2022	AnaSpec (AS-55556), *E. coli* purification	N	N	N
Udeochu et al., 2023	non-disclosed	N	N	N
Perea et al., 2022	ClearColi purification	Y	Y	N/A
Funk et al., 2015	*E. coli* purification	N	N	N
Ising et al., 2019	*E. coli* purification	N	Y	N
Stancu et al., 2019	*E. coli* purification	N	N	N
Pampuscenko et al., 2020	*E. coli* purification	N	Y	Y (0.001-0.007% w/w LPS/tau)
Zilkova et al., 2020	*E. coli* purification	Y	N	N
Das et al., 2020	*E. coli* purification	N	N	N
Pampuscenko et al., 2021	*E. coli* purification	N	Y	Y (0.001-0.007% w/w
Jin et al., 2021	*E. coli* purification	N	N	N
Wang et al., 2022	*E. coli* purification	N	Y	Y (<1 EU/mL in working concentration)
Chinnathambi and Das, 2023	*E. coli* purification	N	N	N

Table 4.1: Endotoxin contamination of recombinant tau preparations used in published studies

4.2 Results

4.2.1 Endotoxin removal from purified recombinant tau preparation represents a major challenge

Human recombinant 2N4R tau was generated by Donatella Di Rienzo at the ODDI, using an adaptation of the original tau purification protocol by Goedert & Jakes, 1990. The method involved a combination of immobilised nickel ion affinity chromatography followed by 6xHis-tag cleavage, with SEC to maximise protein purity (Figure 4.3A). Details of the tau expression plasmid pNIC28-Bsa4_6xHis-tag_TauWT 2N4R can be found in section 2.3.1. The preparation was kindly gifted to me in order to investigate microglial responses to tau protein. However, the preparation was found to contain high endotoxin levels (i.e., 83.47 EU/mL) Figure 4.3C) following an assessment with FDA-approved, gold-standard LAL assay (L. Chen & Mozier, 2013). Therefore, the first approach taken was to test the efficacy of commercially available endotoxin-removal reagents to reduce the endotoxin contamination in recombinant tau preparation to acceptable levels.

Two, widely-used endotoxin removal columns exploiting distinct separation methods were used in the test (Figure 4.3B). Column A (Pierce^{TM} High Capacity Endotoxin Removal Spin Column, 88275) guarantees 2,000,000 EU/mL binding capacity, >99% endotoxin removal, and simultaneous 85% protein recovery. The column matrix is composed of porous cellulose beads covalently modified with cationic ε-poly-L-lysine polymer, trapping the negatively charged endotoxin. As a naturally occurring, food-grade antimicrobial produced by fermentation, ε-poly-L-lysine serves as a safer alternative to the reportedly toxic, polycationic polymixin B, an antibiotic traditionally used for endotoxin decontamination (Bhor et al., 2005). Column B (Endotrap®, Lionex, LET0009) cites best-in-class binding capacity of 5,000,000 EU/mL, removal of 99.9% endotoxin, and higher than 95% sample recovery. The precise column resin composition is proprietary but according to the manufacturer, it is based on a bacteriophage-derived protein, neither polymixin B nor antibody, binding specifically the endotoxin core region conserved across all gram-negative bacteria with high affinity.

Recombinant tau samples were passed through the columns according to the respective manufacturer's instructions. Sterile PBS used to normalise protein concentration was also run through the columns as a negative control. Procedures were carried out in the tissue culture class 2 containment cabinet to avoid introducing further contamination. All buffers were sterile-filtered or sterile, and all labware used was certified pyrogen-free. Endotoxin concentration in the samples was determined with the LAL assay.

Only 5% endotoxin removal was achieved using Column A, 12% with Column B (Figure 4.3C). Neither increasing the sample-resin contact time to an overnight incubation at 4°C nor recycling the sample through the columns up to three consecutive times improved the removal efficiency. As a comparison, human recombinant α-syn (rPeptide, S-1011-1), also purified from *E. coli*, was passed through the columns following the manufacturer's recommendations. Baseline endotoxin levels in α-synuclein preparation before removal were about 50% lower compared with tau. Column A provided 89% removal, whilst column B removed 98% of the endotoxin.

These results confirmed the general efficacy of both columns in removing endotoxin from recombinantly expressed proteins but specifically not from the tau preparation, suggesting a particularly strong endotoxin interaction with tau.

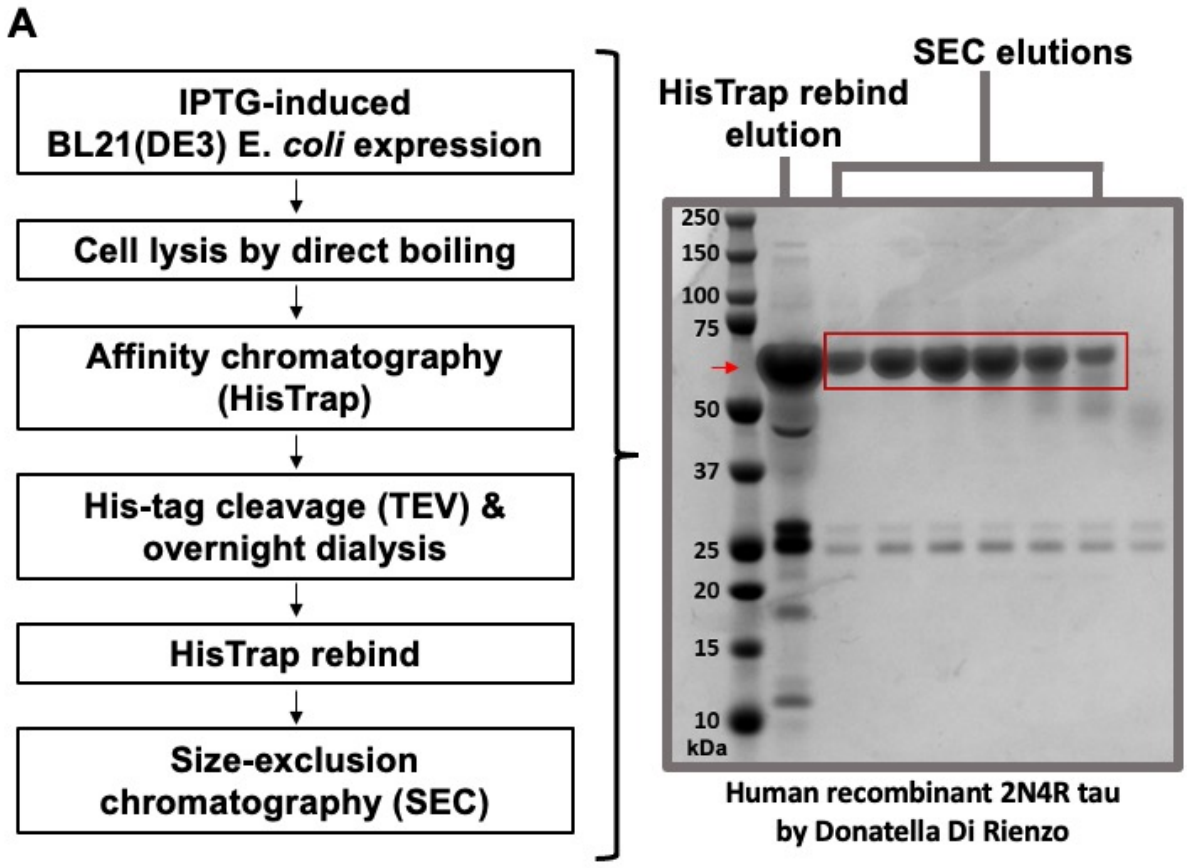

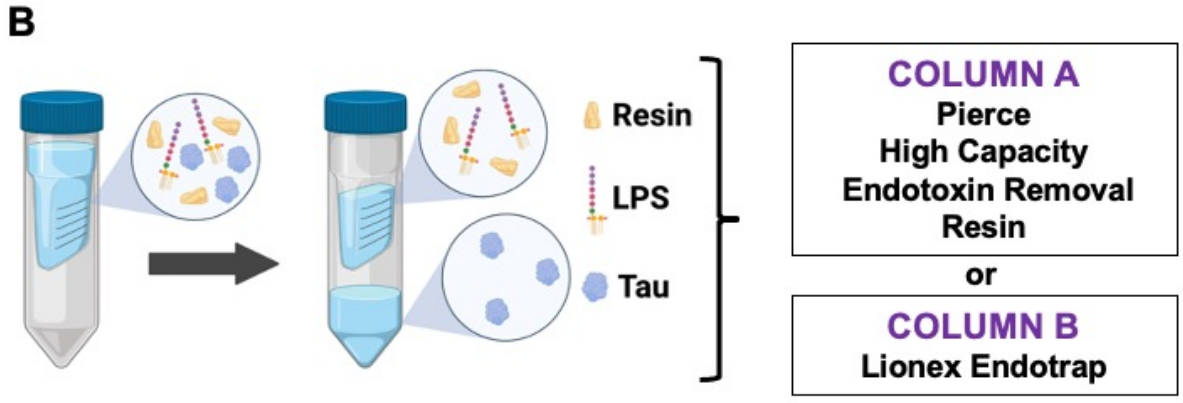

C

			Recombinant 2N4R Tau	Recombinant α-syn	Sterile PBS
Endotoxin levels (EU/mL)	Before endotoxin removal		83.47	46.17	<0.01
	After endotoxin removal	Column A	79.19	4.95	<0.01
		Column B	73.7	0.81	<0.01

Figure legend on the next page.

Figure 4.3: Commercially available endotoxin removal columns fail to remove endotoxin from recombinant tau purified with standard method

(A.) Human recombinant 2N4R tau purification workflow and SimplyBlue™-stained gel depicting final eluted fractions. Work was carried out by Donatella Di Rienzo at the ODDI. Tau is an intrinsically disordered protein with hydrodynamic radius larger than that of a globular protein of similar size, therefore tau MW on a gel is higher than the one predicted (45 kDa) (cite Churion and Bondos). (B.) Workflow diagram of endotoxin removal from tau purified in (A.) using commercially-available products. (C.) LAL assay results showing endotoxin levels (EU/mL) in recombinant tau purified in (A.) and recombinant a-syn gifted by Dr. Nora Bengoa-Vergniory at DPAG, University of Oxford. Protein levels were normalised to 1 mg/mL in sterile PBS.

4.2.2 Endotoxin-free tau purification from ClearColi BL21(DE3) electrocompetent cells provides poor yield

In the absence of an effective, commercially-available method for endotoxin depletion from purified recombinant tau, I next explored the use of ClearColi^{TM} BL21(DE3) cells, an alternative, low-endotoxin protein expression system. ClearColi^{TM} cells have been genetically modified through a series of strain deletions to express Lipid IV_A in place of the regular Lipid A. Lipid IV_A is composed of only 4-acyls instead of the characteristic Lipid A 6-acyl chain recognised by the TLR4 receptor (Figure 4.4A). Lipid IV_A contamination in the purified protein preparation therefore completely bypasses triggering the formation of TLR4-MD-2 complex and downstream proinflammatory signalling in mammalian cells (Mamat et al., 2015).

A pilot tau purification from ClearColi was carried out. 6xHis-tag-TauWT 2N4R expression plasmid was extracted from Mach1 T1^{R} *E. coli* stock donated by Donatella Di Rienzo and transformed into ClearColi by electroporation (section 2.3.1 and 2.3.2). The workflow selected for ClearColi tau expression and purification was identical to the one outlined in Figure 4.3A with two modifications (Figure 4.4B). Specifically, direct boiling cell lysis was replaced with French Press high-pressure cell homogenisation as a preferred technique traditionally used for high volume cell extrusion. The cost-effective and protein yield-sparing cation exchange chromatography (CIEX) was chosen in place of SEC. Detailed expression and purification steps including the list of buffers and elution steps are described in section 2.3.3.

A substantial 6 L volume of bacterial culture provided only a total of 173 µg of concentrated tau protein (Figure 4.4B). The yield was insufficient for downstream *in vitro* application. Therefore, other avenues of producing endotoxin-free recombinant protein had to be investigated.

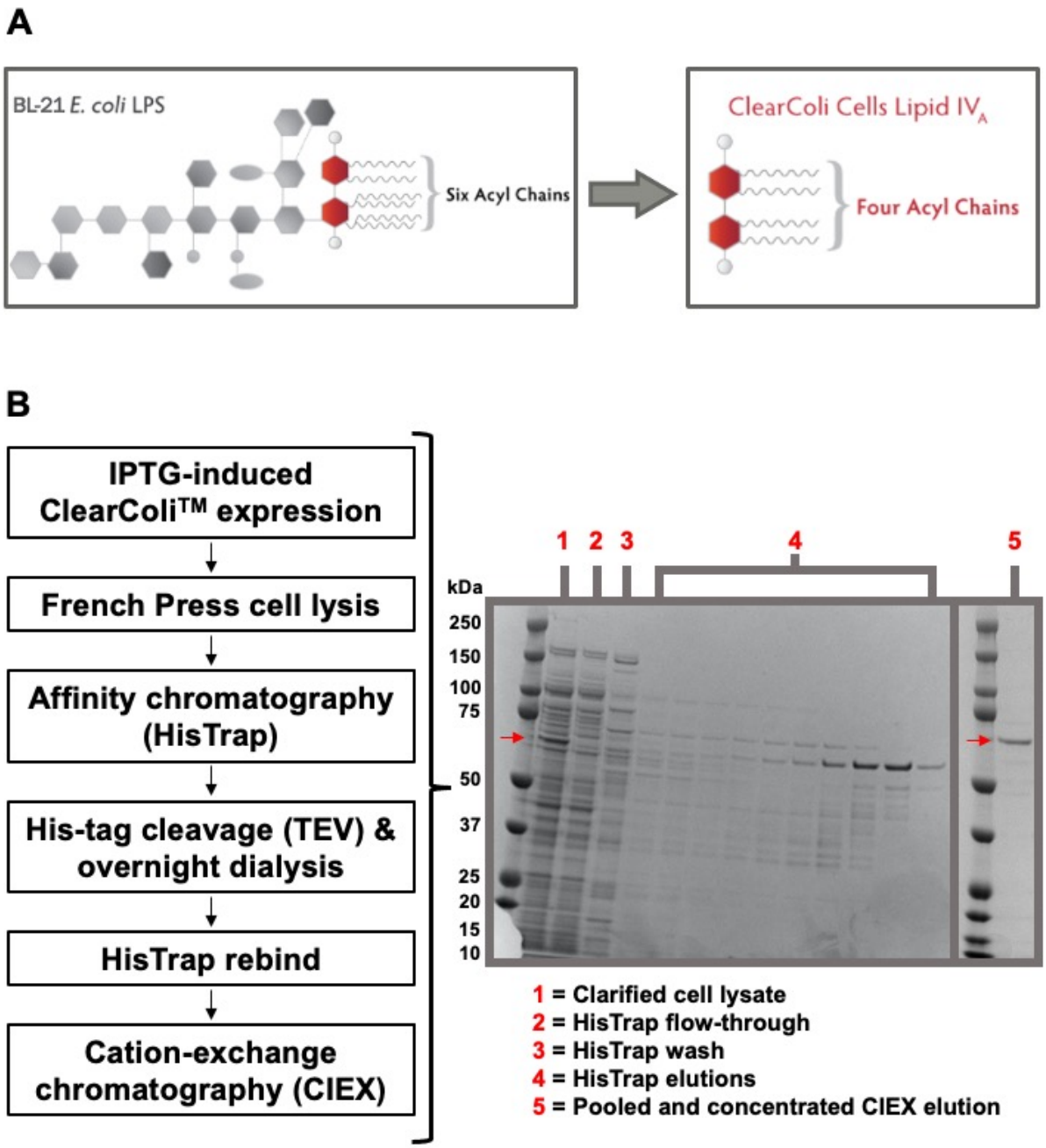

Figure 4.4: Human recombinant 2N4R tau purification from ClearColi™ BL21(DE3) produces poor yield

(A.) ClearColi cells have been genetically modified to express only four acyl chains of the normally 6-acyl Lipid A to avoid triggering the endotoxin response in human cells by TLR4/MD2 complex activation. Image adapted from https://clearcoli.com/technology. (B.) Workflow of tau purification from ClearColi and SimplyBlue™-stained gels depicting eluted fractions. Red arrows point to the bands of interest. 6 L bacterial culture yielded a total of 173 µg of recombinant tau.

4.2.3 Endotoxin-free tau purification from standard BL21(DE3) *E. coli*

Both endotoxin depletion and high yield of tau were critical to continue any work pertinent to this thesis. Since the discovery of recombinant DNA technology, purification from standard *E. coli* cells has remained the simplest, most cost-effective way of producing large quantities of recombinant proteins. The failure to dissociate the strongly-bound endotoxin from purified tau, however, still presented a challenge. I therefore sought to identify a method eliminating endotoxin during rather than after the purification workflow.

The use of non-ionic TritonX-114 detergent is one of the oldest and most effective methods cited to date for removal of endotoxin from purified protein and plasmid DNA preparations (S. Liu et al., 1997). It was first described in 1981 for the purpose of separating amphiphilic membrane proteins from hydrophilic proteins in crude cell extracts, based on its property to undergo phase separation into an aqueous and detergent phase at temperatures above its cloud point (20°C) (Bordier, 1981). The method got later adapted for protein endotoxin decontamination (Aida & Pabst, 1990). Below 20°C, Triton X114 dissociates endotoxin from the protein of interest. Above 20°C, the dissociated, hydrophobic endotoxin precipitates into the detergent phase while the hydrophilic protein remains in the aqueous solution. The initial protocol required multiple, time-consuming cycles of temperature changes. In addition, traces of TritonX-114 remained in the protein preparations, adversely affecting downstream *in vitro* applications. A novel, one-step protocol combining affinity chromatography with TritonX-114 on-column wash step at 4°C was recently described, showing efficient endotoxin reduction of up to 99% and near 100% protein recovery in six separate preparations of varying chemical properties (Reichelt et al., 2006a).

I tested the feasibility of this protocol for endotoxin-free purification of tau. Standard BL21(DE3) *E. coli* cells were transformed with the 6xHis-tag-TauWT 2N4R expression plasmid used for tau purification from ClearColi (section 4.2.2.). The same purification workflow was repeated, with the addition of 0.1% TritonX-114 wash step immediately after the clarified lysate application to HisTrap column (Figure 4.5A, section 2.3.3). LAL assay results confirmed the

protocol was successful at removing the majority of endotoxin from tau already after the first purification step (Figure 4.5B). Standard affinity chromatography lacking the detergent wash can result in protein elution contaminated with upward of 10^3 EU/mL (Reichelt et al., 2006a). In contrast, tau eluted from the HisTrap column with TritonX-114 wash contained only 13.77 EU/mL. The endotoxin concentration was further reduced to 5.4 EU/mL after elution from the CIEX column. Final passage of concentrated tau through Pierce™ High Capacity Endotoxin Removal Spin Column eliminated the remaining endotoxin from tau preparation to below detection level of 0.01 EU/mL.

A total of 3.5 mg of endotoxin-free tau was purified from 6 L bacterial culture, demonstrating the efficacy of this method. Multiple protein bands were detected following SDS-PAGE of the final tau preparation, initially raising concerns about the protein purity. However, subsequent tryptic in-gel digestion and peptide mass fingerprinting (PMF) matched the peptides only to tau protein sequence (Figure 4.5C). LC-MS analysis of intact tau in solution revealed a successful cleavage of the 6xHis-tag and a match to the theoretical 2N4R MAPT amino acid sequence (441aa + an additional serine linker at the artificial N-terminus) (Figure 4.5D). Additionally, C-terminal tau truncation (378aa) was identified, explaining the presence of low-MW contaminants on SimplyBlue™-stained gel.

A

IPTG-induced BL21(DE3) expression

↓

French Press cell lysis

↓

Affinity chromatography (HisTrap) with TritonX-114 wash

↓

His-tag cleavage (TEV) & overnight dialysis

↓

HisTrap rebind

↓

Cation-exchange chromatography (CIEX)

↓

Protein concentration

↓

Endotoxin removal column

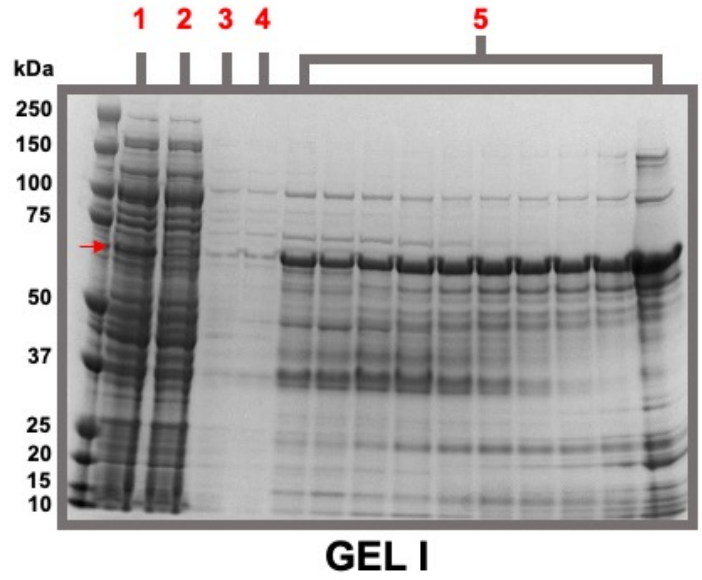

GEL I

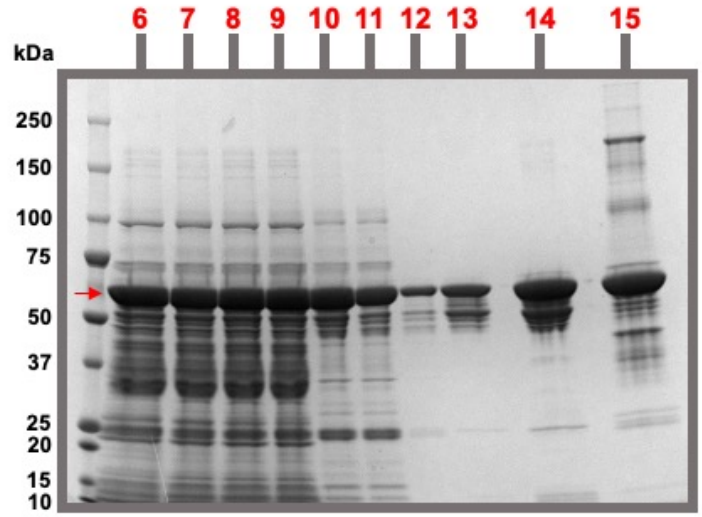

GEL II

1 = Clarified cell lysate
2 = HisTrap flow-through
3 = HisTrap TritonX-114 wash
4 = HisTrap standard wash
5 = HisTrap elutions
6 = Pooled HisTrap elution pre-dialysis
7 = Post-dialysis (1:200 TEV:protein)
8 = Post-dialysis (1:100 TEV:protein
9 = Post-dialysis (1:50 TEV:protein)
10 = Pooled HisTrap rebind elutions
11 = CIEX flow-through
12 = CIEX wash
13 = Pooled CIEX elution
14 = Concentrated CIEX elution, post endo-removal
15 = Recombinant tau by D. Di Rienzo (Figure 4.1)

Figure continued on the next page

B

	Clarified lysate (1)	HisTrap elution (6)	CIEX elution (13)	Concentrated CIEX elution (14)	Sterile ddH2O
Endotoxin levels (EU/mL)	>1 (above detection)	13.77	5.4	<0.01 (below detection)	<0.01 (below detection)

C

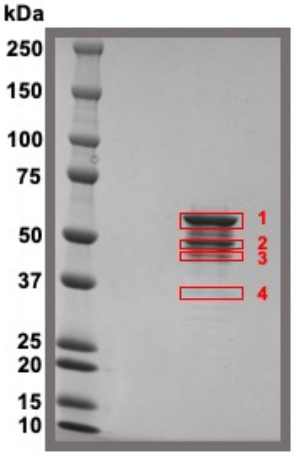

Sample code	Database	Mascot Score	Title	Annotation
Band 1	Swissprot sequences (top 5)	225	Microtubule-associated protein tau OS=Homo sapiens GN=MAPT P	MAPT only
		85	Trypsin OS=Sus scrofa PE=1 SV=1	
		57	30S ribosomal protein S19 OS=Rickettsia prowazekii (strain M	
		57	30S RIBOSOMAL PROTEIN S19 OS=RICKETTSIA PROWAZEKII (STRAIN	
		49	DNA-DIRECTED RNA POLYMERASE SUBUNIT BETA" OS=PHYSCOMITRELL	
Band 2	Swissprot sequences (top 5)	323	Microtubule-associated protein tau OS=Homo sapiens GN=MAPT P	MAPT only
		48	Ribonuclease PH OS=Haemophilus ducreyi (strain 35000HP / ATC	
		43	Flagellar P-ring protein OS=Wolinella succinogenes (strain A	
		43	FLAGELLAR P-RING PROTEIN OS=WOLINELLA SUCCINOGENES (STRAIN	
		42	N-acetylmuramic acid 6-phosphate etherase OS=Clostridium bot	
Band 3	Swissprot sequences (top 5)	80	Microtubule-associated protein tau OS=Homo sapiens GN=MAPT P	MAPT only
		60	Nuclear hormone receptor family member nhr-18 OS=Caenorhabdi	
		52	ATP synthase gamma chain OS=Xylella fastidiosa (strain 9a5c)	
		51	ATP SYNTHASE GAMMA CHAIN OS=XYLELLA FASTIDIOSA (STRAIN 9A5C	
		51	HEAVY METAL-BINDING PROTEIN HIP OS=MYTILUS EDULIS PE=1 SV=1	
Band 4	Swissprot sequences (top 5)	96	Microtubule-associated protein tau OS=Homo sapiens GN=MAPT P	MAPT only
		74	Uncharacterized protein MPN_440 OS=Mycoplasma pneumoniae (st	
		60	UNCHARACTERIZED PROTEIN MPN_440 OS=MYCOPLASMA PNEUMONIAE (S	
		59	Uncharacterized protein MAL13P1.304 OS=Plasmodium falciparum	
		54	UNCHARACTERIZED PROTEIN MAL13P1.304 OS=PLASMODIUM FALCIPARU	

D

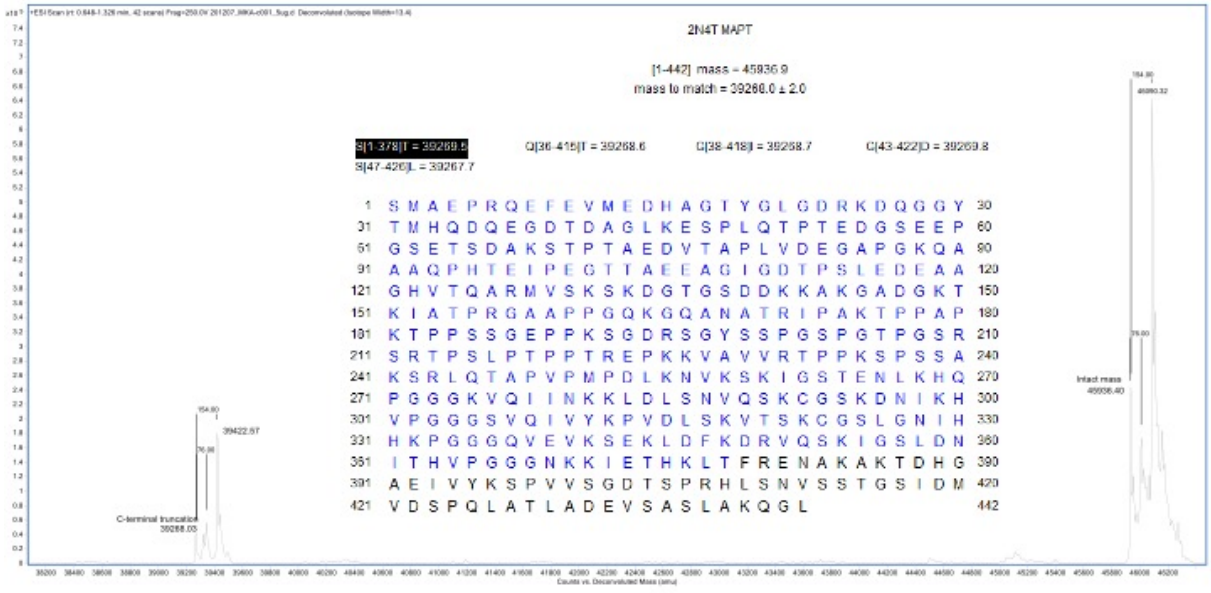

Figure legend on the next page.

Figure 4.5: Combination of affinity chromatography with on-column TritonX-114 detergent wash effectively removes the majority of endotoxin contaminants from tau purified from standard BL21(DE3) E. coli

(A.) Purification workflow and SimplyBlue™-stained gels depicting eluted fractions. Red arrows point to the bands of interest. 6 L bacterial culture yielded a total of 3.5 mg of recombinant tau. Recombinant tau purified by standard, non-endotoxin free purification method by Donatella Di Rienzo (Figure 4.2A) was including on the gel for a reference. (B.) LAL assay results showing endotoxin levels (EU/mL) in individual purified tau fractions. Numbers in red correspond to fractions described in (A.). Protein levels were normalised to 1 mg/mL in sterile ddH_2O. (C.) SimplyBlue™-stained gels showing bands excised for trypsin-digested in-gel protein analysis by LC-MS/MS. Mascot software was used for protein identification from peptide sequence databases. (D.) Results of intact protein characterisation by LC/MS.

4.2.4 Protocol optimisation for the production of endotoxin-free, full-length tau protein in high yield

The presence of truncated products in purified tau preparation fitted the published observations of tau's propensity to truncate (Csokova et al., 2004; Karikari et al., 2017).This occurs most likely due to tau's intrinsically disordered nature (Jeganathan et al., 2008; Mukrasch et al., 2005b; Schwalbe et al., 2014). The lack of well-defined structure in solution makes tau particularly vulnerable to recombinant host proteases targeting foreign material for degradation (Graether, 2022; Rozkov & Enfors, 2004; Uversky, 2002). The most common troubleshooting for proteolytic degradation of IDPs involves recombinant host lysis by direct boiling. The host proteins including proteases denature and aggregate while the hydrophilic IDPs with no structure to lose, remain soluble (Graether, 2022).

Other methods include secretion by the host system into medium (reviewed in Kleiner-Grote et al., 2018), the use of protease inhibitors (Prouty & Goldberg, 1972) or gene fusion systems (Costa et al., 2014; Murby et al., 1996). Multiple fusion systems cloned between the tag and the protein N-terminus have recently been developed to protect against proteolytic degradation via translocation of the fused protein away from the protease-rich cytosol to a different cellular compartment of the recombinant host (Varshavsky, 1996). One such widely-used system is the 6xHis_SUMO (small ubiquitin-like modifier) fusion (Butt et al., 2005; Malakhov et al., 2004). In addition to proteolytic protective effect, SUMO with its amphipathic, detergent-like structure aids the solubility of otherwise insoluble proteins (Butt et al., 2005). Finally, unlike TEV proteases recognising a very short sequence, SUMO proteases (e.g., SENP2) target its tertiary structure, thus offering a highly efficient and specific cleavage, and enabling the release of proteins with desired N-terminus (Marblestone, 2006) (Figure 4.6A).

In the next steps, I therefore sought to explore the 6xHis_SUMO fusion expression system to further optimise recombinant tau yield, remove the non-native aa at the N-terminus post TEV protease tag cleavage, and to eliminate the C-terminus truncated products in the purified preparation.

First, SUMO_TauWT 2N4R_pETM11SUMO3_sense expression plasmid was created using Gibson assembly (section 2.3.1, Figures 2.4 and 2.5), and transformed into BL21(DE3) *E. coli* cells. Subsequently, conditions for optimal tau expression and extraction were investigated. 1 L overnight bacteria culture expressing SUMO_TauWT 2N4R_pETM11SUMO3_sense plasmid was divided into 12 equal aliquots at OD_{600} = 0.6 and subjected to varying IPTG induction concentrations, post-induction expression temperatures, and cell lysis methods. French press homogenisation was replaced with sonication due to the small cell culture volume. Clarified cell lysates were applied to SDS-PAGE and total protein was visualised with SimplyBlue™ stain (Figure 4.6B). 4-hour bacteria growth at 37°C increased tau expression compared to overnight growth at 18°C. 0.5 mM IPTG induction was found to be the best for tau expression at 37°C. The increased temperature seemed to have favoured tau aggregation but a cell lysis by a combination of sonication with direct boiling effectively removed the larger as well as some of the lower MW products.

Purification from 6 L of SUMO_TauWT 2N4R expressing BL21(DE3) *E. coli* was carried out based on the optimised conditions identified in Figure 4.6B. Figure 4.7A shows the selected workflow steps and corresponding elutions visualised on a SimplyBlue™-stained gel. A total yield of 9.1 mg of tau protein was purified and subsequently confirmed endotoxin-free by LAL assay (Figure 4.7B). A few low-MW protein bands additional to the one predicted for tau were still visible on a gel but subsequent PMF confirmed 100% tau sequence match (Figure 4.7C). The SUMO gene fusion system did not eliminate tau C-terminal truncation completely but notably reduced its abundance compared to 6xHis-tagged tau system, according to the LC-MS analysis (Figure 4.7D vs Figure 4.5D).

This purified and QC-ed tau batch was either fibrillised (see section 4.2.5) or aliquoted, snap-frozen in LN, and used in all subsequent experiments in chapter 5.

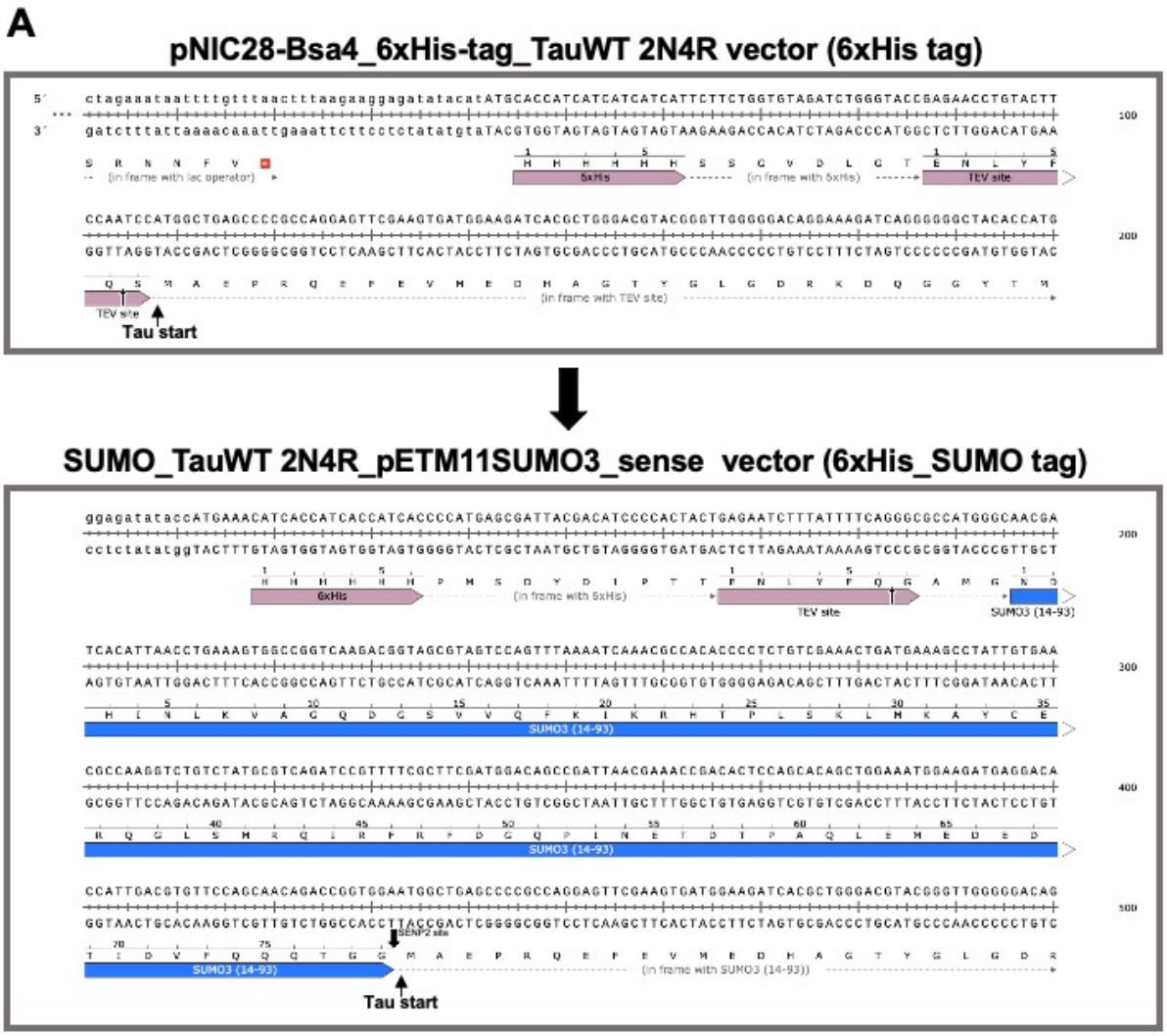

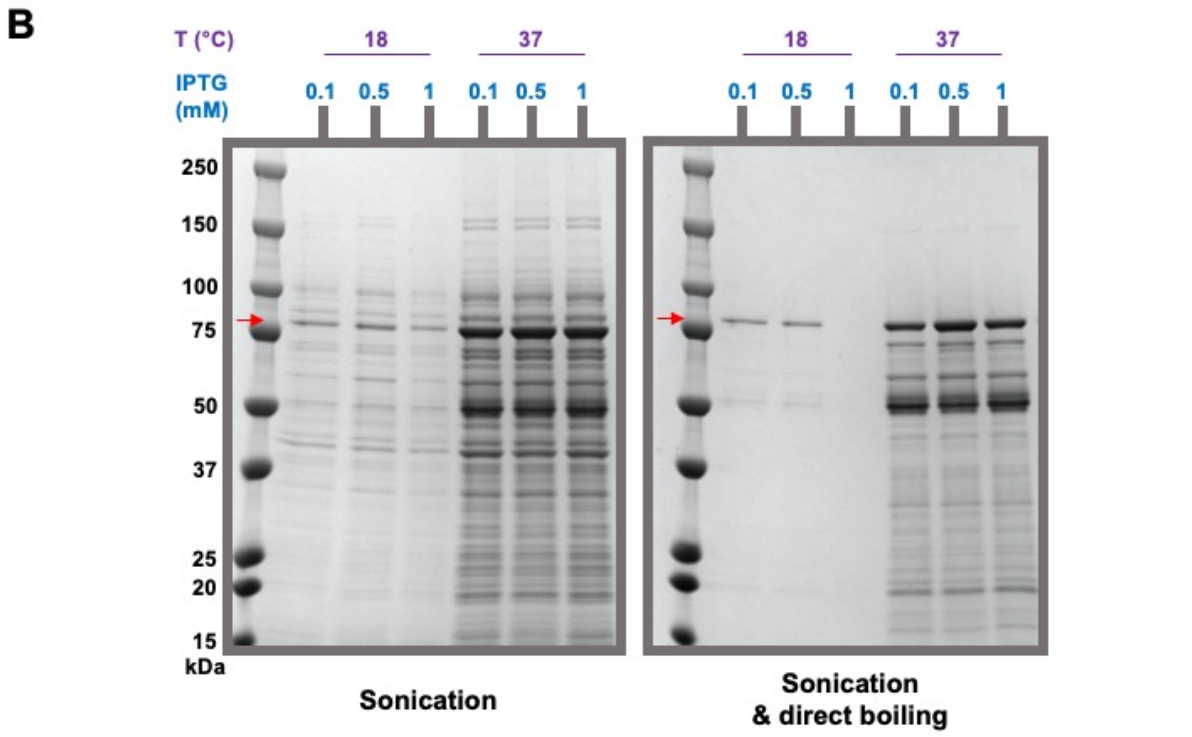

Figure legend on the next page.

Figure 4.6: Optimisation of 2N4R tau expression in SUMO_TauWT 2N4R_pETM11SUMO3_sense-transformed BL21(DE3) cells

(A.) DNA sequences of 6xHis- and 6xHis_SUMO-tagged tau expression vectors. 2N4R tau coding sequence was cloned into the pETM11SUMO3_sense vector to prevent truncation during purification, aid solubility, and to remove artificial N-terminus created by TEV protease cleavage site. (B.) SimplyBlue™-stained gels comparing the effect of varying IPTG concentration, expression temperature, and cell lysis methods on tau protein expression and purity.

A

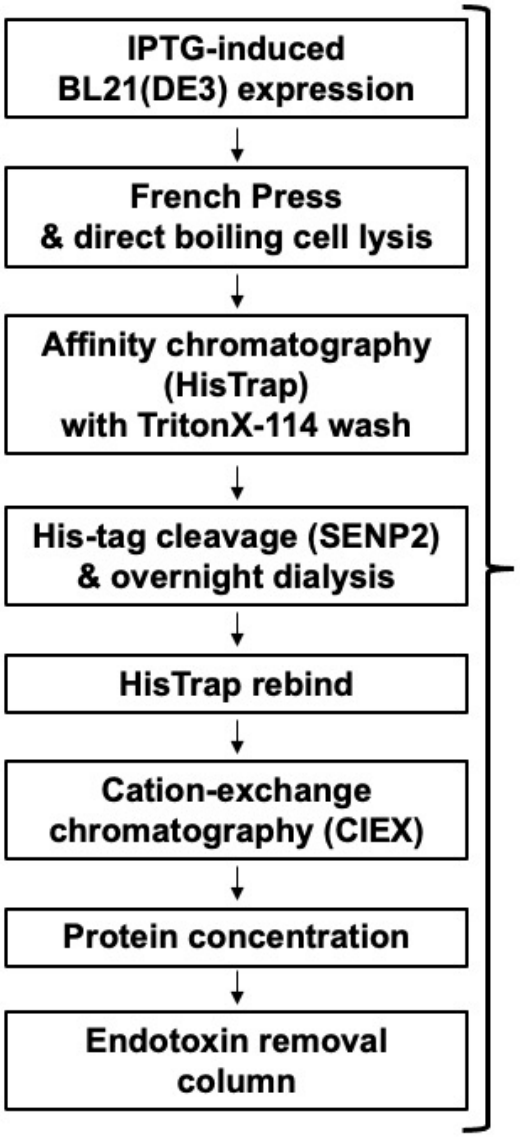

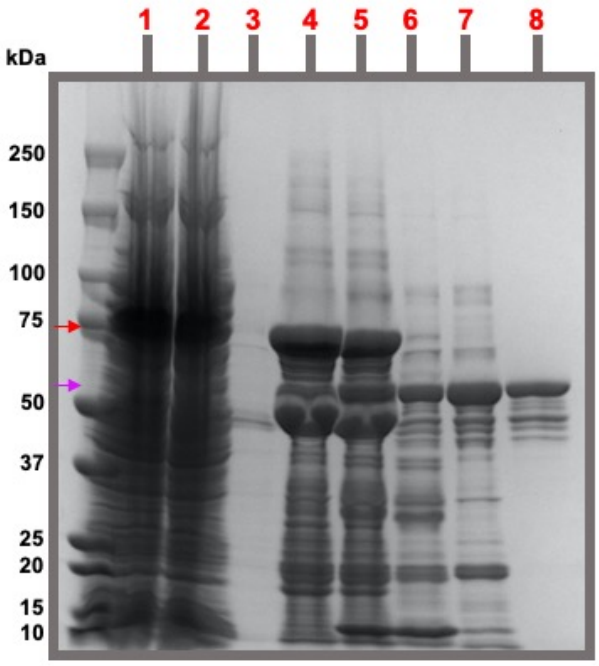

1 = Clarified cell lysate
2 = HisTrap flow-through
3 = HisTrap TritonX-114 wash
4 = Pooled HisTrap elution pre-dialysis
5 = Post-dialysis (1:300 SENP2:protein)
6 = Post-dialysis (1:100 SENP2:protein)
7 = Pooled HisTrap rebind elution
8 = Concentrated CIEX elution, post endo-removal

B

	Clarified lysate (1)	HisTrap elution (4)	CIEX elution (not shown)	Concentrated CIEX elution (8)	Sterile ddH2O
Endotoxin levels (EU/mL)	>1 (above detection)	12.26	6.68	<0.01 (below detection)	<0.01 (below detection)

Figure continued on the next page

C

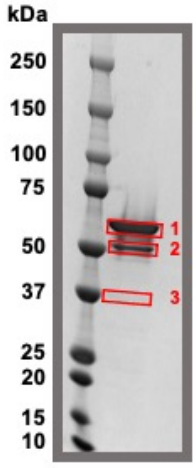

Sample code	Database	Mascot Score	Title	Annotation
Band 1	Swissprot sequences (top 5)	514	Microtubule-associated protein tau OS=Homo sapiens OX=9606 G	MAPT only
		102	Trypsin OS=Sus scrofa OX=9823 PE=1 SV=1	
		56	Proline--tRNA ligase OS=Picrophilus torridus (strain ATCC 70	
		54	Kinesin-like protein KIF15 OS=Strongylocentrotus purpuratus	
		53	KINESIN-LIKE PROTEIN KIF15 OS=STRONGYLOCENTROTUS PURPURATUS	
Band 2	Swissprot sequences (top 5)	445	Microtubule-associated protein tau OS=Hylobates lar OX=9580	MAPT only
		174	Trypsin OS=Sus scrofa OX=9823 PE=1 SV=1	
		69	TRYPSIN OS=SUS SCROFA OX=9823 PE=1 SV=1	
		61	DISEASE RESISTANCE PROTEIN RPP5 OS=ARABIDOPSIS THALIANA OX=	
		54	UPF0102 protein DICTH_1420 OS=Dictyoglomus thermophilum (str	
Band 3	Swissprot sequences (top 5)	250	Microtubule-associated protein tau OS=Hylobates lar OX=9580	MAPT only
		182	Trypsin OS=Sus scrofa OX=9823 PE=1 SV=1	
		77	TRYPSIN OS=SUS SCROFA OX=9823 PE=1 SV=1	
		54	Protein-methionine-sulfoxide reductase heme-binding subunit	
		51	PROTEIN-METHIONINE-SULFOXIDE REDUCTASE HEME-BINDING SUBUNIT	

D

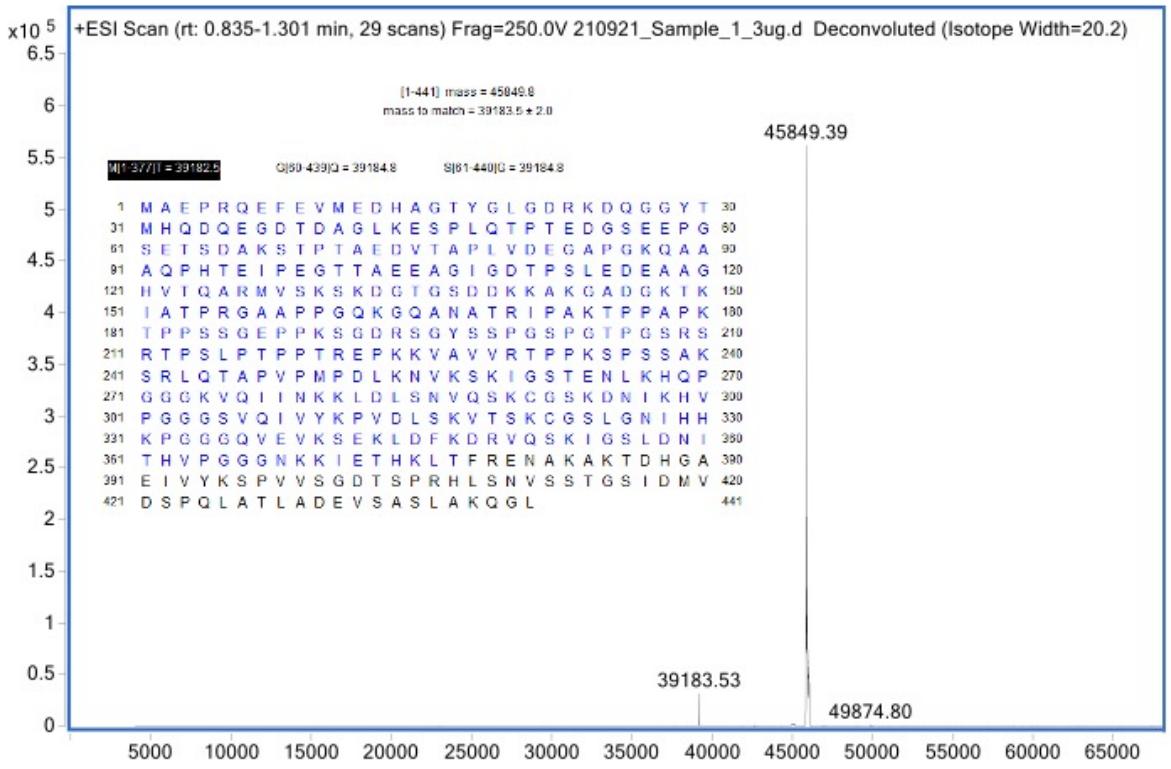

Figure legend on the next page.

Figure 4.7: Tau purification using the SUMO_TauWT 2N4R_pETM11SUMO3_sense construct further improves yield of endotoxin-free tau

(A.) Purification workflow and SimplyBlue™-stained gels showing eluted protein fractions. Red arrow points to the tagged tau, purple arrow points to the tag-less tau post SENP2 cleavage. 6L bacterial culture yielded a total of 9.1 mg of recombinant tau. (B.) Endotoxin levels (EU/mL) in individual purified tau fractions, determined by LAL assay. Numbers in red correspond to fractions shown in (A.). Protein levels were normalised to 1 mg/mL in sterile ddH2O. (C.) SimplyBlue™-stained gels depicting bands excised for trypsin-digested in-gel protein analysis by LC-MS/MS. Protein identification from peptide sequence databases was performed using Mascot software. (D.) Results of intact protein characterisation by LC/MS.

4.2.5 Production of *in vitro* aggregated tau fibrils

Native, unfolded tau assembly into amyloidogenic, cross-β-sheet-structured filaments underlies the pathological signature of tauopathies (Berriman et al., 2003; Goedert et al., 2017; Y. Wang & Mandelkow, 2016). With an optimised protocol for the production of endotoxin-free tau monomer, I next aimed to generate fibrillar tau preparation which is more relevant to the form of tau observed in diseased brains.

Truncated forms of tau efficiently self-assemble into filaments (Crowther et al., 1992; Wille et al., 1992). In contrast, full-length 2N4R requires the addition of negatively-charged co-factors, such as RNA, arachidonic acid, or heparin (Friedhoff et al., 1998; Goedert et al., 1996a; Kampers et al., 1996; Pérez et al., 2002; M. Wilson et al., 2001). Of those, heparin has been widely utilised in the field to investigate the kinetics and potential inhibitors of tau aggregation (reviewed in Fichou et al., 2019).

To facilitate tau fibril formation, recombinant monomeric tau purified as indicated in section 4.2.4 was mixed with heparin at the established optimal stoichiometric ratio of 4 tau molecules per 1 heparin molecule (section 2.3.4) (Figure 4.8A). Aggregation kinetics was monitored at regular intervals with ThT assay (section 2.3.5) (Figure 4.8B). Increase in ThT fluorescence confirmed successful conformation change of soluble tau in mostly random coil formation to β-sheet-rich ordered assemblies induced by heparin. ThT maxima plateau was observed after 7 days. On day 11, negative stain TEM microscopy further visually validated presence of tau fibrils in the preparation (Figures 4.8C and D).

One of the intrinsic features of tau aggregates is their capacity for a seeding behaviour, i.e., the ability to template the distinct conformation onto unfolded monomeric tau substrate (reviewed in Goedert et al., 2017). The seeding competency of heparin-induced *in vitro* generated tau fibrils was assessed with 4R tau RT-QuIC assay (section 2.4.9) in collaboration with Alessia Santambrogio at the University of Cambridge. Unlike recombinant monomeric tau, the synthetic tau fibrils induced aggregation of truncated tau substrate, as confirmed by the

characteristic kinetic curve with a discernible lag phase, followed by an exponential growth and stationary phase (Figure 4.8E) (Kamath et al., 2021).

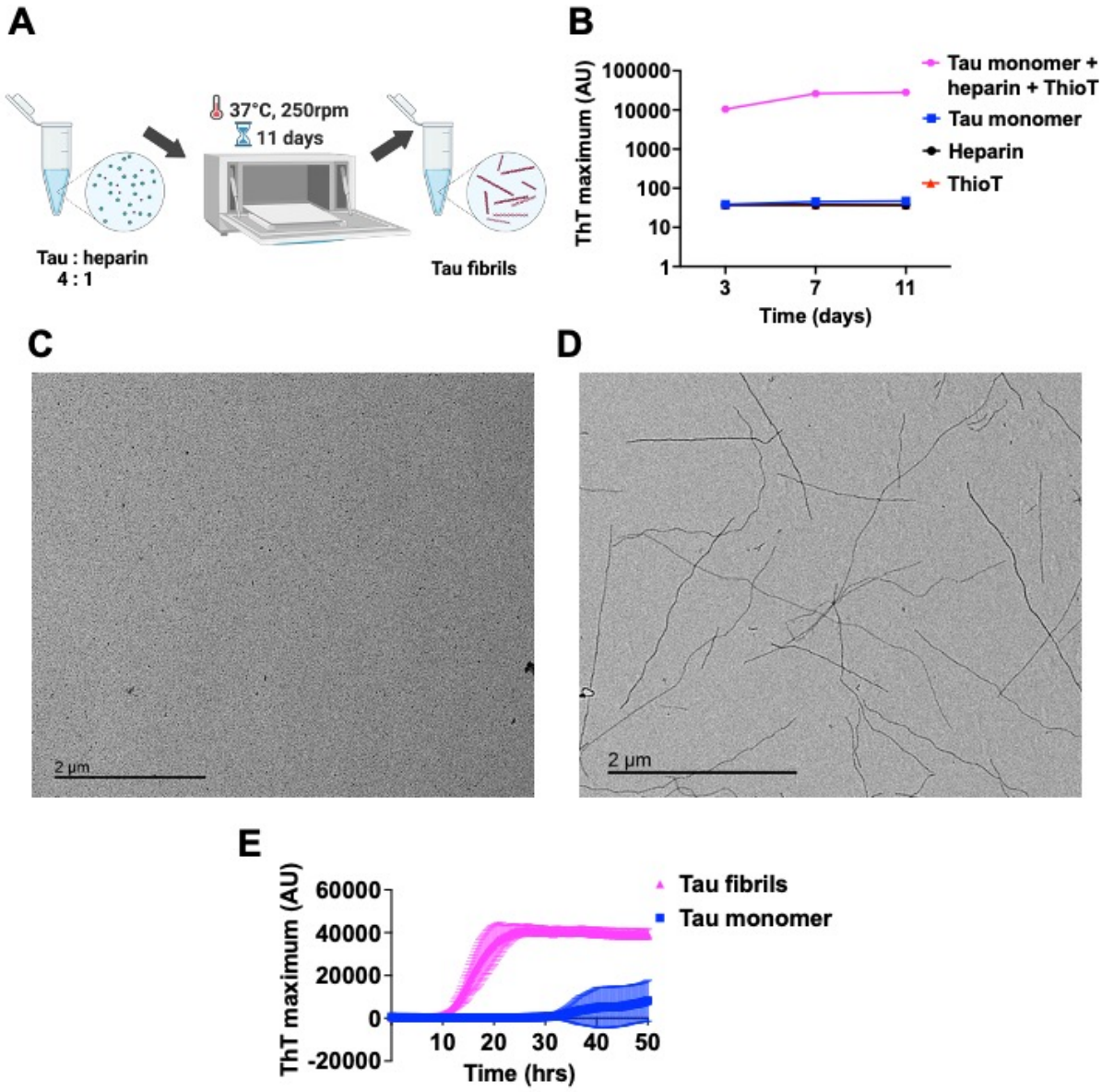

Figure 4.8: Heparin-induced in vitro aggregation of recombinant tau monomer generates tau fibrils

(A.) Workflow diagram. (B.) ThT assay confirming presence of b-sheet structures in recombinant tau preparation, purified as per section 4.2.4 and aggregated with heparin. Negative stain TEM images of recombinant tau monomer (C.) and heparin-aggregated tau fibrils (D.). (E.) Results of 4R tau RT-QuIC assay investigating seeding of truncated tau substrate (K11, tau aa residues 244-394) in presence of purified recombinant tau monomer or heparin-induced fibrils. 4 technical replicates were run per condition. Data is presented as mean±SD.

4.3 Discussion

In this chapter, I present an original protocol for the production of endotoxin-free 2N4R human recombinant tau monomer, and the monomer-derived, *in vitro* aggregated seeding-competent tau fibrils.

All six individual tau isoforms were first recombinantly expressed and purified from *E. coli* by Goedert & Jakes in 1990. Since then, multiple adaptations of the protocol have been published (Barghorn et al., n.d.; Bugiani et al., 1999; Combs et al., 2017; Csokova et al., 2004; Ferrari & Rüdiger, 2018a; Goedert & Jakes, 1990b; Hasegawa et al., 1998; Karikari et al., 2017, 2020; Tepper et al., 2014). All used *E. coli* as the preferred expression host of choice and various chromatography methods or combinations thereof to produce full-length or truncated version of tau. None so far have, however, demonstrated endotoxin concentration compatible with *in vitro* assays investigating microglial response to tau.

The absence of controlling for endotoxin contamination can be explained by a number of reasons. Firstly, the issue of endotoxin contamination needs no addressing for *in vitro* applications of tau to pure cultured neurons or other cell types lacking the TLR4 receptor recognising endotoxin molecules and triggering the innate immune response (Beutler & Rietschel, 2003; Zettel et al., 2017).

Secondly, endotoxins are highly heat and pH stable (Raetz & Whitfield, 2002). Thus, endotoxin removal from recombinant protein preparation typically involves an elaborate and expensive procedure with limited results (reviewed in Miyamoto et al., 2009). Several endotoxin removal methods have been described over the years. Common chromatography approaches, such as immobilised divalent metal (typically Ni^{2+}) affinity chromatography and ion exchange, exploit endotoxin's formation of aggregates that readily adsorb onto cationic surfaces with their exposed, negatively charged phosphate group (Anspach & Hilbeck, 1995; Gorbet & Sefton, 2005; Kozlowski, 2017; Mack et al., 2014; Ongkudon et al., 2012). These methods are, however, only applicable for tagged or net negatively-charged proteins, and risk product loss

due to adsorption. Diverse, convenient-to-use columns have also been developed, packed with beads modified with affinity ligands for endotoxin, including polymyxin B, ε-poly-L-lysine, L-histidine, poly(γ-methyl L-glutamate), activated charcoal, or bacteriophage-derived protein. Other methods utilise detergent-based phase separation, sucrose-gradient centrifugation, or ultrafiltration. Care must be taken particularly using the latter two, as the protein preparations can get easily damaged by physical forces in the process. The following reviews summarise the pros and cons of each of the individual methods in detail: S. Liu et al., 1997; Magalhães et al., 2007; Petsch, 2000; Schneier et al., 2020; Serdakowski London et al., 2012.

The majority of endotoxin removal methods lack broad applicability, as the specific steps must always be adjusted to the biochemical properties of the particular protein to-be-decontaminated. The precise mechanisms by which endotoxins bind various proteins aside from the PRRs are not completely understood. Interactions with neutral and acidic proteins have been shown, ascribed to hydrophobic interactions or possibly the formation of calcium bridges (Petsch, 2000). Electrostatic interactions are thought to underlie the binding of endotoxin to net positive-charged proteins, driving the formation of stable complexes and making endotoxin molecules inaccessible for removal (Petsch, 2000; Reichelt et al., 2006b). In line with the hypothesis, endotoxin removal from basic proteins was shown to be less efficient compared with acidic proteins (Petsch et al., 1998). Our results demonstrating failure to remove high levels of endotoxin contamination from recombinant, net positive-charged tau purified from *E. coli* using two independent affinity columns fit this observation (Figure 4.2).

Complete or near complete endotoxin elimination is required for *E. coli*-derived tau incubation with CD14- and TLR4-expressing myeloid cells, including microglia. Recent recognition of microglial role in neurodegenerative diseases (reviewed in Bartels et al., 2020; X. Chen & Holtzman, 2022; Hickman et al., 2018; Kumari & Gensel, 2023; Odfalk et al., 2022) drove an increase in studies investigating microglial response to tau. The majority, however, failed to show sufficient evidence for endotoxin elimination from their recombinant tau preparations.

I first tried to overcome this limitation by purifying tau from ClearColi, a genetically modified *E. coli* strain that expresses biologically inert version of the immune response-inducing Lipid A. Contrary to the published claims (Mamat et al., 2013), the method did not generate product yield comparable with purification from standard *E. coli* cells (Figure 4.3). This occurred most likely due to the previously-observed slow growth kinetics of the cells and could be potentially bypassed in the future by optimisation of the cell culture conditions (Hunt et al., 2019).

I next returned to purification from standard *E. coli* strain, verified to produce tau quantities sufficient for further *in vitro* work (KrishnaKumar & Gupta, 2017). To eliminate the endotoxin, I adapted a published one-step protocol combining Ni-NTA affinity chromatography with 0.1% TritonX-114 on-column wash step (Reichelt et al., 2006b). The on-column TritonX-114 wash step attenuates protein loss occurring during standard, post-purification endotoxin removal methods. In addition, it increases depyrogenation efficiency by minimising tau-endotoxin contact time and therefore an opportunity for strong interaction. Our results confirmed successful elimination of the majority of endotoxin from tau eluted from the HisTrap column (Figure 4.5B). This method requires a use of 6xHis-tagged tau expression construct which could be perceived as a disadvantage. The tag can, however, be easily removed with an additional overnight cleavage and dialysis step.

Two additional steps were added to the purification protocol; CIEX to increase tau purity, followed by the use of Pierce™ High Capacity Endotoxin Removal Spin Column to achieve a complete endotoxin elimination. LAL assay results subsequently confirmed endotoxin concentration below detection levels (<0.01 EU/mL) in the final preparation.

A substantial amount of tau truncation occurred during the early versions of the purification process, despite the continuous presence of protease inhibitors in all relevant buffers (Figure 4.5). This could most likely be explained by the intrinsically disordered nature of tau, rendering the protein vulnerable to the heterologous host's proteases (Suskiewicz et al., 2011; Uversky, 2019). I attempted to circumvent the issue by cloning tau coding sequence into pET SUMO

expression vector. The plasmid features an N-terminal SUMO3 protein fusion with traditional 6xHis-tag under the standard T7 promoter. Compared with the classical 6xHis-tag, SUMO fusion system favours protein yield by facilitating increased protein solubility and decreased proteolytic degradation by host proteases (Butt et al., 2005; Graether, 2022; Marblestone, 2006). In addition, the high specificity of SUMO proteases enables more precise tag cleavage compared with TEV protease, enabling a release of an authentic protein N-terminus with methionine as the first aa. Finally, the 6xHis_SUMO tag cleavage efficiency can be immediately confirmed by gel electrophoresis unlike cleavage of 6xHis-tag, on account of the more pronounced size differences between the tagged and untagged protein (Figures 4.5A and 4.7A).

Interestingly, 4-hour tau expression at 37°C showed more favourable results compared with overnight expression at 18°C during a pilot expression optimisation experiment. The higher temperature promoted formation of aggregates, in agreement with previous observations (Figure 4.6B). The aggregates were, however, subsequently efficiently removed during the purification process.

Overall, the SUMO system reduced but did not completely eliminate the problematic tau truncation, as evident by LC-MS analysis results (Figure 4.7D). Further separation by SEC could have been utilised to maximise purity but the risk of further product loss outweighed the benefits. Several strategies could be trialled in the future to eliminate the tau truncation completely. The majority of proteolytic degradation occurs during cell lysis (Ryan & Henehan, 2017). French Press homogenisation is used traditionally to lyse large volumes of bacterial cultures. However, the length of time required to lyse cells with homogenisation is sufficient for proteases to degrade the protein of interest, despite presence of protease inhibitors in the cell lysis buffer. Using direct boiling method exclusively to extract the thermostable tau, instead of a combination of French Press and direct boiling as in this thesis, could help reduce the degree of tau degradation by denaturing the bacterial proteases. In addition to the cell lysis method,

CIEX buffer pH optimisation has been reported to significantly influence tau purity with lower pH buffers promoting increased elution of truncated tau products (Ferrari & Rüdiger, 2018b).

Purification of the 6xHis_SUMO-tagged construct from a 6 L bacterial culture yielded 9.1 mg of endotoxin-free tau; that is 2.6-times more product compared with the 6xHis-tagged version (Figures 4.5 and 4.7). The yield was sufficient for the purpose of this thesis. However, the protein quantity could be potentially further improved upon. The final endotoxin removal step using Pierce™ High Capacity Endotoxin Removal Spin Column results in 10% tau loss. This process could potentially be eliminated by optimising the efficacy of TritonX-114 on-column wash step, either by increasing the number of CV washes or performing several consecutive washes alternating with non-detergent buffer wash.

Self-propagating activity is one of fundamental features of pathological, aggregated tau (Goedert & Spillantini, 2019). Clinically, tau pathology spreads throughout neuroanatomically-connected brain regions in a predictable spatio-temporal manner, correlating with the progression of cognitive decline (Goedert et al., 2017; Mudher et al., 2017; Vogels et al., 2020). It was, therefore, important to verify that the purified tau monomer is aggregation- and seeding-competent. Incubation of the monomer with polyanionic cofactor heparin at 37°C with constant orbital shaking induced formation of β-sheet rich tau aggregates, confirmed by the increase in ThT fluorescence and also by negative-stain TEM (Figures 4.7B-D). The fibril formation was in line with previous studies reporting heparin-induced conformation change from random coils to β-sheet filaments in the two aggregation-protein hexapeptide motifs present on tau MBD-region (Berriman et al., 2003; von Bergen et al., 2000, 2005). Furthermore, the *in vitro* aggregated tau fibrils facilitated fibrillizations of monomeric tau fragment in an 4R RT-QuIC assay, thus validating their seeding capacity (Figure 4.7E) (Saijo et al., 2020b).

While the heparin-induced aggregation is a convenient, simple, scalable *in vitro* method for producing tau fibrils, it does not completely reproduce the structure and composition of tau aggregates *in vivo*. The heparin-induced tau fibrils are structurally heterogeneous and capable

of transitioning between at least four conformations. This is in contrast with the brain-derived tau fibrils that adopt a disease-characteristic, stable conformation (Fichou et al., 2018; Morozova et al., 2013; Zhang et al., 2019 Arakhamia et al., 2021; Falcon et al., 2018, 2019; Fitzpatrick et al., 2017; Shi et al., 2021; Zhang et al., 2020). The synthetic tau fibrils are also more resistant to chemical denaturation or proteolytic digestion (Morozova et al., 2013), and display reduced seeding potency compared with the brain-derived fibrils, on account of their overall increase in stability (Falcon et al., 2015). The heparin-induced fibrils show weak affinity for RNA, unlike *in vivo* tau fibrils that were found to extensively associated with RNA and other co-factors (Ginsberg et al., 1997; Jiang et al., 2021). Lastly, unlike the recombinant tau purified from *E. coli,* endogenous tau undergoes extensive PTMs *in vivo*, which heavily influence the protein's biophysical properties, function, and aggregation (Arakhamia et al., 2021; Lövestam et al., 2022; Wesseling et al., 2020b).

The issue of physiological relevance could potentially be overcome by replacing heparin with tauopathy-specific, brain-extracted tau aggregate to propagate relevant fold onto the recombinant tau preparation (Ficulle et al., 2022; Kraus et al., 2019b; Narasimhan et al., 2017b). This is the aim in the next phase of the project, though beyond the scope of this thesis. In the meantime, heparin-induced recombinant tau fibrils still represent a convenient and reproducible method allowing us to gain mechanistic insight into tau aggregation kinetics and the cellular response to the aggregates.

Chapter 5

Characterisation of microglial response to tau protein in native and aggregated form

5.1 Introduction

Having successfully developed a method for purification of endotoxin-free human recombinant tau, and its aggregation to fibrillar form, I focused on the final aim of the thesis; the investigation of microglial response to tau protein.

As discussed in sections 1.7 and 1.8, evidence from the past decade consistently highlights the importance of microglia in tauopathies (reviewed in Chen & Holtzman, 2022; Heneka, 2019; Salter & Stevens, 2017)). Post-mortem tissue analyses (Imamura et al., 2003; Minett et al., 2016; Parachikova et al., 2007; Perez-Nievas et al., 2013) and PET studies have demonstrated a strong association between microglial phenotypic changes, pathological tau deposition, and clinical disease presentation (Cagnin et al., 2001, 2006; Crotti et al., 2014; Dani et al., 2018; Gerhard et al., 2004, 2006a; Pascoal et al., 2021; Terada et al., 2019). Genetic studies showed a large number of tauopathy-associated risk variants is expressed highly or exclusively within microglia (Andersen et al., 2021; Efthymiou & Goate, 2017; Farrell et al., 2022; Langston et al., 2022). Whether microglia directly propagate tau pathology is, however, still unclear. Functional studies are needed to elucidate the precise mechanisms, timing, and consequences of microglial response in tauopathies.

The majority of functional studies investigating the topic has been carried out in rodents, largely due to the limited availability of primary human microglia or protocols for relevant *in vitro* microglia models. Some findings have been informative (summarised in section 1.8). Asai et al., 2015 and van Olst et al., 2020 demonstrated tau uptake by microglia *in vivo*. Following tau

internalisation, rodent microglia actively secreted seeding-competent tau encased in EVs to the extracellular space (Asai et al., 2015; Clayton et al., 2021; Crotti et al., 2019; B. Zhu et al., 2022). Exposure to extracellular tau *in vitro* further promoted microglial phagocytosis of living neurons (Butler et al., 2021; Pampuscenko et al., 2020) but repeated incubation with phospho-tau bearing neurons induced hypophagocytic and senescent microglial phenotype (J. H. Brelstaff et al., 2021). Microglia-specific pharmacological depletion significantly reduced tau propagation in two mice models of tauopathy (Asai et al., 2015).

Together, the findings help provide an insight into the potential mechanisms by which microglia may affect tau pathogenesis. However, as discussed in section 1.10, rodent microglia do not accurately recapitulate human physiology. In addition, the majority of rodent tauopathy models rely on the overexpression of hTau protein (reviewed in Ren et al., 2015), and as such, offer limited value in understanding of the disease pathogenesis.

Recent advances in iPSC technology in combination with genome editing strategies have created an unprecedented platform for studying the role of human microglia in tauopathies. We now have the opportunity to study the impact of tauopathy-associated gene variations on a molecular level, selectively manipulate individual variables to understand the mechanisms of microglial response to tau, and conduct high-throughput screens, all in a more authentic and relevant cell model. Studies using iPSC-microglia and pathogenic tau are already under-way. In a proof-of-concept study, Abud et al., 2017 demonstrated that iPSC-microglia internalise and direct AD brain-derived tau oligomers into the intracellular acidic compartments. Furthermore, Udeochu et al., 2023 showed that aggregated tau can induce cGAS-STING-IFN type 1 inflammatory and anti-viral pathway in iPSC-microglia, potentially underlying the loss of cognitive resilience through reduction in neuronal MEF2C transcription network. However, it should be noted that this study did not use demonstrably endotoxin-free tau protein (see section 3.1).

Crucially, the mechanisms surrounding uptake and clearance of pathogenic tau by iPSC-microglia have never been systematically investigated. In addition, no study has inspected the role of LRRK2 protein in microglial tau processing despite its reported risk for PD development (Nalls et al., 2014a, 2019; Paisán-Ruíz et al., 2004; Simón-Sánchez et al., 2009; Zimprich et al., 2004) and PSP progression ((Herbst et al., 2022; Jabbari et al., 2021; Sanchez-Contreras et al., 2017), association with enhanced tau seeding (Cornblath et al., 2021; Nguyen et al., 2018), macrophage and microglial cargo trafficking (H. Lee et al., 2020; Z. Liu et al., 2020; Moehle et al., 2015), endolysosomal pathway perturbations (Erb & Moore, 2020; Madureira et al., 2020), and overall innate inflammatory responses (I. Russo et al., 2022; Wallings & Tansey, 2019) (see section 1.9 for details). Such studies are critical though, as they may help provide mechanistic insight into the microglial role in tauopathies and uncover potential druggable targets for translation into the clinic.

I address the need in this chapter, using iPSC-macrophages and microglia to characterise microglial functional responses to endotoxin-free, human recombinant 2N4R tau protein in its monomeric and aggregated form. I hypothesize that impaired clearance of internalised tau by microglia may contribute to prion-like tau spreading in tauopathies. I therefore focus the investigation on tau uptake, clearance, and seeding capacity of tau processed by microglia (Figure 5.1). Additionally, I explore the influence of microglial LRRK2 on the aforementioned processes.

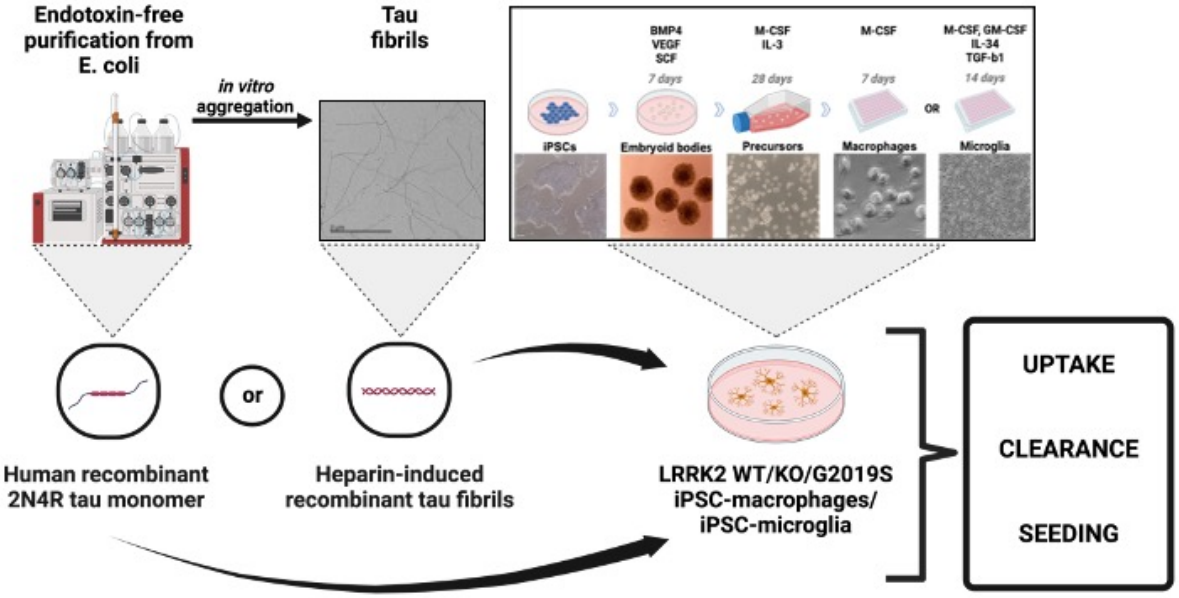

Figure 5.1: Workflow diagram

5.2 Results

All experiments described within this chapter were first carried out using iPSC-macrophages as a simpler surrogate for iPSC-microglia, as previously explained in section 3.2. Some of the critical findings were also reproduced in the iPSC-microglia model. However, time constraints did not all for verification of all findings using both cell models, despite best efforts.

5.2.1 iPSC-macrophages and microglia internalise tau in monomeric and aggregated form

Tau uptake by healthy control-derived iPSC-macrophages and microglia was first visualised using overnight, live, time-course confocal microscopy (Figures 5.2A and B). Image inspection confirmed an overlap between DyLight 488-conjugated tau monomer and fibrils (section 2.3.6), and CellTracker-labelled cytoplasm or LysoTracker-labelled acidic intracellular compartments (section 2.1.7). A considerable portion of tau fibrils appeared to have lined the cell surface, raising questions about microglial ability to fully internalise tau fibrils. Scanning and transmission electron microscopy techniques were therefore selected next to inspect tau fibril uptake at higher resolution. iPSC-macrophages were incubated with vehicle or tau fibrils overnight, and prepared for image acquisition as described in sections 2.4.5 and 2.4.6. Image analyses revealed frequent tau fibril tethering to the cell plasma membrane (Figures 5.2C and E, blue arrows). Red arrows in Figures 5.2D and E point at a potential process of tau fibril uptake. The fibrils appeared to have associated with cell surface but the overall fibril length may have negatively affected the rate of internalisation by iPSC-macrophages. Though beyond the scope of this thesis, the impact of fibril size on uptake by microglia should be systematically investigated in the future. Sonication could be used to generate shorter fibrils. However, biochemical and biophysical properties of the sonicated preparation should be carefully characterised as tau and other amyloid fibril sonication has been reported to produce a mixture of small aggregates and potentially toxic oligomeric species rather than intact, shorter fibrils (Ghag et al., 2018).

Trypan blue fluorescence quenching in combination with flow cytometry readout was examined next to optimise the quantitation of internalised tau monomer and fibrils. Trypan blue is a cell-impermeable azo dye reported to absorb light emitted by the green-yellow fluorescent compounds. It is widely used to quench cellular autofluorescence or extracellular green-fluorescent signal emitted by surface-bound but non-internalised molecules (Graham et al., 2013; Shilova et al., 2017). Following a 6-hour incubation of healthy control-derived iPSC-macrophages with DyLight 488-conjugated tau monomer or fibrils, cells were fixed and harvested for a flow-cytometry analysis (section 2.4.2) in presence or absence of 2.5% trypan blue solution (Figure 5.3A). 488 nm laser with 525/40 detection channel was used to detect the DyLight 488 signal. Figure 5.3B describes the gating strategy. Untreated cells were analysed first to identify the single-cell and tau-negative populations (Figure 5.3B, ‘’Cells only’’ row). Tau-treated samples were analysed next to select for the tau-positive population (Figure 5.3B, ‘’Tau monomer incubation’’ and ‘’Tau fibril incubation’’ rows). Extracellular fluorescence quenching with trypan blue significantly reduced MFI of DyLight 488-tau fibril-positive population but not tau monomer-positive population (Figure 5.3C). These results confirmed the presence of non-internalised tau fibrils at the cell surface and highlighted the need for trypan blue extracellular fluorescence exclusion for an accurate quantitation of tau fibril internalisation. The protocol was therefore adopted in all further experiments.

Tau concentration used thus far, 10 µg/mL (~200 nM for the 2N4R tau isoform), was based on the published literature (Andersson et al., 2019; Asai et al., 2015). While it did not affect cell viability (Figure 5.3D), such concentration is likely higher than physiological. The precise extracellular tau concentration in the human brain is unknown but currently estimated in high pico- to low nanomolar range, based on *in vivo* microdialysis experiments measuring tau levels in the interstitial and cerebrospinal fluid of mice transgenic for human tau (Yamada et al., 2011). Therefore, to optimise the exogenous tau concentration for further use, iPSC-macrophages were treated with 0.1, 1, and 10 µg/mL of tau monomer or fibrils (~ 2, 20, and 200 nM respectively) for 6 hours, and tau internalisation was assessed by flow cytometry.

Significantly higher tau monomer and fibril internalisation was observed after cell treatment with 10 compared with 1 μg/mL treatment but no significant difference was detected between 1 a 0.1 μg/mL tau treatment (Figure 5.3E). To maximise the physiological relevance and still challenge cells with sufficient levels of exogenous tau, I opted to use the tau preparation at 2.5 μg/mL (~50 nM) in all downstream experiments.

A

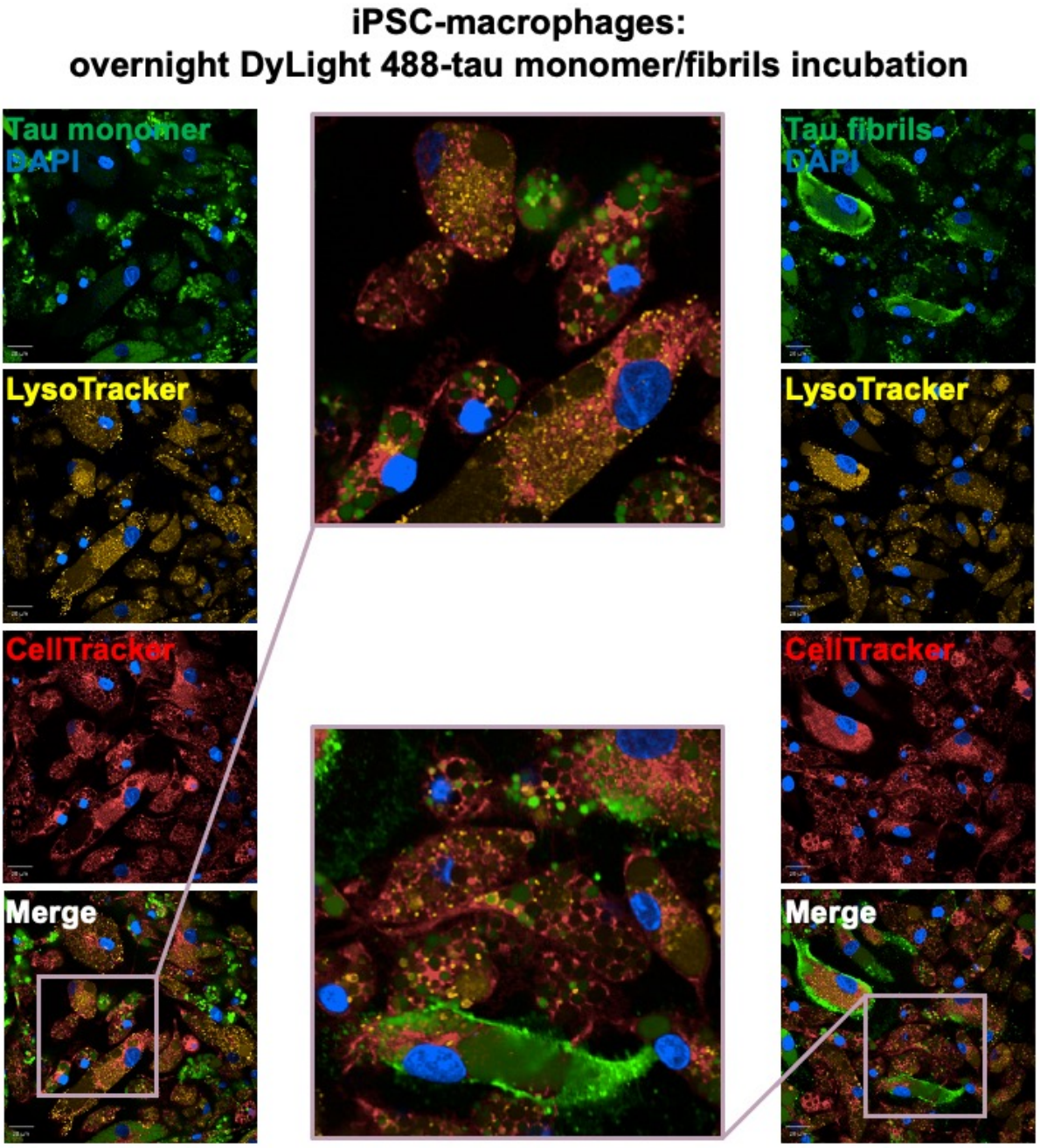

Figure continued on the next page

B

iPSC-microglia:
overnight DyLight 488-tau monomer/fibrils incubation

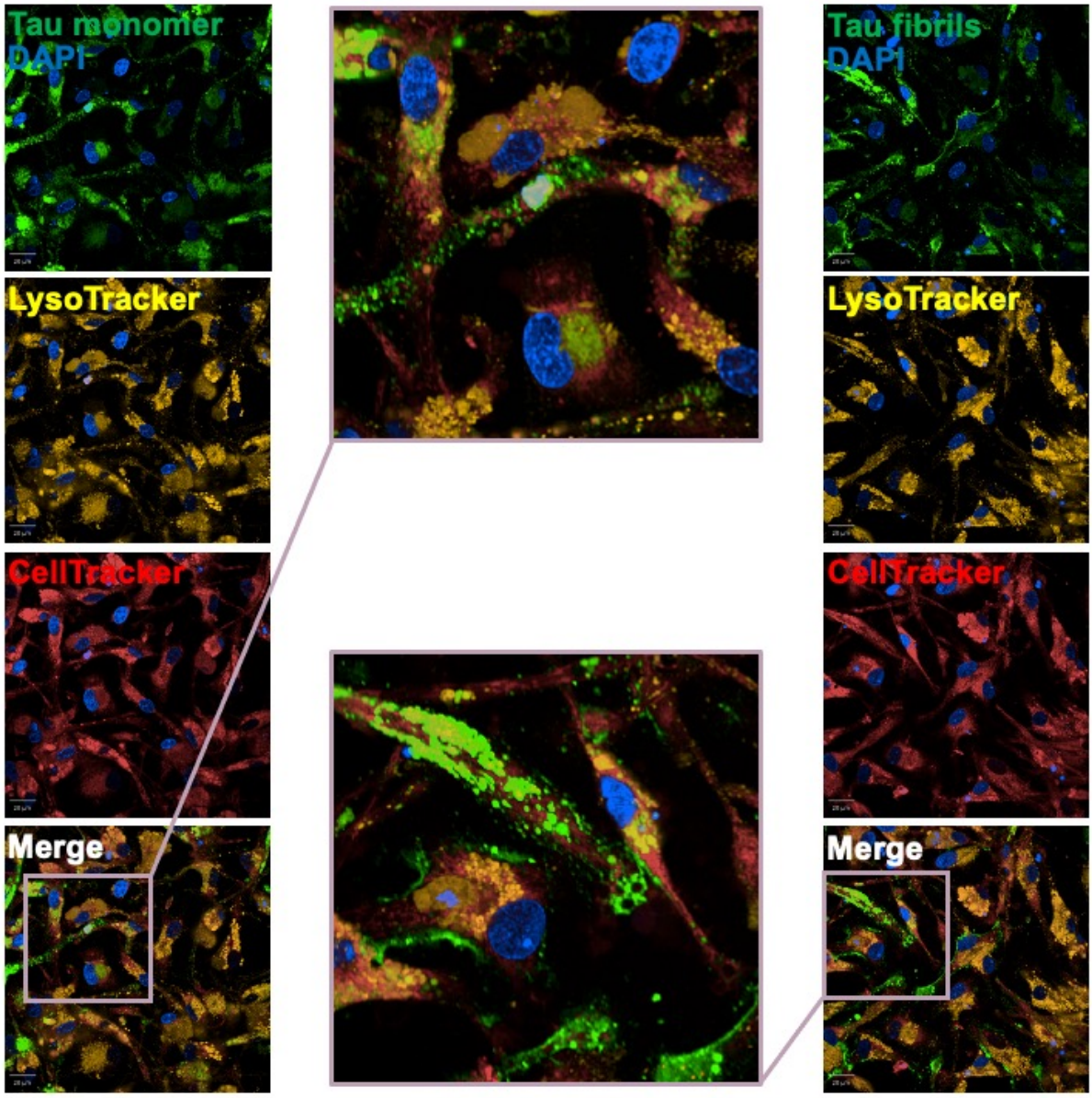

Figure continued on the next page

C

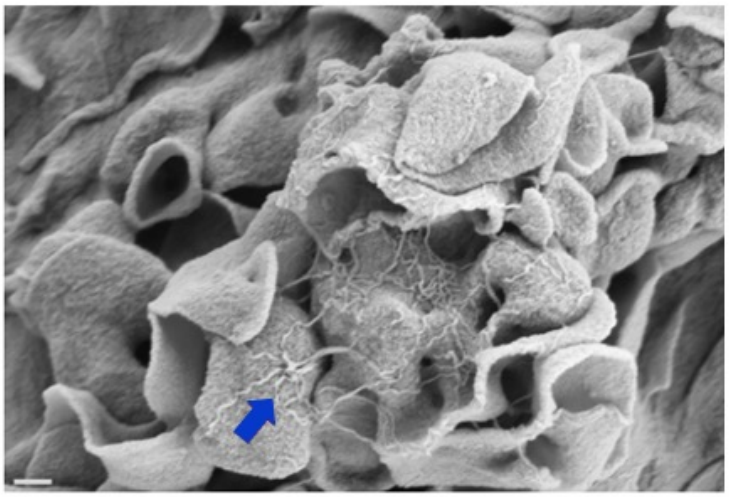

D

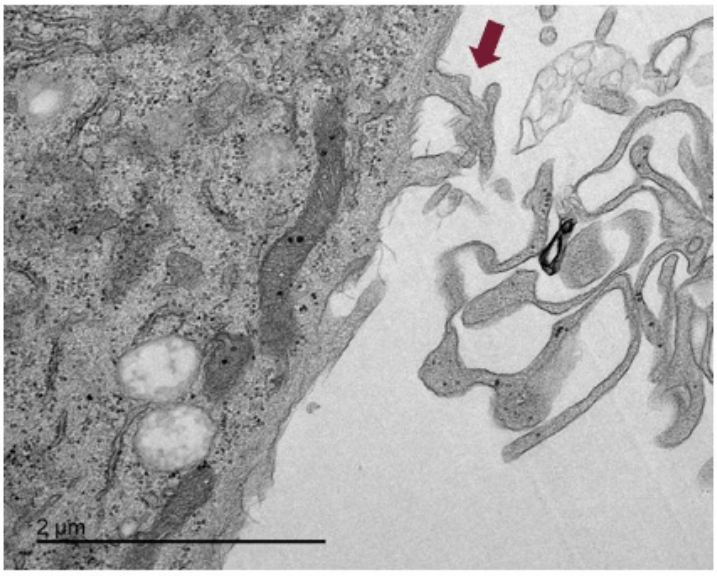

E

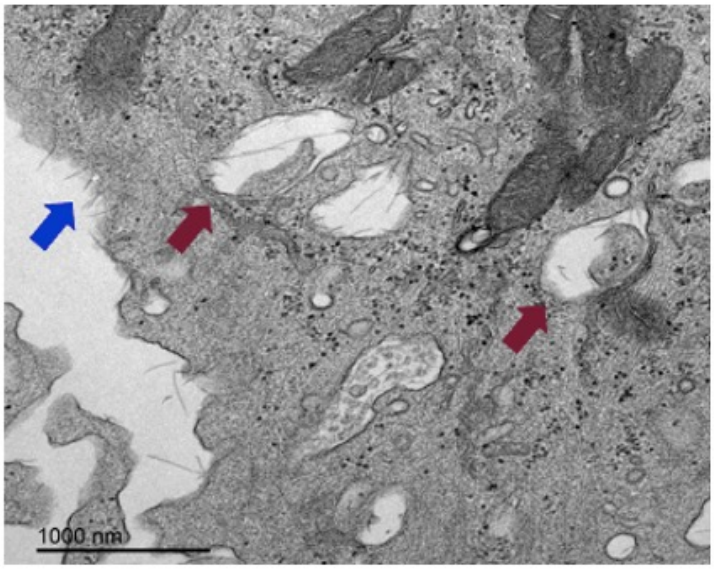

Figure legend on the next page.

Figure 5.2: iPSC-macrophages and microglia can internalise tau in monomeric and fibrillar form

Representative, fluorescent confocal microscopy images of iPSC-macrophages (A.) and iPSC-microglia (B.) derived from a healthy control after 14-hour incubation with DyLight 488- conjugated tau monomer or fibrils. (C.) Scanning and (D., E.) transmission electron micrographs of iPSC-macrophages with tau fibrils tethered to the plasma membrane (blue arrows) and potentially in the process of fibril uptake (red arrows).

(C.) Scale bar = 200 nm, magnification = 69.75K

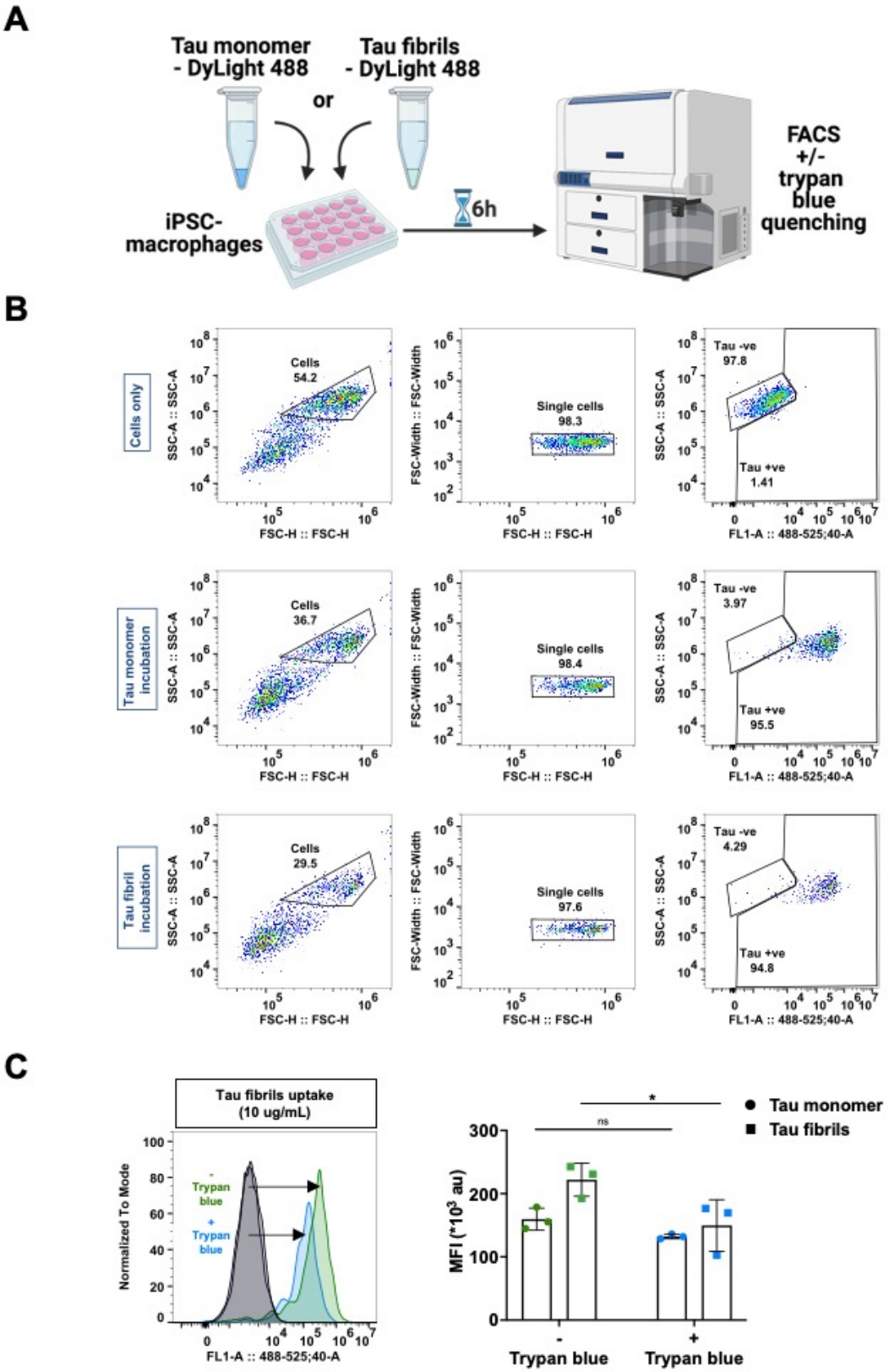

Figure continued on the next page

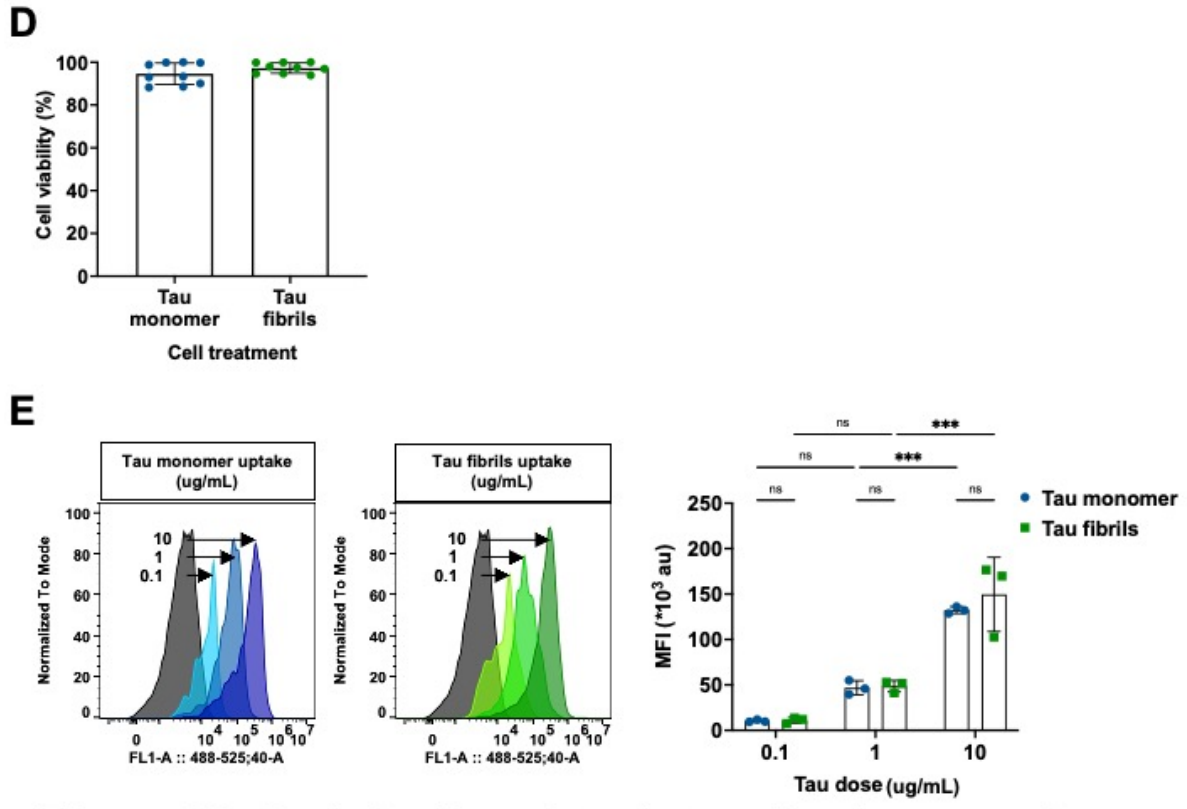

Figure 5.3: Optimisation of tau internalisation assay in iPSC-macrophages

*(A.) Workflow diagram. (B.) Flow cytometry gating strategy. (C.) Flow cytometry analysis of DyLight 488-tau monomer or fibril uptake by iPSC-macrophages in presence or absence of extracellular fluorescence quenching with trypan blue. n=1 in 3 control cell lines, two-way ANOVA with Šídák multiple comparison test, mean±SD, *p<0.05. (D.) Resazurin cell viability assay in healthy donor-derived iPSC-macrophages after 24-hour incubation with 10 μg/mL of tau monomer or fibrils, relative to unstimulated control (n=3 in 3 cell lines). (E.) Flow cytometry analysis of iPSC-macrophage uptake of DyLight 488-tau monomer or fibrils at increasing concentrations. n=1 in 3 control cell lines, two-way ANOVA with Tukey's multiple comparison test, mean±SD, ***p<0.001.*

5.2.2 Microglial LRP1 facilitates tau entry

Next, I explored the mechanisms of tau internalisation by iPSC-macrophages and microglia. LRP1, a large (600 kDa) and ubiquitously expressed endocytic receptor from the family of closely related low-density lipoprotein (LDL) receptors (Beisiegel et al., 1989; Y. Li et al., 2000), has previously been described as the master regulator of tau uptake in neurons (Rauch et al., 2020). Microglial tau receptor has not been clearly identified thus far.

Immunocytochemistry revealed a clear and frequent colocalization of iPSC-macrophage-expressed LRP1 with tau, following a 2-hour tau incubation (Figure 5.4A). The percentage of LRP1-positive tau monomer puncta was significantly higher compared with tau fibrils (Figure 5.4B). I next sought to investigate whether LRP1 inhibition impacts tau internalisation. Receptor-associated protein (RAP) is a 39 kDa molecular chaperon binding LRP1 synthesized at the endoplasmatic reticulum, in order to prevent premature association with other ligands and enable successful delivery to the Golgi apparatus (Herz et al., 1991; Willnow et al., 1995, 1996). RAP binds LRP1 tightly (Figure 5.4C) (De Nardis et al., 2017) but dissociates in acidic environments upon denaturation of its unstable three-helical bundle D3 domain. A synthetic, pH- and heat-stable form of RAP (referred to as sRAP throughout the thesis) was recently engineered by an introduction of disulfide bonds between the second and third helical D3 domain, to maximise LRP1 inhibition (Prasad et al., 2015). iPSC-macrophage and microglia treatment with sRAP reduced tau uptake in a dose-dependent manner, as revealed by confocal microscopy (Figure 5.4E). The effect was not mediated by sRAP-induced cell cytotoxicity (Figure 5.4D). Flow cytometry quantitation confirmed the results. The presence of 500 nM sRAP in culture medium concurrently with tau significantly reduced the percentage of tau monomer- and tau fibril-positive iPSC-macrophages and microglia. Tau monomer MFI but not tau fibril MFI was significantly decreased in both cell models. Overall, these findings suggested human microglia internalise tau monomer via LRP1-mediated endocytosis but an alternative entry route may also exist for tau fibrils (Figure 5.4F)

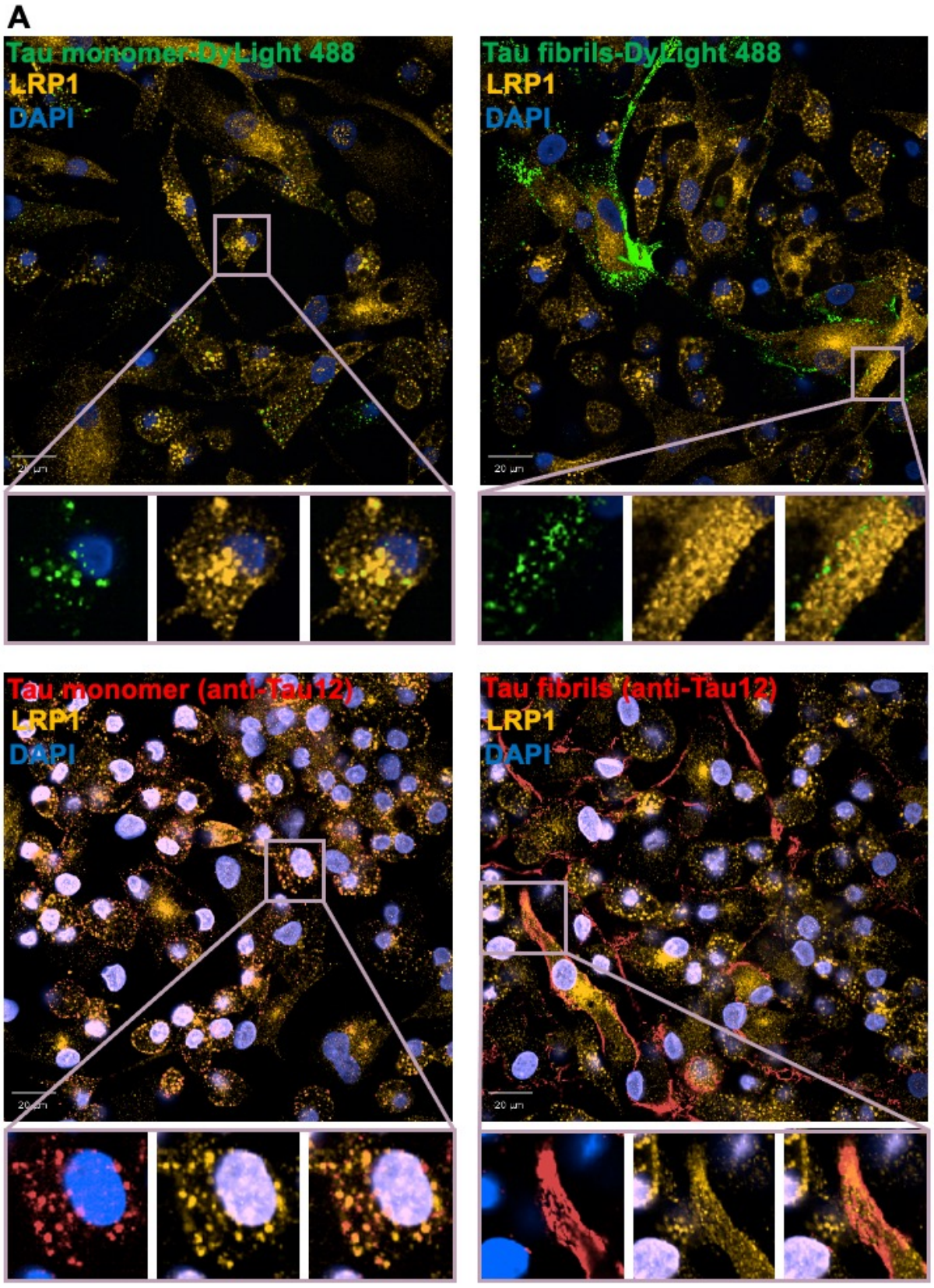

Figure continued on the next page

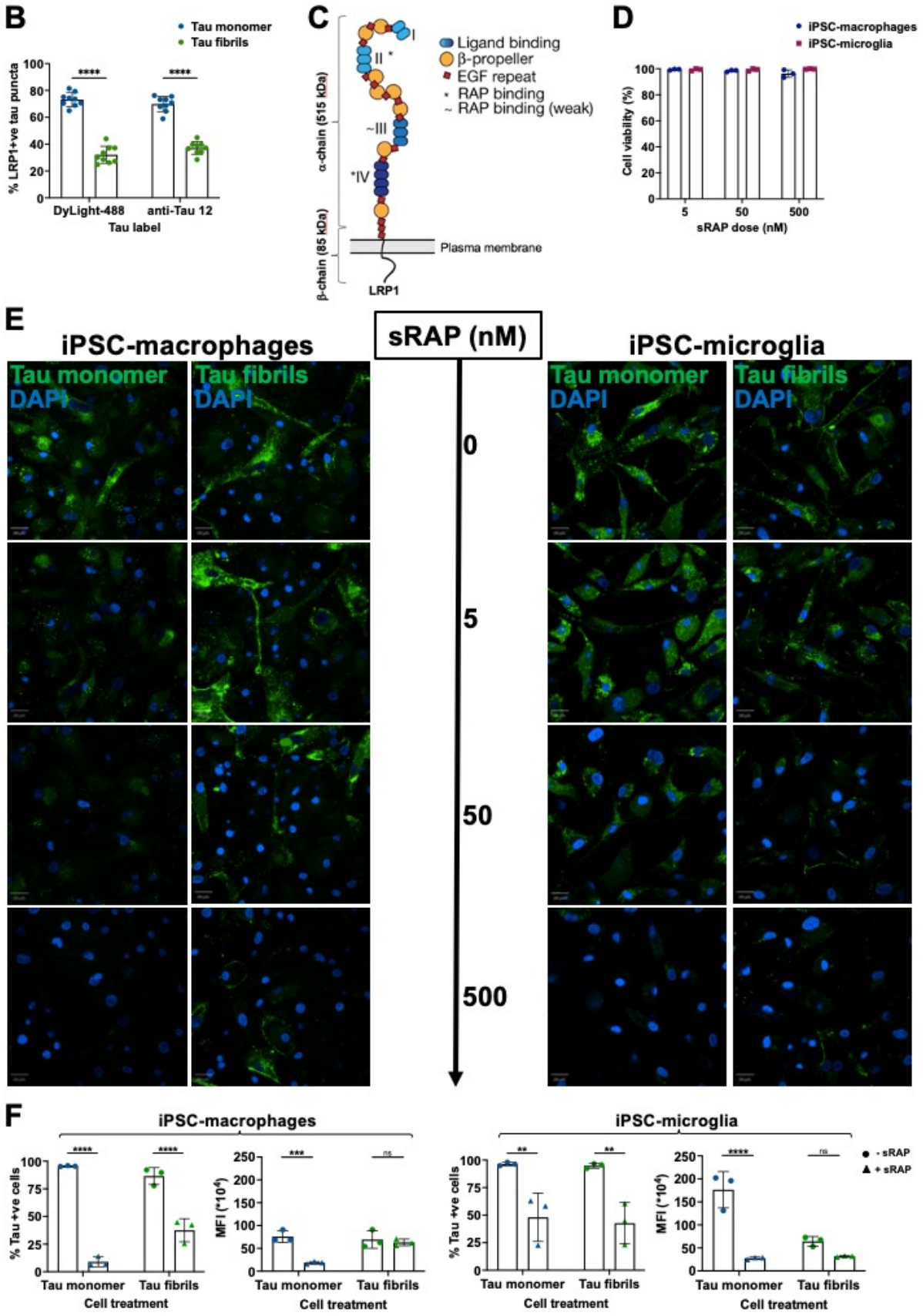

Figure legend on the next page.

Figure 5.4: LRP1 mediates tau entry to iPSC-macrophages and microglia

(A.) Representative confocal microscopy images of LRP1 colocalising with DyLight 488-conjugated or anti-Tau12 immunostained tau monomer and fibrils after 2-hour incubation with iPSC-macrophages. (B.) Quantification of A. Two-way ANOVA with Šídák multiple comparison test, n=3 in 3 control cell lines. (C.) Schematic of LRP1 and LRP1–RAP binding sites (adapted from Rauch et al, 2020). (D.) Resazurin cell viability assay in iPSC-macrophages and microglia following 2-hour sRAP incubation, relative to the unstimulated control (n=1 in 3 control cell lines per cell type). (E.) 2-hour incubation of iPSC-macrophages and microglia with sRAP and tau reduces tau uptake in a dose-dependent manner. Representative confocal microscopy images. (F.) Flow cytometry analysis of 2-hour DyLight 488-tau monomer and fibril uptake in presence or absence of 500 nM sRAP. Two-way ANOVA with Bonferroni's multiple comparison test, n=1 in 3 lines in both iPSC-macrophages and microglia.

*All data is displayed as mean±SD, ** p<0.01, *** p<0.001, **** p<0.0001.*

MFI = mean fluorescence intensity in tau-positive cells.

To supplement the results obtained by pharmacological LRP1 inhibition, I investigated tau uptake in CRISPR/Cas9-induced LRP1 KD iPSC-macrophages.

The lentiviral-mediated CRISPR/Cas9 genome editing has emerged as a powerful way for manipulating gene expression in various iPSC-derived cell types. Unlike neurons or astrocytes, mature microglia are typically resistant to lentiviral transduction owing to the cell's essential role in pathogen defence (reviewed in Maes et al., 2019). Creating a stably-transduced iPSC line or using CRISPR/Cas9 ribonucleoprotein complex to directly KO a gene in iPSCs could bypass the issue. However, the process is lengthy, requires clone selection, and can be further complicated by the population bottleneck arising during the differentiation process.

An alternative platform for gene manipulation directly in iPSC-microglia was recently optimised by Dr Sam Washer in our lab (see section 2.2.2, Figure 5.5A). The method relies on co-transduction of microglia precursors with VLP-packaged Vpx along with the lentiviral Cas9-gRNA pools on differentiation day 0. The HIV-2- and related SIV-encoded accessory protein Vpx facilitates proteasomal degradation of SAMHD1, a potent triphosphohydrolase of deoxynucleotides (dNTPs), thus increasing the pool of cytoplasmic dNTPs available for an efficient RNA reverse transcription (Hofmann et al., 2012; Lahouassa et al., 2012). The use of Vpx was previously demonstrated to improve lentiviral transduction of SAMHD1-expressing myeloid cells (Bobadilla et al., 2013; Dolan et al., 2022; Laguette et al., 2011). Dr Sam Washer showed also a significant transduction efficiency increase in iPSC-microglia when Vpx is included (manuscript in preparation).

I utilised this method to manipulate the LRP1 gene expression in iPSC-macrophages (Figure 5.5A). LRP1- or INTG region-targeting CRISPR/Cas9 lentiviruses were produced in HEK293T cells (sections 2.2.2.1 and 2.2.2.2). A pool of three LRP1, and a pool of eight INTG gRNAs were used to ensure target efficiency. Macrophage precursors were then harvested from differentiation factories (section 2.1.3) and co-transduced at the start of differentiation.

First, lentiviral titer was determined with puromycin selection (section 2.2.2.3). 32.8% and 24.9% of iPSC-macrophages were successfully transduced following the incubation with 1:400 dilution of the LRP1- and INTG-gRNA lentivirus stocks, respectively, corresponding to MOI~0.7 (Figure 5.5B). This MOI was selected for all downstream assays.

WB analysis of macrophage lysates subsequently confirmed significant LRP1 protein reduction upon Cas9-LRP1 gRNA lentivirus transduction (Figure 5.5C). The findings are in line with the expected LRP1 KD as this editing strategy omits the pure clone selection, and results in homozygous and heterozygous population mix. Neither transduction with Vpx VLPs nor Cas9-INTG gRNA lentivirus affected LRP1 protein levels, confirming LRP1 gRNA target specificity.

Functional consequences of LRP1 KD were examined next. Flow cytometry analysis of surface LRP1 expression and tau uptake was performed following 2-hour incubation of LRP1 KD iPSC-macrophages with vehicle, DyLight 488-tau monomer, or DyLight 488-tau fibrils (Figure 5.5A). Puromycin selection was omitted in this experiment to prevent microglial phagocytosis of dead, untransduced cells from affecting the microglial tau uptake. Lentiviral transduction impacted the cell size and granularity. MFI of the cell surface LRP1 and internalised DyLight 488-tau are therefore expressed as relative to the individual condition-associated autofluorescence (Figures 5.5D and E). LRP1 KD in iPSC-macrophages significantly reduced surface LRP1 expression (Figure 5.5D) as well as overall percentage of tau monomer- or tau fibril-positive cells (Figure 5.5E). Gating strategy separating the surface LRP1-negative and positive populations is described in Figure 5.5F. The analysis revealed significant reduction of internalised tau levels in surface LRP1-negative cells following Cas9-LRP1 gRNA lentivirus transduction.

Altogether, both genetic and pharmacological LRP1 inhibition converged on the same finding that LRP1 facilitates tau entry in iPSC-macrophages and microglia. The LRP1 KD-mediated decrease in tau internalisation was smaller compared with that observed after sRAP LRP1

inhibition (Figures 5.5E and F). However, this was most likely caused by the modest % LRP1 KD using this particular genetic approach.

A

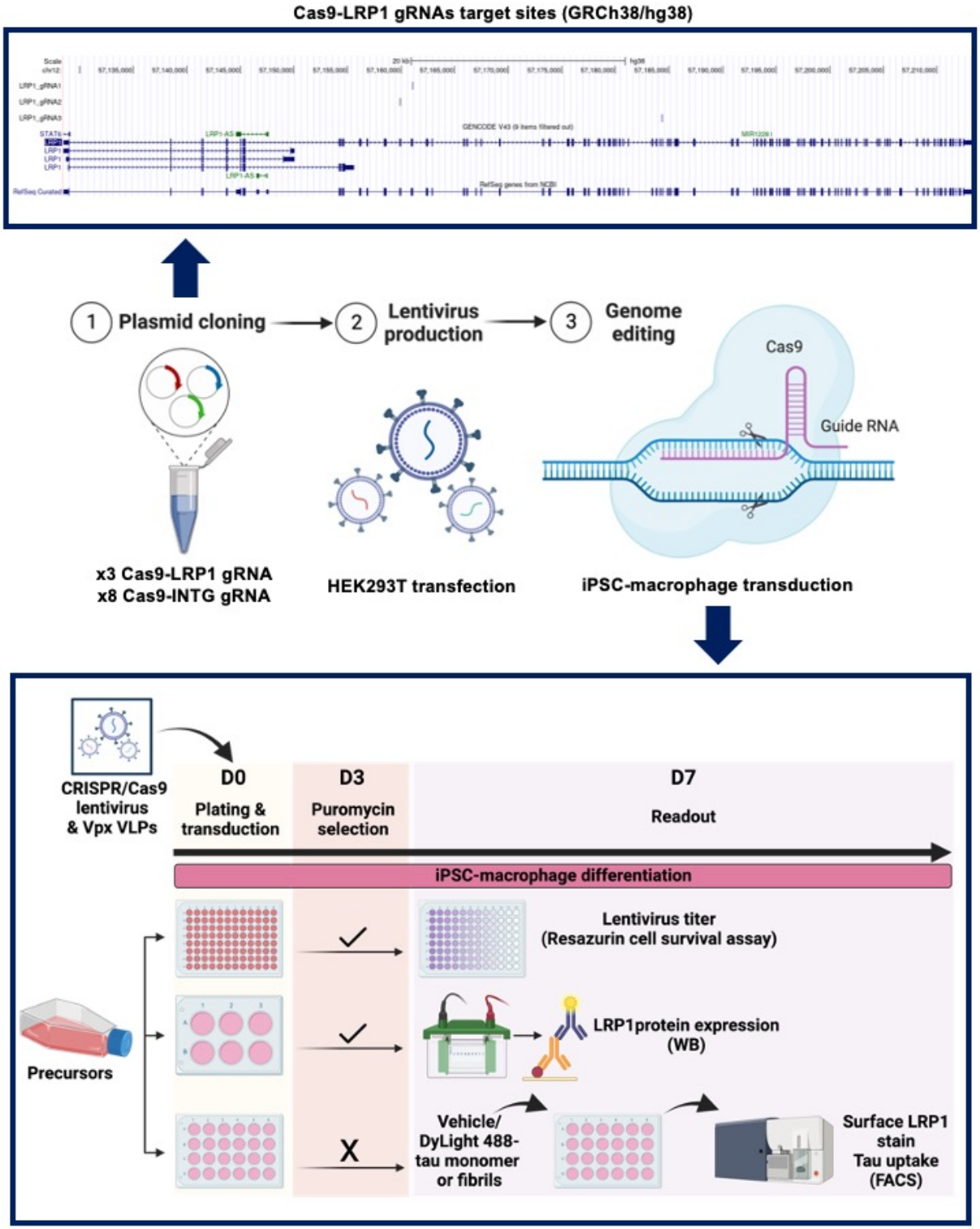

Figure continued on the next page

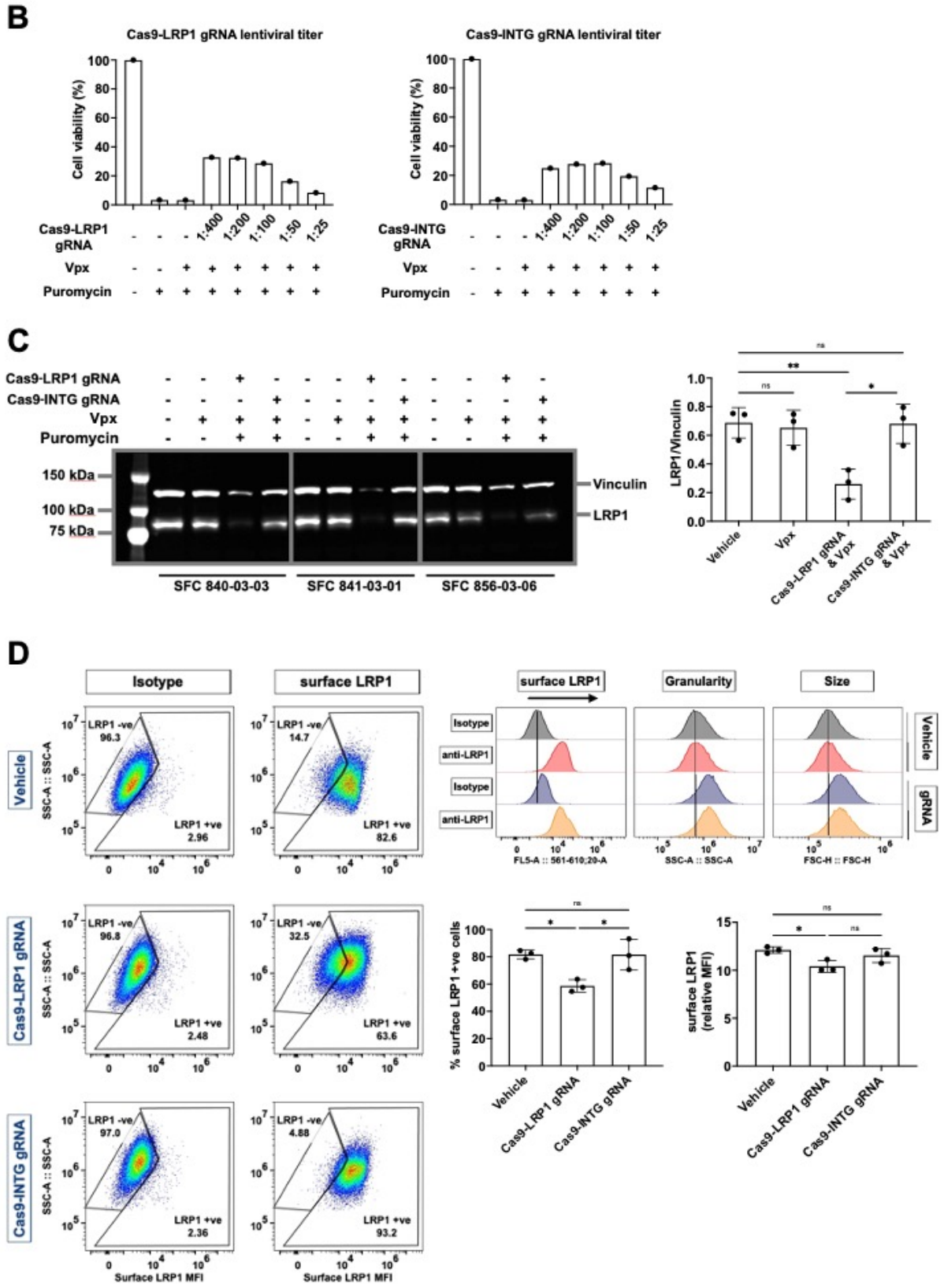

Figure continued on the next page

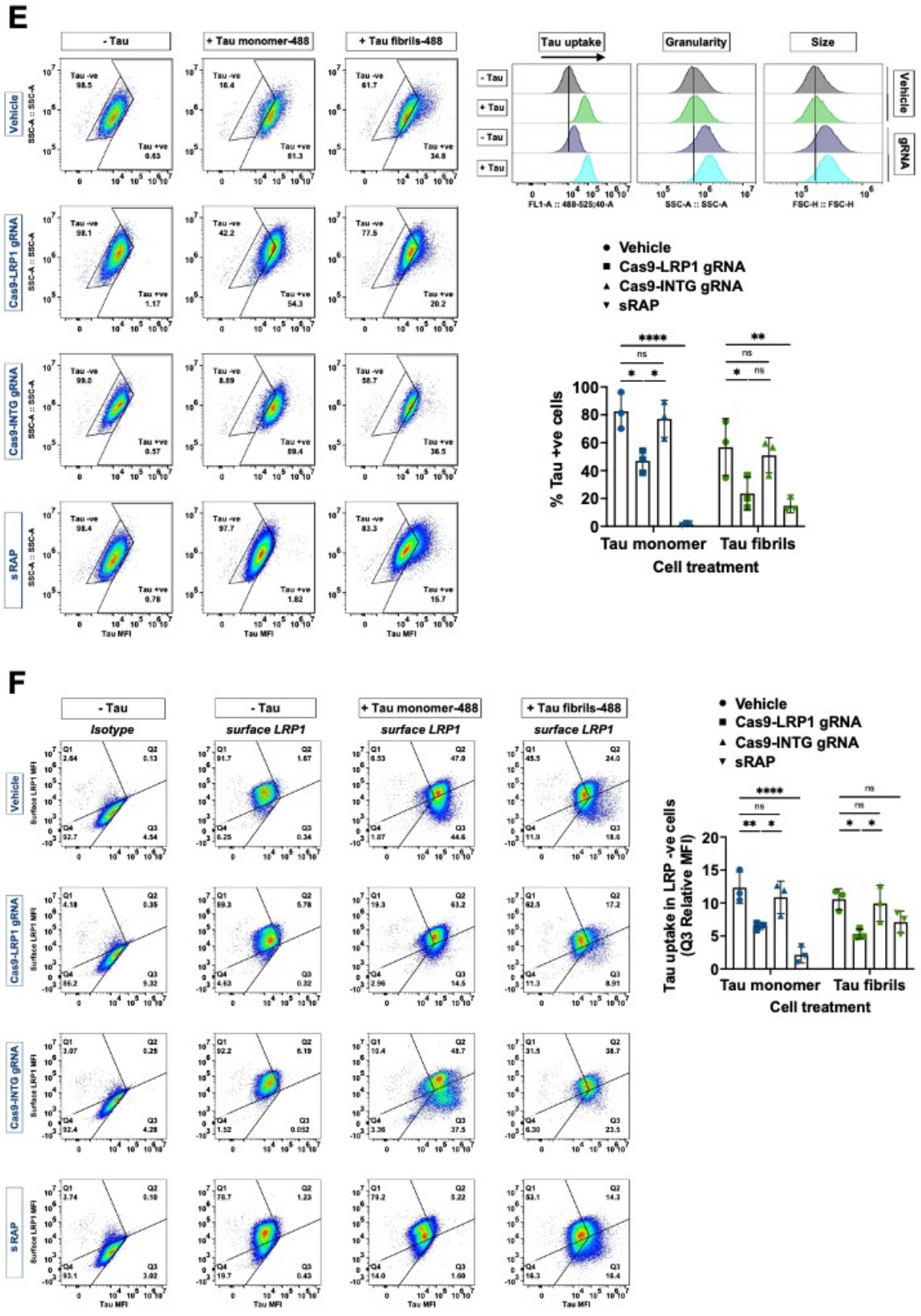

Figure legend on the next page.

Figure 5.5: CRISPR-Cas9 mediated LRP1 KD in iPSC-macrophages reduces tau uptake

(A.) Workflow schematic. To ensure successful genome editing, iPSC-macrophages are co-transduced with Cas9-gRNA lentivirus and VLP-packaged Vpx counteracting SAMHD1-induced inhibition of viral reverse transcription. (B.) Lentiviral titer in iPSC-macrophages determined by resazurin cell viability after puromycin selection. (C.) Western blot confirmation of LRP1 KD. One-way ANOVA with Tukey's multiple comparisons test. (D.) iPSC-macrophage transduction with Cas9-LRP1 gRNA lentivirus reduces % surface LRP1+ve cells and (E.) % tau+ve cells. One-way ANOVA with Šídák's multiple comparisons test for D, two-way ANOVA with Tukey's multiple comparisons test for E. Relative MFI = MFI relative to condition-associated autofluorescence. (F.) Reduction in surface LRP1 following Cas9-LRP1 gRNA transduction of iPSC-macrophages is associated with decreased levels of internalised tau. Two-way ANOVA with Tukey's multiple comparisons test.

*n=1 in in 3 control cell lines. All data is displayed as mean±SD, * p<0.05, ** p<0.01, **** p<0.0001.*

5.2.3 Microglial LRRK2 influences tau uptake

In parallel with the investigation of microglial tau receptor, I explored the role of microglial LRRK2 on tau uptake. Isogenic LRRK2 WT and LRRK2 KO lines, as well as G2019S LRRK2 PD patient-derived lines (sections 1.11, 2.1.1) were differentiated to iPSC-macrophages and microglia, and labelled with CellTracker Deep Red and LysoTracker DND-99 to visualise their cytoplasm and acidic compartments, respectively (section 2.1.7). The cells were then monitored using live using time-course confocal microscopy during an incubation with 2.5 µg/mL DyLight 488-conjugated tau monomer or fibrils. Figures 5.6A and B show representative images taken at 6- and 14-hour timepoints. Visual image inspection indicated that LRRK2 KO cells may have internalised less tau in both monomeric and aggregated form.

A follow-up flow-cytometry analysis of 6-hour tau uptake was performed to quantitate the results and to further elucidate whether tau internalisation is LRRK2 kinase-dependent. (Figure 5.6C). Gating strategy is explained in Figure 5.6D. Similar to the findings in Figure 3.6, the varying cell size and granularity associated with LRRK2 genotype affected baseline intracellular autofluorescence levels (Figure 5.6E). The MFI of internalised tau was therefore expressed as relative to the individual cell line autofluorescence. G2019S iPSC-macrophages internalised significantly more tau monomer and fibrils compared with LRRK2 WT. Conversely, LRRK2 KO cells internalised significantly less tau than LRRK2 WT, but only in the monomeric form (Figure 5.6F). Neither upregulation of endogenous LRRK2 levels with 72-hour IFNγ pre-stimulation (H. Lee et al., 2020), nor inhibition of LRRK2 kinase activity with Mli-2 affected the rate of tau monomer or fibril internalisation by LRRK2 WT and KO cells (Figure 5.6G). Interestingly, IFNγ treatment of G2019S iPSC-macrophages appeared to have significantly decreased monomeric and fibrillar tau uptake (Figure 5.6G). Overall, these findings suggested the LRRK2 genotype does influence tau internalisation by iPSC-macrophages but the effect is not reversed by short-term pharmacological inhibition of LRRK2 kinase activity.

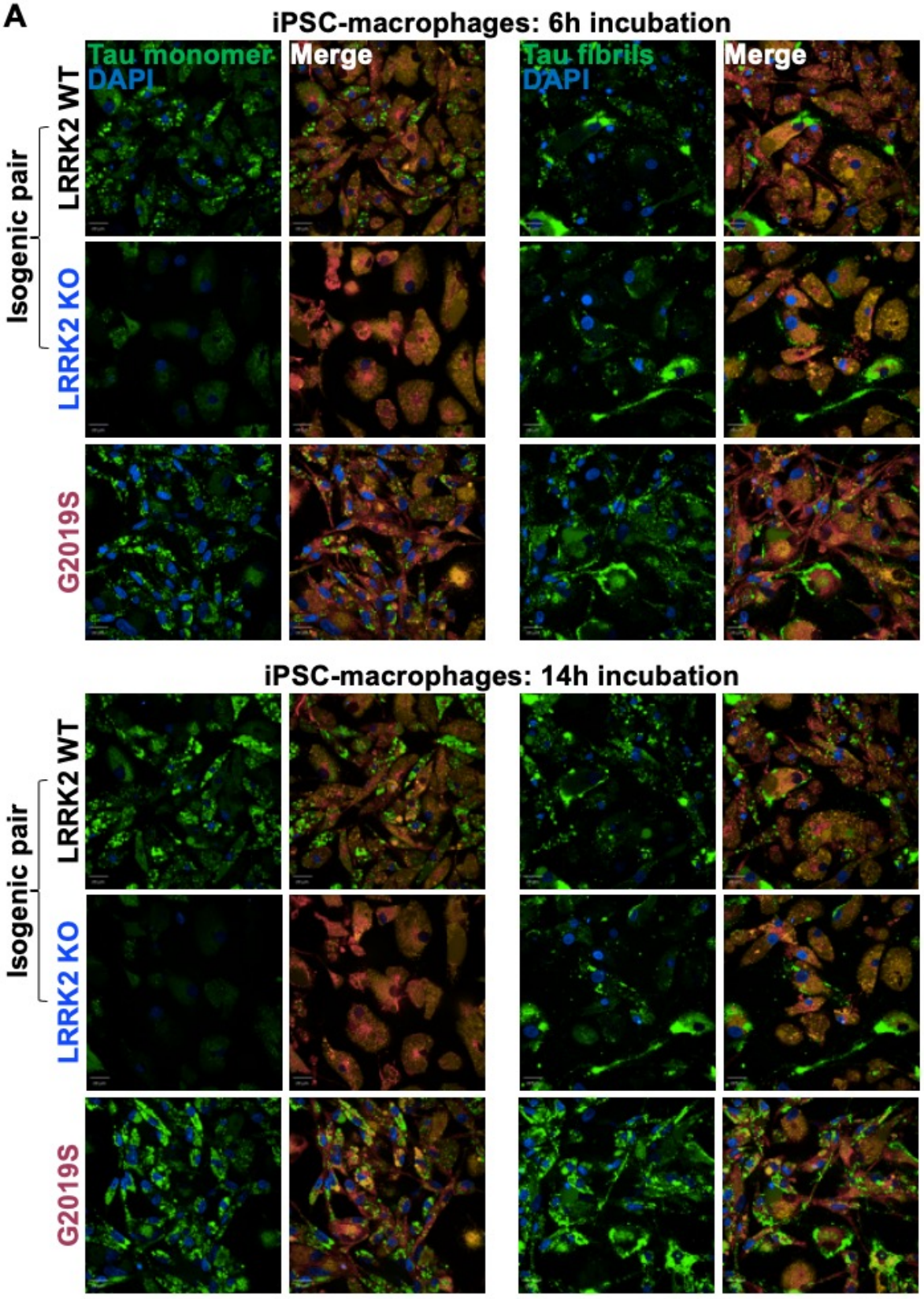

Figure continued on the next page

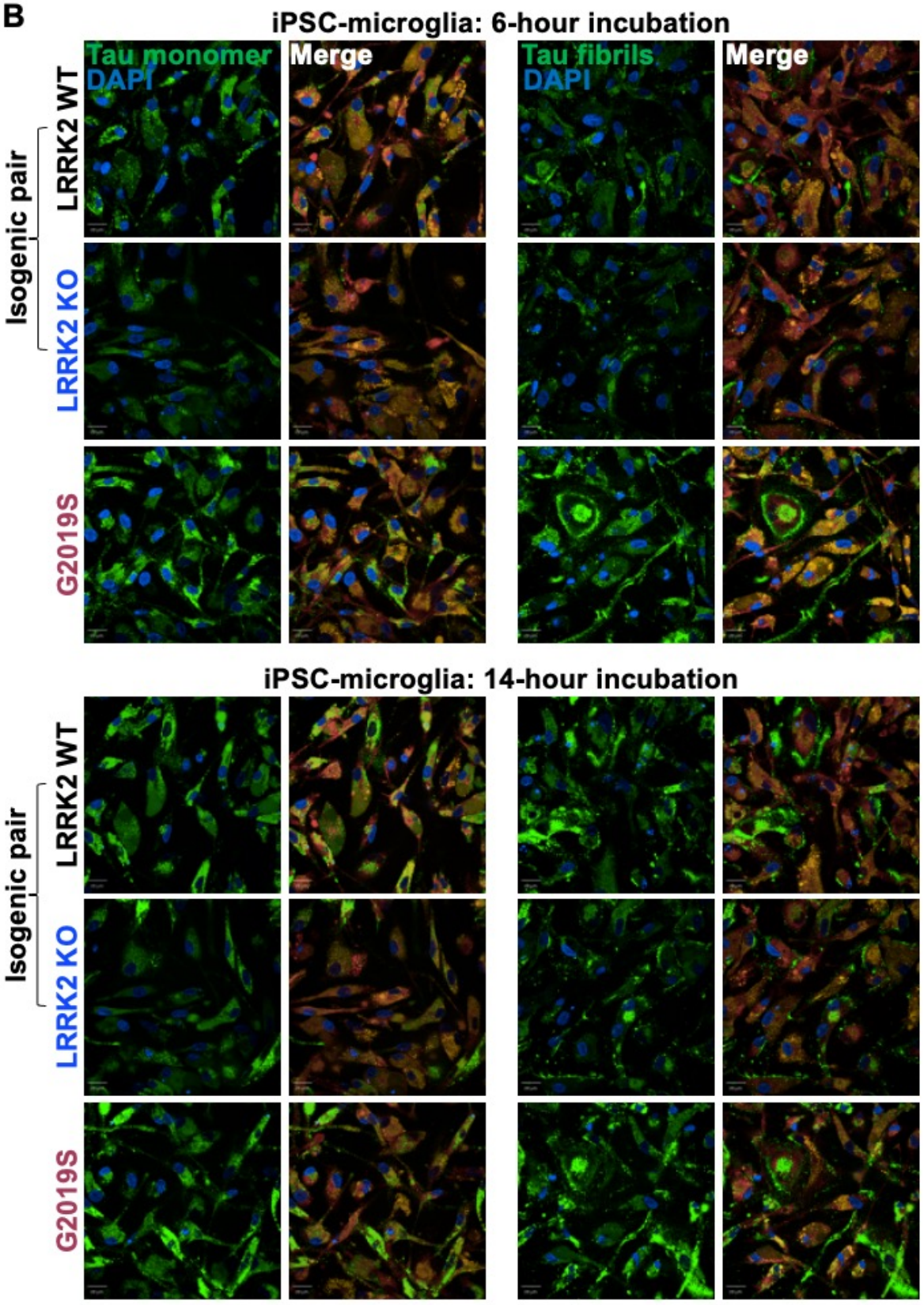

Figure continued on the next page

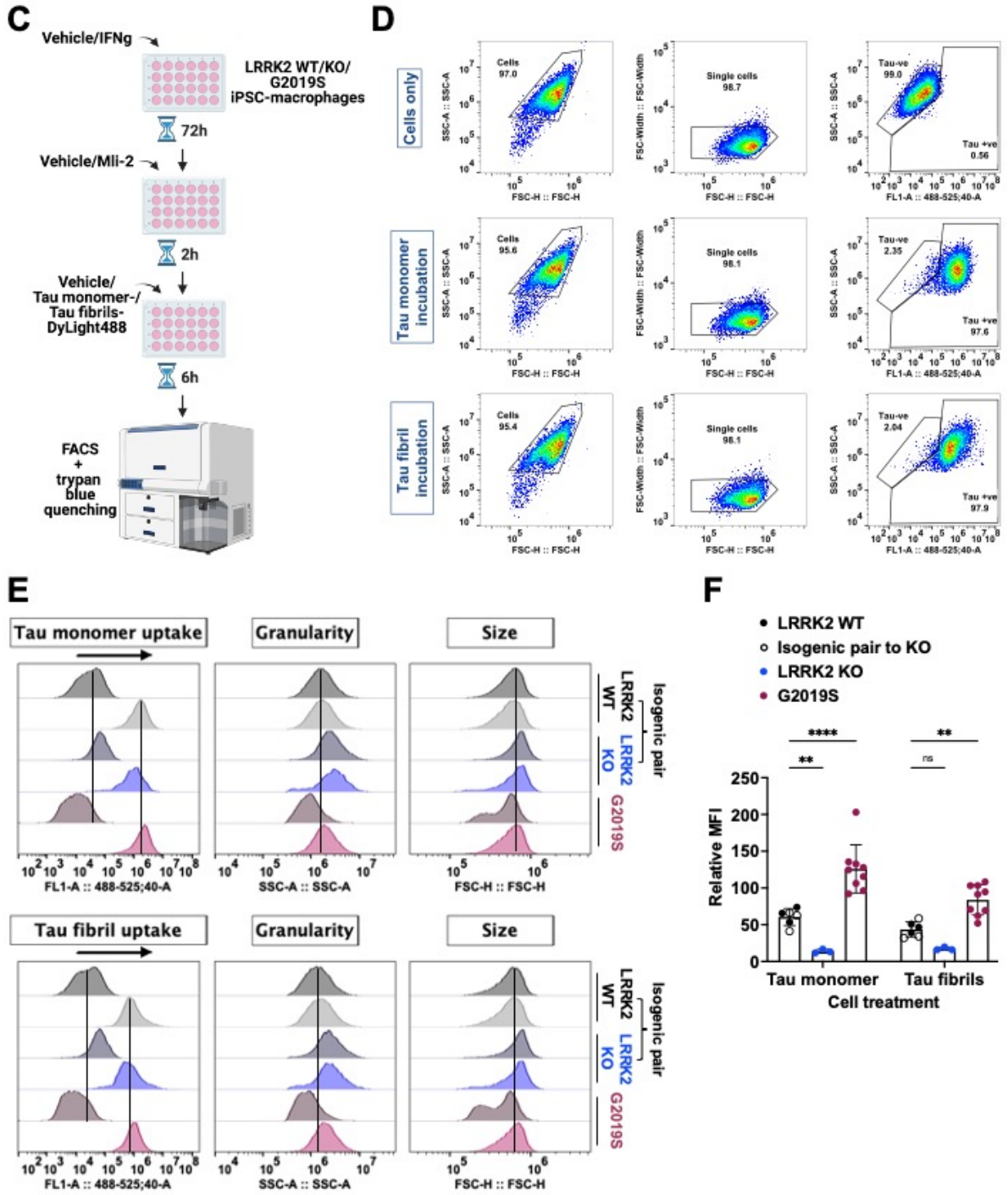

Figure legend on the next page.

Figure 5.6: LRRK2 influences tau uptake

LRRK2 WT, KO, and G2019S iPSC-macrophages (A.) and iPSC-microglia (B.) internalising DyLight 488-conjugated tau monomer or fibrils for 6 or 14 hours. Representative confocal microscopy images. Cell cytoplasm is labelled with CellTracker Deep Red (red) and lysosomes with LysoTracker DND-99 (yellow). (C.) Workflow diagram. (D.) Flow cytometry gating strategy for tau-positive cells. (E.) The difference in cell morphology (size and granularity) between LRRK2 cell lines is associated with varying levels of cell autofluorescence. (F. - G.) MFI of internalised tau monomer or fibrils after 6-hour incubation with iPSC-macrophages, relative to individual cell-line autofluorescence. Open symbols represent values for LRRK2 WT cell line isogenic to the LRRK2 KO.

Two-way ANOVA with Dunnett's multiple comparisons test for F.

Two-way ANOVA with Tukey's multiple comparisons test for G.

n=3 in x2 LRRK2 WT lines, x1 LRRK2 KO line, x3 G2019S LRRK2 lines.

*All data is displayed as mean±SD, ** p<0.01, **** p<0.0001.*

5.2.4 LRRK2 affects LRP1-tau complex recycling in iPSC-macrophages

Further efforts focused on elucidating the mechanisms by which LRRK2 participates in tau internalisation by iPSC-macrophages. Previous work in our lab demonstrated that LRRK2 recruited its bona-fide kinase substrates, Rab8a and Rab10, to maturing phagosomes, possibly regulating the trafficking of the internalised cargo (H. Lee et al., 2020). Coincidentally, a literature search revealed that LRP1 colocalises with Rab8a to signalling sites on micropinosomes in human and mouse primary macrophages (L. Luo et al., 2018), and that in retinal Müller glial cells, Rab10-dependent exocytosis is needed for trafficking of the internalised LRP1 back to the plasma membrane (Jaldín-Fincati et al., 2019). Based on the suggested interplay between LRRK2, LRRK2 substrates, and LRP1, I hypothesised that LRRK2 may influence tau internalisation by regulating the LRP1-tau complex trafficking. I focused on the mechanisms of tau monomer internalisation as previous finding from sections 5.2.2 and 5.2.3 suggested less clear involvement of LRP1 and LRRK2 in tau fibril uptake.

Healthy control-derived iPSC-macrophages were incubated with DyLight 488-conjugated tau monomer for 2 hours, then immunostained for LRRK2, LRP1, pRab8a, and pRab10. Image analysis revealed colocalisation of LRRK2, pRab8a, and pRab10 each with tau monomer alone, as well as with double-positive LRP1-tau puncta (Figure 5.7A). IFNγ-induced increase in LRRK2 expression enhanced the colocalization frequency. LRRK2 and pRab8a but not pRab10 appeared to be recruited to LRP1-tau complex more frequently compared to tau monomer alone. It is important to note, however, that the pRab8a antibody is not entirely target specific and can cross-react pRab3A, pRab10, pRab35 and pRab43 (Lis 2018). Statistical analysis was not performed on this data set as this experiment was carried out only once thus far.

Following the immunocytochemistry results, I sought to examine whether LRRK2 is necessary for the recruitment of pRab8a and pRab10 to LRP1-tau complex using the isogenic LRRK2 WT and LRRK2 KO cell line pair. Time constraints and the lack of reagents allowed only for

n=1 experiment, with no label against the internalised tau. Nevertheless, visual image inspection of LRRK2 KO iPSC-macrophages following 2-hour tau monomer incubation revealed the lack of pRab10 signal compared with the LRRK2 WT iPSC-macrophages (Figure 5.7B). Some pRab8a signal was observed in LRRK2 KO cells but this could potentially be attributed to the non-specificity of the antibody (see above paragraph).

To further examine LRRK2 influence on LRP1-tau complex trafficking, I measured the cell-surface and total LRP1 levels at baseline and post 2-hour tau monomer incubation using two independent techniques. Regardless of their LRRK2 genotype, all iPSC-macrophages expressed the same total LRP1 levels at baseline, confirmed by WB (Figure 5.7C, ‘’- Tau’’) and flow cytometry (Figure 5.7E, ‘’- Tau’’). However, G0291S cells significantly upregulated their total LRP1 levels, following 2-hour tau monomer incubation (Figures 5.7C and E, “+ Tau’’). WB analysis (Figure 5.7D, ‘’- Tau’’) but not flow cytometry analysis (Figure 5.7F, ‘’- Tau’’), indicated that LRRK2 KO iPSC-macrophages may express overall reduced amount of surface LRP1 at baseline. Importantly, both techniques confirmed the surface LRP1 levels decrease significantly upon tau incubation in G2019S macrophages but remain unchanged in LRRK2 KO cells (Figures 5.7D and F, ‘’- Tau’’ vs ‘’+ Tau).

Altogether, the findings confirmed the hypothesis that the enhanced tau monomer internalisation observed in patient-derived G2019S iPSC-macrophages and microglia may be mediated by a more efficient LRRK2-mediated receptor-cargo complex trafficking in these cells.

A

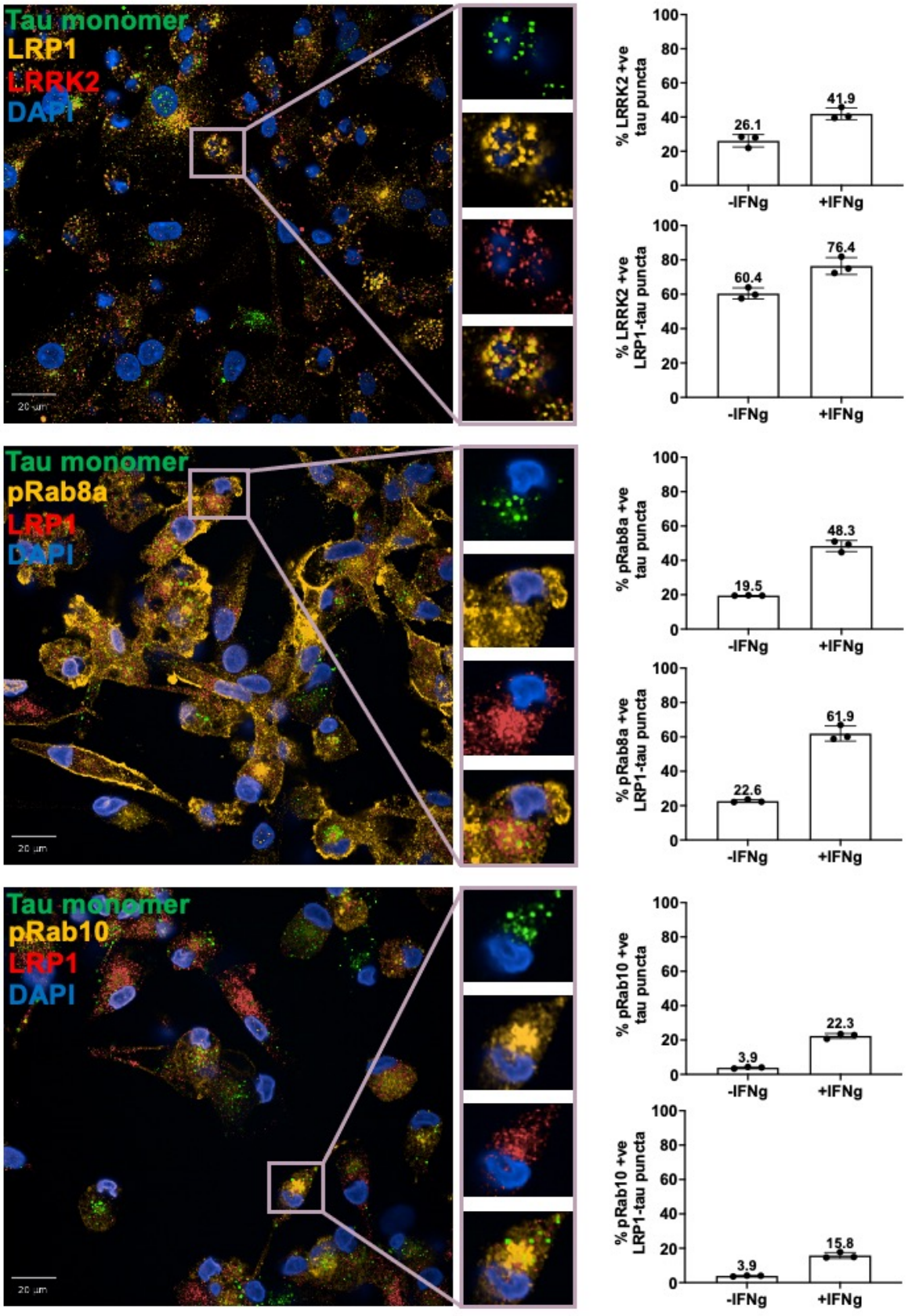
Tau monomer
LRP1
LRRK2
DAPI
20 µm
% LRRK2 +ve tau puncta
26.1
41.9
-IFNg
+IFNg
% LRRK2 +ve LRP1-tau puncta
60.4
76.4
Tau monomer
pRab8a
LRP1
DAPI
% pRab8a +ve tau puncta
19.5
48.3
% pRab8a +ve LRP1-tau puncta
22.6
61.9
Tau monomer
pRab10
LRP1
DAPI
% pRab10 +ve tau puncta
3.9
22.3
% pRab10 +ve LRP1-tau puncta
3.9
15.8

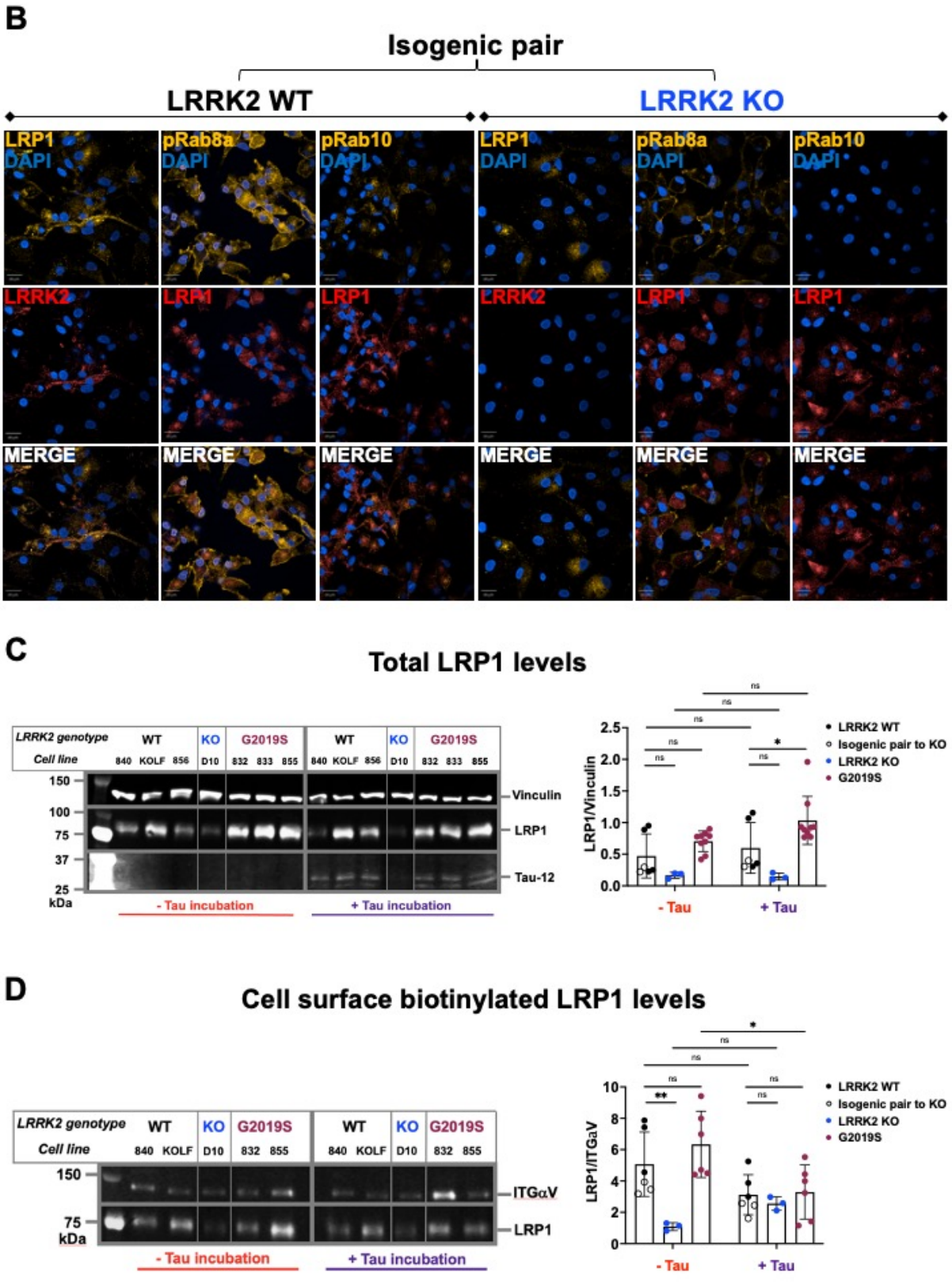

Figure continued on the next page

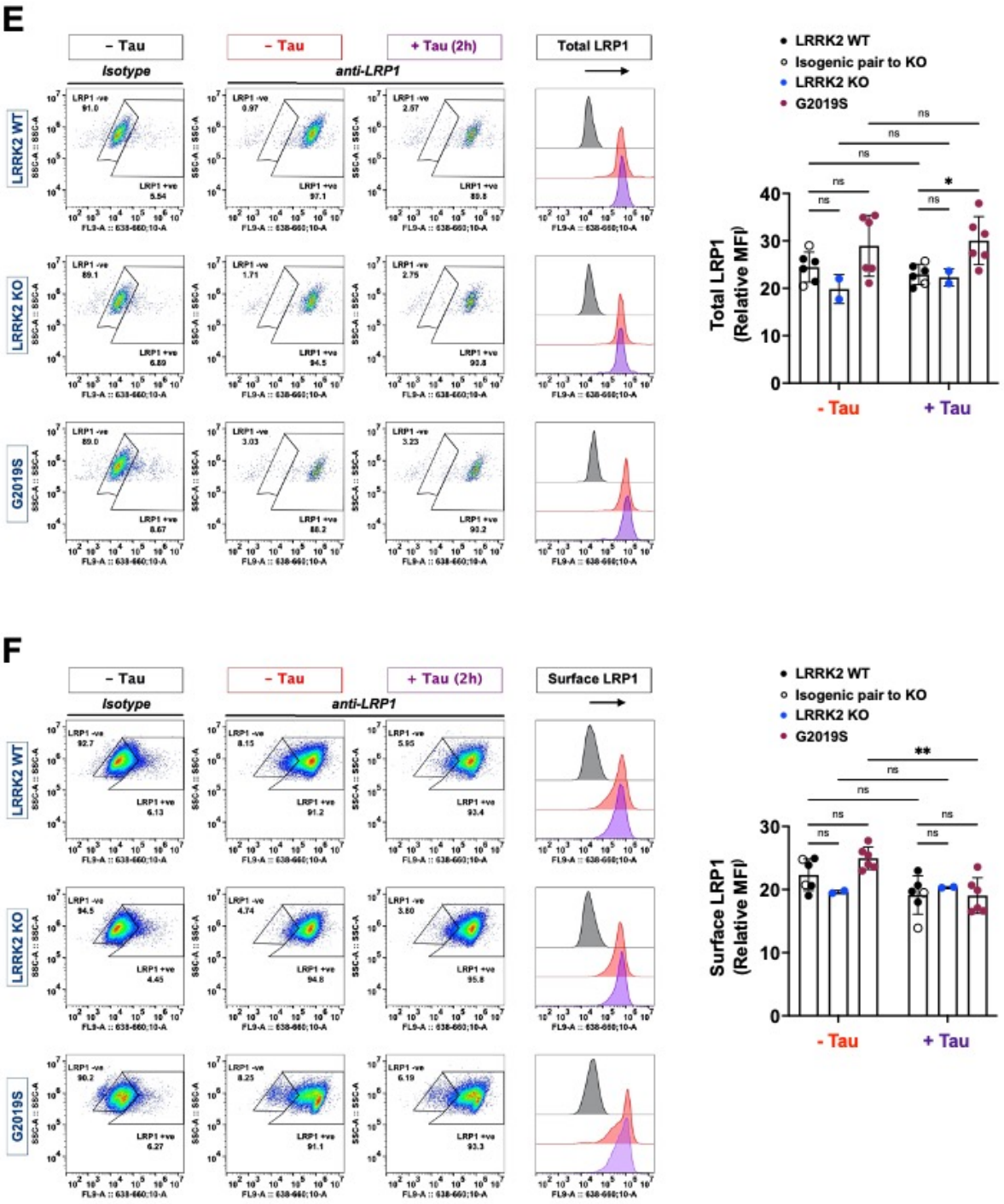

Figure legend on the next page.

Figure 5.7: LRRK2 enhances LRP1-tau complex internalisation

(A.) LRRK2 and its Rab GTP-ase substrates colocalise with LRP1-tau monomer complex in control iPSC-macrophages following 2-hour tau incubation (n=1 in 3 LRRK2 WT cell lines). Representative confocal microscopy images in IFNg-stimulated iPSC-macrophages. (B.) Representative LRRK2, pRab8a, pRab10, and LRP1 immunostaining in isogenic LRRK2 WT and KO iPSC-macrophage pair. (C.) Western blot analysis of total and (D.) biotinylated surface LRP1 levels in iPSC-macrophages at baseline (red) and after 2-hour tau monomer stimulation (purple). n=2 in 3 LRRK2 WT, 1 LRRK2 KO, 3 G2019S lines for the total, and n=3 in 2 LRRK2 WT, 1 LRRK2 KO, 2 G2019S lines for the surface protein levels. (E.) FACS analysis of total and (F.) surface LRP1 levels in iPSC-macrophages at baseline (‘’-Tau,’’ red) and after 2-hour tau monomer stimulation (‘’+Tau,’’ purple). MFI relative to individual cell-line isotype. n=2 in 3 LRRK2 WT, 1 LRRK2 KO, 3 G2019S patient lines.

*C-F. Two-way ANOVA with Šídák’s multiple comparisons test, mean±SD, * p<0.05, ** p<0.01. Open symbols represent values for LRRK2 WT cell line isogenic to the LRRK2 KO.*

5.2.5 iPSC-macrophages efficiently degrade monomeric but not fibrillar tau

Clearance of tau monomer and fibrils internalised by iPSC-macrophages was characterised next.

First, I explored the intracellular degradation pathways by which the internalised tau may get hydrolysed. iPSC-macrophages were either fixed at the end of an overnight incubation with tau monomer or fibrils (Pulse), or allowed to process the internalised tau in presence or absence of degradation pathway-specific drugs for 24 hours (Chase) (Figure 5.8A). Intracellular tau levels were quantified by anti-tau immunostaining and confocal microscopy. The amount of tau remaining within iPSC-macrophages post clearance was plotted as relative to the amount of internalised tau. Neither protease inhibitors (a combination of leupeptin, pepstatin A, and E64d, as per previous use in Chapter 3, nor the 26S proteasome inhibitor (MG-132, section 2.1.8) significantly inhibited tau monomer clearance, though slightly more tau remained intracellularly in the presence of protease inhibitors (29%) compared with vehicle (22%). Fibrillar tau clearance was significantly inhibited by drugs targeting both types of degradation pathways (Figures 5.8B and C).

I then investigated whether clearance of the internalised tau is affected by the exogenous tau concentration, the incubation length, or the length of time allowed for post-uptake processing. Intracellular tau levels were quantified with immunostaining against tau. Tau released to conditioned medium during clearance was determined with total tau ELISA. The experiment design is detailed in Figure 5.9A.

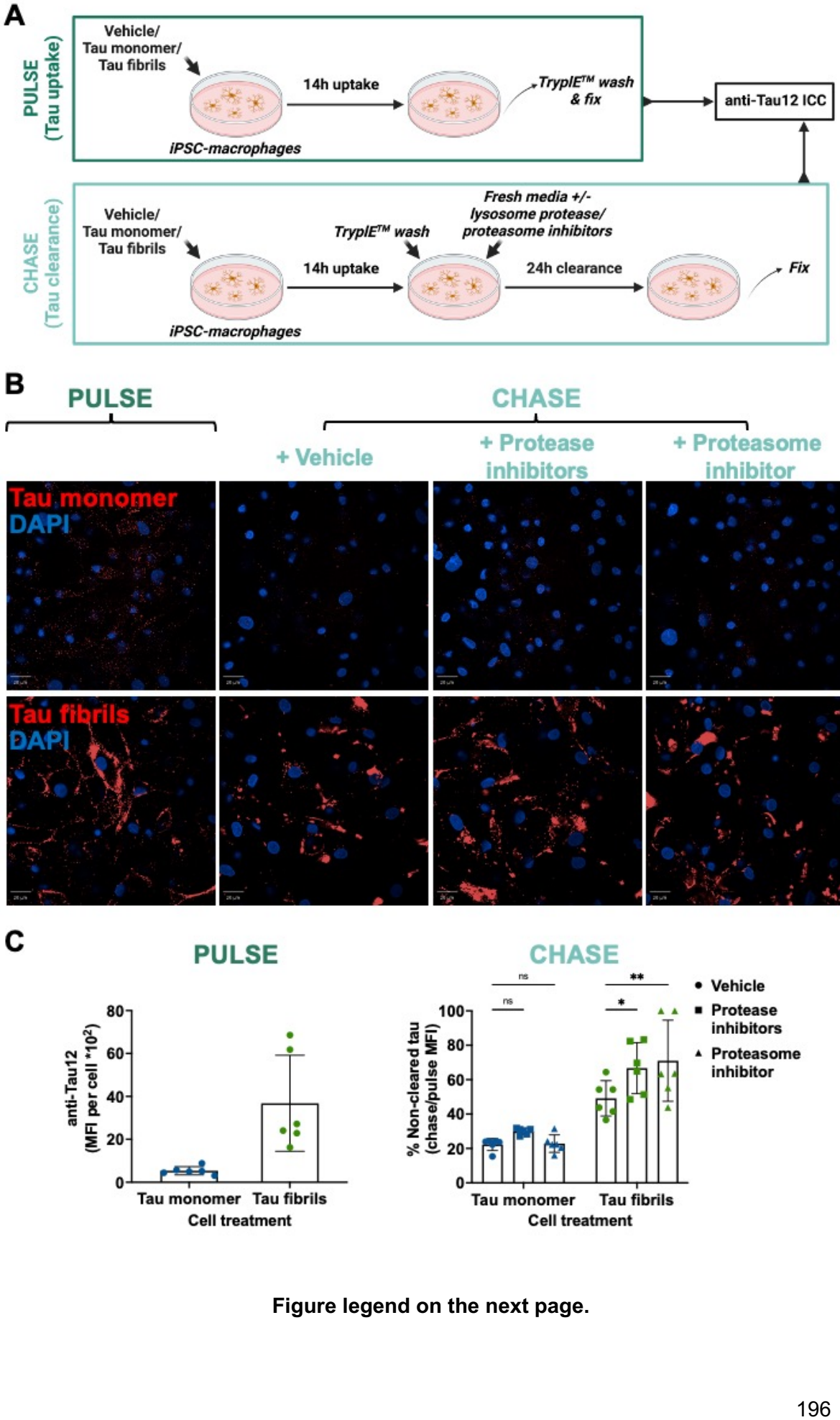

Figure legend on the next page.

Figure 5.8: Investigating degradation of tau internalised by iPSC-macrophages

*(A.) Experimental workflow. (B.) Representative confocal microscopy images of tau uptake (pulse) and clearance (chase) in the presence or absence of lysosomal protease or proteasome inhibitors. iPSC-macrophages are immunostained with anti-Tau12 and DAPI. (C.) Quantification of B. n=2 in 3 control lines, two-way ANOVA with Dunnett's multiple comparisons test, mean±SD, * p<0.05, ** p<0.01. Both chase and pulse MFI are normalised to the number of cells.*

A

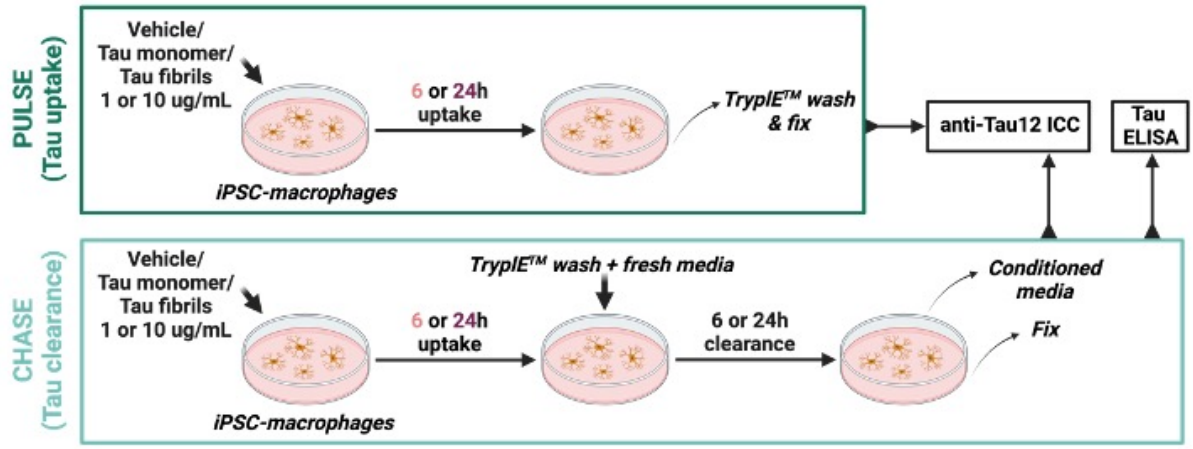

B

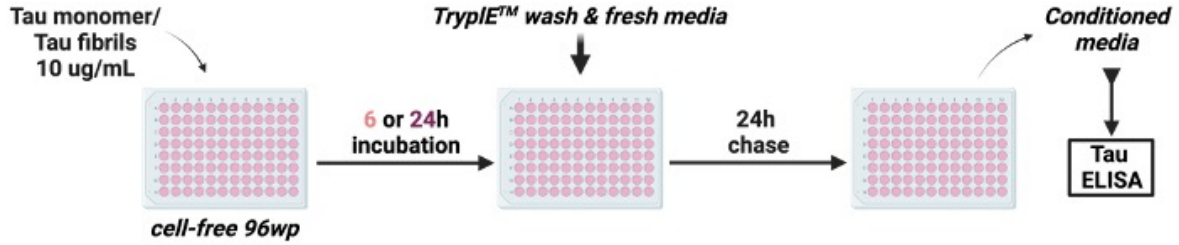

Plate treatment	Incubation length (h)	Tau detected in media (pg/mL)
Tau monomer	6	<31
	24	<31
Tau fibrils	6	<31
	24	<31

Figure continued on the next page

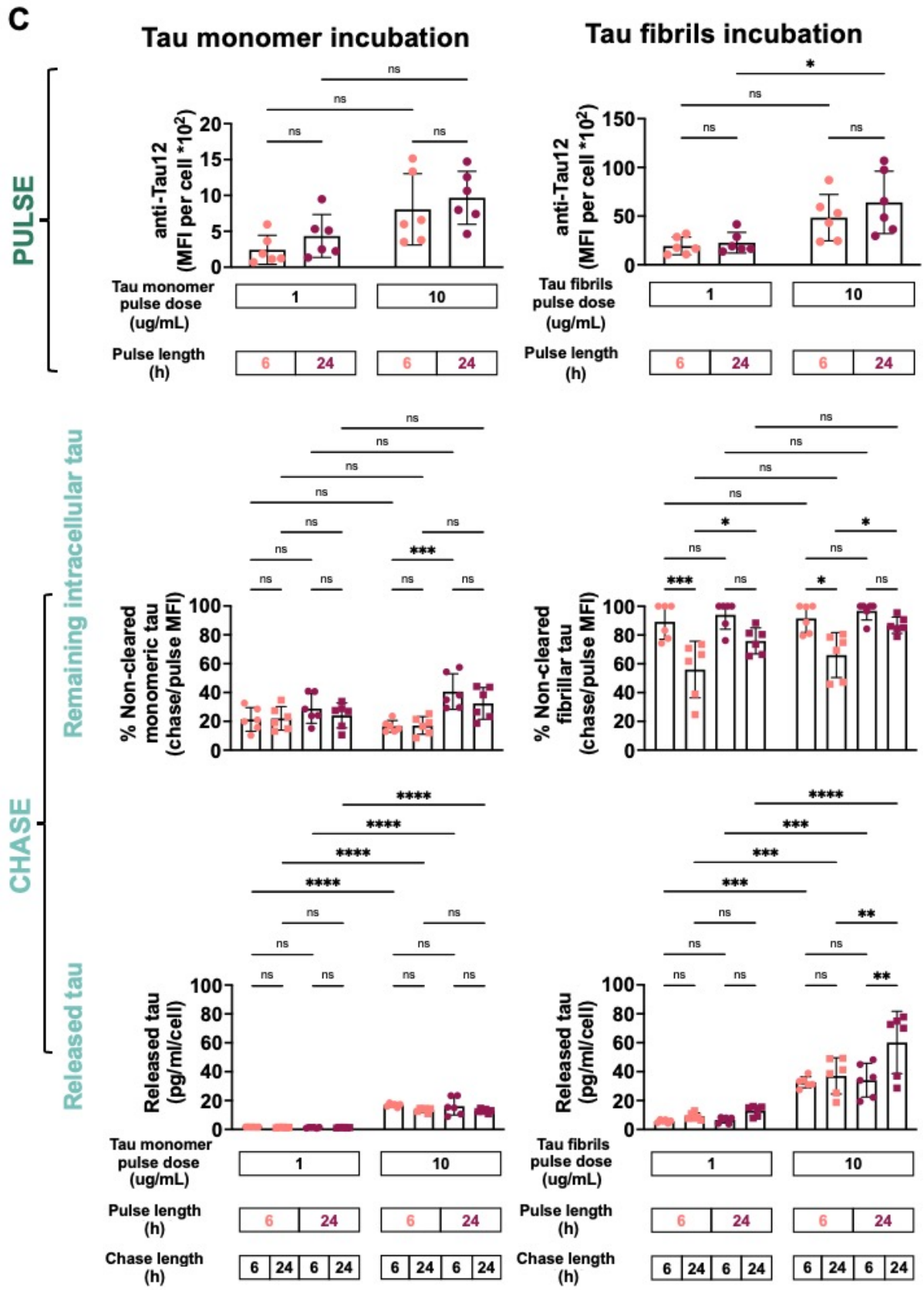

Figure legend on the next page.

Figure 5.9: Tau clearance is dependent on its conformation, concentration and incubation length

(A.) Experimental workflow. (B.) Passive dissociation of tau from tissue-culture plate does not explain the presence of tau in the conditioned media. (C.) Quantification of tau monomer/fibril internalisation (pulse) and clearance (chase) by iPSC-macrophages. Intracellular tau levels were quantified by anti-Tau 12 immunostaining (MFI), relative to the number of cells. The amount of tau in the conditioned media was determined with total tau ELISA relative to the number of cells.

n=2 in x3 control cell lines.

*Two-way ANOVA with Tukey's multiple comparisons test, mean±SD, * p<0.05, ** p<0.01, *** p<0.001.*

The percentage of non-cleared tau monomer was on average lower compared with the fibrils, suggesting tau monomer clearance is more efficient (Figure 5.9C, % Non-cleared monomeric tau vs % Non-clear fibrillar tau). Long-term (24-hour) incubation of cells with tau monomer at high concentration (10 µg/mL) significantly reduced the internalised tau clearance compared with short-term (6-hour) incubation at the same concentration. However, the effect was only evident at short-term (6-hour) clearance timepoint, indicating that iPSC-macrophages may be able to successfully process tau monomer even at high concentrations, if sufficient processing time is allowed (Figure 5.9C, % Non-cleared monomeric tau).

Tau fibril clearance appeared dependent on the length of the clearance phase (Figure 5.9C, % Non-cleared fibrillar tau). Significantly more tau fibrils were cleared after 24 hours compared with the 6-hour clearance timepoint but only following a short-term fibril uptake (6 hours). In contrast, after 24-hour fibril incubation, the cells have cleared less than 75% of the internalised fibrils, regardless of the length of time allowed for cargo processing. Altogether, the data indicated tau fibril clearance by iPSC-macrophages may be possible if low internalised quantities can be processed over a sufficient period of time. However, long-term tau fibril uptake significantly impairs their clearance.

Tau release to conditioned medium during the clearance phase was strongly affected by the exogenous tau concentration. Significantly more tau was detected in the medium after cells had been presented with high exogenous concentrations of tau, regardless of tau conformation (Figure 5.9C, Released tau graphs). However, fibrillar tau incubation resulted in overall more tau release than monomeric tau incubation. Importantly, the data revealed a potential relationship between fibrillar tau clearance and release to medium. Following a long-term (24-hour) fibrillar tau uptake at high concentration, the internalised tau accumulated within the cells (Figure 5.9C, % Non-cleared fibrillar tau), and significantly more tau was released to medium after 24 hours compared with the short-term fibrillar tau uptake (Figure 5.9C, Released tau graph, Tau fibrils incubation panel). The association between the lack of intracellular fibrillar tau clearance and enhanced extracellular tau release indicates that tau release to medium

may serve as a mechanism by which cells alleviate stress from the accumulating intracellular load.

In parallel with the investigation, a control experiment was performed to ensure the tau detected in the conditioned medium had been actually processed and released by iPSC-macrophages and not a contamination from tau adhered to the plate surface (Figure 5.9B). High concentration (10 µg/mL) of tau monomer and fibrils was allowed to adhere to the plastic surface of a cell-free, standard, 96-well tissue culture plate for 6 or 24 hours. After the incubation, the tissue culture plate was washed with TryplE^{TM} and PBS to remove non-adherent tau (Michel et al., 2014), and incubated for 24 hours in iPSC-macrophage medium. The amount of tau detected in the medium by tau ELISA at the end of the incubation was below detection point (<31 pg/ mL). The results minimise the possibility that tau present in the conditioned medium following incubation with iPSC-macrophages (Figure 5.9C, Released tau) passively diffused into medium from the tissue-culture plate surface.

5.2.6 LRRK2 affects tau clearance

Following the characterisation of tau clearance by healthy control-derived iPSC-macrophages, I sought to test the impact of LRRK2 genotype on the process (Figure 5.10A). To increase detection accuracy, intracellular tau levels were quantified with two independent methods; anti-tau immunostaining of fixed cells and tau ELISA of cell lysates. Tau ELISA was also used to determine tau amount in the conditioned medium.

LRRK2 genotype had no significant effect on clearance of the internalised tau monomer (Figures 5.10B-E). In contrast, fibrillar tau clearance was strongly affected by LRRK2. Significantly lower amount of tau fibrils remained unprocessed within G2019S iPSC-macrophages compared to LRRK2 WT. Conversely, unprocessed tau fibrils appeared to accumulate within LRRK2 KO macrophages (Figures 5.10B-D). Moreover, without LRRK2, cells released significantly more tau to conditioned medium, in line with findings from section 5.2.5 suggesting that intracellular fibril accumulation leads to enhanced extracellular tau

release (Figure 5.10 E). Overall, the results suggest LRRK2 may be needed for successful intracellular degradation of tau fibrils.

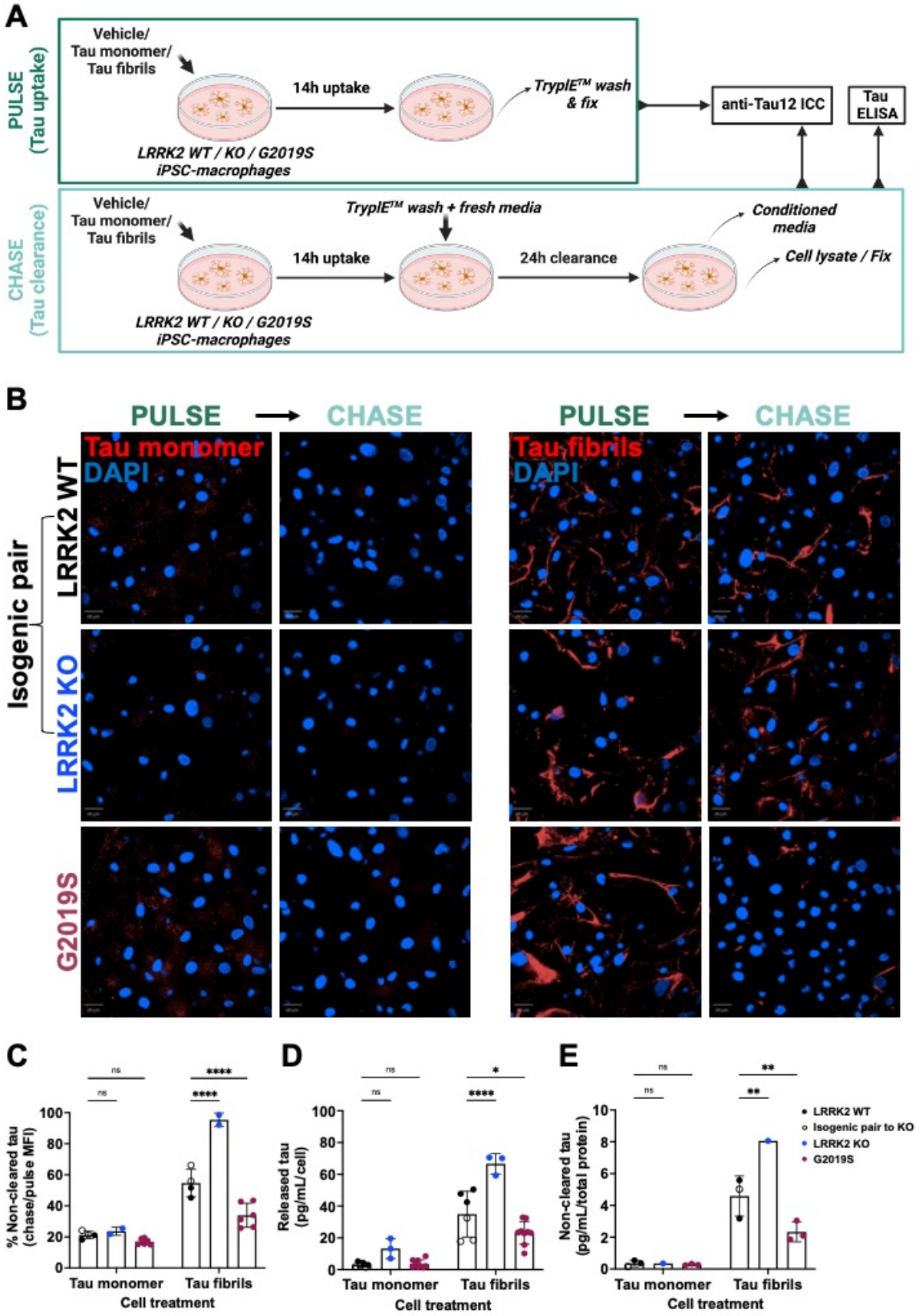

Figure legend on the next page.

Figure 5.10: LRRK2 influences tau clearance

(A.) Experiment workflow. (B.) Representative confocal microscopy images of tau uptake (Pulse) and intracellular clearance (Chase) in LRRK2 WT, KO, and G2019S iPSC-macrophages immunostained with anti-Tau12 and DAPI. (C.) Quantification of B. n=2 in x2 LRRK2 WT, x1 LRRK2 KO, and x3 G2019S lines. (D.) Total tau ELISA quantification of non-cleared intracellular tau remaining in iPSC-macrophages lysates post 24-hour clearance. n=1 in x3 LRRK2 WT, x1 LRRK2 KO, and x3 G2019S lines. (E.) Total tau ELISA quantification of tau in the conditioned media post 24-hour clearance. n=3 in x2 LRRK2 WT, x1 KO, and x3 G2019S lines.

*Two-way ANOVA with Dunnett's multiple comparisons test. All data is displayed as mean±SD, * p<0.05, ** p<0.01, **** p<0.0001.*

5.2.7 Prion-like capacity of tau processed by iPSC-macrophages

The final set of experiments interrogates the contribution of human microglia and microglial LRRK2 to prion-like tau propagation.

LRRK2 WT, KO, and G2019S iPSC-macrophages were pulsed with vehicle, monomeric, or fibrillar tau overnight, followed by a 24-hour clearance period. Conditioned medium, and cell lysates containing soluble (Triton fraction in 1% Triton lysis buffer) or sarkosyl-insoluble (SDS fraction in 1% SDS lysis buffer) tau were then collected and applied to 4R tau RT-QuIC assay in collaboration with Alessia Santambrogio from the Vendruscolo lab at the University of Cambridge (Figure 5.11A, section 2.4.9).

RT-QuIC is an ultra-sensitive and specific biochemical assay providing insight into the dosage and conformational strain of proteopathic aggregates in biospecimen. Initially developed for the diagnosis of prion diseases (Atarashi et al., 2011; Wilham et al., 2010), the assay has been lately adapted to test the presence of α-syn (Bongianni et al., 2019; Candelise et al., 2019; Fairfoul et al., 2016; Groveman et al., 2018; Shahnawaz et al., 2017) and tau seeds (Kraus et al., 2019a; Metrick et al., 2020a; Saijo et al., 2017, 2020a; Tennant et al., 2020) in clinical samples (reviewed in Vascellari et al., 2022). The 4R tau RT-QuIC assay utilised in this thesis detects the ability of 4R tau in sample to induce templated conversion of a monomeric tau substrate to an aggregate. The conversion is measured by a time-dependent increase in ThT fluorescence intensity above background threshold upon detection of β-sheet structures (Figure 5.11B). Previous version of the assay (Saijo et al., 2020a) used a cysteine-free, poly-histidine-tagged K18 tau fragment as the monomeric tau substrate (von Bergen et al., 2001). Following the determination of cryo-EM structures of tau filaments from 4R tauopathy patient brains (Y. Shi et al., 2021; W. Zhang et al., 2020), the K18 fragment was extended to tau aa residue 400 to create a novel K11 substrate used in this thesis to encompass the entire fibril core of typical 4R tau aggregates (Figure 5.11C).

No seeding activity was detected in neither of the cell lysate fractions nor in the conditioned medium collected from cells treated with vehicle or tau monomer. In contrast, SDS-soluble cell lysate fraction and conditioned medium collected from tau fibril-treated cells both showed positive K11 seeding. The SDS-soluble cell lysate fraction containing non-cleared, sarkosyl-insoluble tau produced strong, kinetically fast, and consistent ThT responses, regardless of LRRK2 genotype. In comparison, tau released to the conditioned medium by iPSC-macrophages treated with tau fibrils showed more variable ThT fluorescence, weaker in amplitude, and longer nucleation time (Figure 5.11D).

Potential confounding effect of the Triton and SDS lysis buffers as well as the iPSC-macrophage culture medium on the reaction kinetics was also investigated (Figure 5.11E). Interestingly, SDS lysis buffer alone showed efficient templation of the K11 substrate, unlike Triton lysis buffer or macrophage culture medium. We speculate that the effect could have been caused by SDS-induced fragmentation of the spontaneously-forming K11 aggregates, leading to multiple secondary nucleation events. Due to this potentially confounding effect, data described in Figure 5.11D (SDS fraction) should be interpreted with caution.

Lastly, we analysed the reaction half-times (t1/2) to understand the influence of LRRK2 on the seeding kinetics (Figure 5.11F). T1/2 refers to time required for ThT fluorescence to increase by 50% of its maximum intensity. No significant differences were found between any of the conditions tested. However, sarkosyl-insoluble tau accumulating in G1029S iPSC-macrophage lysates post tau fibril clearance, exhibited faster reaction times (mean t1/2 = 8.97 hours) compared with the LRRK2 WT (mean t1/2 = 12.11 hours). Conversely, insoluble tau accumulating in LRRK2 KO cells following tau fibril incubation showed slower ThT increase compared with LRRK2 WT (mean t1/2 = 13.27 hours). The opposite was true for conditioned medium samples. Without LRRK2, cells released tau capable of slightly faster seeding activity (mean t1/2 = 41.53 hrs) compared to LRRK2 WT cells (mean t1/2 = 54.74 hrs).

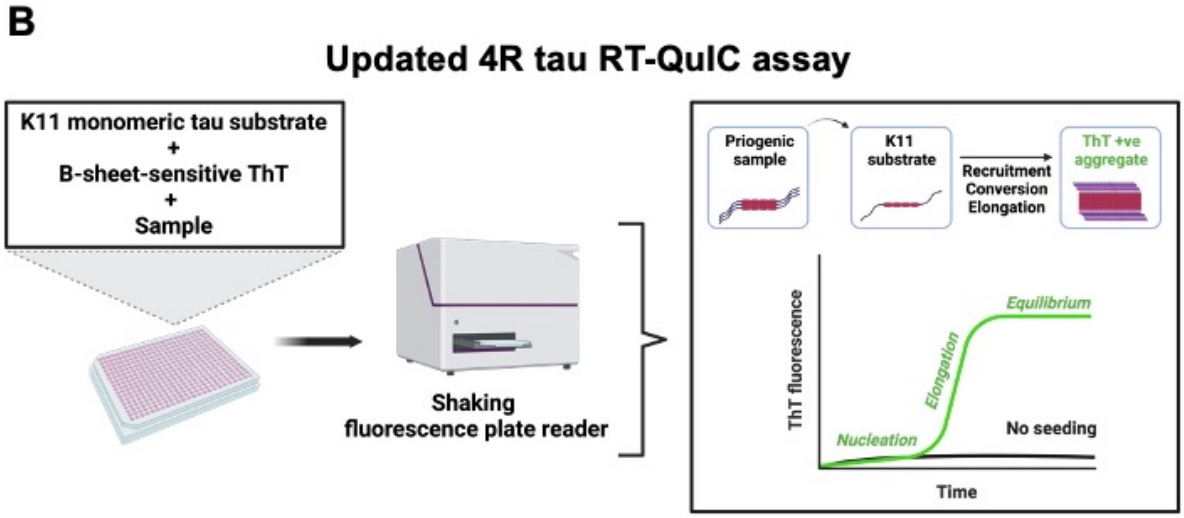

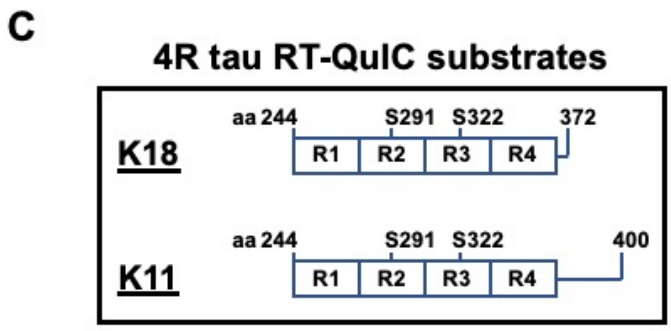

Figure continued on the next page

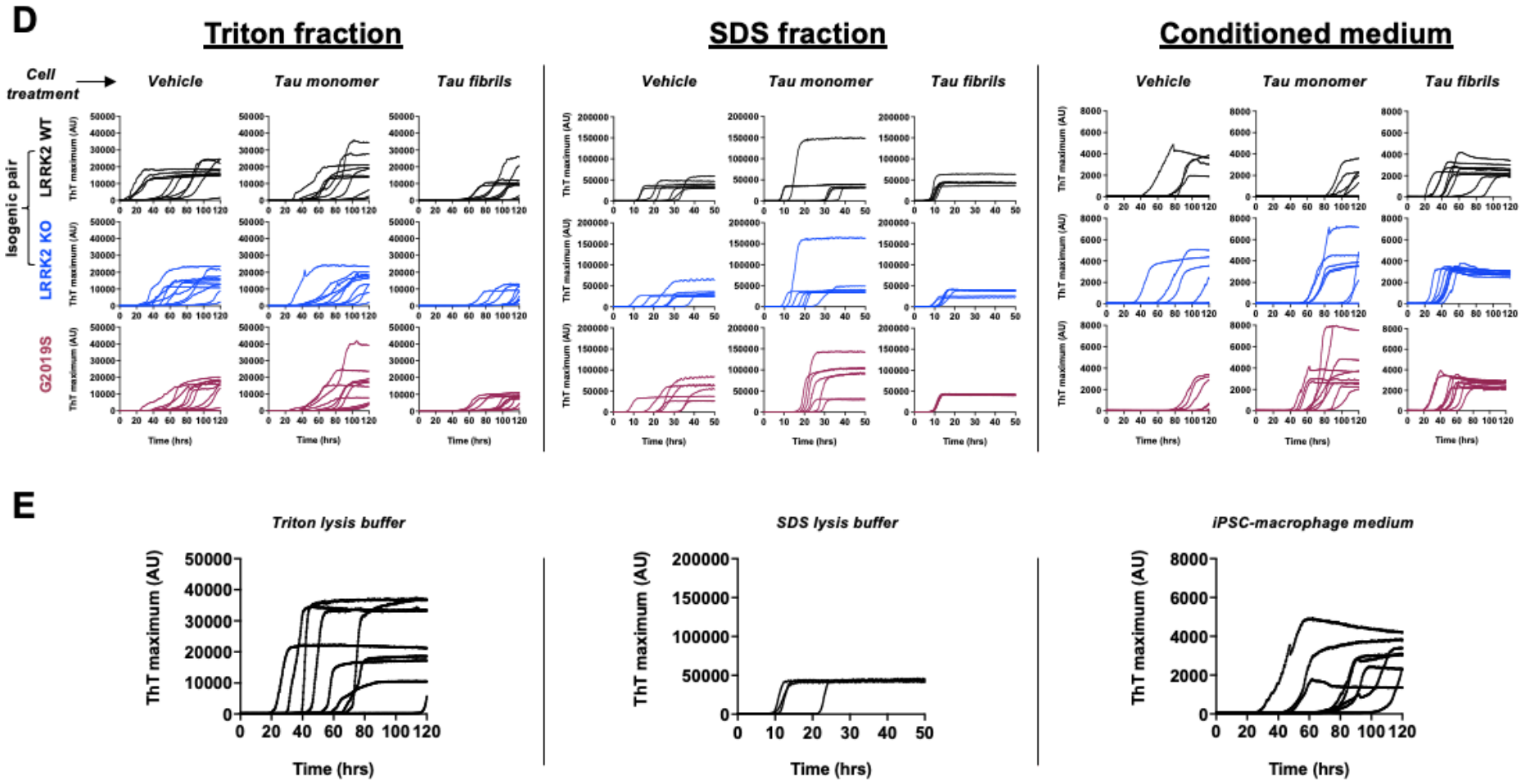

Figure continued on the next page

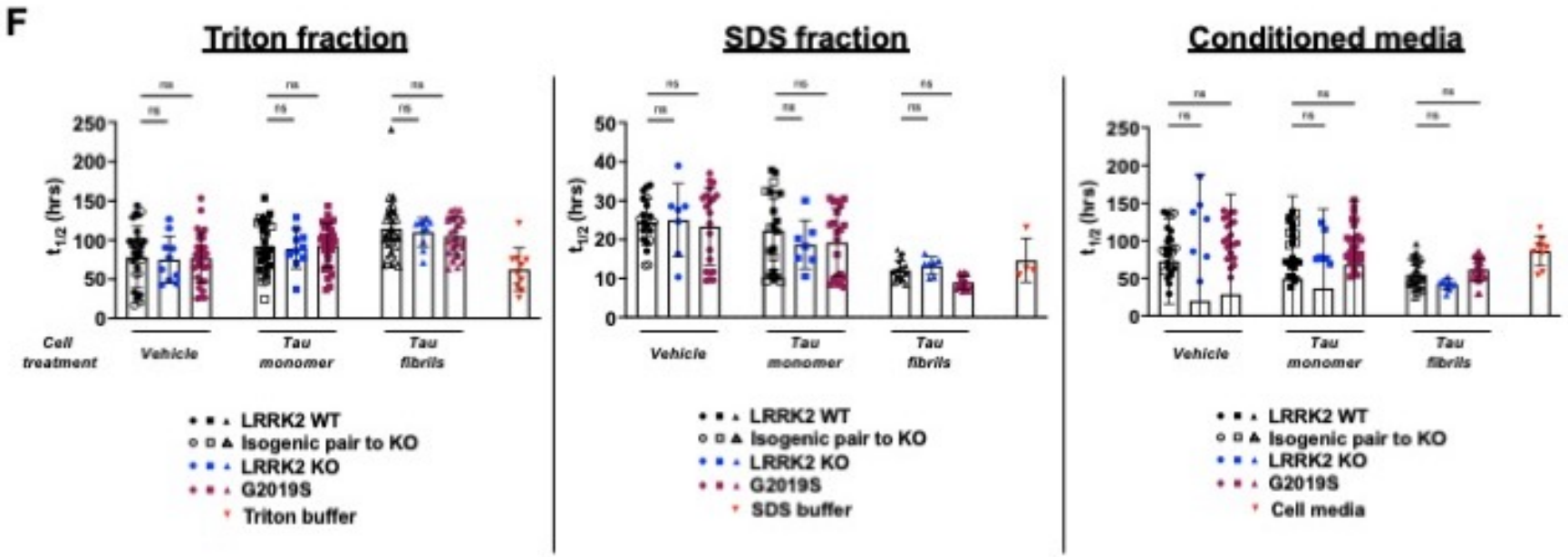

Figure legend on the next page.

Figure 5.11: Investigating the seeding competency of tau processed by iPSC-macrophages

(A.) Workflow diagram. Conditioned media and cell lysates from iPSC-macrophages were collected following tau uptake and clearance, and applied to 4R tau RT-QuIC assay. (B.) ThT readout is used to detect the sample capacity to template K11 monomeric tau fragment to b-sheet-rich aggregates in the updated assay version. (C.) Schematics of K18 and K11 4R tau RT-QuIC assay substrates. (D.) Representative seeding activity of samples collected LRRK2 WT, KO and G2019S iPSC-macrophages in (A.). Total protein levels in cell lysates and media were normalised to the 1 and 5 mg/mL, respectively. Cell lysates were applied to the reaction buffer at 1:10,000 dilution, conditioned media at 1:100, to account for tau concentration differences. Individual, technical replicate reactions are shown in each panel (minimum of n=7). Biological replicates: n=1 in x3 LRRK2 WT, x1 LRRK2 KO, x3 G2019S lines. (E.) Seeding capacity of cell lysate buffers and iPSC-macrophage media alone. Minimum of 4 individual technical replicate is shown. (F.) t1/2 calculated from (D.): sigmoidal dose-response, variable slope, logEC50. Values are displayed as mean±SD. Two-way ANOVA with Tukey's multiple comparisons test.

5.3 Discussion

Genetic, epidemiological, as well as interventional studies in rodents have consistently implicated microglia in tau pathogenesis. But direct evidence of human microglial contribution to tau pathogenesis in tauopathies is missing. In this chapter, I investigated whether impaired microglial processing of tau may underlie the propagation of prion-like tau species, using iPSC-macrophages and microglia and endotoxin-free, human recombinant 2N4R tau.

First, I focused on characterising microglial tau internalisation. Past functional studies have already showed that various microglia models can take up tau from the extracellular space (Abud et al., 2017; Asai et al., 2015; Bolós et al., 2016b; W. Luo et al., 2015; Majerova et al., 2014; Stancu et al., 2019; B. Zhu et al., 2022; Zilkova et al., 2020) as well as tau-containing neurons (J. Brelstaff et al., 2018; J. H. Brelstaff et al., 2021; Pampuscenko et al., 2020). Little is still known about the precise mechanisms by which microglia internalise tau. Soluble monomeric and oligomeric tau were found to interact with CX3CR1 (Bolós et al., 2016b) and P2Y12 (Chinnathambi & Das, 2023) microglial chemoattractant receptors. Considerable attention has also focused on the TREM2 receptor based on previous reports of Aβ uptake via TREM2 (Yeh et al., 2016; Zhao et al., 2018) but Zhu et al., 2022 recently clearly showed no difference in tau uptake following microglial TREM2 KO *in vitro*.

Our data demonstrates for the first time that human microglia internalise tau via LRP1. LRP1, also known as the ApoE receptor, is type I glycosylated, ubiquitously expressed, transmembrane protein involved in the endocytosis of extracellular molecules as well as in signal transduction regulating lipid homeostasis and inflammatory processes (reviewed in Gonias & Campana, 2014). Following 2-hour tau monomer incubation with iPSC-macrophages, we observed 73.2% and 69.9% LRP1-positive, anti-tau12-stained or DyLight 488-conjugated tau puncta, respectively (Figure 5.4). Pharmacological and genetic LRP1 perturbations significantly reduced monomeric tau uptake, overall pointing to LRP1-mediated monomeric tau endocytosis (Figures 5.4 and 5.5).

Receptor mediated endocytosis is a form of micropinocytosis by which cells selectively internalise small soluble molecules into vesicles formed by the invagination of plasma membrane. Micropinocytosis may further require vesicle scaffold proteins, including clathrin and caveolin, or can be clathrin/caveolin-independent (Solé-Domènech et al., 2016). Whether scaffold proteins are necessary for LRP1-mediated monomeric tau endocytosis in microglia was beyond the scope of this thesis. Such investigation could, however, provide valuable insight into internalised tau processing pathways, since the mode of cargo uptake by microglia shapes their effector function (Kiss & Botos, 2009; S. Kumari et al., 2010). Interestingly, a vascular smooth muscle cell study demonstrated increased LRP1 expression following P2Y12 receptor (P2Y12R) activation with ADP (J. Chen et al., 2020). Considering the previously reported P2Y12R and tau interaction (Chinnathambi & Das, 2023), P2Y12R-LRP1 interplay in monomeric tau uptake could be another valuable hypothesis to examine in the future.

Only 32.1 and 37.1% anti-tau12-stained and DyLight 488-conjugated tau puncta colocalised with LRP1 following 2-hour tau fibril incubation with iPSC-macrophages (Figure 5.4). Tau fibril uptake was also less affected by LRP1 inhibition with sRAP and LRP1 knockdown, compared with tau monomer uptake (Figures 5.4 and 5.5). The data suggests an alternative route of entry, besides LRP1, may exist for tau fibrils in human microglia. Reduced but not inhibited tau fibril uptake following LRP1 silencing in neurons (Rauch et al., 2020) confirms our findings. Aggregated tau species were previously reported to bind HSPGs on microglial surface (Funk et al., 2015a). HSPGs are highly interactive, ubiquitously expressed, cell surface and extracellular matrix glycoproteins. HSPGs are constitutively endocytosed via fluid-phase macropinocytosis (Christianson & Belting, 2014; Sarrazin et al., 2011). Given that homeostatic microglia use pinocytosis to constantly survey their environment (Booth & Thomas, 1991; Canton, 2018; Ranson & Thomas, 1991), macropinocytic uptake of tau fibrils bound to HSPGs should be investigated in the future. Importantly, LRP1 often forms a co-receptor complex with HSPGs (Bres & Faissner, 2019), as was shown in the case of Aβ (Kanekiyo et al., 2011) and ApoE/lipoprotein particle (Wilsie & Orlando, 2003) uptake. Such co-dependent uptake

regulation could explain why inhibition of microglial LRP1 only partially affected tau fibril uptake in our results.

Overall, LRP1 has emerged from this thesis as an important regulator of tau uptake in microglia. Given its reported involvement in the uptake of tau in neurons (Rauch et al., 2020) as well as other proteopathic seeds, including aβ (Shinohara) (Shinohara et al., 2017), α-syn (Chen et al., 2022), and cellular prion protein (Jen et al., 2010; Taylor & Hooper, 2007), manipulation of LRP1 levels could potentially be explored for therapeutic purposes across multiple neurodegenerative diseases.

Of note is also the CRISPR/Cas9-mediated gene editing platform used in this chapter to knockdown LRP1. Dr Sam Washer (manuscript in preparation) and Dolan et al., 2022 independently demonstrated that SAMHD1 degradation by Vpx delivered simultaneously with Cas9-gRNA of interest to iPSC-microglia, overcomes the long-standing issues with lentiviral transduction of SAMHD1-expresing myeloid cells (Navarro-Guerrero et al., 2021). Successful LRP1 KD in iPSC-macrophages shown in this chapter further demonstrates the method suitable for stable gene delivery in an *in vitro* model of human microglia (Figure 5.5)

Microglial internalisation of neurodegeneration-associated proteins has been traditionally considered a beneficial phenomenon, similar to microglial phagocytosis of pathogens and cellular debris (Sierra et al., 2013). Translational efforts into potentiating microglial effector function via TREM2-activating antibodies are already under way (Schlepckow et al., 2020; van Lengerich et al., 2023; S. Wang et al., 2020). Yet, no direct evidence exists confirming microglial ability to fully degrade the internalised tau. In fact, very few studies have systematically investigated the downstream tau processing by microglia.

Data emerging from the tau clearance-focused experiments presented in this chapter (Figures 5.8 and 5.9) significantly expands our understanding of the topic. Internalised monomeric tau is readily degraded by iPSC-macrophages, as very little tau was detected intra- or extracellularly already post 6-hour clearance. In contrast, processing of internalised tau fibrils

appears to be slower. At least 50% of tau fibrils could still be detected within iPSC-macrophages post clearance phase, regardless of the examined condition (Figure 5.9). In agreement with our findings, Luo et al., 2015 previously reported degradation of internalised sarkosyl-insoluble, brain-derived tau at low concentration (1 μg/mL) by primary rodent microglia. According to Andersson et al., 2019, lysosomal acidification but not proteasomal degradation was necessary for successful insoluble tau clearance by rodent microglia. In contrast, our data in relevant, human microglial model indicates both degradation pathways may be involved (Figure 5.8).

Immunocytochemistry was used as a quick and simple method for quantification of intracellular tau levels in the tau clearance-focused experiments, due to the number of conditions examined. However, a significant amount of tau fibrils can be bound to the cellular surface at the end of incubation, as evident by Figures 5.2C and 5.3C. It will be therefore essential to verify the findings on tau clearance with quantification methods excluding the membrane-bound tau, such as flow cytometry with trypan-blue quenching. It will be equally important to examine whether microglia can fully clear the internalised tau, given long-enough time-course beyond 24 hours, and how the intracellular clearance relates to the extracellular tau release in this scenario.

The detection of tau in the conditioned medium from iPSC-macrophages (Figure 5.9) confirms previous evidence of extracellular tau release by rodent microglia (Asai et al., 2015; J. H. Brelstaff et al., 2021; Clayton et al., 2021; Crotti et al., 2019; Hopp et al., 2018; B. Zhu et al., 2022). The amount of tau released by iPSC-macrophages depended strongly on the pulsed tau conformation and concentration. Cells stimulated with tau fibrils at high concentrations released the most tau. Future quantification of tau levels in the conditioned medium following the inhibition of microglial secretory pathways could provide an important proof of active tau secretion. Given the accumulating reports of microglia secreting tau packaged in EVs (Asai et al., 2015; Clayton et al., 2021; Crotti et al., 2019; B. Zhu et al., 2022), determining the

proportion of tau secreted freely vs in EVs in our samples could help further elucidate microglial processing of the internalised tau.

Furthermore, data presented in this chapter indicates a potential coupling of tau fibril uptake, degradation, and release. Specifically, I found that the length of tau fibril incubation with iPSC-macrophages negatively affects their clearance, followed by an enhanced release of tau to conditioned medium (Figure 5.9). Importantly, the non-cleared, insoluble tau accumulating within iPSC-macrophages, as well as tau released by the cells following tau fibril stimulation, show capacity to template β-sheet rich conformation onto a native, monomeric tau substrate (Figure 5.11). The data provides important evidence supporting the putative role of microglia in tau prion-like spreading.

Interestingly, the released tau showed weaker seeding capacity compared with the cell lysate-contained tau (Figure 5.11). It is conceivable that microglial processing of tau partially neutralises tau seeding capacity. Alternatively, microglia may release the partially neutralised tau in a free form while seeding-competent tau is specifically destined for EV-packaged release. These speculations would fit previous preliminary findings of seeding-competent tau in EVs derived from rodent microglia (Crotti et al., 2019; B. Zhu et al., 2022).

It is important to note that the RT-QuIC assay used in this thesis reports only on the sample capacity to seed cell-free tau substrate. Currently, direct evidence for templated aggregation of endogenous tau expressed in neurons by microglial-processed tau is lacking. The majority of studies published on the topic utilised tau-biosensor cell lines (Hitt et al., 2021; Holmes et al., 2014) in place of neurons. Reduced phospho-tau spreading *in vivo* was reported following inhibition of microglial EV secretion (Asai et al., 2015; Crotti et al., 2019) but only one study so far demonstrated neurons can internalise tau released by microglia (Asai et al., 2015). Following up on our RT-QuIC data with an *in vitro* tau seeding assay in neurons could therefore confirm the physiological relevance of our data and, crucially, provide the missing direct evidence of microglia-mediated pathological tau propagation.

Genetic studies have consistently highlighted several molecular components of microglial phagolysosomal pathways as key variants associated with development and progression of tauopathies (reviewed in Podleśny-Drabiniok et al., 2020; Romero-Molina et al., 2022). LRRK2 protein represents one such candidate variant. The LRRK2 kinase activity-increasing G2019S mutation, associated with the most common, tau pathology-featuring form of PD (Bonifati, 2006, Henderson et al., 2019) and PSP (Sanchez-Contreras et al., 2017) is an example of one such variant. As discussed throughout the thesis, microglia become the highest LRRK2-expressing brain cells under inflammatory conditions (H. Lee et al., 2020). Yet the role of microglial LRRK2 in tau pathogenesis has never been examined.

This thesis provides pioneering evidence of LRRK2 influence on all aspects of microglial tau processing, including uptake, clearance, and tau seeding activity. G2019S LRRK2 iPSC-macrophages and microglia show enhanced tau uptake, potentially mediated via accelerated LRP1-tau complex trafficking. Conversely, LRRK2 absence decreases tau uptake but short-term LRRK2 kinase pharmacological inhibition did not phenocopy the KO, implying that the effect is not mediated through simple transient LRRK2 kinase activity (Figure 5.6). It is possible that other, G2019S LRRK2-mutation-induced phenotypic changes besides the increased LRRK2 kinase activity, underlie the increased tau uptake.

Furthermore, our data suggests LRRK2 may be needed for tau fibril degradation. Compared with LRRK2 WT, internalised tau fibrils accumulated in LRRK2 KO cells, followed by an enhanced extracellular tau release. The opposite was true in G2019S iPSC-macrophages (Figure 5.10). The data agrees with our earlier observations linking impaired tau fibril degradation with an enhanced tau release in healthy control-derived iPSC-macrophages (Figure 5.9). Tau in the conditioned medium from LRRK2 KO iPSC-macrophages trended towards faster seeding activity compared with LRRK2 WT or G2019S cells, though the data did not reach significance (Figure 5.11). Altogether, these observations potentially fit our speculations about the importance of microglial processing for neutralisation of tau fibril seeding capacity.

The data would also appear to support the initial hypothesis that impaired microglial tau clearance mediates prion-like tau spreading in tauopathies. However, *in vivo* evidence from rodents and humans indicate that pathogenic tau spread is associated with the LRRK2-activity-increasing G2019S mutation rather that LRRK2 KO (Henderson et al., 2019; Nguyen et al., 2018). Interestingly, insoluble non-degraded tau within G2019S macrophage lysates, though reduced in the amount compared with LRRK2 WT or KO, showed tendency towards faster and more consistent seeding capacity (Figure 5.11). It is therefore possible that not only degradation efficiency but also the identity of processed tau species may underlie prion-like tau spreading by microglia. Proteomic analysis could help further elucidate how LRRK2 affects microglia tau clearance to species with varying seeding competencies.

Chapter 6

General Discussion

The overarching aim of this thesis was to examine the contribution of human microglia to the propagation of tau pathology in tauopathies. Using iPSC-macrophage and microglia as a relevant and authentic *in vitro* model of human microglia, I have provided novel insight into the molecular mechanisms underlying microglial processing of exogenous native and aggregated tau at healthy baseline and in disease.

The thesis workflow is divided into three complementing stages:
In the first stage (Chapter 3), I interrogate the influence of LRRK2 protein on microglial baseline phagocytic and degradative capacity. LRR2K has emerged as candidate genetic determinant of microglia-mediated tauopathy progression (Herbst et al., 2022; Nalls et al., 2014a; Nguyen et al., 2018; Podleśny-Drabiniok et al., 2020; Sanchez-Contreras et al., 2017; Zimprich et al., 2004) but little is known about its precise mechanistic involvement in the process. Previous studies have suggested LRRK2 may regulate phagocytic cargo uptake by microglia but inconsistencies between experimental approaches and contradictory evidence have prevented consensus on the topic. To address the gap in our knowledge, I have first optimised a protocol to simultaneously monitor phagocytosis and degradation of a basic, versatile cargo in IPSC-macrophages, a simple, yet authentic *in vitro* model human microglia. Next, I applied the assay to investigate the influence of microglial LRRK2 on the processes. Neither genetic nor pharmacological manipulation of LRRK2 altered iPSC-macrophage uptake of double-labelled reporter beads. However, the disease-associated G2019S LRRK2 mutation appeared to have enhanced iPSC-macrophage proteolytic activity. Collectively, the results implied that LRRK2 may not be involved in the initial step of phagocytic cargo engulfment but may be needed for proteolytic activity necessary to degrade the internalised cargo.

Subsequently, I aimed to compare these findings with the influence of LRRK2 on microglial tau-specific processing. To do so, I needed sufficient quantities of tau preparation, in native and aggregated form. I addressed the need in the second stage of the workflow, summarised in Chapter 4, Here, I present an optimised protocol for the production of human recombinant tau protein from *E. coli*, having overcome the highly challenging removal of residual bacterial endotoxin from the preparation in order to measure accurate microglial responses to the protein alone. The method is the first to provide an effective, scalable workflow for the purification of endotoxin-free, human recombinant 2N4R tau in respectable yield and purity. The purified tau can be further aggregated into seeding-competent fibrils in presence of heparin co-factor. There are known structural, biochemical, and biophysical differences between the recombinant tau fibril preparation and disease-associated tau extracted from the brains of tauopathy patients (Fichou et al., 2018; Fichou, Oberholtzer, et al., 2019; Y. Shi et al., 2021). However, the use of recombinant fibrils in experimental settings can be viewed as complementary to the use of brain-extracted tau preparation, as it offers a modular, reproducible system for the systematic investigation of cellular response to the individual tau isoforms and modifications.

Having succeeded in the production of recombinant tau monomer and aggregates, I examined the role of human microglia and microglial LRRK2 in tau pathogenesis in the last stage. The results are summarised in Chapter 5. Using iPSC-macrophages and microglia, and endotoxin-free human recombinant tau, I provide novel observation that LRP1 mediates tau internalisation by microglia. I further show that degradation of internalised tau involves both the proteasomal and lysosomal system in iPSC-macrophages, and is more efficient for the soluble compared with the aggregated tau. Intracellular clearance of the insoluble fibrils is concentration- and incubation-length dependent, and inversely associated with tau release to conditioned medium. Following tau fibril incubation, the intracellular non-cleared tau and tau released by microglia to the conditioned medium, shows seeding competency, supporting the role for microglia in tau prion-like spreading.

Importantly, the results here demonstrate that the PD and PSP-associated G2019S LRRK2 mutation enhances tau uptake by microglia. The effect is potentially mediated by LRRK2 phosphorylation of Rab8a and Rab10 GTPases involved in the LRP1-tau complex trafficking and influences the monomeric tau LRP1-mediated endocytosis more prominently than the hypothesised phagocytosis of aggregated tau. These observations would agree with the Chapter 3 findings of no LRRK2 involvement in bead phagocytosis. Intriguingly, the G2019S LRRK2 iPSC-macrophages also exhibited enhanced tau fibrillar clearance, in line with the observed increase in baseline proteolytic capacity, described in Chapter 3. Precisely how these observed phenotypes relate to the progression of pathology *in vivo* is yet to be elucidated. Despite the enhanced fibrillar tau clearance by G2019S iPSC-macrophages, the non-cleared fibrillar tau retained in G2019S iPSC-macrophages post 24-hour clearance showed faster seeding capacity compared with the non-cleared fibrillar tau in LRRK2 WT cells. It is conceivable that tau degradation by microglia may generate species with enhanced seeding capacity. Future proteomic and conformation analyses of the processed tau, including the Fourier-transform infrared spectroscopy, could help provide mechanistic insight into how microglia may affect tau prion-like behaviour.

To conclude, dysregulation of microglial homeostatic phenotype had long been recognized as a secondary pathological hallmark of tauopathies. Substantial evidence from rodents have indicated that microglia play a more direct role in the propagation of tau pathology. This thesis importantly extends the evidence by providing detailed characterisation of human iPSC-macrophage and microglial response to tau protein in its native and aggregated form. The results presented here support the putative role of human microglia in tau pathogenesis and provide further reasoning for investigating microglia-enriched tauopathy risk variants as potential druggable targets.

Appendix

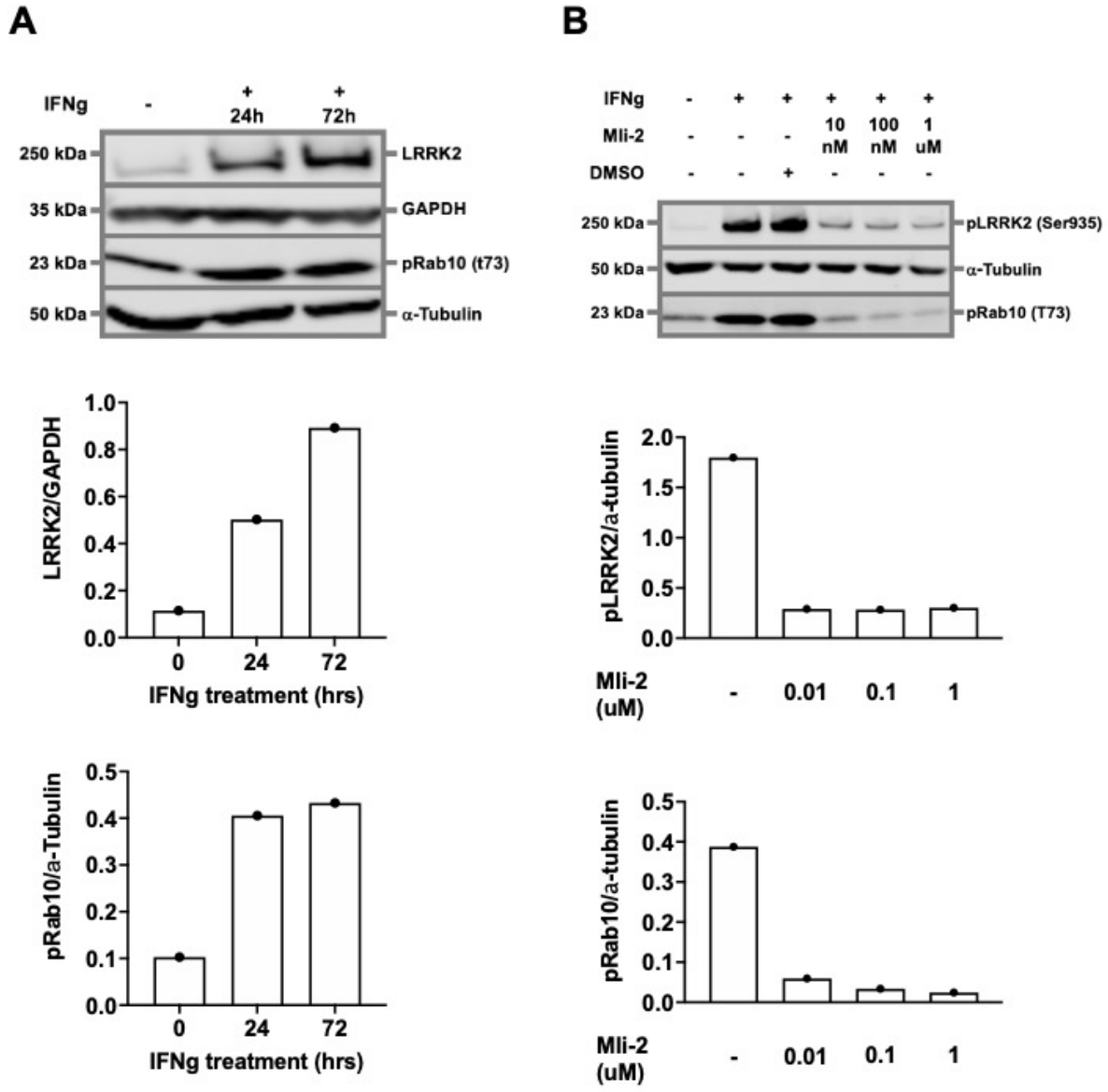

Figure 7.1: IFNγ- and Mli-2-induced changes in LRRK2 protein expression levels and LRRK2 kinase activity in OXM macrophage media-cultured iPSC-macrophages
(A.) Western blot analysis confirms upregulation of LRRK2 and pRab 10 (T73) protein levels upon 24- and 72-hour IFNγ treatment. (B.) Mli-2, a LRRK2 kinase inhibitor, effectively decreases pLRRK2 (Ser 935) and pRab10 (T73) levels in iPSC-macrophages. n=1 in LRRK2 WT line.

References

Abels, E. R., Nieland, L., Hickman, S., Broekman, M. L. D., El Khoury, J., & Maas, S. L. N. (2021). Comparative Analysis Identifies Similarities between the Human and Murine Microglial Sensomes. *International Journal of Molecular Sciences*, *22*(3), 1495. https://doi.org/10.3390/ijms22031495

Abounit, S., Bousset, L., Loria, F., Zhu, S., de Chaumont, F., Pieri, L., Olivo-Marin, J., Melki, R., & Zurzolo, C. (2016). Tunneling nanotubes spread fibrillar α-synuclein by intercellular trafficking of lysosomes. *The EMBO Journal*, *35*(19), 2120–2138. https://doi.org/10.15252/embj.201593411

Abud, E. M., Ramirez, R. N., Martinez, E. S., Healy, L. M., Nguyen, C. H. H., Newman, S. A., Yeromin, A. V., Scarfone, V. M., Marsh, S. E., Fimbres, C., Caraway, C. A., Fote, G. M., Madany, A. M., Agrawal, A., Kayed, R., Gylys, K. H., Cahalan, M. D., Cummings, B. J., Antel, J. P., … Blurton-Jones, M. (2017). iPSC-Derived Human Microglia-like Cells to Study Neurological Diseases. *Neuron*, *94*(2), 278-293.e9. https://doi.org/10.1016/j.neuron.2017.03.042

Aderem, A., & Underhill, D. M. (1999). MECHANISMS OF PHAGOCYTOSIS IN MACROPHAGES. *Annual Review of Immunology*, *17*(1), 593–623. https://doi.org/10.1146/annurev.immunol.17.1.593

Ahmadi Rastegar, D., & Dzamko, N. (2020). Leucine Rich Repeat Kinase 2 and Innate Immunity. *Frontiers in Neuroscience*, *14*. https://doi.org/10.3389/fnins.2020.00193

Ahmadi Rastegar, D., Hughes, L. P., Perera, G., Keshiya, S., Zhong, S., Gao, J., Halliday, G. M., Schüle, B., & Dzamko, N. (2022). Effect of LRRK2 protein and activity on stimulated cytokines in human monocytes and macrophages. *Npj Parkinson's Disease*, *8*(1), 34. https://doi.org/10.1038/s41531-022-00297-9

Ahmed, Z., Cooper, J., Murray, T. K., Garn, K., McNaughton, E., Clarke, H., Parhizkar, S., Ward, M. A., Cavallini, A., Jackson, S., Bose, S., Clavaguera, F., Tolnay, M., Lavenir, I., Goedert, M., Hutton, M. L., & O'Neill, M. J. (2014). A novel in vivo model of tau propagation with rapid and progressive neurofibrillary tangle pathology: the pattern of spread is determined by connectivity, not proximity. *Acta Neuropathologica*, *127*(5), 667–683. https://doi.org/10.1007/s00401-014-1254-6

Aida, Y., & Pabst, M. J. (1990). Removal of endotoxin from protein solutions by phase separation using triton X-114. *Journal of Immunological Methods*, *132*(2), 191–195. https://doi.org/10.1016/0022-1759(90)90029-U

Akira, S., Uematsu, S., & Takeuchi, O. (2006). Pathogen Recognition and Innate Immunity. *Cell*, *124*(4), 783–801. https://doi.org/10.1016/j.cell.2006.02.015

Alliot, F., Godin, I., & Pessac, B. (1999). Microglia derive from progenitors, originating from the yolk sac, and which proliferate in the brain. *Developmental Brain Research*, *117*(2), 145–152. https://doi.org/10.1016/S0165-3806(99)00113-3

Alliot, F., Lecain, E., Grima, B., & Pessac, B. (1991). Microglial progenitors with a high proliferative potential in the embryonic and adult mouse brain. *Proceedings of the National Academy of Sciences*, *88*(4), 1541–1545. https://doi.org/10.1073/pnas.88.4.1541

Alonso, A. del C., Zaidi, T., Novak, M., Grundke-Iqbal, I., & Iqbal, K. (2001). Hyperphosphorylation induces self-assembly of τ into tangles of paired helical filaments/straight filaments. *Proceedings of the National Academy of Sciences*, *98*(12), 6923–6928. https://doi.org/10.1073/pnas.121119298

Alster, P., Madetko, N., Koziorowski, D., & Friedman, A. (2020). Microglial Activation and Inflammation as a Factor in the Pathogenesis of Progressive Supranuclear Palsy (PSP). *Frontiers in Neuroscience*, *14*. https://doi.org/10.3389/fnins.2020.00893

Alzforum. (n.d.). *MAPT mutations*. Https://Www.Alzforum.Org/Mutations/Mapt.

Anand, V. S., Reichling, L. J., Lipinski, K., Stochaj, W., Duan, W., Kelleher, K., Pungaliya, P., Brown, E. L., Reinhart, P. H., Somberg, R., Hirst, W. D., Riddle, S. M., & Braithwaite, S. P. (2009). Investigation of leucine-rich repeat kinase 2. *FEBS Journal*, *276*(2), 466–478. https://doi.org/10.1111/j.1742-4658.2008.06789.x

Andersen, M. S., Bandres-Ciga, S., Reynolds, R. H., Hardy, J., Ryten, M., Krohn, L., Gan-Or, Z., Holtman, I. R., & Pihlstrøm, L. (2021). Heritability Enrichment Implicates Microglia in Parkinson's Disease Pathogenesis. *Annals of Neurology*, *89*(5), 942–951. https://doi.org/10.1002/ana.26032

Andersson, C. R., Falsig, J., Stavenhagen, J. B., Christensen, S., Kartberg, F., Rosenqvist, N., Finsen, B., & Pedersen, J. T. (2019). Antibody-mediated clearance of tau in primary mouse microglial cultures requires Fcγ-receptor binding and functional lysosomes. *Scientific Reports*, *9*(1), 4658. https://doi.org/10.1038/s41598-019-41105-4

Anspach, F. B., & Hilbeck, O. (1995). Removal of endotoxins by affinity sorbents. *Journal of Chromatography A*, *711*(1), 81–92. https://doi.org/10.1016/0021-9673(95)00126-8

Antón-Fernández, A., Vallés-Saiz, L., Avila, J., & Hernández, F. (2023). Neuronal nuclear tau and neurodegeneration. *Neuroscience*, *518*, 178–184. https://doi.org/10.1016/j.neuroscience.2022.07.015

Arakhamia, T., Lee, C. E., Carlomagno, Y., Kumar, M., Duong, D. M., Wesseling, H., Kundinger, S. R., Wang, K., Williams, D., DeTure, M., Dickson, D. W., Cook, C. N., Seyfried, N. T., Petrucelli, L., Steen, J. A., & Fitzpatrick, A. W. P. (2021).

Posttranslational Modifications Mediate the Structural Diversity of Tauopathy Strains. *Cell*, *184*(25), 6207–6210. https://doi.org/10.1016/j.cell.2021.11.029

Arendt, T., Stieler, J., Strijkstra, A. M., Hut, R. A., Rüdiger, J., Van der Zee, E. A., Harkany, T., Holzer, M., & Härtig, W. (2003). Reversible Paired Helical Filament-Like Phosphorylation of Tau Is an Adaptive Process Associated with Neuronal Plasticity in Hibernating Animals. *The Journal of Neuroscience*, *23*(18), 6972–6981. https://doi.org/10.1523/JNEUROSCI.23-18-06972.2003

Arendt, T., Stieler, J. T., & Holzer, M. (2016). Tau and tauopathies. *Brain Research Bulletin*, *126*, 238–292. https://doi.org/10.1016/j.brainresbull.2016.08.018

Arima, K., Hirai, S., Sunohara, N., Aoto, K., Izumiyama, Y., Uéda, K., Ikeda, K., & Kawai, M. (1999). Cellular co-localization of phosphorylated tau- and NACP/α-synuclein-epitopes in Lewy bodies in sporadic Parkinson's disease and in dementia with Lewy bodies. *Brain Research*, *843*(1–2), 53–61. https://doi.org/10.1016/S0006-8993(99)01848-X

Arnold, S. E., Hyman, B. T., Flory, J., Damasio, A. R., & Van Hoesen, G. W. (1991). The Topographical and Neuroanatomical Distribution of Neurofibrillary Tangles and Neuritic Plaques in the Cerebral Cortex of Patients with Alzheimer's Disease. *Cerebral Cortex*, *1*(1), 103–116. https://doi.org/10.1093/cercor/1.1.103

Aronov, S., Aranda, G., Behar, L., & Ginzburg, I. (2002). Visualization of translated tau protein in the axons of neuronal P19 cells and characterization of tau RNP granules. *Journal of Cell Science*, *115*(19), 3817–3827. https://doi.org/10.1242/jcs.00058

Asai, H., Ikezu, S., Tsunoda, S., Medalla, M., Luebke, J., Haydar, T., Wolozin, B., Butovsky, O., Kügler, S., & Ikezu, T. (2015). Depletion of microglia and inhibition of exosome synthesis halt tau propagation. *Nature Neuroscience*, *18*(11), 1584–1593. https://doi.org/10.1038/nn.4132

Askew, K., Li, K., Olmos-Alonso, A., Garcia-Moreno, F., Liang, Y., Richardson, P., Tipton, T., Chapman, M. A., Riecken, K., Beccari, S., Sierra, A., Molnár, Z., Cragg, M. S., Garaschuk, O., Perry, V. H., & Gomez-Nicola, D. (2017). Coupled Proliferation and Apoptosis Maintain the Rapid Turnover of Microglia in the Adult Brain. *Cell Reports*, *18*(2), 391–405. https://doi.org/10.1016/j.celrep.2016.12.041

Atarashi, R., Satoh, K., Sano, K., Fuse, T., Yamaguchi, N., Ishibashi, D., Matsubara, T., Nakagaki, T., Yamanaka, H., Shirabe, S., Yamada, M., Mizusawa, H., Kitamoto, T., Klug, G., McGlade, A., Collins, S. J., & Nishida, N. (2011). Ultrasensitive human prion detection in cerebrospinal fluid by real-time quaking-induced conversion. *Nature Medicine*, *17*(2), 175–178. https://doi.org/10.1038/nm.2294

Babcock, A. A., Kuziel, W. A., Rivest, S., & Owens, T. (2003). Chemokine Expression by Glial Cells Directs Leukocytes to Sites of Axonal Injury in the CNS. *The Journal of*

Neuroscience, *23*(21), 7922–7930. https://doi.org/10.1523/JNEUROSCI.23-21-07922.2003

Baeuerle, E., Zhang, N., Musi, N., & Orr, M. E. (2019). WHOLE-BODY TAU-KNOCKOUT MICE DEVELOP AGE-ASSOCIATED METABOLIC DYSFUNCTION AND OBESITY. *Innovation in Aging*, *3*(Supplement_1), S89–S89. https://doi.org/10.1093/geroni/igz038.341

Barbier, P., Zejneli, O., Martinho, M., Lasorsa, A., Belle, V., Smet-Nocca, C., Tsvetkov, P. O., Devred, F., & Landrieu, I. (2019). Role of Tau as a Microtubule-Associated Protein: Structural and Functional Aspects. *Frontiers in Aging Neuroscience*, *11*. https://doi.org/10.3389/fnagi.2019.00204

Barghorn, S., Biernat, J., & Mandelkow, E. (n.d.). Purification of Recombinant Tau Protein and Preparation of Alzheimer-Paired Helical Filaments In Vitro. In *Amyloid Proteins* (pp. 035–052). Humana Press. https://doi.org/10.1385/1-59259-874-9:035

Barghorn, S., Zheng-Fischhöfer, Q., Ackmann, M., Biernat, J., von Bergen, M., Mandelkow, E.-M., & Mandelkow, E. (2000). Structure, Microtubule Interactions, and Paired Helical Filament Aggregation by Tau Mutants of Frontotemporal Dementias. *Biochemistry*, *39*(38), 11714–11721. https://doi.org/10.1021/bi000850r

Bartels, T., De Schepper, S., & Hong, S. (2020). Microglia modulate neurodegeneration in Alzheimer's and Parkinson's diseases. *Science*, *370*(6512), 66–69. https://doi.org/10.1126/science.abb8587

Batchelor, P. E., Liberatore, G. T., Wong, J. Y. F., Porritt, M. J., Frerichs, F., Donnan, G. A., & Howells, D. W. (1999). Activated Macrophages and Microglia Induce Dopaminergic Sprouting in the Injured Striatum and Express Brain-Derived Neurotrophic Factor and Glial Cell Line-Derived Neurotrophic Factor. *The Journal of Neuroscience*, *19*(5), 1708–1716. https://doi.org/10.1523/JNEUROSCI.19-05-01708.1999

Beers, J., Gulbranson, D. R., George, N., Siniscalchi, L. I., Jones, J., Thomson, J. A., & Chen, G. (2012). Passaging and colony expansion of human pluripotent stem cells by enzyme-free dissociation in chemically defined culture conditions. *Nature Protocols*, *7*(11), 2029–2040. https://doi.org/10.1038/nprot.2012.130

Beisiegel, U., Weber, W., Ihrke, G., Herz, J., & Stanley, K. K. (1989). The LDL–receptor–related protein, LRP, is an apolipoprotein E-binding protein. *Nature*, *341*(6238), 162–164. https://doi.org/10.1038/341162a0

Bejanin, A., Schonhaut, D. R., La Joie, R., Kramer, J. H., Baker, S. L., Sosa, N., Ayakta, N., Cantwell, A., Janabi, M., Lauriola, M., O'Neil, J. P., Gorno-Tempini, M. L., Miller, Z. A., Rosen, H. J., Miller, B. L., Jagust, W. J., & Rabinovici, G. D. (2017). Tau

pathology and neurodegeneration contribute to cognitive impairment in Alzheimer's disease. *Brain*, *140*(12), 3286–3300. https://doi.org/10.1093/brain/awx243

Bennett, F. C., Bennett, M. L., Yaqoob, F., Mulinyawe, S. B., Grant, G. A., Hayden Gephart, M., Plowey, E. D., & Barres, B. A. (2018). A Combination of Ontogeny and CNS Environment Establishes Microglial Identity. *Neuron*, *98*(6), 1170-1183.e8. https://doi.org/10.1016/j.neuron.2018.05.014

Berlec, A., & Štrukelj, B. (2013). Current state and recent advances in biopharmaceutical production in *Escherichia coli* , yeasts and mammalian cells. *Journal of Industrial Microbiology and Biotechnology*, *40*(3–4), 257–274. https://doi.org/10.1007/s10295-013-1235-0

Berriman, J., Serpell, L. C., Oberg, K. A., Fink, A. L., Goedert, M., & Crowther, R. A. (2003). Tau filaments from human brain and from in vitro assembly of recombinant protein show cross-beta structure. *Proceedings of the National Academy of Sciences of the United States of America*, *100*(15), 9034–9038. https://doi.org/10.1073/pnas.1530287100

Beutler, B., & Rietschel, E. Th. (2003). Innate immune sensing and its roots: the story of endotoxin. *Nature Reviews Immunology*, *3*(2), 169–176. https://doi.org/10.1038/nri1004

Bhaskar, K., Konerth, M., Kokiko-Cochran, O. N., Cardona, A., Ransohoff, R. M., & Lamb, B. T. (2010). Regulation of Tau Pathology by the Microglial Fractalkine Receptor. *Neuron*, *68*(1), 19–31. https://doi.org/10.1016/j.neuron.2010.08.023

Bhor, V. M., Thomas, C. J., Surolia, N., & Surolia, A. (2005). Polymyxin B: An ode to an old antidote for endotoxic shock. *Molecular BioSystems*, *1*(3), 213. https://doi.org/10.1039/b500756a

Biancalana, M., & Koide, S. (2010). Molecular mechanism of Thioflavin-T binding to amyloid fibrils. *Biochimica et Biophysica Acta (BBA) - Proteins and Proteomics*, *1804*(7), 1405–1412. https://doi.org/10.1016/j.bbapap.2010.04.001

Block, M. L., Zecca, L., & Hong, J.-S. (2007). Microglia-mediated neurotoxicity: uncovering the molecular mechanisms. *Nature Reviews Neuroscience*, *8*(1), 57–69. https://doi.org/10.1038/nrn2038

Bobadilla, S., Sunseri, N., & Landau, N. R. (2013). Efficient transduction of myeloid cells by an HIV-1-derived lentiviral vector that packages the Vpx accessory protein. *Gene Therapy*, *20*(5), 514–520. https://doi.org/10.1038/gt.2012.61

Boche, D., & Gordon, M. N. (2022). Diversity of transcriptomic microglial phenotypes in aging and Alzheimer's disease. *Alzheimer's & Dementia*, *18*(2), 360–376. https://doi.org/10.1002/alz.12389

Bode, J. G., Ehlting, C., & Häussinger, D. (2012). The macrophage response towards LPS and its control through the p38MAPK–STAT3 axis. *Cellular Signalling*, *24*(6), 1185–1194. https://doi.org/10.1016/j.cellsig.2012.01.018

Bohlen, C. J., Bennett, F. C., Tucker, A. F., Collins, H. Y., Mulinyawe, S. B., & Barres, B. A. (2017). Diverse Requirements for Microglial Survival, Specification, and Function Revealed by Defined-Medium Cultures. *Neuron*, *94*(4), 759-773.e8. https://doi.org/10.1016/j.neuron.2017.04.043

Boje, K. M., & Arora, P. K. (1992). Microglial-produced nitric oxide and reactive nitrogen oxides mediate neuronal cell death. *Brain Research*, *587*(2), 250–256. https://doi.org/10.1016/0006-8993(92)91004-X

Bolós, M., Llorens-Martín, M., Jurado-Arjona, J., Hernández, F., Rábano, A., & Avila, J. (2016a). Direct Evidence of Internalization of Tau by Microglia In Vitro and In Vivo. *Journal of Alzheimer's Disease*, *50*(1), 77–87. https://doi.org/10.3233/JAD-150704

Bolós, M., Llorens-Martín, M., Jurado-Arjona, J., Hernández, F., Rábano, A., & Avila, J. (2016b). Direct Evidence of Internalization of Tau by Microglia In Vitro and In Vivo. *Journal of Alzheimer's Disease*, *50*(1), 77–87. https://doi.org/10.3233/JAD-150704

Boluda, S., Iba, M., Zhang, B., Raible, K. M., Lee, V. M.-Y., & Trojanowski, J. Q. (2015). Differential induction and spread of tau pathology in young PS19 tau transgenic mice following intracerebral injections of pathological tau from Alzheimer's disease or corticobasal degeneration brains. *Acta Neuropathologica*, *129*(2), 221–237. https://doi.org/10.1007/s00401-014-1373-0

Bonet-Ponce, L., & Cookson, M. R. (2022). LRRK2 recruitment, activity, and function in organelles. *The FEBS Journal*, *289*(22), 6871–6890. https://doi.org/10.1111/febs.16099

Bongianni, M., Ladogana, A., Capaldi, S., Klotz, S., Baiardi, S., Cagnin, A., Perra, D., Fiorini, M., Poleggi, A., Legname, G., Cattaruzza, T., Janes, F., Tabaton, M., Ghetti, B., Monaco, S., Kovacs, G. G., Parchi, P., Pocchiari, M., & Zanusso, G. (2019). α-Synuclein RT-QuIC assay in cerebrospinal fluid of patients with dementia with Lewy bodies. *Annals of Clinical and Translational Neurology*, *6*(10), 2120–2126. https://doi.org/10.1002/acn3.50897

Bonifati, V. (2006). Parkinson's Disease: The LRRK2-G2019S mutation: opening a novel era in Parkinson's disease genetics. *European Journal of Human Genetics*, *14*(10), 1061–1062. https://doi.org/10.1038/sj.ejhg.5201695

Booth, P. L., & Thomas, W. E. (1991). Evidence for motility and pinocytosis in ramified microglia in tissue culture. *Brain Research*, *548*(1–2), 163–171. https://doi.org/10.1016/0006-8993(91)91118-K

Bordier, C. (1981). Phase separation of integral membrane proteins in Triton X-114 solution. *The Journal of Biological Chemistry*, *256*(4), 1604–1607.

Bou Samra, E., Buhagiar-Labarchède, G., Machon, C., Guitton, J., Onclercq-Delic, R., Green, M. R., Alibert, O., Gazin, C., Veaute, X., & Amor-Guéret, M. (2017). A role for Tau protein in maintaining ribosomal DNA stability and cytidine deaminase-deficient cell survival. *Nature Communications*, *8*(1), 693. https://doi.org/10.1038/s41467-017-00633-1

Braak, H., & Braak, E. (1991). Neuropathological stageing of Alzheimer-related changes. *Acta Neuropathologica*, *82*(4), 239–259. https://doi.org/10.1007/BF00308809

Braak, H., & Braak, E. (1996). Development of Alzheimer-related neurofibrillary changes in the neocortex inversely recapitulates cortical myelogenesis. *Acta Neuropathologica*, *92*(2), 197–201. https://doi.org/10.1007/s004010050508

Brelstaff, J. H., Mason, M., Katsinelos, T., McEwan, W. A., Ghetti, B., Tolkovsky, A. M., & Spillantini, M. G. (2021). Microglia become hypofunctional and release metalloproteases and tau seeds when phagocytosing live neurons with P301S tau aggregates. *Science Advances*, *7*(43). https://doi.org/10.1126/sciadv.abg4980

Brelstaff, J., Tolkovsky, A. M., Ghetti, B., Goedert, M., & Spillantini, M. G. (2018). Living Neurons with Tau Filaments Aberrantly Expose Phosphatidylserine and Are Phagocytosed by Microglia. *Cell Reports*, *24*(8), 1939-1948.e4. https://doi.org/10.1016/j.celrep.2018.07.072

Bres, E. E., & Faissner, A. (2019). Low Density Receptor-Related Protein 1 Interactions With the Extracellular Matrix: More Than Meets the Eye. *Frontiers in Cell and Developmental Biology*, *7*. https://doi.org/10.3389/fcell.2019.00031

Brunello, C. A., Merezhko, M., Uronen, R.-L., & Huttunen, H. J. (2020). Mechanisms of secretion and spreading of pathological tau protein. *Cellular and Molecular Life Sciences*, *77*(9), 1721–1744. https://doi.org/10.1007/s00018-019-03349-1

Bruttger, J., Karram, K., Wörtge, S., Regen, T., Marini, F., Hoppmann, N., Klein, M., Blank, T., Yona, S., Wolf, Y., Mack, M., Pinteaux, E., Müller, W., Zipp, F., Binder, H., Bopp, T., Prinz, M., Jung, S., & Waisman, A. (2015). Genetic Cell Ablation Reveals Clusters of Local Self-Renewing Microglia in the Mammalian Central Nervous System. *Immunity*, *43*(1), 92–106. https://doi.org/10.1016/j.immuni.2015.06.012

Buchrieser, J., James, W., & Moore, M. D. (2017). Human Induced Pluripotent Stem Cell-Derived Macrophages Share Ontogeny with MYB-Independent Tissue-Resident Macrophages. *Stem Cell Reports*, *8*(2), 334–345. https://doi.org/10.1016/j.stemcr.2016.12.020

Bugiani, O., Murrell, J. R., Giaccone, G., Hasegawa, M., Ghigo, G., Tabaton, M., Morbin, M., Primavera, A., Carella, F., Solaro, C., Grisoli, M., Savoiardo, M., Spillantini, M. G.,

Tagliavini, F., Goedert, M., & Ghetti, B. (1999). Frontotemporal Dementia and Corticobasal Degeneration in a Family with a P301S Mutation in Tau. *Journal of Neuropathology and Experimental Neurology*, *58*(6), 667–677. https://doi.org/10.1097/00005072-199906000-00011

Butler, C. A., Popescu, A. S., Kitchener, E. J. A., Allendorf, D. H., Puigdellívol, M., & Brown, G. C. (2021). Microglial phagocytosis of neurons in neurodegeneration, and its regulation. *Journal of Neurochemistry*, *158*(3), 621–639. https://doi.org/10.1111/jnc.15327

Butovsky, O., Jedrychowski, M. P., Moore, C. S., Cialic, R., Lanser, A. J., Gabriely, G., Koeglsperger, T., Dake, B., Wu, P. M., Doykan, C. E., Fanek, Z., Liu, L., Chen, Z., Rothstein, J. D., Ransohoff, R. M., Gygi, S. P., Antel, J. P., & Weiner, H. L. (2014). Identification of a unique TGF-β–dependent molecular and functional signature in microglia. *Nature Neuroscience*, *17*(1), 131–143. https://doi.org/10.1038/nn.3599

Butovsky, O., & Weiner, H. L. (2018). Microglial signatures and their role in health and disease. *Nature Reviews Neuroscience*, *19*(10), 622–635. https://doi.org/10.1038/s41583-018-0057-5

Butt, T. R., Edavettal, S. C., Hall, J. P., & Mattern, M. R. (2005). SUMO fusion technology for difficult-to-express proteins. *Protein Expression and Purification*, *43*(1), 1–9. https://doi.org/10.1016/j.pep.2005.03.016

Cagnin, A., Brooks, D. J., Kennedy, A. M., Gunn, R. N., Myers, R., Turkheimer, F. E., Jones, T., & Banati, R. B. (2001). In-vivo measurement of activated microglia in dementia. *The Lancet*, *358*(9280), 461–467. https://doi.org/10.1016/S0140-6736(01)05625-2

Cagnin, A., Kassiou, M., Meikle, S. R., & Banati, R. B. (2006). In vivo evidence for microglial activation in neurodegenerative dementia. *Acta Neurologica Scandinavica*, *114*(s185), 107–114. https://doi.org/10.1111/j.1600-0404.2006.00694.x

Calafate, S., Buist, A., Miskiewicz, K., Vijayan, V., Daneels, G., de Strooper, B., de Wit, J., Verstreken, P., & Moechars, D. (2015). Synaptic Contacts Enhance Cell-to-Cell Tau Pathology Propagation. *Cell Reports*, *11*(8), 1176–1183. https://doi.org/10.1016/j.celrep.2015.04.043

Calafate, S., Flavin, W., Verstreken, P., & Moechars, D. (2016). Loss of Bin1 Promotes the Propagation of Tau Pathology. *Cell Reports*, *17*(4), 931–940. https://doi.org/10.1016/j.celrep.2016.09.063

Candelise, N., Schmitz, M., Llorens, F., Villar-Piqué, A., Cramm, M., Thom, T., Silva Correia, S. M., Cunha, J. E. G., Möbius, W., Outeiro, T. F., Álvarez, V. G., Banchelli, M., D'Andrea, C., Angelis, M., Zafar, S., Rabano, A., Matteini, P., & Zerr, I. (2019).

Seeding variability of different alpha synuclein strains in synucleinopathies. *Annals of Neurology*, *85*(5), 691–703. https://doi.org/10.1002/ana.25446

Canton, J. (2018). Macropinocytosis: New Insights Into Its Underappreciated Role in Innate Immune Cell Surveillance. *Frontiers in Immunology*, *9*. https://doi.org/10.3389/fimmu.2018.02286

Chakrabarty, P., Ceballos-Diaz, C., Lin, W.-L., Beccard, A., Jansen-West, K., McFarland, N. R., Janus, C., Dickson, D., Das, P., & Golde, T. E. (2011). Interferon-γ induces progressive nigrostriatal degeneration and basal ganglia calcification. *Nature Neuroscience*, *14*(6), 694–696. https://doi.org/10.1038/nn.2829

Champion, J. A., Walker, A., & Mitragotri, S. (2008). Role of Particle Size in Phagocytosis of Polymeric Microspheres. *Pharmaceutical Research*, *25*(8), 1815–1821. https://doi.org/10.1007/s11095-008-9562-y

Chen, J., Kanai, Y., Cowan, N. J., & Hirokawa, N. (1992). Projection domains of MAP2 and tau determine spacings between microtubules in dendrites and axons. *Nature*, *360*(6405), 674–677. https://doi.org/10.1038/360674a0

Chen, J., Pi, S., Yu, C., Shi, H., Liu, Y., Guo, X., Zhou, L., Li, Y., He, H., Xia, Y., Mao, L., & Hu, B. (2020). sLRP1 (Soluble Low-Density Lipoprotein Receptor-Related Protein 1). *Arteriosclerosis, Thrombosis, and Vascular Biology*, *40*(6). https://doi.org/10.1161/ATVBAHA.120.314350

Chen, K., Martens, Y. A., Meneses, A., Ryu, D. H., Lu, W., Raulin, A. C., Li, F., Zhao, J., Chen, Y., Jin, Y., Linares, C., Goodwin, M., Li, Y., Liu, C.-C., Kanekiyo, T., Holtzman, D. M., Golde, T. E., Bu, G., & Zhao, N. (2022). LRP1 is a neuronal receptor for α-synuclein uptake and spread. *Molecular Neurodegeneration*, *17*(1), 57. https://doi.org/10.1186/s13024-022-00560-w

Chen, L., & Mozier, N. (2013). Comparison of Limulus amebocyte lysate test methods for endotoxin measurement in protein solutions. *Journal of Pharmaceutical and Biomedical Analysis*, *80*, 180–185. https://doi.org/10.1016/j.jpba.2013.03.011

Chen, R. (2012). Bacterial expression systems for recombinant protein production: E. coli and beyond. *Biotechnology Advances*, *30*(5), 1102–1107. https://doi.org/10.1016/j.biotechadv.2011.09.013

Chen, X., Firulyova, M., Manis, M., Herz, J., Smirnov, I., Aladyeva, E., Wang, C., Bao, X., Finn, M. B., Hu, H., Shchukina, I., Kim, M. W., Yuede, C. M., Kipnis, J., Artyomov, M. N., Ulrich, J. D., & Holtzman, D. M. (2023). Microglia-mediated T cell infiltration drives neurodegeneration in tauopathy. *Nature*, *615*(7953), 668–677. https://doi.org/10.1038/s41586-023-05788-0

Chen, X., & Holtzman, D. M. (2022). Emerging roles of innate and adaptive immunity in Alzheimer's disease. *Immunity*, *55*(12), 2236–2254. https://doi.org/10.1016/j.immuni.2022.10.016

Cherry, J. D., Olschowka, J. A., & O'Banion, M. K. (2014). Neuroinflammation and M2 microglia: the good, the bad, and the inflamed. *Journal of Neuroinflammation*, *11*(1), 98. https://doi.org/10.1186/1742-2094-11-98

Cheung, S., Greene, C., & Yates, R. M. (2017). *Simultaneous Analysis of Multiple Lumenal Parameters of Individual Phagosomes Using High-Content Imaging* (pp. 227–239). https://doi.org/10.1007/978-1-4939-6581-6_15

Chinnathambi, S., & Das, R. (2023). Microglia degrade Tau oligomers deposit via purinergic P2Y12-associated podosome and filopodia formation and induce chemotaxis. *Cell & Bioscience*, *13*(1), 95. https://doi.org/10.1186/s13578-023-01028-0

Chirita, C. N., Congdon, E. E., Yin, H., & Kuret, J. (2005). Triggers of Full-Length Tau Aggregation: A Role for Partially Folded Intermediates. *Biochemistry*, *44*(15), 5862–5872. https://doi.org/10.1021/bi0500123

Christianson, H. C., & Belting, M. (2014). Heparan sulfate proteoglycan as a cell-surface endocytosis receptor. *Matrix Biology*, *35*, 51–55. https://doi.org/10.1016/j.matbio.2013.10.004

Chung, D. C., Roemer, S., Petrucelli, L., & Dickson, D. W. (2021). Cellular and pathological heterogeneity of primary tauopathies. *Molecular Neurodegeneration*, *16*(1), 57. https://doi.org/10.1186/s13024-021-00476-x

Civiero, L., Cogo, S., Biosa, A., & Greggio, E. (2018). The role of LRRK2 in cytoskeletal dynamics. *Biochemical Society Transactions*, *46*(6), 1653–1663. https://doi.org/10.1042/BST20180469

Clavaguera, F., Akatsu, H., Fraser, G., Crowther, R. A., Frank, S., Hench, J., Probst, A., Winkler, D. T., Reichwald, J., Staufenbiel, M., Ghetti, B., Goedert, M., & Tolnay, M. (2013). Brain homogenates from human tauopathies induce tau inclusions in mouse brain. *Proceedings of the National Academy of Sciences*, *110*(23), 9535–9540. https://doi.org/10.1073/pnas.1301175110

Clavaguera, F., Bolmont, T., Crowther, R. A., Abramowski, D., Frank, S., Probst, A., Fraser, G., Stalder, A. K., Beibel, M., Staufenbiel, M., Jucker, M., Goedert, M., & Tolnay, M. (2009). Transmission and spreading of tauopathy in transgenic mouse brain. *Nature Cell Biology*, *11*(7), 909–913. https://doi.org/10.1038/ncb1901

Clavaguera, F., Hench, J., Lavenir, I., Schweighauser, G., Frank, S., Goedert, M., & Tolnay, M. (2014). Peripheral administration of tau aggregates triggers intracerebral

tauopathy in transgenic mice. *Acta Neuropathologica*, *127*(2), 299–301. https://doi.org/10.1007/s00401-013-1231-5

Clayton, K., Delpech, J. C., Herron, S., Iwahara, N., Ericsson, M., Saito, T., Saido, T. C., Ikezu, S., & Ikezu, T. (2021). Plaque associated microglia hyper-secrete extracellular vesicles and accelerate tau propagation in a humanized APP mouse model. *Molecular Neurodegeneration*, *16*(1), 18. https://doi.org/10.1186/s13024-021-00440-9

Cleveland, D. W., Hwo, S.-Y., & Kirschner, M. W. (1977). Physical and chemical properties of purified tau factor and the role of tau in microtubule assembly. *Journal of Molecular Biology*, *116*(2), 227–247. https://doi.org/10.1016/0022-2836(77)90214-5

Collinge, J., & Clarke, A. R. (2007). A General Model of Prion Strains and Their Pathogenicity. *Science*, *318*(5852), 930–936. https://doi.org/10.1126/science.1138718

Combs, B., Tiernan, C. T., Hamel, C., & Kanaan, N. M. (2017). *Production of recombinant tau oligomers in vitro* (pp. 45–64). https://doi.org/10.1016/bs.mcb.2017.06.005

Cornblath, E. J., Li, H. L., Changolkar, L., Zhang, B., Brown, H. J., Gathagan, R. J., Olufemi, M. F., Trojanowski, J. Q., Bassett, D. S., Lee, V. M. Y., & Henderson, M. X. (2021). Computational modeling of tau pathology spread reveals patterns of regional vulnerability and the impact of a genetic risk factor. *Science Advances*, *7*(24). https://doi.org/10.1126/sciadv.abg6677

Costa, S., Almeida, A., Castro, A., & Domingues, L. (2014). Fusion tags for protein solubility, purification and immunogenicity in Escherichia coli: the novel Fh8 system. *Frontiers in Microbiology*, *5*. https://doi.org/10.3389/fmicb.2014.00063

Couchie, D., Mavilia, C., Georgieff, I. S., Liem, R. K., Shelanski, M. L., & Nunez, J. (1992). Primary structure of high molecular weight tau present in the peripheral nervous system. *Proceedings of the National Academy of Sciences*, *89*(10), 4378–4381. https://doi.org/10.1073/pnas.89.10.4378

Criado-Marrero, M., Sabbagh, J. J., Jones, M. R., Chaput, D., Dickey, C. A., & Blair, L. J. (2020). Hippocampal Neurogenesis Is Enhanced in Adult Tau Deficient Mice. *Cells*, *9*(1), 210. https://doi.org/10.3390/cells9010210

Cronk, J. C., Filiano, A. J., Louveau, A., Marin, I., Marsh, R., Ji, E., Goldman, D. H., Smirnov, I., Geraci, N., Acton, S., Overall, C. C., & Kipnis, J. (2018). Peripherally derived macrophages can engraft the brain independent of irradiation and maintain an identity distinct from microglia. *Journal of Experimental Medicine*, *215*(6), 1627–1647. https://doi.org/10.1084/jem.20180247

Crotti, A., Benner, C., Kerman, B. E., Gosselin, D., Lagier-Tourenne, C., Zuccato, C., Cattaneo, E., Gage, F. H., Cleveland, D. W., & Glass, C. K. (2014). Mutant Huntingtin

promotes autonomous microglia activation via myeloid lineage-determining factors. *Nature Neuroscience*, *17*(4), 513–521. https://doi.org/10.1038/nn.3668

Crotti, A., Sait, H. R., McAvoy, K. M., Estrada, K., Ergun, A., Szak, S., Marsh, G., Jandreski, L., Peterson, M., Reynolds, T. L., Dalkilic-Liddle, I., Cameron, A., Cahir-McFarland, E., & Ransohoff, R. M. (2019). BIN1 favors the spreading of Tau via extracellular vesicles. *Scientific Reports*, *9*(1), 9477. https://doi.org/10.1038/s41598-019-45676-0

Crowther, R. A., Olesen, O. F., Jakes, R., & Goedert, M. (1992). The microtubule binding repeats of tau protein assemble into filaments like those found in Alzheimer's disease. *FEBS Letters*, *309*(2), 199–202. https://doi.org/10.1016/0014-5793(92)81094-3

Csokova, N., Skrabana, R., Liebig, H.-D., Mederlyova, A., Kontsek, P., & Novak, M. (2004). Rapid purification of truncated tau proteins: model approach to purification of functionally active fragments of disordered proteins, implication for neurodegenerative diseases. *Protein Expression and Purification*, *35*(2), 366–372. https://doi.org/10.1016/j.pep.2004.01.012

Dachet, F., Brown, J. B., Valyi-Nagy, T., Narayan, K. D., Serafini, A., Boley, N., Gingeras, T. R., Celniker, S. E., Mohapatra, G., & Loeb, J. A. (2021). Selective time-dependent changes in activity and cell-specific gene expression in human postmortem brain. *Scientific Reports*, *11*(1), 6078. https://doi.org/10.1038/s41598-021-85801-6

Dai, C., Tung, Y. C., Liu, F., Gong, C.-X., & Iqbal, K. (2017). Tau passive immunization inhibits not only tau but also Aβ pathology. *Alzheimer's Research & Therapy*, *9*(1), 1. https://doi.org/10.1186/s13195-016-0227-5

Dani, M., Wood, M., Mizoguchi, R., Fan, Z., Walker, Z., Morgan, R., Hinz, R., Biju, M., Kuruvilla, T., Brooks, D. J., & Edison, P. (2018). Microglial activation correlates in vivo with both tau and amyloid in Alzheimer's disease. *Brain*. https://doi.org/10.1093/brain/awy188

Das, R., Balmik, A. A., & Chinnathambi, S. (2020). Phagocytosis of full-length Tau oligomers by Actin-remodeling of activated microglia. *Journal of Neuroinflammation*, *17*(1), 10. https://doi.org/10.1186/s12974-019-1694-y

Dasari, A. K. R., Kayed, R., Wi, S., & Lim, K. H. (2019). Tau Interacts with the C-Terminal Region of α-Synuclein, Promoting Formation of Toxic Aggregates with Distinct Molecular Conformations. *Biochemistry*, *58*(25), 2814–2821. https://doi.org/10.1021/acs.biochem.9b00215

Davalos, D., Grutzendler, J., Yang, G., Kim, J. V, Zuo, Y., Jung, S., Littman, D. R., Dustin, M. L., & Gan, W.-B. (2005). ATP mediates rapid microglial response to local brain injury in vivo. *Nature Neuroscience*, *8*(6), 752–758. https://doi.org/10.1038/nn1472

de Calignon, A., Fox, L. M., Pitstick, R., Carlson, G. A., Bacskai, B. J., Spires-Jones, T. L., & Hyman, B. T. (2010). Caspase activation precedes and leads to tangles. *Nature*, *464*(7292), 1201–1204. https://doi.org/10.1038/nature08890

De Nardis, C., Lössl, P., van den Biggelaar, M., Madoori, P. K., Leloup, N., Mertens, K., Heck, A. J. R., & Gros, P. (2017). Recombinant Expression of the Full-length Ectodomain of LDL Receptor-related Protein 1 (LRP1) Unravels pH-dependent Conformational Changes and the Stoichiometry of Binding with Receptor-associated Protein (RAP). *Journal of Biological Chemistry*, *292*(3), 912–924. https://doi.org/10.1074/jbc.M116.758862

de Calignon, A., Polydoro, M., Suárez-Calvet, M., William, C., Adamowicz, D. H., Kopeikina, K. J., Pitstick, R., Sahara, N., Ashe, K. H., Carlson, G. A., Spires-Jones, T. L., & Hyman, B. T. (2012). Propagation of Tau Pathology in a Model of Early Alzheimer's Disease. *Neuron*, *73*(4), 685–697. https://doi.org/10.1016/j.neuron.2011.11.033

del Río-Hortega, P. (1919). El "tercer elemento" de los centros nerviosos. I. La microglía en estado normal. II. Intervención de la microglía en los procesos patológicos (células en bastoncito y cuerpos gránulo-adiposos). *Bol. Scoc. Esp. Biol.*, *8*, 69–109.

Del-Aguila, J. L., Li, Z., Dube, U., Mihindukulasuriya, K. A., Budde, J. P., Fernandez, M. V., Ibanez, L., Bradley, J., Wang, F., Bergmann, K., Davenport, R., Morris, J. C., Holtzman, D. M., Perrin, R. J., Benitez, B. A., Dougherty, J., Cruchaga, C., & Harari, O. (2019). A single-nuclei RNA sequencing study of Mendelian and sporadic AD in the human brain. *Alzheimer's Research & Therapy*, *11*(1), 71. https://doi.org/10.1186/s13195-019-0524-x

Dello Russo, C., Cappoli, N., Coletta, I., Mezzogori, D., Paciello, F., Pozzoli, G., Navarra, P., & Battaglia, A. (2018). The human microglial HMC3 cell line: where do we stand? A systematic literature review. *Journal of Neuroinflammation*, *15*(1), 259. https://doi.org/10.1186/s12974-018-1288-0

Desjardins, M., & Griffiths, G. (2003). Phagocytosis: latex leads the way. *Current Opinion in Cell Biology*, *15*(4), 498–503. https://doi.org/10.1016/S0955-0674(03)00083-8

DeVos, S. L., Corjuc, B. T., Oakley, D. H., Nobuhara, C. K., Bannon, R. N., Chase, A., Commins, C., Gonzalez, J. A., Dooley, P. M., Frosch, M. P., & Hyman, B. T. (2018). Synaptic Tau Seeding Precedes Tau Pathology in Human Alzheimer's Disease Brain. *Frontiers in Neuroscience*, *12*. https://doi.org/10.3389/fnins.2018.00267

Dickson, D. W. (2018). Neuropathology of Parkinson disease. *Parkinsonism & Related Disorders*, *46*, S30–S33. https://doi.org/10.1016/j.parkreldis.2017.07.033

Dodd, D. A., LaCroix, M., Valdez, C., Knox, G. M., Vega, A. R., Kumar, A., Xing, C., White, C. L., & Diamond, M. I. (2022). Tau seeds translocate across the cell membrane to initiate aggregation . *BioRxiv*.

Dolan, M.-J., Therrien, M., Jereb, S., Kamath, T., Epstein, C., Macosko, E. Z., & Stevens, B. (2022). A resource for generating and manipulating human microglial states in vitro. *BioRxiv*.

Dujardin, S., Bégard, S., Caillierez, R., Lachaud, C., Carrier, S., Lieger, S., Gonzalez, J. A., Deramecourt, V., Déglon, N., Maurage, C.-A., Frosch, M. P., Hyman, B. T., Colin, M., & Buée, L. (2018). Different tau species lead to heterogeneous tau pathology propagation and misfolding. *Acta Neuropathologica Communications*, *6*(1), 132. https://doi.org/10.1186/s40478-018-0637-7

Dujardin, S., Commins, C., Lathuiliere, A., Beerepoot, P., Fernandes, A. R., Kamath, T. V., De Los Santos, M. B., Klickstein, N., Corjuc, D. L., Corjuc, B. T., Dooley, P. M., Viode, A., Oakley, D. H., Moore, B. D., Mullin, K., Jean-Gilles, D., Clark, R., Atchison, K., Moore, R., … Hyman, B. T. (2020). Tau molecular diversity contributes to clinical heterogeneity in Alzheimer's disease. *Nature Medicine*, *26*(8), 1256–1263. https://doi.org/10.1038/s41591-020-0938-9

Dujardin, S., Lécolle, K., Caillierez, R., Bégard, S., Zommer, N., Lachaud, C., Carrier, S., Dufour, N., Aurégan, G., Winderickx, J., Hantraye, P., Déglon, N., Colin, M., & Buée, L. (2014). Neuron-to-neuron wild-type Tau protein transfer through a trans-synaptic mechanism: relevance to sporadic tauopathies. *Acta Neuropathologica Communications*, *2*(1), 14. https://doi.org/10.1186/2051-5960-2-14

Duyckaerts, C., & Hauw, J.-J. (1997). Diagnosis and Staging of Alzheimer Disease. *Neurobiology of Aging*, *18*(4), S33–S42. https://doi.org/10.1016/S0197-4580(97)00067-5

Duyckaerts, C., Uchihara, T., Seilhean, D., He, Y., & Hauw, J.-J. (1997). Dissociation of Alzheimer type pathology in a disconnected piece of cortex. *Acta Neuropathologica*, *93*(5), 501–507. https://doi.org/10.1007/s004010050645

Ebner, F., Brandt, C., Thiele, P., Richter, D., Schliesser, U., Siffrin, V., Schueler, J., Stubbe, T., Ellinghaus, A., Meisel, C., Sawitzki, B., & Nitsch, R. (2013). Microglial Activation Milieu Controls Regulatory T Cell Responses. *The Journal of Immunology*, *191*(11), 5594–5602. https://doi.org/10.4049/jimmunol.1203331

Eckermann, K., Mocanu, M.-M., Khlistunova, I., Biernat, J., Nissen, A., Hofmann, A., Schönig, K., Bujard, H., Haemisch, A., Mandelkow, E., Zhou, L., Rune, G., & Mandelkow, E.-M. (2007). The β-Propensity of Tau Determines Aggregation and Synaptic Loss in Inducible Mouse Models of Tauopathy. *Journal of Biological Chemistry*, *282*(43), 31755–31765. https://doi.org/10.1074/jbc.M705282200

Edwards, T. L., Scott, W. K., Almonte, C., Burt, A., Powell, E. H., Beecham, G. W., Wang, L., Züchner, S., Konidari, I., Wang, G., Singer, C., Nahab, F., Scott, B., Stajich, J. M., Pericak-Vance, M., Haines, J., Vance, J. M., & Martin, E. R. (2010). Genome-Wide Association Study Confirms SNPs in *SNCA* and the *MAPT* Region as Common Risk Factors for Parkinson Disease. *Annals of Human Genetics*, *74*(2), 97–109. https://doi.org/10.1111/j.1469-1809.2009.00560.x

Efthymiou, A. G., & Goate, A. M. (2017). Late onset Alzheimer's disease genetics implicates microglial pathways in disease risk. *Molecular Neurodegeneration*, *12*(1), 43. https://doi.org/10.1186/s13024-017-0184-x

Eguchi, T., Kuwahara, T., Sakurai, M., Komori, T., Fujimoto, T., Ito, G., Yoshimura, S., Harada, A., Fukuda, M., Koike, M., & Iwatsubo, T. (2018). LRRK2 and its substrate Rab GTPases are sequentially targeted onto stressed lysosomes and maintain their homeostasis. *Proceedings of the National Academy of Sciences*, *115*(39). https://doi.org/10.1073/pnas.1812196115

Elbaum-Garfinkle, S., & Rhoades, E. (2012). Identification of an Aggregation-Prone Structure of Tau. *Journal of the American Chemical Society*, *134*(40), 16607–16613. https://doi.org/10.1021/ja305206m

Engler, C., Gruetzner, R., Kandzia, R., & Marillonnet, S. (2009). Golden Gate Shuffling: A One-Pot DNA Shuffling Method Based on Type IIs Restriction Enzymes. *PLoS ONE*, *4*(5), e5553. https://doi.org/10.1371/journal.pone.0005553

Engler, C., Kandzia, R., & Marillonnet, S. (2008). A One Pot, One Step, Precision Cloning Method with High Throughput Capability. *PLoS ONE*, *3*(11), e3647. https://doi.org/10.1371/journal.pone.0003647

Erb, M. L., & Moore, D. J. (2020). LRRK2 and the Endolysosomal System in Parkinson's Disease. *Journal of Parkinson's Disease*, *10*(4), 1271–1291. https://doi.org/10.3233/JPD-202138

Evans, L. D., Strano, A., Campbell, A., Karakoc, E., Iorio, F., Bassett, A. R., & Livesey, F. J. (2020). Whole genome CRISPR screens identify LRRK2-regulated endocytosis as a major mechanism for extracellular tau uptake by human neurons. *BioRxiv*.

Evans, L. D., Wassmer, T., Fraser, G., Smith, J., Perkinton, M., Billinton, A., & Livesey, F. J. (2018). Extracellular Monomeric and Aggregated Tau Efficiently Enter Human Neurons through Overlapping but Distinct Pathways. *Cell Reports*, *22*(13), 3612–3624. https://doi.org/10.1016/j.celrep.2018.03.021

Fabrik, I., Bilkei-Gorzo, O., Öberg, M., Fabrikova, D., Fuchs, J., Sihlbom, C., Göransson, M., & Härtlova, A. (2023). Lung macrophages utilize unique cathepsin K–dependent phagosomal machinery to degrade intracellular collagen. *Life Science Alliance*, *6*(4), e202201535. https://doi.org/10.26508/lsa.202201535

Fairfoul, G., McGuire, L. I., Pal, S., Ironside, J. W., Neumann, J., Christie, S., Joachim, C., Esiri, M., Evetts, S. G., Rolinski, M., Baig, F., Ruffmann, C., Wade-Martins, R., Hu, M. T. M., Parkkinen, L., & Green, A. J. E. (2016). Alpha-synuclein <scp>RT</scp> -Qu <scp>IC</scp> in the <scp>CSF</scp> of patients with alpha-synucleinopathies. *Annals of Clinical and Translational Neurology*, *3*(10), 812–818. https://doi.org/10.1002/acn3.338

Falcon, B., Cavallini, A., Angers, R., Glover, S., Murray, T. K., Barnham, L., Jackson, S., O'Neill, M. J., Isaacs, A. M., Hutton, M. L., Szekeres, P. G., Goedert, M., & Bose, S. (2015). Conformation Determines the Seeding Potencies of Native and Recombinant Tau Aggregates. *Journal of Biological Chemistry*, *290*(2), 1049–1065. https://doi.org/10.1074/jbc.M114.589309

Falcon, B., Noad, J., McMahon, H., Randow, F., & Goedert, M. (2018). Galectin-8–mediated selective autophagy protects against seeded tau aggregation. *Journal of Biological Chemistry*, *293*(7), 2438–2451. https://doi.org/10.1074/jbc.M117.809293

Falcon, B., Zhang, W., Murzin, A. G., Murshudov, G., Garringer, H. J., Vidal, R., Crowther, R. A., Ghetti, B., Scheres, S. H. W., & Goedert, M. (2018). Structures of filaments from Pick's disease reveal a novel tau protein fold. *Nature*, *561*(7721), 137–140. https://doi.org/10.1038/s41586-018-0454-y

Falcon, B., Zhang, W., Schweighauser, M., Murzin, A. G., Vidal, R., Garringer, H. J., Ghetti, B., Scheres, S. H. W., & Goedert, M. (2018). Tau filaments from multiple cases of sporadic and inherited Alzheimer's disease adopt a common fold. *Acta Neuropathologica*, *136*(5), 699–708. https://doi.org/10.1007/s00401-018-1914-z

Falcon, B., Zivanov, J., Zhang, W., Murzin, A. G., Garringer, H. J., Vidal, R., Crowther, R. A., Newell, K. L., Ghetti, B., Goedert, M., & Scheres, S. H. W. (2019). Novel tau filament fold in chronic traumatic encephalopathy encloses hydrophobic molecules. *Nature*, *568*(7752), 420–423. https://doi.org/10.1038/s41586-019-1026-5

Farrell, K., Kim, S., Han, N., Iida, M. A., Gonzalez, E. M., Otero-Garcia, M., Walker, J. M., Richardson, T. E., Renton, A. E., Andrews, S. J., Fulton-Howard, B., Humphrey, J., Vialle, R. A., Bowles, K. R., de Paiva Lopes, K., Whitney, K., Dangoor, D. K., Walsh, H., Marcora, E., … Crary, J. F. (2022). Genome-wide association study and functional validation implicates JADE1 in tauopathy. *Acta Neuropathologica*, *143*(1), 33–53. https://doi.org/10.1007/s00401-021-02379-z

Fattorelli, N., Martinez-Muriana, A., Wolfs, L., Geric, I., De Strooper, B., & Mancuso, R. (2021). Stem-cell-derived human microglia transplanted into mouse brain to study human disease. *Nature Protocols*, *16*(2), 1013–1033. https://doi.org/10.1038/s41596-020-00447-4

Fell, M. J., Mirescu, C., Basu, K., Cheewatrakoolpong, B., DeMong, D. E., Ellis, J. M., Hyde, L. A., Lin, Y., Markgraf, C. G., Mei, H., Miller, M., Poulet, F. M., Scott, J. D., Smith, M. D., Yin, Z., Zhou, X., Parker, E. M., Kennedy, M. E., & Morrow, J. A. (2015). MLi-2, a Potent, Selective, and Centrally Active Compound for Exploring the Therapeutic Potential and Safety of LRRK2 Kinase Inhibition. *Journal of Pharmacology and Experimental Therapeutics*, *355*(3), 397–409. https://doi.org/10.1124/jpet.115.227587

FELLOUS, A., FRANCON, J., LENNON, A.-M., & NUNEZ, J. (1977). Microtubule Assembly in vitro. Purification of Assembly-Promoting Factors. *European Journal of Biochemistry*, *78*(1), 167–174. https://doi.org/10.1111/j.1432-1033.1977.tb11726.x

Fenyi, A., Coens, A., Bellande, T., Melki, R., & Bousset, L. (2018). Assessment of the efficacy of different procedures that remove and disassemble alpha-synuclein, tau and A-beta fibrils from laboratory material and surfaces. *Scientific Reports*, *8*(1), 10788. https://doi.org/10.1038/s41598-018-28856-2

Ferrari, L., & Rüdiger, S. G. D. (2018a). Recombinant production and purification of the human protein Tau. *Protein Engineering, Design and Selection*, *31*(12), 447–455. https://doi.org/10.1093/protein/gzz010

Ferrari, L., & Rüdiger, S. G. D. (2018b). Recombinant production and purification of the human protein Tau. *Protein Engineering, Design and Selection*, *31*(12), 447–455. https://doi.org/10.1093/protein/gzz010

Fichou, Y., Al-Hilaly, Y. K., Devred, F., Smet-Nocca, C., Tsvetkov, P. O., Verelst, J., Winderickx, J., Geukens, N., Vanmechelen, E., Perrotin, A., Serpell, L., Hanseeuw, B. J., Medina, M., Buée, L., & Landrieu, I. (2019). The elusive tau molecular structures: can we translate the recent breakthroughs into new targets for intervention? *Acta Neuropathologica Communications*, *7*(1), 31. https://doi.org/10.1186/s40478-019-0682-x

Fichou, Y., Oberholtzer, Z. R., Ngo, H., Cheng, C.-Y., Keller, T. J., Eschmann, N. A., & Han, S. (2019). Tau-Cofactor Complexes as Building Blocks of Tau Fibrils. *Frontiers in Neuroscience*, *13*. https://doi.org/10.3389/fnins.2019.01339

Fichou, Y., Vigers, M., Goring, A. K., Eschmann, N. A., & Han, S. (2018). Heparin-induced tau filaments are structurally heterogeneous and differ from Alzheimer's disease filaments. *Chemical Communications*, *54*(36), 4573–4576. https://doi.org/10.1039/C8CC01355A

Ficulle, E., Kananathan, S., Airey, D., Gharbi, S. I., Humphryes-Kirilov, N., Scherschel, J., Dunbar, C., Eastwood, B. J., Laing, E., Collier, D. A., & Bose, S. (2022). A human tau seeded neuronal cell model recapitulates molecular responses associated with

Alzheimer's disease. *Scientific Reports*, *12*(1), 2673. https://doi.org/10.1038/s41598-022-06411-4

Filipello, F., You, S.-F., Mirfakhar, F. S., Mahali, S., Bollman, B., Acquarone, M., Korvatska, O., Marsh, J. A., Sivaraman, A., Martinez, R., Cantoni, C., De Feo, L., Ghezzi, L., Minaya, M. A., Renganathan, A., Cashikar, A. G., Satoh, J.-I., Beatty, W., Iyer, A. K., … Karch, C. M. (2023). Defects in lysosomal function and lipid metabolism in human microglia harboring a TREM2 loss of function mutation. *Acta Neuropathologica*, *145*(6), 749–772. https://doi.org/10.1007/s00401-023-02568-y

Fischer, I. (2023). Big Tau: What We Know, and We Need to Know. *Eneuro*, *10*(5), ENEURO.0052-23.2023. https://doi.org/10.1523/ENEURO.0052-23.2023

Fitzpatrick, A. W. P., Falcon, B., He, S., Murzin, A. G., Murshudov, G., Garringer, H. J., Crowther, R. A., Ghetti, B., Goedert, M., & Scheres, S. H. W. (2017). Cryo-EM structures of tau filaments from Alzheimer's disease. *Nature*, *547*(7662), 185–190. https://doi.org/10.1038/nature23002

Flament, S., Delacourte, A., Verny, M., Hauw, J.-J., & Javoy-Agid, F. (1991). Abnormal Tau proteins in progressive supranuclear palsy. *Acta Neuropathologica*, *81*(6), 591–596. https://doi.org/10.1007/BF00296367

Flannagan, R. S., Jaumouillé, V., & Grinstein, S. (2012). The Cell Biology of Phagocytosis. *Annual Review of Pathology: Mechanisms of Disease*, *7*(1), 61–98. https://doi.org/10.1146/annurev-pathol-011811-132445

Flavin, W. P., Bousset, L., Green, Z. C., Chu, Y., Skarpathiotis, S., Chaney, M. J., Kordower, J. H., Melki, R., & Campbell, E. M. (2017). Endocytic vesicle rupture is a conserved mechanism of cellular invasion by amyloid proteins. *Acta Neuropathologica*, *134*(4), 629–653. https://doi.org/10.1007/s00401-017-1722-x

Fontaine, S. N., Zheng, D., Sabbagh, J. J., Martin, M. D., Chaput, D., Darling, A., Trotter, J. H., Stothert, A. R., Nordhues, B. A., Lussier, A., Baker, J., Shelton, L., Kahn, M., Blair, L. J., Stevens, S. M., & Dickey, C. A. (2016). DnaJ/Hsc70 chaperone complexes control the extracellular release of neurodegenerative-associated proteins. *The EMBO Journal*, *35*(14), 1537–1549. https://doi.org/10.15252/embj.201593489

Fowler, S. L., Behr, T. S., Turkes, E., Maglio Cauhy, P., Foiani, M. S., Schaler, A., Crowley, G., Bez, S., Ficulle, E., Fischer, R., Geary, B., Gaur, P., Miller, C., D'Acunzo, P., Levy, E., Duff, K. E., & Ryskeldi-Faocn, B. (2023). Tau filaments are tethered within brain extracellular vesicles in Alzheimer's disease. *BioRxiv*.

Frankenberg, T., Kirschnek, S., Häcker, H., & Häcker, G. (2008). Phagocytosis-induced apoptosis of macrophages is linked to uptake, killing and degradation of bacteria. *European Journal of Immunology*, *38*(1), 204–215. https://doi.org/10.1002/eji.200737379

Friedhoff, P., Schneider, A., Mandelkow, E. M., & Mandelkow, E. (1998). Rapid assembly of Alzheimer-like paired helical filaments from microtubule-associated protein tau monitored by fluorescence in solution. *Biochemistry*, *37*(28), 10223–10230. https://doi.org/10.1021/bi980537d

Friedman, B. A., Srinivasan, K., Ayalon, G., Meilandt, W. J., Lin, H., Huntley, M. A., Cao, Y., Lee, S.-H., Haddick, P. C. G., Ngu, H., Modrusan, Z., Larson, J. L., Kaminker, J. S., van der Brug, M. P., & Hansen, D. V. (2018). Diverse Brain Myeloid Expression Profiles Reveal Distinct Microglial Activation States and Aspects of Alzheimer's Disease Not Evident in Mouse Models. *Cell Reports*, *22*(3), 832–847. https://doi.org/10.1016/j.celrep.2017.12.066

Frost, B., Jacks, R. L., & Diamond, M. I. (2009). Propagation of Tau Misfolding from the Outside to the Inside of a Cell. *Journal of Biological Chemistry*, *284*(19), 12845–12852. https://doi.org/10.1074/jbc.M808759200

Frost, L. S., Dhingra, A., Reyes-Reveles, J., & Boesze-Battaglia, K. (2017). *The Use of DQ-BSA to Monitor the Turnover of Autophagy-Associated Cargo* (pp. 43–54). https://doi.org/10.1016/bs.mie.2016.09.052

Fu, H., Hardy, J., & Duff, K. E. (2018). Selective vulnerability in neurodegenerative diseases. *Nature Neuroscience*, *21*(10), 1350–1358. https://doi.org/10.1038/s41593-018-0221-2

Funk, K. E., Mirbaha, H., Jiang, H., Holtzman, D. M., & Diamond, M. I. (2015a). Distinct Therapeutic Mechanisms of Tau Antibodies. *Journal of Biological Chemistry*, *290*(35), 21652–21662. https://doi.org/10.1074/jbc.M115.657924

Funk, K. E., Mirbaha, H., Jiang, H., Holtzman, D. M., & Diamond, M. I. (2015b). Distinct Therapeutic Mechanisms of Tau Antibodies. *Journal of Biological Chemistry*, *290*(35), 21652–21662. https://doi.org/10.1074/jbc.M115.657924

Galatro, T. F., Holtman, I. R., Lerario, A. M., Vainchtein, I. D., Brouwer, N., Sola, P. R., Veras, M. M., Pereira, T. F., Leite, R. E. P., Möller, T., Wes, P. D., Sogayar, M. C., Laman, J. D., den Dunnen, W., Pasqualucci, C. A., Oba-Shinjo, S. M., Boddeke, E. W. G. M., Marie, S. K. N., & Eggen, B. J. L. (2017). Transcriptomic analysis of purified human cortical microglia reveals age-associated changes. *Nature Neuroscience*, *20*(8), 1162–1171. https://doi.org/10.1038/nn.4597

Gautier, E. L., Shay, T., Miller, J., Greter, M., Jakubzick, C., Ivanov, S., Helft, J., Chow, A., Elpek, K. G., Gordonov, S., Mazloom, A. R., Ma'ayan, A., Chua, W.-J., Hansen, T. H., Turley, S. J., Merad, M., & Randolph, G. J. (2012). Gene-expression profiles and transcriptional regulatory pathways that underlie the identity and diversity of mouse tissue macrophages. *Nature Immunology*, *13*(11), 1118–1128. https://doi.org/10.1038/ni.2419

Geirsdottir, L., David, E., Keren-Shaul, H., Weiner, A., Bohlen, S. C., Neuber, J., Balic, A., Giladi, A., Sheban, F., Dutertre, C.-A., Pfeifle, C., Peri, F., Raffo-Romero, A., Vizioli, J., Matiasek, K., Scheiwe, C., Meckel, S., Mätz-Rensing, K., van der Meer, F., … Prinz, M. (2019). Cross-Species Single-Cell Analysis Reveals Divergence of the Primate Microglia Program. *Cell*, *179*(7), 1609-1622.e16. https://doi.org/10.1016/j.cell.2019.11.010

Gerhard, A., Trender-Gerhard, I., Turkheimer, F., Quinn, N. P., Bhatia, K. P., & Brooks, D. J. (2006a). In vivo imaging of microglial activation with [11C](R)-PK11195 PET in progressive supranuclear palsy. *Movement Disorders*, *21*(1), 89–93. https://doi.org/10.1002/mds.20668

Gerhard, A., Trender-Gerhard, I., Turkheimer, F., Quinn, N. P., Bhatia, K. P., & Brooks, D. J. (2006b). In vivo imaging of microglial activation with [11C](R)-PK11195 PET in progressive supranuclear palsy. *Movement Disorders*, *21*(1), 89–93. https://doi.org/10.1002/mds.20668

Gerhard, A., Watts, J., Trender-Gerhard, I., Turkheimer, F., Banati, R. B., Bhatia, K., & Brooks, D. J. (2004). In vivo imaging of microglial activation with [11C](R)-PK11195 PET in corticobasal degeneration. *Movement Disorders*, *19*(10), 1221–1226. https://doi.org/10.1002/mds.20162

Giannakopoulos, P., Herrmann, F. R., Bussiere, T., Bouras, C., Kovari, E., Perl, D. P., Morrison, J. H., Gold, G., & Hof, P. R. (2003). Tangle and neuron numbers, but not amyloid load, predict cognitive status in Alzheimer's disease. *Neurology*, *60*(9), 1495–1500. https://doi.org/10.1212/01.WNL.0000063311.58879.01

Giasson, B. I., Forman, M. S., Higuchi, M., Golbe, L. I., Graves, C. L., Kotzbauer, P. T., Trojanowski, J. Q., & Lee, V. M.-Y. (2003). Initiation and Synergistic Fibrillization of Tau and Alpha-Synuclein. *Science*, *300*(5619), 636–640. https://doi.org/10.1126/science.1082324

Gibbons, G. S., Banks, R. A., Kim, B., Xu, H., Changolkar, L., Leight, S. N., Riddle, D. M., Li, C., Gathagan, R. J., Brown, H. J., Zhang, B., Trojanowski, J. Q., & Lee, V. M.-Y. (2017). GFP-Mutant Human Tau Transgenic Mice Develop Tauopathy Following CNS Injections of Alzheimer's Brain-Derived Pathological Tau or Synthetic Mutant Human Tau Fibrils. *The Journal of Neuroscience*, *37*(47), 11485–11494. https://doi.org/10.1523/JNEUROSCI.2393-17.2017

Gibson, D. G., Young, L., Chuang, R.-Y., Venter, J. C., Hutchison, C. A., & Smith, H. O. (2009). Enzymatic assembly of DNA molecules up to several hundred kilobases. *Nature Methods*, *6*(5), 343–345. https://doi.org/10.1038/nmeth.1318

Ginhoux, F., Greter, M., Leboeuf, M., Nandi, S., See, P., Gokhan, S., Mehler, M. F., Conway, S. J., Ng, L. G., Stanley, E. R., Samokhvalov, I. M., & Merad, M. (2010). Fate

Mapping Analysis Reveals That Adult Microglia Derive from Primitive Macrophages. *Science*, *330*(6005), 841–845. https://doi.org/10.1126/science.1194637

Ginhoux, F., Lim, S., Hoeffel, G., Low, D., & Huber, T. (2013a). Origin and differentiation of microglia. *Frontiers in Cellular Neuroscience*, *7*. https://doi.org/10.3389/fncel.2013.00045

Ginhoux, F., Lim, S., Hoeffel, G., Low, D., & Huber, T. (2013b). Origin and differentiation of microglia. *Frontiers in Cellular Neuroscience*, *7*. https://doi.org/10.3389/fncel.2013.00045

Ginsberg, S. D., Crino, P. B., Lee, V. M.-Y., Eberwine, J. H., & Trojanowski, J. Q. (1997). Sequestration of RNA in Alzheimer's disease neurofibrillary tangles and senile plaques. *Annals of Neurology*, *41*(2), 200–209. https://doi.org/10.1002/ana.410410211

Giustiniani, J., Chambraud, B., Sardin, E., Dounane, O., Guillemeau, K., Nakatani, H., Paquet, D., Kamah, A., Landrieu, I., Lippens, G., Baulieu, E.-E., & Tawk, M. (2014). Immunophilin FKBP52 induces Tau-P301L filamentous assembly in vitro and modulates its activity in a model of tauopathy. *Proceedings of the National Academy of Sciences*, *111*(12), 4584–4589. https://doi.org/10.1073/pnas.1402645111

Goedert, M., Eisenberg, D. S., & Crowther, R. A. (2017). Propagation of Tau Aggregates and Neurodegeneration. *Annual Review of Neuroscience*, *40*(1), 189–210. https://doi.org/10.1146/annurev-neuro-072116-031153

Goedert, M., & Jakes, R. (1990a). Expression of separate isoforms of human tau protein: correlation with the tau pattern in brain and effects on tubulin polymerization. *The EMBO Journal*, *9*(13), 4225–4230. https://doi.org/10.1002/j.1460-2075.1990.tb07870.x

Goedert, M., & Jakes, R. (1990b). Expression of separate isoforms of human tau protein: correlation with the tau pattern in brain and effects on tubulin polymerization. *The EMBO Journal*, *9*(13), 4225–4230. https://doi.org/10.1002/j.1460-2075.1990.tb07870.x

Goedert, M., Jakes, R., Spillantini, M. G., Hasegawa, M., Smith, M. J., & Crowther, R. A. (1996a). Assembly of microtubule-associated protein tau into Alzheimer-like filaments induced by sulphated glycosaminoglycans. *Nature*, *383*(6600), 550–553. https://doi.org/10.1038/383550a0

Goedert, M., Jakes, R., Spillantini, M. G., Hasegawa, M., Smith, M. J., & Crowther, R. A. (1996b). Assembly of microtubule-associated protein tau into Alzheimer-like filaments induced by sulphated glycosaminoglycans. *Nature*, *383*(6600), 550–553. https://doi.org/10.1038/383550a0

Goedert, M., & Spillantini, M. G. (2019). *Ordered Assembly of Tau Protein and Neurodegeneration* (pp. 3–21). https://doi.org/10.1007/978-981-32-9358-8_1

Goedert, M., Spillantini, M. G., & Crowther, R. A. (1992). Cloning of a big tau microtubule-associated protein characteristic of the peripheral nervous system. *Proceedings of the National Academy of Sciences*, *89*(5), 1983–1987. https://doi.org/10.1073/pnas.89.5.1983

Goedert, M., Spillantini, M. G., Potier, M. C., Ulrich, J., & Crowther, R. A. (1989). Cloning and sequencing of the cDNA encoding an isoform of microtubule-associated protein tau containing four tandem repeats: differential expression of tau protein mRNAs in human brain. *The EMBO Journal*, *8*(2), 393–399. https://doi.org/10.1002/j.1460-2075.1989.tb03390.x

Goedert, M., Wischik, C. M., Crowther, R. A., Walker, J. E., & Klug, A. (1988). Cloning and sequencing of the cDNA encoding a core protein of the paired helical filament of Alzheimer disease: identification as the microtubule-associated protein tau. *Proceedings of the National Academy of Sciences*, *85*(11), 4051–4055. https://doi.org/10.1073/pnas.85.11.4051

Gomez Perdiguero, E., Klapproth, K., Schulz, C., Busch, K., Azzoni, E., Crozet, L., Garner, H., Trouillet, C., de Bruijn, M. F., Geissmann, F., & Rodewald, H.-R. (2015). Tissue-resident macrophages originate from yolk-sac-derived erythro-myeloid progenitors. *Nature*, *518*(7540), 547–551. https://doi.org/10.1038/nature13989

Gómez-Ramos, A., Díaz-Hernández, M., Cuadros, R., Hernández, F., & Avila, J. (2006). Extracellular tau is toxic to neuronal cells. *FEBS Letters*, *580*(20), 4842–4850. https://doi.org/10.1016/j.febslet.2006.07.078

Gonçalves, R. A., Wijesekara, N., Fraser, P. E., & De Felice, F. G. (2020). Behavioral Abnormalities in Knockout and Humanized Tau Mice. *Frontiers in Endocrinology*, *11*. https://doi.org/10.3389/fendo.2020.00124

Gonias, S. L., & Campana, W. M. (2014). LDL Receptor–Related Protein-1. *The American Journal of Pathology*, *184*(1), 18–27. https://doi.org/10.1016/j.ajpath.2013.08.029

Goode, B., & Feinstein, S. (1994). Identification of a novel microtubule binding and assembly domain in the developmentally regulated inter-repeat region of tau. *The Journal of Cell Biology*, *124*(5), 769–782. https://doi.org/10.1083/jcb.124.5.769

Goode, B. L., Denis, P. E., Panda, D., Radeke, M. J., Miller, H. P., Wilson, L., & Feinstein, S. C. (1997). Functional interactions between the proline-rich and repeat regions of tau enhance microtubule binding and assembly. *Molecular Biology of the Cell*, *8*(2), 353–365. https://doi.org/10.1091/mbc.8.2.353

Gorbet, M. B., & Sefton, M. V. (2005). Endotoxin: The uninvited guest. *Biomaterials*, *26*(34), 6811–6817. https://doi.org/10.1016/j.biomaterials.2005.04.063

Gordon, S. (2002). Pattern Recognition Receptors. *Cell*, *111*(7), 927–930. https://doi.org/10.1016/S0092-8674(02)01201-1

Gosselin, D., Skola, D., Coufal, N. G., Holtman, I. R., Schlachetzki, J. C. M., Sajti, E., Jaeger, B. N., O'Connor, C., Fitzpatrick, C., Pasillas, M. P., Pena, M., Adair, A., Gonda, D. D., Levy, M. L., Ransohoff, R. M., Gage, F. H., & Glass, C. K. (2017). An environment-dependent transcriptional network specifies human microglia identity. *Science*, *356*(6344). https://doi.org/10.1126/science.aal3222

Götz, J., Halliday, G., & Nisbet, R. M. (2019). Molecular Pathogenesis of the Tauopathies. *Annual Review of Pathology: Mechanisms of Disease*, *14*(1), 239–261. https://doi.org/10.1146/annurev-pathmechdis-012418-012936

Goujon, C., Jarrosson-Wuillème, L., Bernaud, J., Rigal, D., Darlix, J.-L., & Cimarelli, A. (2006). With a little help from a friend: increasing HIV transduction of monocyte-derived dendritic cells with virion-like particles of SIVMAC. *Gene Therapy*, *13*(12), 991–994. https://doi.org/10.1038/sj.gt.3302753

Grabert, K., Michoel, T., Karavolos, M. H., Clohisey, S., Baillie, J. K., Stevens, M. P., Freeman, T. C., Summers, K. M., & McColl, B. W. (2016). Microglial brain region−dependent diversity and selective regional sensitivities to aging. *Nature Neuroscience*, *19*(3), 504–516. https://doi.org/10.1038/nn.4222

Graether, S. P. (2022). Methods for recombinant production and purification of intrinsically disordered proteins. In *Advances in Protein Molecular and Structural Biology Methods* (pp. 41–48). Elsevier. https://doi.org/10.1016/B978-0-323-90264-9.00004-0

Graham, J. P., Rauf, M. A., Hisaindee, S., & Nawaz, M. (2013). Experimental and theoretical study of the spectral behavior of Trypan Blue in various solvents. *Journal of Molecular Structure*, *1040*, 1–8. https://doi.org/10.1016/j.molstruc.2013.02.015

Gray, M. A., Choy, C. H., Dayam, R. M., Ospina-Escobar, E., Somerville, A., Xiao, X., Ferguson, S. M., & Botelho, R. J. (2016). Phagocytosis Enhances Lysosomal and Bactericidal Properties by Activating the Transcription Factor TFEB. *Current Biology*, *26*(15), 1955–1964. https://doi.org/10.1016/j.cub.2016.05.070

Greggio, E., Jain, S., Kingsbury, A., Bandopadhyay, R., Lewis, P., Kaganovich, A., van der Brug, M. P., Beilina, A., Blackinton, J., Thomas, K. J., Ahmad, R., Miller, D. W., Kesavapany, S., Singleton, A., Lees, A., Harvey, R. J., Harvey, K., & Cookson, M. R. (2006). Kinase activity is required for the toxic effects of mutant LRRK2/dardarin. *Neurobiology of Disease*, *23*(2), 329–341. https://doi.org/10.1016/j.nbd.2006.04.001

Greter, M., Lelios, I., Pelczar, P., Hoeffel, G., Price, J., Leboeuf, M., Kündig, T. M., Frei, K., Ginhoux, F., Merad, M., & Becher, B. (2012). Stroma-Derived Interleukin-34 Controls the Development and Maintenance of Langerhans Cells and the Maintenance of Microglia. *Immunity*, *37*(6), 1050–1060. https://doi.org/10.1016/j.immuni.2012.11.001

Groveman, B. R., Orrù, C. D., Hughson, A. G., Raymond, L. D., Zanusso, G., Ghetti, B., Campbell, K. J., Safar, J., Galasko, D., & Caughey, B. (2018). Rapid and ultra-sensitive quantitation of disease-associated α-synuclein seeds in brain and cerebrospinal fluid by αSyn RT-QuIC. *Acta Neuropathologica Communications*, *6*(1), 7. https://doi.org/10.1186/s40478-018-0508-2

Grundke-Iqbal, I., Iqbal, K., Quinlan, M., Tung, Y. C., Zaidi, M. S., & Wisniewski, H. M. (1986). Microtubule-associated protein tau. A component of Alzheimer paired helical filaments. *The Journal of Biological Chemistry*, *261*(13), 6084–6089.

Grundke-Iqbal, I., Iqbal, K., Tung, Y. C., Quinlan, M., Wisniewski, H. M., & Binder, L. I. (1986). Abnormal phosphorylation of the microtubule-associated protein tau (tau) in Alzheimer cytoskeletal pathology. *Proceedings of the National Academy of Sciences*, *83*(13), 4913–4917. https://doi.org/10.1073/pnas.83.13.4913

Grüning, C. S. R., Mirecka, E. A., Klein, A. N., Mandelkow, E., Willbold, D., Marino, S. F., Stoldt, M., & Hoyer, W. (2014). Alternative Conformations of the Tau Repeat Domain in Complex with an Engineered Binding Protein. *Journal of Biological Chemistry*, *289*(33), 23209–23218. https://doi.org/10.1074/jbc.M114.560920

Guérin, I., & de Chastellier, C. (2000). Disruption of the actin filament network affects delivery of endocytic contents marker to phagosomes with early endosome characteristics: The case of phagosomes with pathogenic mycobacteria. *European Journal of Cell Biology*, *79*(10), 735–749. https://doi.org/10.1078/0171-9335-00092

Guo, J. L., & Lee, V. M.-Y. (2011a). Seeding of Normal Tau by Pathological Tau Conformers Drives Pathogenesis of Alzheimer-like Tangles. *Journal of Biological Chemistry*, *286*(17), 15317–15331. https://doi.org/10.1074/jbc.M110.209296

Guo, J. L., & Lee, V. M.-Y. (2011b). Seeding of Normal Tau by Pathological Tau Conformers Drives Pathogenesis of Alzheimer-like Tangles. *Journal of Biological Chemistry*, *286*(17), 15317–15331. https://doi.org/10.1074/jbc.M110.209296

Guo, L., Gandhi, P. N., Wang, W., Petersen, R. B., Wilson-Delfosse, A. L., & Chen, S. G. (2007). The Parkinson's disease-associated protein, leucine-rich repeat kinase 2 (LRRK2), is an authentic GTPase thatstimulates kinase activity. *Experimental Cell Research*, *313*(16), 3658–3670. https://doi.org/10.1016/j.yexcr.2007.07.007

Haenseler, W., & Rajendran, L. (2019). Concise Review: Modeling Neurodegenerative Diseases with Human Pluripotent Stem Cell-Derived Microglia. *Stem Cells*, *37*(6), 724–730. https://doi.org/10.1002/stem.2995

Haenseler, W., Sansom, S. N., Buchrieser, J., Newey, S. E., Moore, C. S., Nicholls, F. J., Chintawar, S., Schnell, C., Antel, J. P., Allen, N. D., Cader, M. Z., Wade-Martins, R., James, W. S., & Cowley, S. A. (2017). A Highly Efficient Human Pluripotent Stem Cell Microglia Model Displays a Neuronal-Co-culture-Specific Expression Profile and

Inflammatory Response. *Stem Cell Reports*, *8*(6), 1727–1742. https://doi.org/10.1016/j.stemcr.2017.05.017

Haenseler, W., Zambon, F., Lee, H., Vowles, J., Rinaldi, F., Duggal, G., Houlden, H., Gwinn, K., Wray, S., Luk, K. C., Wade-Martins, R., James, W. S., & Cowley, S. A. (2017). Excess α-synuclein compromises phagocytosis in iPSC-derived macrophages. *Scientific Reports*, *7*(1), 9003. https://doi.org/10.1038/s41598-017-09362-3

Hagemeyer, N., Hanft, K.-M., Akriditou, M.-A., Unger, N., Park, E. S., Stanley, E. R., Staszewski, O., Dimou, L., & Prinz, M. (2017). Microglia contribute to normal myelinogenesis and to oligodendrocyte progenitor maintenance during adulthood. *Acta Neuropathologica*, *134*(3), 441–458. https://doi.org/10.1007/s00401-017-1747-1

Hakimi, M., Selvanantham, T., Swinton, E., Padmore, R. F., Tong, Y., Kabbach, G., Venderova, K., Girardin, S. E., Bulman, D. E., Scherzer, C. R., LaVoie, M. J., Gris, D., Park, D. S., Angel, J. B., Shen, J., Philpott, D. J., & Schlossmacher, M. G. (2011). Parkinson's disease-linked LRRK2 is expressed in circulating and tissue immune cells and upregulated following recognition of microbial structures. *Journal of Neural Transmission*, *118*(5), 795–808. https://doi.org/10.1007/s00702-011-0653-2

Hallinan, G. I., Vargas-Caballero, M., West, J., & Deinhardt, K. (2019). Tau Misfolding Efficiently Propagates between Individual Intact Hippocampal Neurons. *The Journal of Neuroscience*, *39*(48), 9623–9632. https://doi.org/10.1523/JNEUROSCI.1590-19.2019

Hanger, D. P., Goniotaki, D., & Noble, W. (2019). *Synaptic Localisation of Tau* (pp. 105–112). https://doi.org/10.1007/978-981-32-9358-8_9

Harris, J. A., Koyama, A., Maeda, S., Ho, K., Devidze, N., Dubal, D. B., Yu, G.-Q., Masliah, E., & Mucke, L. (2012). Human P301L-Mutant Tau Expression in Mouse Entorhinal-Hippocampal Network Causes Tau Aggregation and Presynaptic Pathology but No Cognitive Deficits. *PLoS ONE*, *7*(9), e45881. https://doi.org/10.1371/journal.pone.0045881

Hartlage-Rübsamen, M., Lemke, R., & Schliebs, R. (1999). Interleukin-1beta, inducible nitric oxide synthase, and nuclear factor-kappaB are induced in morphologically distinct microglia after rat hippocampal lipopolysaccharide/interferon-gamma injection. *Journal of Neuroscience Research*, *57*(3), 388–398.

Härtlova, A., Herbst, S., Peltier, J., Rodgers, A., Bilkei-Gorzo, O., Fearns, A., Dill, B. D., Lee, H., Flynn, R., Cowley, S. A., Davies, P., Lewis, P. A., Ganley, I. G., Martinez, J., Alessi, D. R., Reith, A. D., Trost, M., & Gutierrez, M. G. (2018a). LRRK2 is a negative regulator of *Mycobacterium tuberculosis* phagosome maturation in macrophages. *The EMBO Journal*, *37*(12). https://doi.org/10.15252/embj.201798694

Härtlova, A., Herbst, S., Peltier, J., Rodgers, A., Bilkei-Gorzo, O., Fearns, A., Dill, B. D., Lee, H., Flynn, R., Cowley, S. A., Davies, P., Lewis, P. A., Ganley, I. G., Martinez, J., Alessi, D. R., Reith, A. D., Trost, M., & Gutierrez, M. G. (2018b). LRRK2 is a negative regulator of *Mycobacterium tuberculosis* phagosome maturation in macrophages. *The EMBO Journal*, *37*(12). https://doi.org/10.15252/embj.201798694

Härtlova, A., Herbst, S., Peltier, J., Rodgers, A., Bilkei-Gorzo, O., Fearns, A., Dill, B. D., Lee, H., Flynn, R., Cowley, S. A., Davies, P., Lewis, P. A., Ganley, I. G., Martinez, J., Alessi, D. R., Reith, A. D., Trost, M., & Gutierrez, M. G. (2018c). LRRK2 is a negative regulator of *Mycobacterium tuberculosis* phagosome maturation in macrophages. *The EMBO Journal*, *37*(12). https://doi.org/10.15252/embj.201798694

Hasegawa, M., Smith, M. J., & Goedert, M. (1998). Tau proteins with FTDP-17 mutations have a reduced ability to promote microtubule assembly. *FEBS Letters*, *437*(3), 207–210. https://doi.org/10.1016/S0014-5793(98)01217-4

Hasselmann, J., & Blurton-Jones, M. (2020a). Human iPSC-derived microglia: A growing toolset to study the brain's innate immune cells. *Glia*, *68*(4), 721–739. https://doi.org/10.1002/glia.23781

Hasselmann, J., & Blurton-Jones, M. (2020b). Human iPSC-derived microglia: A growing toolset to study the brain's innate immune cells. *Glia*, *68*(4), 721–739. https://doi.org/10.1002/glia.23781

Haynes, S. E., Hollopeter, G., Yang, G., Kurpius, D., Dailey, M. E., Gan, W.-B., & Julius, D. (2006). The P2Y12 receptor regulates microglial activation by extracellular nucleotides. *Nature Neuroscience*, *9*(12), 1512–1519. https://doi.org/10.1038/nn1805

He, Z., Wilson, A., Rich, F., Kenwright, D., Stevens, A., Low, Y. S., & Thunders, M. (2023). Chromosomal instability and its effect on cell lines. *Cancer Reports*. https://doi.org/10.1002/cnr2.1822

Hedegaard, A., Stodolak, S., James, W. S., & Cowley, S. A. (2020). Honing the Double-Edged Sword: Improving Human iPSC-Microglia Models. *Frontiers in Immunology*, *11*. https://doi.org/10.3389/fimmu.2020.614972

Henderson, M. X., Changolkar, L., Trojanowski, J. Q., & Lee, V. M. Y. (2021). LRRK2 Kinase Activity Does Not Alter Cell-Autonomous Tau Pathology Development in Primary Neurons. *Journal of Parkinson's Disease*, *11*(3), 1187–1196. https://doi.org/10.3233/JPD-212562

Henderson, M. X., Sengupta, M., Trojanowski, J. Q., & Lee, V. M. Y. (2019). Alzheimer's disease tau is a prominent pathology in LRRK2 Parkinson's disease. *Acta Neuropathologica Communications*, *7*(1), 183. https://doi.org/10.1186/s40478-019-0836-x

Heneka, M. T. (2019). Microglia take centre stage in neurodegenerative disease. *Nature Reviews Immunology*, *19*(2), 79–80. https://doi.org/10.1038/s41577-018-0112-5

Henry, A. G., Aghamohammadzadeh, S., Samaroo, H., Chen, Y., Mou, K., Needle, E., & Hirst, W. D. (2015). Pathogenic LRRK2 mutations, through increased kinase activity, produce enlarged lysosomes with reduced degradative capacity and increase ATP13A2 expression. *Human Molecular Genetics*, *24*(21), 6013–6028. https://doi.org/10.1093/hmg/ddv314

Herbst, S., Campbell, P., Harvey, J., Bernard, E. M., Papayannopoulos, V., Wood, N. W., Morris, H. R., & Gutierrez, M. G. (2020). <scp>LRRK</scp> 2 activation controls the repair of damaged endomembranes in macrophages. *The EMBO Journal*, *39*(18). https://doi.org/10.15252/embj.2020104494

Herbst, S., Lewis, P. A., & Morris, H. R. (2022). The emerging role of LRRK2 in tauopathies. *Clinical Science*, *136*(13), 1071–1079. https://doi.org/10.1042/CS20220067

Herms, J., Tings, T., Gall, S., Madlung, A., Giese, A., Siebert, H., Schürmann, P., Windl, O., Brose, N., & Kretzschmar, H. (1999). Evidence of Presynaptic Location and Function of the Prion Protein. *The Journal of Neuroscience*, *19*(20), 8866–8875. https://doi.org/10.1523/JNEUROSCI.19-20-08866.1999

Herz, J., Goldstein, J. L., Strickland, D. K., Ho, Y. K., & Brown, M. S. (1991). 39-kDa protein modulates binding of ligands to low density lipoprotein receptor-related protein/alpha 2-macroglobulin receptor. *Journal of Biological Chemistry*, *266*(31), 21232–21238. https://doi.org/10.1016/S0021-9258(18)54845-6

Hickman, S. E., Kingery, N. D., Ohsumi, T. K., Borowsky, M. L., Wang, L., Means, T. K., & El Khoury, J. (2013). The microglial sensome revealed by direct RNA sequencing. *Nature Neuroscience*, *16*(12), 1896–1905. https://doi.org/10.1038/nn.3554

Hickman, S., Izzy, S., Sen, P., Morsett, L., & El Khoury, J. (2018). Microglia in neurodegeneration. *Nature Neuroscience*, *21*(10), 1359–1369. https://doi.org/10.1038/s41593-018-0242-x

Himmler, A., Drechsel, D., Kirschner, M. W., & Martin, D. W. (1989). Tau Consists of a Set of Proteins with Repeated C-Terminal Microtubule-Binding Domains and Variable N-Terminal Domains. *Molecular and Cellular Biology*, *9*(4), 1381–1388. https://doi.org/10.1128/mcb.9.4.1381-1388.1989

Hirayama, C., & Sakata, M. (2002). Chromatographic removal of endotoxin from protein solutions by polymer particles. *Journal of Chromatography B*, *781*(1–2), 419–432. https://doi.org/10.1016/S1570-0232(02)00430-0

Hirokawa, N., Funakoshi, T., Sato-Harada, R., & Kanai, Y. (1996). Selective stabilization of tau in axons and microtubule-associated protein 2C in cell bodies and dendrites

contributes to polarized localization of cytoskeletal proteins in mature neurons. *The Journal of Cell Biology*, *132*(4), 667–679. https://doi.org/10.1083/jcb.132.4.667

Hitt, B. D., Vaquer-Alicea, J., Manon, V. A., Beaver, J. D., Kashmer, O. M., Garcia, J. N., & Diamond, M. I. (2021). Ultrasensitive tau biosensor cells detect no seeding in Alzheimer's disease CSF. *Acta Neuropathologica Communications*, *9*(1), 99. https://doi.org/10.1186/s40478-021-01185-8

Hoenig, M. C., Bischof, G. N., Seemiller, J., Hammes, J., Kukolja, J., Onur, Ö. A., Jessen, F., Fliessbach, K., Neumaier, B., Fink, G. R., van Eimeren, T., & Drzezga, A. (2018). Networks of tau distribution in Alzheimer's disease. *Brain*, *141*(2), 568–581. https://doi.org/10.1093/brain/awx353

Hofmann, H., Logue, E. C., Bloch, N., Daddacha, W., Polsky, S. B., Schultz, M. L., Kim, B., & Landau, N. R. (2012). The Vpx Lentiviral Accessory Protein Targets SAMHD1 for Degradation in the Nucleus. *Journal of Virology*, *86*(23), 12552–12560. https://doi.org/10.1128/JVI.01657-12

Holmes, B. B., DeVos, S. L., Kfoury, N., Li, M., Jacks, R., Yanamandra, K., Ouidja, M. O., Brodsky, F. M., Marasa, J., Bagchi, D. P., Kotzbauer, P. T., Miller, T. M., Papy-Garcia, D., & Diamond, M. I. (2013). Heparan sulfate proteoglycans mediate internalization and propagation of specific proteopathic seeds. *Proceedings of the National Academy of Sciences*, *110*(33). https://doi.org/10.1073/pnas.1301440110

Holmes, B. B., Furman, J. L., Mahan, T. E., Yamasaki, T. R., Mirbaha, H., Eades, W. C., Belaygorod, L., Cairns, N. J., Holtzman, D. M., & Diamond, M. I. (2014). Proteopathic tau seeding predicts tauopathy in vivo. *Proceedings of the National Academy of Sciences*, *111*(41). https://doi.org/10.1073/pnas.1411649111

Holtman, I. R., Raj, D. D., Miller, J. A., Schaafsma, W., Yin, Z., Brouwer, N., Wes, P. D., Möller, T., Orre, M., Kamphuis, W., Hol, E. M., Boddeke, E. W. G. M., & Eggen, B. J. L. (2015). Induction of a common microglia gene expression signature by aging and neurodegenerative conditions: a co-expression meta-analysis. *Acta Neuropathologica Communications*, *3*(1), 31. https://doi.org/10.1186/s40478-015-0203-5

Hong, M. (1998). Mutation-Specific Functional Impairments in Distinct Tau Isoforms of Hereditary FTDP-17. *Science*, *282*(5395), 1914–1917. https://doi.org/10.1126/science.282.5395.1914

Hopp, S. C., Lin, Y., Oakley, D., Roe, A. D., DeVos, S. L., Hanlon, D., & Hyman, B. T. (2018). The role of microglia in processing and spreading of bioactive tau seeds in Alzheimer's disease. *Journal of Neuroinflammation*, *15*(1), 269. https://doi.org/10.1186/s12974-018-1309-z

Hu, W., Zhang, X., Tung, Y. C., Xie, S., Liu, F., & Iqbal, K. (2016). Hyperphosphorylation determines both the spread and the morphology of tau pathology. *Alzheimer's & Dementia*, *12*(10), 1066–1077. https://doi.org/10.1016/j.jalz.2016.01.014

Huang, Y., Xu, Z., Xiong, S., Sun, F., Qin, G., Hu, G., Wang, J., Zhao, L., Liang, Y.-X., Wu, T., Lu, Z., Humayun, M. S., So, K.-F., Pan, Y., Li, N., Yuan, T.-F., Rao, Y., & Peng, B. (2018). Repopulated microglia are solely derived from the proliferation of residual microglia after acute depletion. *Nature Neuroscience*, *21*(4), 530–540. https://doi.org/10.1038/s41593-018-0090-8

Hunt, J. P., Zhao, E. L., Soltani, M., Frei, M., Nelson, J. A. D., & Bundy, B. C. (2019). Streamlining the preparation of "endotoxin-free" ClearColi cell extract with autoinduction media for cell-free protein synthesis of the therapeutic protein crisantaspase. *Synthetic and Systems Biotechnology*, *4*(4), 220–224. https://doi.org/10.1016/j.synbio.2019.11.003

Hur, E.-M., Jang, E.-H., Jeong, G. R., & Lee, B. D. (2019). LRRK2 and membrane trafficking: nexus of Parkinson's disease. *BMB Reports*, *52*(9), 533–539. https://doi.org/10.5483/BMBRep.2019.52.9.186

Hutton, M., Lendon, C. L., Rizzu, P., Baker, M., Froelich, S., Houlden, H., Pickering-Brown, S., Chakraverty, S., Isaacs, A., Grover, A., Hackett, J., Adamson, J., Lincoln, S., Dickson, D., Davies, P., Petersen, R. C., Stevens, M., de Graaff, E., Wauters, E., … Heutink, P. (1998). Association of missense and 5′-splice-site mutations in tau with the inherited dementia FTDP-17. *Nature*, *393*(6686), 702–705. https://doi.org/10.1038/31508

Iba, M., McBride, J. D., Guo, J. L., Zhang, B., Trojanowski, J. Q., & Lee, V. M.-Y. (2015a). Tau pathology spread in PS19 tau transgenic mice following locus coeruleus (LC) injections of synthetic tau fibrils is determined by the LC's afferent and efferent connections. *Acta Neuropathologica*, *130*(3), 349–362. https://doi.org/10.1007/s00401-015-1458-4

Iba, M., McBride, J. D., Guo, J. L., Zhang, B., Trojanowski, J. Q., & Lee, V. M.-Y. (2015b). Tau pathology spread in PS19 tau transgenic mice following locus coeruleus (LC) injections of synthetic tau fibrils is determined by the LC's afferent and efferent connections. *Acta Neuropathologica*, *130*(3), 349–362. https://doi.org/10.1007/s00401-015-1458-4

Imamura, K., Hishikawa, N., Sawada, M., Nagatsu, T., Yoshida, M., & Hashizume, Y. (2003). Distribution of major histocompatibility complex class II-positive microglia and cytokine profile of Parkinson's disease brains. *Acta Neuropathologica*, *106*(6), 518–526. https://doi.org/10.1007/s00401-003-0766-2

Iqbal, K., Wiśniewski, H. M., Shelanski, M. L., Brostoff, S., Liwnicz, B. H., & Terry, R. D. (1974). Protein changes in senile dementia. *Brain Research*, *77*(2), 337–343. https://doi.org/10.1016/0006-8993(74)90798-7

Irwin, D. J., Brettschneider, J., McMillan, C. T., Cooper, F., Olm, C., Arnold, S. E., Van Deerlin, V. M., Seeley, W. W., Miller, B. L., Lee, E. B., Lee, V. M.-Y., Grossman, M., & Trojanowski, J. Q. (2016). Deep clinical and neuropathological phenotyping of Pick disease. *Annals of Neurology*, *79*(2), 272–287. https://doi.org/10.1002/ana.24559

Ising, C., Venegas, C., Zhang, S., Scheiblich, H., Schmidt, S. V., Vieira-Saecker, A., Schwartz, S., Albasset, S., McManus, R. M., Tejera, D., Griep, A., Santarelli, F., Brosseron, F., Opitz, S., Stunden, J., Merten, M., Kayed, R., Golenbock, D. T., Blum, D., … Heneka, M. T. (2019). NLRP3 inflammasome activation drives tau pathology. *Nature*, *575*(7784), 669–673. https://doi.org/10.1038/s41586-019-1769-z

Ittner, L. M., Ke, Y. D., Delerue, F., Bi, M., Gladbach, A., van Eersel, J., Wölfing, H., Chieng, B. C., Christie, M. J., Napier, I. A., Eckert, A., Staufenbiel, M., Hardeman, E., & Götz, J. (2010). Dendritic Function of Tau Mediates Amyloid-β Toxicity in Alzheimer's Disease Mouse Models. *Cell*, *142*(3), 387–397. https://doi.org/10.1016/j.cell.2010.06.036

Jabbari, E., Koga, S., Valentino, R. R., Reynolds, R. H., Ferrari, R., Tan, M. M. X., Rowe, J. B., Dalgard, C. L., Scholz, S. W., Dickson, D. W., Warner, T. T., Revesz, T., Höglinger, G. U., Ross, O. A., Ryten, M., Hardy, J., Shoai, M., Morris, H. R., Mok, K. Y., … T.M. Hu, M. (2021). Genetic determinants of survival in progressive supranuclear palsy: a genome-wide association study. *The Lancet Neurology*, *20*(2), 107–116. https://doi.org/10.1016/S1474-4422(20)30394-X

Jackson, S. J., Kerridge, C., Cooper, J., Cavallini, A., Falcon, B., Cella, C. V., Landi, A., Szekeres, P. G., Murray, T. K., Ahmed, Z., Goedert, M., Hutton, M., O'Neill, M. J., & Bose, S. (2016). Short Fibrils Constitute the Major Species of Seed-Competent Tau in the Brains of Mice Transgenic for Human P301S Tau. *The Journal of Neuroscience*, *36*(3), 762–772. https://doi.org/10.1523/JNEUROSCI.3542-15.2016

Jaldín-Fincati, J. R., Actis Dato, V., Díaz, N. M., Sánchez, M. C., Barcelona, P. F., & Chiabrando, G. A. (2019). Activated α2-Macroglobulin Regulates LRP1 Levels at the Plasma Membrane through the Activation of a Rab10-dependent Exocytic Pathway in Retinal Müller Glial Cells. *Scientific Reports*, *9*(1), 13234. https://doi.org/10.1038/s41598-019-49072-6

Janova, H., Böttcher, C., Holtman, I. R., Regen, T., van Rossum, D., Götz, A., Ernst, A.-S., Fritsche, C., Gertig, U., Saiepour, N., Gronke, K., Wrzos, C., Ribes, S., Rolfes, S., Weinstein, J., Ehrenreich, H., Pukrop, T., Kopatz, J., Stadelmann, C., … Hanisch, U.-

K. (2016). CD14 is a key organizer of microglial responses to CNS infection and injury. *Glia*, *64*(4), 635–649. https://doi.org/10.1002/glia.22955

Jeganathan, S., von Bergen, M., Brutlach, H., Steinhoff, H.-J., & Mandelkow, E. (2006). Global Hairpin Folding of Tau in Solution. *Biochemistry*, *45*(7), 2283–2293. https://doi.org/10.1021/bi0521543

Jeganathan, S., von Bergen, M., Mandelkow, E.-M., & Mandelkow, E. (2008). The Natively Unfolded Character of Tau and Its Aggregation to Alzheimer-like Paired Helical Filaments. *Biochemistry*, *47*(40), 10526–10539. https://doi.org/10.1021/bi800783d

Jen, A., Parkyn, C. J., Mootoosamy, R. C., Ford, M. J., Warley, A., Liu, Q., Bu, G., Baskakov, I. V., Moestrup, S., McGuinness, L., Emptage, N., & Morris, R. J. (2010). Neuronal low-density lipoprotein receptor-related protein 1 binds and endocytoses prion fibrils via receptor cluster 4. *Journal of Cell Science*, *123*(2), 246–255. https://doi.org/10.1242/jcs.058099

Jiang, L., Lin, W., Zhang, C., Ash, P. E. A., Verma, M., Kwan, J., van Vliet, E., Yang, Z., Cruz, A. L., Boudeau, S., Maziuk, B. F., Lei, S., Song, J., Alvarez, V. E., Hovde, S., Abisambra, J. F., Kuo, M.-H., Kanaan, N., Murray, M. E., … Wolozin, B. (2021). Interaction of tau with HNRNPA2B1 and N6-methyladenosine RNA mediates the progression of tauopathy. *Molecular Cell*, *81*(20), 4209-4227.e12. https://doi.org/10.1016/j.molcel.2021.07.038

Jin, M., Shiwaku, H., Tanaka, H., Obita, T., Ohuchi, S., Yoshioka, Y., Jin, X., Kondo, K., Fujita, K., Homma, H., Nakajima, K., Mizuguchi, M., & Okazawa, H. (2021). Tau activates microglia via the PQBP1-cGAS-STING pathway to promote brain inflammation. *Nature Communications*, *12*(1), 6565. https://doi.org/10.1038/s41467-021-26851-2

Jucker, M., & Walker, L. C. (2013). Self-propagation of pathogenic protein aggregates in neurodegenerative diseases. *Nature*, *501*(7465), 45–51. https://doi.org/10.1038/nature12481

Kadavath, H., Hofele, R. V., Biernat, J., Kumar, S., Tepper, K., Urlaub, H., Mandelkow, E., & Zweckstetter, M. (2015a). Tau stabilizes microtubules by binding at the interface between tubulin heterodimers. *Proceedings of the National Academy of Sciences*, *112*(24), 7501–7506. https://doi.org/10.1073/pnas.1504081112

Kadavath, H., Hofele, R. V., Biernat, J., Kumar, S., Tepper, K., Urlaub, H., Mandelkow, E., & Zweckstetter, M. (2015b). Tau stabilizes microtubules by binding at the interface between tubulin heterodimers. *Proceedings of the National Academy of Sciences*, *112*(24), 7501–7506. https://doi.org/10.1073/pnas.1504081112

Kalia, L. V., Lang, A. E., Hazrati, L.-N., Fujioka, S., Wszolek, Z. K., Dickson, D. W., Ross, O. A., Van Deerlin, V. M., Trojanowski, J. Q., Hurtig, H. I., Alcalay, R. N., Marder, K.

S., Clark, L. N., Gaig, C., Tolosa, E., Ruiz-Martínez, J., Marti-Masso, J. F., Ferrer, I., López de Munain, A., … Marras, C. (2015). Clinical Correlations With Lewy Body Pathology in *LRRK2* -Related Parkinson Disease. *JAMA Neurology*, *72*(1), 100. https://doi.org/10.1001/jamaneurol.2014.2704

Kamath, T. V, Klickstein, N., Commins, C., Fernandes, A. R., Oakley, D. H., Frosch, M. P., Hyman, B. T., & Dujardin, S. (2021). Kinetics of tau aggregation reveals patient-specific tau characteristics among Alzheimer's cases. *Brain Communications*, *3*(2). https://doi.org/10.1093/braincomms/fcab096

Kampers, T., Friedhoff, P., Biernat, J., Mandelkow, E.-M., & Mandelkow, E. (1996). RNA stimulates aggregation of microtubule-associated protein tau into Alzheimer-like paired helical filaments. *FEBS Letters*, *399*(3), 344–349. https://doi.org/10.1016/S0014-5793(96)01386-5

Kanekiyo, T., Zhang, J., Liu, Q., Liu, C.-C., Zhang, L., & Bu, G. (2011). Heparan Sulphate Proteoglycan and the Low-Density Lipoprotein Receptor-Related Protein 1 Constitute Major Pathways for Neuronal Amyloid-β Uptake. *The Journal of Neuroscience*, *31*(5), 1644–1651. https://doi.org/10.1523/JNEUROSCI.5491-10.2011

Kanemaru, K., Takio, K., Miura, R., Titani, K., & Ihara, Y. (1992). Fetal-Type Phosphorylation of the ? in Paired Helical Filaments. *Journal of Neurochemistry*, *58*(5), 1667–1675. https://doi.org/10.1111/j.1471-4159.1992.tb10039.x

Kann, O., Almouhanna, F., & Chausse, B. (2022). Interferon γ: a master cytokine in microglia-mediated neural network dysfunction and neurodegeneration. *Trends in Neurosciences*, *45*(12), 913–927. https://doi.org/10.1016/j.tins.2022.10.007

Kapetanovic, R., Nahori, M.-A., Balloy, V., Fitting, C., Philpott, D. J., Cavaillon, J.-M., & Adib-Conquy, M. (2007). Contribution of Phagocytosis and Intracellular Sensing for Cytokine Production by *Staphylococcus aureus* -Activated Macrophages. *Infection and Immunity*, *75*(2), 830–837. https://doi.org/10.1128/IAI.01199-06

Karikari, T. K., Keeling, S., Hill, E., Lantero Rodríguez, J., Nagel, D. A., Becker, B., Höglund, K., Zetterberg, H., Blennow, K., Hill, E. J., & Moffat, K. G. (2020). Extensive Plasmid Library to Prepare Tau Protein Variants and Study Their Functional Biochemistry. *ACS Chemical Neuroscience*, *11*(19), 3117–3129. https://doi.org/10.1021/acschemneuro.0c00469

Karikari, T. K., Turner, A., Stass, R., Lee, L. C. Y., Wilson, B., Nagel, D. A., Hill, E. J., & Moffat, K. G. (2017). Expression and purification of tau protein and its frontotemporal dementia variants using a cleavable histidine tag. *Protein Expression and Purification*, *130*, 44–54. https://doi.org/10.1016/j.pep.2016.09.009

Karlsson, K. R., Cowley, S., Martinez, F. O., Shaw, M., Minger, S. L., & James, W. (2008). Homogeneous monocytes and macrophages from human embryonic stem cells

following coculture-free differentiation in M-CSF and IL-3. *Experimental Hematology*, *36*(9), 1167–1175. https://doi.org/10.1016/j.exphem.2008.04.009

Kato, G., Inada, H., Wake, H., Akiyoshi, R., Miyamoto, A., Eto, K., Ishikawa, T., Moorhouse, A. J., Strassman, A. M., & Nabekura, J. (2016). Microglial Contact Prevents Excess Depolarization and Rescues Neurons from Excitotoxicity. *Eneuro*, *3*(3), ENEURO.0004-16.2016. https://doi.org/10.1523/ENEURO.0004-16.2016

Katsinelos, T., Zeitler, M., Dimou, E., Karakatsani, A., Müller, H.-M., Nachman, E., Steringer, J. P., Ruiz de Almodovar, C., Nickel, W., & Jahn, T. R. (2018). Unconventional Secretion Mediates the Trans-cellular Spreading of Tau. *Cell Reports*, *23*(7), 2039–2055. https://doi.org/10.1016/j.celrep.2018.04.056

Kaufman, S. K., Sanders, D. W., Thomas, T. L., Ruchinskas, A. J., Vaquer-Alicea, J., Sharma, A. M., Miller, T. M., & Diamond, M. I. (2016). Tau Prion Strains Dictate Patterns of Cell Pathology, Progression Rate, and Regional Vulnerability In Vivo. *Neuron*, *92*(4), 796–812. https://doi.org/10.1016/j.neuron.2016.09.055

Kavanagh, T., Halder, A., & Drummond, E. (2022). Tau interactome and RNA binding proteins in neurodegenerative diseases. *Molecular Neurodegeneration*, *17*(1), 66. https://doi.org/10.1186/s13024-022-00572-6

Kawai, T., & Akira, S. (2010). The role of pattern-recognition receptors in innate immunity: update on Toll-like receptors. *Nature Immunology*, *11*(5), 373–384. https://doi.org/10.1038/ni.1863

Keren-Shaul, H., Spinrad, A., Weiner, A., Matcovitch-Natan, O., Dvir-Szternfeld, R., Ulland, T. K., David, E., Baruch, K., Lara-Astaiso, D., Toth, B., Itzkovitz, S., Colonna, M., Schwartz, M., & Amit, I. (2017). A Unique Microglia Type Associated with Restricting Development of Alzheimer's Disease. *Cell*, *169*(7), 1276-1290.e17. https://doi.org/10.1016/j.cell.2017.05.018

Kettenmann, H., Hanisch, U.-K., Noda, M., & Verkhratsky, A. (2011). Physiology of Microglia. *Physiological Reviews*, *91*(2), 461–553. https://doi.org/10.1152/physrev.00011.2010

Kettenmann, H., Kirchhoff, F., & Verkhratsky, A. (2013). Microglia: New Roles for the Synaptic Stripper. *Neuron*, *77*(1), 10–18. https://doi.org/10.1016/j.neuron.2012.12.023

Kfoury, N., Holmes, B. B., Jiang, H., Holtzman, D. M., & Diamond, M. I. (2012). Trans-cellular Propagation of Tau Aggregation by Fibrillar Species. *Journal of Biological Chemistry*, *287*(23), 19440–19451. https://doi.org/10.1074/jbc.M112.346072

Khlistunova, I., Biernat, J., Wang, Y., Pickhardt, M., von Bergen, M., Gazova, Z., Mandelkow, E., & Mandelkow, E.-M. (2006). Inducible Expression of Tau Repeat

Domain in Cell Models of Tauopathy. *Journal of Biological Chemistry*, *281*(2), 1205–1214. https://doi.org/10.1074/jbc.M507753200

KIDD, M. (1963). Paired Helical Filaments in Electron Microscopy of Alzheimer's Disease. *Nature*, *197*(4863), 192–193. https://doi.org/10.1038/197192b0

Kierdorf, K., Erny, D., Goldmann, T., Sander, V., Schulz, C., Perdiguero, E. G., Wieghofer, P., Heinrich, A., Riemke, P., Hölscher, C., Müller, D. N., Luckow, B., Brocker, T., Debowski, K., Fritz, G., Opdenakker, G., Diefenbach, A., Biber, K., Heikenwalder, M., … Prinz, M. (2013). Microglia emerge from erythromyeloid precursors via Pu.1- and Irf8-dependent pathways. *Nature Neuroscience*, *16*(3), 273–280. https://doi.org/10.1038/nn.3318

Kim, B., Suh, Y. H., & Joe, E. (2022). LRRK2 decreases microglial actin dynamics by filamentous actin depolymerization and Rac1 inhibition. *Animal Cells and Systems*, *26*(6), 380–387. https://doi.org/10.1080/19768354.2022.2158219

Kim, D., Lim, S., Haque, Md. M., Ryoo, N., Hong, H. S., Rhim, H., Lee, D.-E., Chang, Y.-T., Lee, J.-S., Cheong, E., Kim, D. J., & Kim, Y. K. (2015). Identification of disulfide cross-linked tau dimer responsible for tau propagation. *Scientific Reports*, *5*(1), 15231. https://doi.org/10.1038/srep15231

Kim, K. S., Marcogliese, P. C., Yang, J., Callaghan, S. M., Resende, V., Abdel-Messih, E., Marras, C., Visanji, N. P., Huang, J., Schlossmacher, M. G., Trinkle-Mulcahy, L., Slack, R. S., Lang, A. E., Park, D. S., Brown, E., Gibbings, D., Hayley, S., Park, D., Philpott, D. C., … Schurr, E. (2018a). Regulation of myeloid cell phagocytosis by LRRK2 via WAVE2 complex stabilization is altered in Parkinson's disease. *Proceedings of the National Academy of Sciences*, *115*(22). https://doi.org/10.1073/pnas.1718946115

Kim, K. S., Marcogliese, P. C., Yang, J., Callaghan, S. M., Resende, V., Abdel-Messih, E., Marras, C., Visanji, N. P., Huang, J., Schlossmacher, M. G., Trinkle-Mulcahy, L., Slack, R. S., Lang, A. E., Park, D. S., Brown, E., Gibbings, D., Hayley, S., Park, D., Philpott, D. C., … Schurr, E. (2018b). Regulation of myeloid cell phagocytosis by LRRK2 via WAVE2 complex stabilization is altered in Parkinson's disease. *Proceedings of the National Academy of Sciences*, *115*(22). https://doi.org/10.1073/pnas.1718946115

Kim, S. J., & Li, J. (2013). Caspase blockade induces RIP3-mediated programmed necrosis in Toll-like receptor-activated microglia. *Cell Death & Disease*, *4*(7), e716–e716. https://doi.org/10.1038/cddis.2013.238

Kimura, T., Whitcomb, D. J., Jo, J., Regan, P., Piers, T., Heo, S., Brown, C., Hashikawa, T., Murayama, M., Seok, H., Sotiropoulos, I., Kim, E., Collingridge, G. L., Takashima, A., & Cho, K. (2014). Microtubule-associated protein tau is essential for long-term

depression in the hippocampus. *Philosophical Transactions of the Royal Society B: Biological Sciences*, *369*(1633), 20130144. https://doi.org/10.1098/rstb.2013.0144

Kiss, A. L., & Botos, E. (2009). Endocytosis *via* caveolae: alternative pathway with distinct cellular compartments to avoid lysosomal degradation? *Journal of Cellular and Molecular Medicine*, *13*(7), 1228–1237. https://doi.org/10.1111/j.1582-4934.2009.00754.x

Kitazawa, M., Cheng, D., Tsukamoto, M. R., Koike, M. A., Wes, P. D., Vasilevko, V., Cribbs, D. H., & LaFerla, F. M. (2011). Blocking IL-1 Signaling Rescues Cognition, Attenuates Tau Pathology, and Restores Neuronal β-Catenin Pathway Function in an Alzheimer's Disease Model. *The Journal of Immunology*, *187*(12), 6539–6549. https://doi.org/10.4049/jimmunol.1100620

Kjeken, R., Egeberg, M., Habermann, A., Kuehnel, M., Peyron, P., Floetenmeyer, M., Walther, P., Jahraus, A., Defacque, H., Kuznetsov, S. A., & Griffiths, G. (2004). Fusion between Phagosomes, Early and Late Endosomes: A Role for Actin in Fusion between Late, but Not Early Endocytic Organelles. *Molecular Biology of the Cell*, *15*(1), 345–358. https://doi.org/10.1091/mbc.e03-05-0334

Kleiner-Grote, G. R. M., Risse, J. M., & Friehs, K. (2018). Secretion of recombinant proteins from *E. coli*. *Engineering in Life Sciences*, *18*(8), 532–550. https://doi.org/10.1002/elsc.201700200

Kodama, L., Guzman, E., Etchegaray, J. I., Li, Y., Sayed, F. A., Zhou, L., Zhou, Y., Zhan, L., Le, D., Udeochu, J. C., Clelland, C. D., Cheng, Z., Yu, G., Li, Q., Kosik, K. S., & Gan, L. (2020). Microglial microRNAs mediate sex-specific responses to tau pathology. *Nature Neuroscience*, *23*(2), 167–171. https://doi.org/10.1038/s41593-019-0560-7

Köpke, E., Tung, Y. C., Shaikh, S., Alonso, A. C., Iqbal, K., & Grundke-Iqbal, I. (1993). Microtubule-associated protein tau. Abnormal phosphorylation of a non-paired helical filament pool in Alzheimer disease. *The Journal of Biological Chemistry*, *268*(32), 24374–24384.

Kosik, K., & Finch, E. (1987). MAP2 and tau segregate into dendritic and axonal domains after the elaboration of morphologically distinct neurites: an immunocytochemical study of cultured rat cerebrum. *The Journal of Neuroscience*, *7*(10), 3142–3153. https://doi.org/10.1523/JNEUROSCI.07-10-03142.1987

Kosik, K. S., Orecchio, L. D., Bakalis, S., & Neve, R. L. (1989). Developmentally regulated expression of specific tau sequences. *Neuron*, *2*(4), 1389–1397. https://doi.org/10.1016/0896-6273(89)90077-9

Kovac, A., Zilka, N., Kazmerova, Z., Cente, M., Zilkova, M., & Novak, M. (2011). Misfolded Truncated Protein τ Induces Innate Immune Response via MAPK Pathway. *The*

Journal of Immunology, *187*(5), 2732–2739. https://doi.org/10.4049/jimmunol.1100216

Kozlowski, L. P. (2017). Proteome-pI: proteome isoelectric point database. *Nucleic Acids Research*, *45*(D1), D1112–D1116. https://doi.org/10.1093/nar/gkw978

Krasemann, S., Madore, C., Cialic, R., Baufeld, C., Calcagno, N., El Fatimy, R., Beckers, L., O'Loughlin, E., Xu, Y., Fanek, Z., Greco, D. J., Smith, S. T., Tweet, G., Humulock, Z., Zrzavy, T., Conde-Sanroman, P., Gacias, M., Weng, Z., Chen, H., … Butovsky, O. (2017). The TREM2-APOE Pathway Drives the Transcriptional Phenotype of Dysfunctional Microglia in Neurodegenerative Diseases. *Immunity*, *47*(3), 566-581.e9. https://doi.org/10.1016/j.immuni.2017.08.008

Kraus, A., Saijo, E., Metrick, M. A., Newell, K., Sigurdson, C. J., Zanusso, G., Ghetti, B., & Caughey, B. (2019a). Seeding selectivity and ultrasensitive detection of tau aggregate conformers of Alzheimer disease. *Acta Neuropathologica*, *137*(4), 585–598. https://doi.org/10.1007/s00401-018-1947-3

Kraus, A., Saijo, E., Metrick, M. A., Newell, K., Sigurdson, C. J., Zanusso, G., Ghetti, B., & Caughey, B. (2019b). Seeding selectivity and ultrasensitive detection of tau aggregate conformers of Alzheimer disease. *Acta Neuropathologica*, *137*(4), 585–598. https://doi.org/10.1007/s00401-018-1947-3

Krebs, M. R. H., Bromley, E. H. C., & Donald, A. M. (2005). The binding of thioflavin-T to amyloid fibrils: localisation and implications. *Journal of Structural Biology*, *149*(1), 30–37. https://doi.org/10.1016/j.jsb.2004.08.002

Kremlev, S. (2004). Differential expression of chemokines and chemokine receptors during microglial activation and inhibition. *Journal of Neuroimmunology*, *149*(1–2), 1–9. https://doi.org/10.1016/j.jneuroim.2003.11.012

KrishnaKumar, V. G., & Gupta, S. (2017). Simplified method to obtain enhanced expression of tau protein from *E. coli* and one-step purification by direct boiling. *Preparative Biochemistry & Biotechnology*, *47*(5), 530–538. https://doi.org/10.1080/10826068.2016.1275012

Kumari, R., & Gensel, J. C. (2023). Microglia as drivers of neurodegeneration: The role of innate-adaptive immune signaling. *Neuron*, *111*(5), 597–598. https://doi.org/10.1016/j.neuron.2023.02.005

Kumari, S., MG, S., & Mayor, S. (2010). Endocytosis unplugged: multiple ways to enter the cell. *Cell Research*, *20*(3), 256–275. https://doi.org/10.1038/cr.2010.19

Kustrimovic, N., Comi, C., Magistrelli, L., Rasini, E., Legnaro, M., Bombelli, R., Aleksic, I., Blandini, F., Minafra, B., Riboldazzi, G., Sturchio, A., Mauri, M., Bono, G., Marino, F., & Cosentino, M. (2018). Parkinson's disease patients have a complex phenotypic and functional Th1 bias: cross-sectional studies of CD4+ Th1/Th2/T17 and Treg in drug-

naïve and drug-treated patients. *Journal of Neuroinflammation*, *15*(1), 205. https://doi.org/10.1186/s12974-018-1248-8

Laguette, N., Sobhian, B., Casartelli, N., Ringeard, M., Chable-Bessia, C., Ségéral, E., Yatim, A., Emiliani, S., Schwartz, O., & Benkirane, M. (2011). SAMHD1 is the dendritic- and myeloid-cell-specific HIV-1 restriction factor counteracted by Vpx. *Nature*, *474*(7353), 654–657. https://doi.org/10.1038/nature10117

Lahouassa, H., Daddacha, W., Hofmann, H., Ayinde, D., Logue, E. C., Dragin, L., Bloch, N., Maudet, C., Bertrand, M., Gramberg, T., Pancino, G., Priet, S., Canard, B., Laguette, N., Benkirane, M., Transy, C., Landau, N. R., Kim, B., & Margottin-Goguet, F. (2012). SAMHD1 restricts the replication of human immunodeficiency virus type 1 by depleting the intracellular pool of deoxynucleoside triphosphates. *Nature Immunology*, *13*(3), 223–228. https://doi.org/10.1038/ni.2236

Lancaster, C. E., Fountain, A., Dayam, R. M., Somerville, E., Sheth, J., Jacobelli, V., Somerville, A., Terebiznik, M. R., & Botelho, R. J. (2021). Phagosome resolution regenerates lysosomes and maintains the degradative capacity in phagocytes. *Journal of Cell Biology*, *220*(9). https://doi.org/10.1083/jcb.202005072

Langston, R. G., Beilina, A., Reed, X., Kaganovich, A., Singleton, A. B., Blauwendraat, C., Gibbs, J. R., & Cookson, M. R. (2022). Association of a common genetic variant with Parkinson's disease is mediated by microglia. *Science Translational Medicine*, *14*(655). https://doi.org/10.1126/scitranslmed.abp8869

Lee, G., Cowan, N., & Kirschner, M. (1988). The Primary Structure and Heterogeneity of Tau Protein from Mouse Brain. *Science*, *239*(4837), 285–288. https://doi.org/10.1126/science.3122323

Lee, H., Flynn, R., Sharma, I., Haberman, E., Carling, P. J., Nicholls, F. J., Stegmann, M., Vowles, J., Haenseler, W., Wade-Martins, R., James, W. S., & Cowley, S. A. (2020). LRRK2 Is Recruited to Phagosomes and Co-recruits RAB8 and RAB10 in Human Pluripotent Stem Cell-Derived Macrophages. *Stem Cell Reports*, *14*(5), 940–955. https://doi.org/10.1016/j.stemcr.2020.04.001

Lee, H., James, W. S., & Cowley, S. A. (2017). LRRK2 in peripheral and central nervous system innate immunity: its link to Parkinson's disease. *Biochemical Society Transactions*, *45*(1), 131–139. https://doi.org/10.1042/BST20160262

Lee, M., McGeer, E., & McGeer, P. L. (2015). Activated human microglia stimulate neuroblastoma cells to upregulate production of beta amyloid protein and tau: implications for Alzheimer's disease pathogenesis. *Neurobiology of Aging*, *36*(1), 42–52. https://doi.org/10.1016/j.neurobiolaging.2014.07.024

Lei, P., Ayton, S., Finkelstein, D. I., Spoerri, L., Ciccotosto, G. D., Wright, D. K., Wong, B. X. W., Adlard, P. A., Cherny, R. A., Lam, L. Q., Roberts, B. R., Volitakis, I., Egan, G.

F., McLean, C. A., Cappai, R., Duce, J. A., & Bush, A. I. (2012). Tau deficiency induces parkinsonism with dementia by impairing APP-mediated iron export. *Nature Medicine*, *18*(2), 291–295. https://doi.org/10.1038/nm.2613

Leng, K., Li, E., Eser, R., Piergies, A., Sit, R., Tan, M., Neff, N., Li, S. H., Rodriguez, R. D., Suemoto, C. K., Leite, R. E. P., Ehrenberg, A. J., Pasqualucci, C. A., Seeley, W. W., Spina, S., Heinsen, H., Grinberg, L. T., & Kampmann, M. (2021). Molecular characterization of selectively vulnerable neurons in Alzheimer's disease. *Nature Neuroscience*, *24*(2), 276–287. https://doi.org/10.1038/s41593-020-00764-7

Leschziner, A. E., & Reck-Peterson, S. L. (2021). Structural Biology of <scp>LRRK2</scp> and its Interaction with Microtubules. *Movement Disorders*, *36*(11), 2494–2504. https://doi.org/10.1002/mds.28755

Lester, E., Ooi, F. K., Bakkar, N., Ayers, J., Woerman, A. L., Wheeler, J., Bowser, R., Carlson, G. A., Prusiner, S. B., & Parker, R. (2021). Tau aggregates are RNA-protein assemblies that mislocalize multiple nuclear speckle components. *Neuron*, *109*(10), 1675-1691.e9. https://doi.org/10.1016/j.neuron.2021.03.026

Li, D., & Wu, M. (2021). Pattern recognition receptors in health and diseases. *Signal Transduction and Targeted Therapy*, *6*(1), 291. https://doi.org/10.1038/s41392-021-00687-0

Li, Q., & Barres, B. A. (2018). Microglia and macrophages in brain homeostasis and disease. *Nature Reviews Immunology*, *18*(4), 225–242. https://doi.org/10.1038/nri.2017.125

Li, Q., Cheng, Z., Zhou, L., Darmanis, S., Neff, N. F., Okamoto, J., Gulati, G., Bennett, M. L., Sun, L. O., Clarke, L. E., Marschallinger, J., Yu, G., Quake, S. R., Wyss-Coray, T., & Barres, B. A. (2019). Developmental Heterogeneity of Microglia and Brain Myeloid Cells Revealed by Deep Single-Cell RNA Sequencing. *Neuron*, *101*(2), 207-223.e10. https://doi.org/10.1016/j.neuron.2018.12.006

Li, X., Kumar, Y., Zempel, H., Mandelkow, E.-M., Biernat, J., & Mandelkow, E. (2011). Novel diffusion barrier for axonal retention of Tau in neurons and its failure in neurodegeneration. *The EMBO Journal*, *30*(23), 4825–4837. https://doi.org/10.1038/emboj.2011.376

Li, Y., Liu, L., Barger, S. W., & Griffin, W. S. T. (2003). Interleukin-1 Mediates Pathological Effects of Microglia on Tau Phosphorylation and on Synaptophysin Synthesis in Cortical Neurons through a p38-MAPK Pathway. *The Journal of Neuroscience*, *23*(5), 1605–1611. https://doi.org/10.1523/JNEUROSCI.23-05-01605.2003

Li, Y., Paz Marzolo, M., van Kerkhof, P., Strous, G. J., & Bu, G. (2000). The YXXL Motif, but Not the Two NPXY Motifs, Serves as the Dominant Endocytosis Signal for Low

Density Lipoprotein Receptor-related Protein. *Journal of Biological Chemistry*, *275*(22), 17187–17194. https://doi.org/10.1074/jbc.M000490200

Liebl, D., & Griffiths, G. (2009). Transient assembly of F-actin by phagosomes delays phagosome fusion with lysosomes in cargo-overloaded macrophages. *Journal of Cell Science*, *122*(16), 2935–2945. https://doi.org/10.1242/jcs.048355

Liscovitch, N., & French, L. (2014). Differential Co-Expression between α-Synuclein and IFN-γ Signaling Genes across Development and in Parkinson's Disease. *PLoS ONE*, *9*(12), e115029. https://doi.org/10.1371/journal.pone.0115029

Liu, C., & Götz, J. (2013). Profiling Murine Tau with 0N, 1N and 2N Isoform-Specific Antibodies in Brain and Peripheral Organs Reveals Distinct Subcellular Localization, with the 1N Isoform Being Enriched in the Nucleus. *PLoS ONE*, *8*(12), e84849. https://doi.org/10.1371/journal.pone.0084849

Liu, L., Drouet, V., Wu, J. W., Witter, M. P., Small, S. A., Clelland, C., & Duff, K. (2012). Trans-Synaptic Spread of Tau Pathology In Vivo. *PLoS ONE*, *7*(2), e31302. https://doi.org/10.1371/journal.pone.0031302

Liu, S., Liu, Y., Hao, W., Wolf, L., Kiliaan, A. J., Penke, B., Rübe, C. E., Walter, J., Heneka, M. T., Hartmann, T., Menger, M. D., & Fassbender, K. (2012). TLR2 Is a Primary Receptor for Alzheimer's Amyloid β Peptide To Trigger Neuroinflammatory Activation. *The Journal of Immunology*, *188*(3), 1098–1107. https://doi.org/10.4049/jimmunol.1101121

Liu, S., Tobias, R., McClure, S., Styba, G., Shi, Q., & Jackowski, G. (1997). Removal of Endotoxin from Recombinant Protein Preparations. *Clinical Biochemistry*, *30*(6), 455–463. https://doi.org/10.1016/S0009-9120(97)00049-0

Liu, T., Zhang, L., Joo, D., & Sun, S.-C. (2017). NF-κB signaling in inflammation. *Signal Transduction and Targeted Therapy*, *2*(1), 17023. https://doi.org/10.1038/sigtrans.2017.23

Liu, Z., Xu, E., Zhao, H. T., Cole, T., & West, A. B. (2020). LRRK2 and Rab10 coordinate macropinocytosis to mediate immunological responses in phagocytes. *The EMBO Journal*, *39*(20). https://doi.org/10.15252/embj.2020104862

LoPresti, P., Szuchet, S., Papasozomenos, S. C., Zinkowski, R. P., & Binder, L. I. (1995). Functional implications for the microtubule-associated protein tau: localization in oligodendrocytes. *Proceedings of the National Academy of Sciences*, *92*(22), 10369–10373. https://doi.org/10.1073/pnas.92.22.10369

Lövestam, S., Koh, F. A., van Knippenberg, B., Kotecha, A., Murzin, A. G., Goedert, M., & Scheres, S. H. (2022). Assembly of recombinant tau into filaments identical to those of Alzheimer's disease and chronic traumatic encephalopathy. *ELife*, *11*. https://doi.org/10.7554/eLife.76494

Lu, M., & Kosik, K. S. (2001). Competition for Microtubule-binding with Dual Expression of Tau Missense and Splice Isoforms. *Molecular Biology of the Cell*, *12*(1), 171–184. https://doi.org/10.1091/mbc.12.1.171

Lu, Y.-C., Yeh, W.-C., & Ohashi, P. S. (2008). LPS/TLR4 signal transduction pathway. *Cytokine*, *42*(2), 145–151. https://doi.org/10.1016/j.cyto.2008.01.006

Luan, W., Li, M., Wu, C., Shen, X., & Sun, Z. (2022). Proteomic dissimilarities of primary microglia and BV2 cells under stimuli. *European Journal of Neuroscience*, *55*(7), 1709–1723. https://doi.org/10.1111/ejn.15637

Luciani, M., Montalbano, M., Troncone, L., Bacchin, C., Uchida, K., Daniele, G., Jacobs Wolf, B., Butler, H. M., Kiel, J., Berto, S., Gensemer, C., Moore, K., Morningstar, J., Diteepeng, T., Albayram, O., Abisambra, J. F., Norris, R. A., Di Salvo, T. G., Prosser, B., … del Monte, F. (2023). Big tau aggregation disrupts microtubule tyrosination and causes myocardial diastolic dysfunction: from discovery to therapy. *European Heart Journal*, *44*(17), 1560–1570. https://doi.org/10.1093/eurheartj/ehad205

Lue, Beach, & Walker. (2019). Alzheimer's Disease Research Using Human Microglia. *Cells*, *8*(8), 838. https://doi.org/10.3390/cells8080838

Lui, H., Zhang, J., Makinson, S. R., Cahill, M. K., Kelley, K. W., Huang, H.-Y., Shang, Y., Oldham, M. C., Martens, L. H., Gao, F., Coppola, G., Sloan, S. A., Hsieh, C. L., Kim, C. C., Bigio, E. H., Weintraub, S., Mesulam, M.-M., Rademakers, R., Mackenzie, I. R., … Huang, E. J. (2016). Progranulin Deficiency Promotes Circuit-Specific Synaptic Pruning by Microglia via Complement Activation. *Cell*, *165*(4), 921–935. https://doi.org/10.1016/j.cell.2016.04.001

Luo, L., Wall, A. A., Tong, S. J., Hung, Y., Xiao, Z., Tarique, A. A., Sly, P. D., Fantino, E., Marzolo, M.-P., & Stow, J. L. (2018). TLR Crosstalk Activates LRP1 to Recruit Rab8a and PI3Kγ for Suppression of Inflammatory Responses. *Cell Reports*, *24*(11), 3033–3044. https://doi.org/10.1016/j.celrep.2018.08.028

Luo, W., Liu, W., Hu, X., Hanna, M., Caravaca, A., & Paul, S. M. (2015). Microglial internalization and degradation of pathological tau is enhanced by an anti-tau monoclonal antibody. *Scientific Reports*, *5*(1), 11161. https://doi.org/10.1038/srep11161

Luzon-Toro, B., de la Torre, E. R., Delgado, A., Perez-Tur, J., & Hilfiker, S. (2007). Mechanistic insight into the dominant mode of the Parkinson's disease-associated G2019S LRRK2 mutation. *Human Molecular Genetics*, *16*(17), 2031–2039. https://doi.org/10.1093/hmg/ddm151

Mack, L., Brill, B., Delis, N., & Groner, B. (2014). Endotoxin depletion of recombinant protein preparations through their preferential binding to histidine tags. *Analytical Biochemistry*, *466*, 83–88. https://doi.org/10.1016/j.ab.2014.08.020

MacLeod, D., Dowman, J., Hammond, R., Leete, T., Inoue, K., & Abeliovich, A. (2006). The Familial Parkinsonism Gene LRRK2 Regulates Neurite Process Morphology. *Neuron*, *52*(4), 587–593. https://doi.org/10.1016/j.neuron.2006.10.008

Madureira, M., Connor-Robson, N., & Wade-Martins, R. (2020). "LRRK2: Autophagy and Lysosomal Activity." *Frontiers in Neuroscience*, *14*. https://doi.org/10.3389/fnins.2020.00498

Maekawa, T., Sasaoka, T., Azuma, S., Ichikawa, T., Melrose, H. L., Farrer, M. J., & Obata, F. (2016). Leucine-rich repeat kinase 2 (LRRK2) regulates α-synuclein clearance in microglia. *BMC Neuroscience*, *17*(1), 77. https://doi.org/10.1186/s12868-016-0315-2

Maes, M. E., Colombo, G., Schulz, R., & Siegert, S. (2019). Targeting microglia with lentivirus and AAV: Recent advances and remaining challenges. *Neuroscience Letters*, *707*, 134310. https://doi.org/10.1016/j.neulet.2019.134310

Maeshima, N., & Fernandez, R. C. (2013). Recognition of lipid A variants by the TLR4-MD-2 receptor complex. *Frontiers in Cellular and Infection Microbiology*, *3*. https://doi.org/10.3389/fcimb.2013.00003

Magalhães, P. O., Lopes, A. M., Mazzola, P. G., Rangel-Yagui, C., Penna, T. C. V, & Pessoa, A. (2007). Methods of endotoxin removal from biological preparations: a review. *Journal of Pharmacy & Pharmaceutical Sciences : A Publication of the Canadian Society for Pharmaceutical Sciences, Societe Canadienne Des Sciences Pharmaceutiques*, *10*(3), 388–404.

Majerova, P., Zilkova, M., Kazmerova, Z., Kovac, A., Paholikova, K., Kovacech, B., Zilka, N., & Novak, M. (2014). Microglia display modest phagocytic capacity for extracellular tau oligomers. *Journal of Neuroinflammation*, *11*(1), 161. https://doi.org/10.1186/s12974-014-0161-z

Malakhov, M. P., Mattern, M. R., Malakhova, O. A., Drinker, M., Weeks, S. D., & Butt, T. R. (2004). SUMO fusions and SUMO-specific protease for efficient expression and purification of proteins. *Journal of Structural and Functional Genomics*, *5*(1/2), 75–86. https://doi.org/10.1023/B:JSFG.0000029237.70316.52

Malpetti, M., Passamonti, L., Jones, P. S., Street, D., Rittman, T., Fryer, T. D., Hong, Y. T., Vàsquez Rodriguez, P., Bevan-Jones, W. R., Aigbirhio, F. I., O'Brien, J. T., & Rowe, J. B. (2021). Neuroinflammation predicts disease progression in progressive supranuclear palsy. *Journal of Neurology, Neurosurgery & Psychiatry*, *92*(7), 769–775. https://doi.org/10.1136/jnnp-2020-325549

Mamat, U., Wilke, K., Bramhill, D., Schromm, A. B., Lindner, B., Kohl, T. A., Corchero, J. L., Villaverde, A., Schaffer, L., Head, S. R., Souvignier, C., Meredith, T. C., & Woodard, R. W. (2015). Detoxifying Escherichia coli for endotoxin-free production of

recombinant proteins. *Microbial Cell Factories*, *14*(1), 57. https://doi.org/10.1186/s12934-015-0241-5

Mamat, U., Woodard, R. W., Wilke, K., Souvignier, C., Mead, D., Steinmetz, E., Terry, K., Kovacich, C., Zegers, A., & Knox, C. (2013). Endotoxin-free protein production—ClearColi™ technology. *Nature Methods*, *10*(9), 916–916. https://doi.org/10.1038/nmeth.f.367

Mancuso, R., Van Den Daele, J., Fattorelli, N., Wolfs, L., Balusu, S., Burton, O., Liston, A., Sierksma, A., Fourne, Y., Poovathingal, S., Arranz-Mendiguren, A., Sala Frigerio, C., Claes, C., Serneels, L., Theys, T., Perry, V. H., Verfaillie, C., Fiers, M., & De Strooper, B. (2019). Stem-cell-derived human microglia transplanted in mouse brain to study human disease. *Nature Neuroscience*, *22*(12), 2111–2116. https://doi.org/10.1038/s41593-019-0525-x

Mandelkow, E.-M., & Mandelkow, E. (2012). Biochemistry and Cell Biology of Tau Protein in Neurofibrillary Degeneration. *Cold Spring Harbor Perspectives in Medicine*, *2*(7), a006247–a006247. https://doi.org/10.1101/cshperspect.a006247

Manos, J. D., Preiss, C. N., Venkat, N., Tamm, J., Reinhardt, P., Kwon, T., Wu, J., Winter, A. D., Jahn, T. R., Yanamandra, K., Titterton, K., Karran, E., & Langlois, X. (2022). Uncovering specificity of endogenous TAU aggregation in a human iPSC-neuron TAU seeding model. *IScience*, *25*(1), 103658. https://doi.org/10.1016/j.isci.2021.103658

Mantovani, , Alberto, Sica, , Antonio, & Locati, M. (2005). Macrophage Polarization Comes of Age. *Immunity*, *23*(4), 344–346. https://doi.org/10.1016/j.immuni.2005.10.001

Manzoni, C., Mamais, A., Dihanich, S., McGoldrick, P., Devine, M. J., Zerle, J., Kara, E., Taanman, J.-W., Healy, D. G., Marti-Masso, J.-F., Schapira, A. H., Plun-Favreau, H., Tooze, S., Hardy, J., Bandopadhyay, R., & Lewis, P. A. (2013). Pathogenic Parkinson's disease mutations across the functional domains of LRRK2 alter the autophagic/lysosomal response to starvation. *Biochemical and Biophysical Research Communications*, *441*(4), 862–866. https://doi.org/10.1016/j.bbrc.2013.10.159

Maphis, N., Xu, G., Kokiko-Cochran, O. N., Jiang, S., Cardona, A., Ransohoff, R. M., Lamb, B. T., & Bhaskar, K. (2015). Reactive microglia drive tau pathology and contribute to the spreading of pathological tau in the brain. *Brain*, *138*(6), 1738–1755. https://doi.org/10.1093/brain/awv081

Marblestone, J. G. (2006). Comparison of SUMO fusion technology with traditional gene fusion systems: Enhanced expression and solubility with SUMO. *Protein Science*, *15*(1), 182–189. https://doi.org/10.1110/ps.051812706

Marciniak, E., Leboucher, A., Caron, E., Ahmed, T., Tailleux, A., Dumont, J., Issad, T., Gerhardt, E., Pagesy, P., Vileno, M., Bournonville, C., Hamdane, M., Bantubungi, K., Lancel, S., Demeyer, D., Eddarkaoui, S., Vallez, E., Vieau, D., Humez, S., … Blum,

D. (2017). Tau deletion promotes brain insulin resistance. *Journal of Experimental Medicine*, *214*(8), 2257–2269. https://doi.org/10.1084/jem.20161731

Marín-Teva, J. L., Dusart, I., Colin, C., Gervais, A., van Rooijen, N., & Mallat, M. (2004). Microglia Promote the Death of Developing Purkinje Cells. *Neuron*, *41*(4), 535–547. https://doi.org/10.1016/S0896-6273(04)00069-8

Marker, D. F., Puccini, J. M., Mockus, T. E., Barbieri, J., Lu, S.-M., & Gelbard, H. A. (2012). LRRK2 kinase inhibition prevents pathological microglial phagocytosis in response to HIV-1 Tat protein. *Journal of Neuroinflammation*, *9*(1), 752. https://doi.org/10.1186/1742-2094-9-261

Marschallinger, J., Iram, T., Zardeneta, M., Lee, S. E., Lehallier, B., Haney, M. S., Pluvinage, J. V., Mathur, V., Hahn, O., Morgens, D. W., Kim, J., Tevini, J., Felder, T. K., Wolinski, H., Bertozzi, C. R., Bassik, M. C., Aigner, L., & Wyss-Coray, T. (2020a). Lipid-droplet-accumulating microglia represent a dysfunctional and proinflammatory state in the aging brain. *Nature Neuroscience*, *23*(2), 194–208. https://doi.org/10.1038/s41593-019-0566-1

Marschallinger, J., Iram, T., Zardeneta, M., Lee, S. E., Lehallier, B., Haney, M. S., Pluvinage, J. V., Mathur, V., Hahn, O., Morgens, D. W., Kim, J., Tevini, J., Felder, T. K., Wolinski, H., Bertozzi, C. R., Bassik, M. C., Aigner, L., & Wyss-Coray, T. (2020b). Lipid-droplet-accumulating microglia represent a dysfunctional and proinflammatory state in the aging brain. *Nature Neuroscience*, *23*(2), 194–208. https://doi.org/10.1038/s41593-019-0566-1

Martinez, F. O., & Gordon, S. (2014). The M1 and M2 paradigm of macrophage activation: time for reassessment. *F1000Prime Reports*, *6*. https://doi.org/10.12703/P6-13

Martini-Stoica, H., Cole, A. L., Swartzlander, D. B., Chen, F., Wan, Y.-W., Bajaj, L., Bader, D. A., Lee, V. M. Y., Trojanowski, J. Q., Liu, Z., Sardiello, M., & Zheng, H. (2018). TFEB enhances astroglial uptake of extracellular tau species and reduces tau spreading. *Journal of Experimental Medicine*, *215*(9), 2355–2377. https://doi.org/10.1084/jem.20172158

Marwaha, R., & Sharma, M. (2017). DQ-Red BSA Trafficking Assay in Cultured Cells to Assess Cargo Delivery to Lysosomes. *BIO-PROTOCOL*, *7*(19). https://doi.org/10.21769/BioProtoc.2571

Masuda, T., Sankowski, R., Staszewski, O., Böttcher, C., Amann, L., Sagar, Scheiwe, C., Nessler, S., Kunz, P., van Loo, G., Coenen, V. A., Reinacher, P. C., Michel, A., Sure, U., Gold, R., Grün, D., Priller, J., Stadelmann, C., & Prinz, M. (2019). Spatial and temporal heterogeneity of mouse and human microglia at single-cell resolution. *Nature*, *566*(7744), 388–392. https://doi.org/10.1038/s41586-019-0924-x

Mathys, H., Davila-Velderrain, J., Peng, Z., Gao, F., Mohammadi, S., Young, J. Z., Menon, M., He, L., Abdurrob, F., Jiang, X., Martorell, A. J., Ransohoff, R. M., Hafler, B. P., Bennett, D. A., Kellis, M., & Tsai, L.-H. (2019). Single-cell transcriptomic analysis of Alzheimer's disease. *Nature*, *570*(7761), 332–337. https://doi.org/10.1038/s41586-019-1195-2

McNamara, N. B., Munro, D. A. D., Bestard-Cuche, N., Uyeda, A., Bogie, J. F. J., Hoffmann, A., Holloway, R. K., Molina-Gonzalez, I., Askew, K. E., Mitchell, S., Mungall, W., Dodds, M., Dittmayer, C., Moss, J., Rose, J., Szymkowiak, S., Amann, L., McColl, B. W., Prinz, M., … Miron, V. E. (2023). Microglia regulate central nervous system myelin growth and integrity. *Nature*, *613*(7942), 120–129. https://doi.org/10.1038/s41586-022-05534-y

Metrick, M. A., Ferreira, N. do C., Saijo, E., Kraus, A., Newell, K., Zanusso, G., Vendruscolo, M., Ghetti, B., & Caughey, B. (2020a). A single ultrasensitive assay for detection and discrimination of tau aggregates of Alzheimer and Pick diseases. *Acta Neuropathologica Communications*, *8*(1), 22. https://doi.org/10.1186/s40478-020-0887-z

Metrick, M. A., Ferreira, N. do C., Saijo, E., Kraus, A., Newell, K., Zanusso, G., Vendruscolo, M., Ghetti, B., & Caughey, B. (2020b). A single ultrasensitive assay for detection and discrimination of tau aggregates of Alzheimer and Pick diseases. *Acta Neuropathologica Communications*, *8*(1), 22. https://doi.org/10.1186/s40478-020-0887-z

Michel, C. H., Kumar, S., Pinotsi, D., Tunnacliffe, A., St. George-Hyslop, P., Mandelkow, E., Mandelkow, E.-M., Kaminski, C. F., & Kaminski Schierle, G. S. (2014). Extracellular Monomeric Tau Protein Is Sufficient to Initiate the Spread of Tau Protein Pathology. *Journal of Biological Chemistry*, *289*(2), 956–967. https://doi.org/10.1074/jbc.M113.515445

Minett, T., Classey, J., Matthews, F. E., Fahrenhold, M., Taga, M., Brayne, C., Ince, P. G., Nicoll, J. A. R., & Boche, D. (2016). Microglial immunophenotype in dementia with Alzheimer's pathology. *Journal of Neuroinflammation*, *13*(1), 135. https://doi.org/10.1186/s12974-016-0601-z

Miyamoto, A., Wake, H., Ishikawa, A. W., Eto, K., Shibata, K., Murakoshi, H., Koizumi, S., Moorhouse, A. J., Yoshimura, Y., & Nabekura, J. (2016). Microglia contact induces synapse formation in developing somatosensory cortex. *Nature Communications*, *7*(1), 12540. https://doi.org/10.1038/ncomms12540

Miyamoto, T., Okano, S., & Kasai, N. (2009). Inactivation of *Escherichia coli* Endotoxin by Soft Hydrothermal Processing. *Applied and Environmental Microbiology*, *75*(15), 5058–5063. https://doi.org/10.1128/AEM.00122-09

Miyoshi, E., Bilousova, T., Melnik, M., Fakhrutdinov, D., Poon, W. W., Vinters, H. V., Miller, C. A., Corrada, M., Kawas, C., Bohannan, R., Caraway, C., Elias, C., Maina, K. N., Campagna, J. J., John, V., & Gylys, K. H. (2021). Exosomal tau with seeding activity is released from Alzheimer's disease synapses, and seeding potential is associated with amyloid beta. *Laboratory Investigation*, *101*(12), 1605–1617. https://doi.org/10.1038/s41374-021-00644-z

Mizee, M. R., Miedema, S. S. M., van der Poel, M., Adelia, Schuurman, K. G., van Strien, M. E., Melief, J., Smolders, J., Hendrickx, D. A., Heutinck, K. M., Hamann, J., & Huitinga, I. (2017). Isolation of primary microglia from the human post-mortem brain: effects of ante- and post-mortem variables. *Acta Neuropathologica Communications*, *5*(1), 16. https://doi.org/10.1186/s40478-017-0418-8

Mocanu, M.-M., Nissen, A., Eckermann, K., Khlistunova, I., Biernat, J., Drexler, D., Petrova, O., Schönig, K., Bujard, H., Mandelkow, E., Zhou, L., Rune, G., & Mandelkow, E.-M. (2008). The Potential for β-Structure in the Repeat Domain of Tau Protein Determines Aggregation, Synaptic Decay, Neuronal Loss, and Coassembly with Endogenous Tau in Inducible Mouse Models of Tauopathy. *The Journal of Neuroscience*, *28*(3), 737–748. https://doi.org/10.1523/JNEUROSCI.2824-07.2008

Moehle, M. S., Daher, J. P. L., Hull, T. D., Boddu, R., Abdelmotilib, H. A., Mobley, J., Kannarkat, G. T., Tansey, M. G., & West, A. B. (2015). The G2019S LRRK2 mutation increases myeloid cell chemotactic responses and enhances LRRK2 binding to actin-regulatory proteins. *Human Molecular Genetics*, *24*(15), 4250–4267. https://doi.org/10.1093/hmg/ddv157

Mogi, M., Kondo, T., Mizuno, Y., & Nagatsu, T. (2007). p53 protein, interferon-γ, and NF-κB levels are elevated in the parkinsonian brain. *Neuroscience Letters*, *414*(1), 94–97. https://doi.org/10.1016/j.neulet.2006.12.003

Monier, A., Adle-Biassette, H., Delezoide, A.-L., Evrard, P., Gressens, P., & Verney, C. (2007). Entry and Distribution of Microglial Cells in Human Embryonic and Fetal Cerebral Cortex. *Journal of Neuropathology and Experimental Neurology*, *66*(5), 372–382. https://doi.org/10.1097/nen.0b013e3180517b46

Morita, T., & Sobue, K. (2009). Specification of Neuronal Polarity Regulated by Local Translation of CRMP2 and Tau via the mTOR-p70S6K Pathway. *Journal of Biological Chemistry*, *284*(40), 27734–27745. https://doi.org/10.1074/jbc.M109.008177

Morozova, O. A., March, Z. M., Robinson, A. S., & Colby, D. W. (2013). Conformational Features of Tau Fibrils from Alzheimer's Disease Brain Are Faithfully Propagated by Unmodified Recombinant Protein. *Biochemistry*, *52*(40), 6960–6967. https://doi.org/10.1021/bi400866w

Morrison, M., Klein, C., Clemann, N., Collier, D. A., Hardy, J., Heiβerer, B., Cader, M. Z., Graf, M., & Kaye, J. (2015). StemBANCC: Governing Access to Material and Data in a Large Stem Cell Research Consortium. *Stem Cell Reviews and Reports*, *11*(5), 681–687. https://doi.org/10.1007/s12015-015-9599-3

Mosiman, V. L., Patterson, B. K., Canterero, L., & Goolsby, C. L. (1997). Reducing cellular autofluorescence in flow cytometry: an in situ method. *Cytometry*, *30*(3), 151–156.

Mosser, D. M. (2003). The many faces of macrophage activation. *Journal of Leukocyte Biology*, *73*(2), 209–212. https://doi.org/10.1189/jlb.0602325

Mount, M. P., Lira, A., Grimes, D., Smith, P. D., Faucher, S., Slack, R., Anisman, H., Hayley, S., & Park, D. S. (2007). Involvement of Interferon-γ in Microglial-Mediated Loss of Dopaminergic Neurons. *The Journal of Neuroscience*, *27*(12), 3328–3337. https://doi.org/10.1523/JNEUROSCI.5321-06.2007

Moussaud, S., Jones, D. R., Moussaud-Lamodière, E. L., Delenclos, M., Ross, O. A., & McLean, P. J. (2014). Alpha-synuclein and tau: teammates in neurodegeneration? *Molecular Neurodegeneration*, *9*(1), 43. https://doi.org/10.1186/1750-1326-9-43

Moyes, K. W., Lieberman, N. A. P., Kreuser, S. A., Chinn, H., Winter, C., Deutsch, G., Hoglund, V., Watson, R., & Crane, C. A. (2017). Genetically Engineered Macrophages: A Potential Platform for Cancer Immunotherapy. *Human Gene Therapy*, *28*(2), 200–215. https://doi.org/10.1089/hum.2016.060

Mudher, A., Colin, M., Dujardin, S., Medina, M., Dewachter, I., Alavi Naini, S. M., Mandelkow, E.-M., Mandelkow, E., Buée, L., Goedert, M., & Brion, J.-P. (2017). What is the evidence that tau pathology spreads through prion-like propagation? *Acta Neuropathologica Communications*, *5*(1), 99. https://doi.org/10.1186/s40478-017-0488-7

Mukherjee, S., Ghosh, R. N., & Maxfield, F. R. (1997). Endocytosis. *Physiological Reviews*, *77*(3), 759–803. https://doi.org/10.1152/physrev.1997.77.3.759

Mukrasch, M. D., Bibow, S., Korukottu, J., Jeganathan, S., Biernat, J., Griesinger, C., Mandelkow, E., & Zweckstetter, M. (2009). Structural Polymorphism of 441-Residue Tau at Single Residue Resolution. *PLoS Biology*, *7*(2), e1000034. https://doi.org/10.1371/journal.pbio.1000034

Mukrasch, M. D., Biernat, J., von Bergen, M., Griesinger, C., Mandelkow, E., & Zweckstetter, M. (2005a). Sites of Tau Important for Aggregation Populate β-Structure and Bind to Microtubules and Polyanions. *Journal of Biological Chemistry*, *280*(26), 24978–24986. https://doi.org/10.1074/jbc.M501565200

Mukrasch, M. D., Biernat, J., von Bergen, M., Griesinger, C., Mandelkow, E., & Zweckstetter, M. (2005b). Sites of Tau Important for Aggregation Populate β-Structure

and Bind to Microtubules and Polyanions. *Journal of Biological Chemistry*, *280*(26), 24978–24986. https://doi.org/10.1074/jbc.M501565200

Murby, M., Uhlén, M., & Ståhl, S. (1996). Upstream Strategies to Minimize Proteolytic Degradation upon Recombinant Production inEscherichia coli. *Protein Expression and Purification*, *7*(2), 129–136. https://doi.org/10.1006/prep.1996.0018

Nakano, M., Riku, Y., Nishioka, K., Hasegawa, M., Washimi, Y., Arahata, Y., Takeda, A., Horibe, K., Yamaoka, A., Suzuki, K., Tsujimoto, M., Li, Y., Yoshino, H., Hattori, N., Akagi, A., Miyahara, H., Iwasaki, Y., & Yoshida, M. (2020). Unclassified four-repeat tauopathy associated with familial parkinsonism and progressive respiratory failure. *Acta Neuropathologica Communications*, *8*(1), 148. https://doi.org/10.1186/s40478-020-01025-1

Nakata, T., & Hirokawa, N. (2003). Microtubules provide directional cues for polarized axonal transport through interaction with kinesin motor head. *The Journal of Cell Biology*, *162*(6), 1045–1055. https://doi.org/10.1083/jcb.200302175

Nalls, M. A., Blauwendraat, C., Vallerga, C. L., Heilbron, K., Bandres-Ciga, S., Chang, D., Tan, M., Kia, D. A., Noyce, A. J., Xue, A., Bras, J., Young, E., von Coelln, R., Simón-Sánchez, J., Schulte, C., Sharma, M., Krohn, L., Pihlstrøm, L., Siitonen, A., … Zhang, F. (2019). Identification of novel risk loci, causal insights, and heritable risk for Parkinson's disease: a meta-analysis of genome-wide association studies. *The Lancet Neurology*, *18*(12), 1091–1102. https://doi.org/10.1016/S1474-4422(19)30320-5

Nalls, M. A., Pankratz, N., Lill, C. M., Do, C. B., Hernandez, D. G., Saad, M., DeStefano, A. L., Kara, E., Bras, J., Sharma, M., Schulte, C., Keller, M. F., Arepalli, S., Letson, C., Edsall, C., Stefansson, H., Liu, X., Pliner, H., Lee, J. H., … Singleton, A. B. (2014a). Large-scale meta-analysis of genome-wide association data identifies six new risk loci for Parkinson's disease. *Nature Genetics*, *46*(9), 989–993. https://doi.org/10.1038/ng.3043

Nalls, M. A., Pankratz, N., Lill, C. M., Do, C. B., Hernandez, D. G., Saad, M., DeStefano, A. L., Kara, E., Bras, J., Sharma, M., Schulte, C., Keller, M. F., Arepalli, S., Letson, C., Edsall, C., Stefansson, H., Liu, X., Pliner, H., Lee, J. H., … Singleton, A. B. (2014b). Large-scale meta-analysis of genome-wide association data identifies six new risk loci for Parkinson's disease. *Nature Genetics*, *46*(9), 989–993. https://doi.org/10.1038/ng.3043

Narasimhan, S., Guo, J. L., Changolkar, L., Stieber, A., McBride, J. D., Silva, L. V., He, Z., Zhang, B., Gathagan, R. J., Trojanowski, J. Q., & Lee, V. M. Y. (2017a). Pathological Tau Strains from Human Brains Recapitulate the Diversity of Tauopathies in

Nontransgenic Mouse Brain. *The Journal of Neuroscience*, *37*(47), 11406–11423. https://doi.org/10.1523/JNEUROSCI.1230-17.2017

Narasimhan, S., Guo, J. L., Changolkar, L., Stieber, A., McBride, J. D., Silva, L. V., He, Z., Zhang, B., Gathagan, R. J., Trojanowski, J. Q., & Lee, V. M. Y. (2017b). Pathological Tau Strains from Human Brains Recapitulate the Diversity of Tauopathies in Nontransgenic Mouse Brain. *The Journal of Neuroscience*, *37*(47), 11406–11423. https://doi.org/10.1523/JNEUROSCI.1230-17.2017

Navarro-Guerrero, E., Tay, C., Whalley, J. P., Cowley, S. A., Davies, B., Knight, J. C., & Ebner, D. (2021). Genome-wide CRISPR/Cas9-knockout in human induced Pluripotent Stem Cell (iPSC)-derived macrophages. *Scientific Reports*, *11*(1), 4245. https://doi.org/10.1038/s41598-021-82137-z

Nègre, D., Mangeot, P.-E., Duisit, G., Blanchard, S., Vidalain, P.-O., Leissner, P., Winter, A.-J., Rabourdin-Combe, C., Mehtali, M., Moullier, P., Darlix, J.-L., & Cosset, F.-L. (2000). Characterization of novel safe lentiviral vectors derived from simian immunodeficiency virus (SIVmac251) that efficiently transduce mature human dendritic cells. *Gene Therapy*, *7*(19), 1613–1623. https://doi.org/10.1038/sj.gt.3301292

Neve, R. L., Harris, P., Kosik, K. S., Kurnit, D. M., & Donlon, T. A. (1986). Identification of cDNA clones for the human microtubule-associated protein tau and chromosomal localization of the genes for tau and microtubule-associated protein 2. *Molecular Brain Research*, *1*(3), 271–280. https://doi.org/10.1016/0169-328X(86)90033-1

Nguyen, A. P. T., Daniel, G., Valdés, P., Islam, M. S., Schneider, B. L., & Moore, D. J. (2018). G2019S LRRK2 enhances the neuronal transmission of tau in the mouse brain. *Human Molecular Genetics*, *27*(1), 120–134. https://doi.org/10.1093/hmg/ddx389

Nimmerjahn, A., Kirchhoff, F., & Helmchen, F. (2005). Resting Microglial Cells Are Highly Dynamic Surveillants of Brain Parenchyma in Vivo. *Science*, *308*(5726), 1314–1318. https://doi.org/10.1126/science.1110647

Noble, W., Garwood, C., Stephenson, J., Kinsey, A. M., Hanger, D. P., & Anderton, B. H. (2009). Minocycline reduces the development of abnormal tau species in models of Alzheimer's disease. *The FASEB Journal*, *23*(3), 739–750. https://doi.org/10.1096/fj.08-113795

Nonaka, T., Watanabe, S. T., Iwatsubo, T., & Hasegawa, M. (2010). Seeded Aggregation and Toxicity of α-Synuclein and Tau. *Journal of Biological Chemistry*, *285*(45), 34885–34898. https://doi.org/10.1074/jbc.M110.148460

Nott, A., Holtman, I. R., Coufal, N. G., Schlachetzki, J. C. M., Yu, M., Hu, R., Han, C. Z., Pena, M., Xiao, J., Wu, Y., Keulen, Z., Pasillas, M. P., O'Connor, C., Nickl, C. K.,

Schafer, S. T., Shen, Z., Rissman, R. A., Brewer, J. B., Gosselin, D., … Glass, C. K. (2019). Brain cell type–specific enhancer–promoter interactome maps and disease-risk association. *Science*, *366*(6469), 1134–1139. https://doi.org/10.1126/science.aay0793

Oakley, D. H., Klickstein, N., Commins, C., Chung, M., Dujardin, S., Bennett, R. E., Hyman, B. T., & Frosch, M. P. (2021). Continuous Monitoring of Tau-Induced Neurotoxicity in Patient-Derived iPSC-Neurons. *The Journal of Neuroscience*, *41*(19), 4335–4348. https://doi.org/10.1523/JNEUROSCI.2590-20.2021

Obergasteiger, J., Frapporti, G., Lamonaca, G., Pizzi, S., Picard, A., Lavdas, A. A., Pischedda, F., Piccoli, G., Hilfiker, S., Lobbestael, E., Baekelandt, V., Hicks, A. A., Corti, C., Pramstaller, P. P., & Volta, M. (2020). Kinase inhibition of G2019S-LRRK2 enhances autolysosome formation and function to reduce endogenous alpha-synuclein intracellular inclusions. *Cell Death Discovery*, *6*(1), 45. https://doi.org/10.1038/s41420-020-0279-y

Odfalk, K. F., Bieniek, K. F., & Hopp, S. C. (2022). Microglia: Friend and foe in tauopathy. *Progress in Neurobiology*, *216*, 102306. https://doi.org/10.1016/j.pneurobio.2022.102306

Olah, M., Patrick, E., Villani, A.-C., Xu, J., White, C. C., Ryan, K. J., Piehowski, P., Kapasi, A., Nejad, P., Cimpean, M., Connor, S., Yung, C. J., Frangieh, M., McHenry, A., Elyaman, W., Petyuk, V., Schneider, J. A., Bennett, D. A., De Jager, P. L., & Bradshaw, E. M. (2018a). A transcriptomic atlas of aged human microglia. *Nature Communications*, *9*(1), 539. https://doi.org/10.1038/s41467-018-02926-5

Olah, M., Patrick, E., Villani, A.-C., Xu, J., White, C. C., Ryan, K. J., Piehowski, P., Kapasi, A., Nejad, P., Cimpean, M., Connor, S., Yung, C. J., Frangieh, M., McHenry, A., Elyaman, W., Petyuk, V., Schneider, J. A., Bennett, D. A., De Jager, P. L., & Bradshaw, E. M. (2018b). A transcriptomic atlas of aged human microglia. *Nature Communications*, *9*(1), 539. https://doi.org/10.1038/s41467-018-02926-5

Ongkudon, C. M., Chew, J. H., Liu, B., & Danquah, M. K. (2012). Chromatographic Removal of Endotoxins: A Bioprocess Engineer's Perspective. *ISRN Chromatography*, *2012*, 1–9. https://doi.org/10.5402/2012/649746

Ossenkoppele, R., Schonhaut, D. R., Schöll, M., Lockhart, S. N., Ayakta, N., Baker, S. L., O'Neil, J. P., Janabi, M., Lazaris, A., Cantwell, A., Vogel, J., Santos, M., Miller, Z. A., Bettcher, B. M., Vossel, K. A., Kramer, J. H., Gorno-Tempini, M. L., Miller, B. L., Jagust, W. J., & Rabinovici, G. D. (2016). Tau PET patterns mirror clinical and neuroanatomical variability in Alzheimer's disease. *Brain*, *139*(5), 1551–1567. https://doi.org/10.1093/brain/aww027

Padmanabhan, P., Martínez-Mármol, R., Xia, D., Götz, J., & Meunier, F. A. (2019). Frontotemporal dementia mutant Tau promotes aberrant Fyn nanoclustering in hippocampal dendritic spines. *ELife*, *8*. https://doi.org/10.7554/eLife.45040

Paisán-Ruíz, C., Jain, S., Evans, E. W., Gilks, W. P., Simón, J., van der Brug, M., de Munain, A. L., Aparicio, S., Gil, A. M., Khan, N., Johnson, J., Martinez, J. R., Nicholl, D., Carrera, I. M., Peňa, A. S., de Silva, R., Lees, A., Martí-Massó, J. F., Pérez-Tur, J., … Singleton, A. B. (2004). Cloning of the Gene Containing Mutations that Cause PARK8-Linked Parkinson's Disease. *Neuron*, *44*(4), 595–600. https://doi.org/10.1016/j.neuron.2004.10.023

Palis, J., Robertson, S., Kennedy, M., Wall, C., & Keller, G. (1999). Development of erythroid and myeloid progenitors in the yolk sac and embryo proper of the mouse. *Development*, *126*(22), 5073–5084. https://doi.org/10.1242/dev.126.22.5073

Pallas-Bazarra, N., Draffin, J., Cuadros, R., Antonio Esteban, J., & Avila, J. (2019). Tau is required for the function of extrasynaptic NMDA receptors. *Scientific Reports*, *9*(1), 9116. https://doi.org/10.1038/s41598-019-45547-8

Pallas-Bazarra, N., Jurado-Arjona, J., Navarrete, M., Esteban, J. A., Hernández, F., Ávila, J., & Llorens-Martín, M. (2016). Novel function of Tau in regulating the effects of external stimuli on adult hippocampal neurogenesis. *The EMBO Journal*, *35*(13), 1417–1436. https://doi.org/10.15252/embj.201593518

Pampuscenko, K., Morkuniene, R., Krasauskas, L., Smirnovas, V., Tomita, T., & Borutaite, V. (2021). Distinct Neurotoxic Effects of Extracellular Tau Species in Primary Neuronal-Glial Cultures. *Molecular Neurobiology*, *58*(2), 658–667. https://doi.org/10.1007/s12035-020-02150-7

Pampuscenko, K., Morkuniene, R., Sneideris, T., Smirnovas, V., Budvytyte, R., Valincius, G., Brown, G. C., & Borutaite, V. (2020). Extracellular tau induces microglial phagocytosis of living neurons in cell cultures. *Journal of Neurochemistry*, *154*(3), 316–329. https://doi.org/10.1111/jnc.14940

Pan, K. M., Baldwin, M., Nguyen, J., Gasset, M., Serban, A., Groth, D., Mehlhorn, I., Huang, Z., Fletterick, R. J., & Cohen, F. E. (1993). Conversion of alpha-helices into beta-sheets features in the formation of the scrapie prion proteins. *Proceedings of the National Academy of Sciences*, *90*(23), 10962–10966. https://doi.org/10.1073/pnas.90.23.10962

Pan, L., Meng, L., He, M., & Zhang, Z. (2021). Tau in the Pathophysiology of Parkinson's Disease. *Journal of Molecular Neuroscience*, *71*(11), 2179–2191. https://doi.org/10.1007/s12031-020-01776-5

Panagiotakopoulou, V., Ivanyuk, D., De Cicco, S., Haq, W., Arsić, A., Yu, C., Messelodi, D., Oldrati, M., Schöndorf, D. C., Perez, M.-J., Cassatella, R. P., Jakobi, M.,

Schneiderhan-Marra, N., Gasser, T., Nikić-Spiegel, I., & Deleidi, M. (2020). Interferon-γ signaling synergizes with LRRK2 in neurons and microglia derived from human induced pluripotent stem cells. *Nature Communications*, *11*(1), 5163. https://doi.org/10.1038/s41467-020-18755-4

Paolicelli, R. C., Bolasco, G., Pagani, F., Maggi, L., Scianni, M., Panzanelli, P., Giustetto, M., Ferreira, T. A., Guiducci, E., Dumas, L., Ragozzino, D., & Gross, C. T. (2011). Synaptic Pruning by Microglia Is Necessary for Normal Brain Development. *Science*, *333*(6048), 1456–1458. https://doi.org/10.1126/science.1202529

Paolicelli, R. C., Sierra, A., Stevens, B., Tremblay, M.-E., Aguzzi, A., Ajami, B., Amit, I., Audinat, E., Bechmann, I., Bennett, M., Bennett, F., Bessis, A., Biber, K., Bilbo, S., Blurton-Jones, M., Boddeke, E., Brites, D., Brône, B., Brown, G. C., … Wyss-Coray, T. (2022). Microglia states and nomenclature: A field at its crossroads. *Neuron*, *110*(21), 3458–3483. https://doi.org/10.1016/j.neuron.2022.10.020

Parachikova, A., Agadjanyan, M. G., Cribbs, D. H., Blurton-Jones, M., Perreau, V., Rogers, J., Beach, T. G., & Cotman, C. W. (2007). Inflammatory changes parallel the early stages of Alzheimer disease. *Neurobiology of Aging*, *28*(12), 1821–1833. https://doi.org/10.1016/j.neurobiolaging.2006.08.014

Park, B. S., & Lee, J.-O. (2013). Recognition of lipopolysaccharide pattern by TLR4 complexes. *Experimental & Molecular Medicine*, *45*(12), e66–e66. https://doi.org/10.1038/emm.2013.97

Park, I.-H., Arora, N., Huo, H., Maherali, N., Ahfeldt, T., Shimamura, A., Lensch, M. W., Cowan, C., Hochedlinger, K., & Daley, G. Q. (2008). Disease-Specific Induced Pluripotent Stem Cells. *Cell*, *134*(5), 877–886. https://doi.org/10.1016/j.cell.2008.07.041

Park, T. I.-H., Smyth, L. C. D., Aalderink, M., Woolf, Z. R., Rustenhoven, J., Lee, K., Jansson, D., Smith, A., Feng, S., Correia, J., Heppner, P., Schweder, P., Mee, E., & Dragunow, M. (2022). Routine culture and study of adult human brain cells from neurosurgical specimens. *Nature Protocols*, *17*(2), 190–221. https://doi.org/10.1038/s41596-021-00637-8

Parkhurst, C. N., Yang, G., Ninan, I., Savas, J. N., Yates, J. R., Lafaille, J. J., Hempstead, B. L., Littman, D. R., & Gan, W.-B. (2013). Microglia Promote Learning-Dependent Synapse Formation through Brain-Derived Neurotrophic Factor. *Cell*, *155*(7), 1596–1609. https://doi.org/10.1016/j.cell.2013.11.030

Pascoal, T. A., Benedet, A. L., Ashton, N. J., Kang, M. S., Therriault, J., Chamoun, M., Savard, M., Lussier, F. Z., Tissot, C., Karikari, T. K., Ottoy, J., Mathotaarachchi, S., Stevenson, J., Massarweh, G., Schöll, M., de Leon, M. J., Soucy, J.-P., Edison, P., Blennow, K., … Rosa-Neto, P. (2021). Microglial activation and tau propagate jointly

across Braak stages. *Nature Medicine*, *27*(9), 1592–1599. https://doi.org/10.1038/s41591-021-01456-w

Pauwels, A.-M., Trost, M., Beyaert, R., & Hoffmann, E. (2017). Patterns, Receptors, and Signals: Regulation of Phagosome Maturation. *Trends in Immunology*, *38*(6), 407–422. https://doi.org/10.1016/j.it.2017.03.006

Peeraer, E., Bottelbergs, A., Van Kolen, K., Stancu, I.-C., Vasconcelos, B., Mahieu, M., Duytschaever, H., Ver Donck, L., Torremans, A., Sluydts, E., Van Acker, N., Kemp, J. A., Mercken, M., Brunden, K. R., Trojanowski, J. Q., Dewachter, I., Lee, V. M. Y., & Moechars, D. (2015). Intracerebral injection of preformed synthetic tau fibrils initiates widespread tauopathy and neuronal loss in the brains of tau transgenic mice. *Neurobiology of Disease*, *73*, 83–95. https://doi.org/10.1016/j.nbd.2014.08.032

Pei, G., Repnik, U., Griffiths, G., & Gutierrez, M. G. (2014). Identification of an immune regulated phagosomal Rab cascade in macrophages. *Journal of Cell Science*. https://doi.org/10.1242/jcs.144923

Penney, J., Ralvenius, W. T., & Tsai, L.-H. (2020). Modeling Alzheimer's disease with iPSC-derived brain cells. *Molecular Psychiatry*, *25*(1), 148–167. https://doi.org/10.1038/s41380-019-0468-3

Perea, J. R., Bolós, M., Cuadros, R., García, E., García-Escudero, V., Hernández, F., McManus, R. M., Heneka, M. T., & Avila, J. (2022). p38 Inhibition Decreases Tau Toxicity in Microglia and Improves Their Phagocytic Function. *Molecular Neurobiology*, *59*(3), 1632–1648. https://doi.org/10.1007/s12035-021-02715-0

Perea, J. R., López, E., Díez-Ballesteros, J. C., Ávila, J., Hernández, F., & Bolós, M. (2019). Extracellular Monomeric Tau Is Internalized by Astrocytes. *Frontiers in Neuroscience*, *13*. https://doi.org/10.3389/fnins.2019.00442

Pereira, J. B., Janelidze, S., Strandberg, O., Whelan, C. D., Zetterberg, H., Blennow, K., Palmqvist, S., Stomrud, E., Mattsson-Carlgren, N., & Hansson, O. (2022). Microglial activation protects against accumulation of tau aggregates in nondemented individuals with underlying Alzheimer's disease pathology. *Nature Aging*, *2*(12), 1138–1144. https://doi.org/10.1038/s43587-022-00310-z

Pérez, M., Valpuesta, J. M., Medina, M., Montejo de Garcini, E., & Avila, J. (2002). Polymerization of τ into Filaments in the Presence of Heparin: The Minimal Sequence Required for τ - τ Interaction. *Journal of Neurochemistry*, *67*(3), 1183–1190. https://doi.org/10.1046/j.1471-4159.1996.67031183.x

Perez-Nievas, B. G., Stein, T. D., Tai, H.-C., Dols-Icardo, O., Scotton, T. C., Barroeta-Espar, I., Fernandez-Carballo, L., de Munain, E. L., Perez, J., Marquie, M., Serrano-Pozo, A., Frosch, M. P., Lowe, V., Parisi, J. E., Petersen, R. C., Ikonomovic, M. D., López, O. L., Klunk, W., Hyman, B. T., & Gómez-Isla, T. (2013). Dissecting phenotypic

traits linked to human resilience to Alzheimer's pathology. *Brain*, *136*(8), 2510–2526. https://doi.org/10.1093/brain/awt171

Peri, F., & Nüsslein-Volhard, C. (2008). Live Imaging of Neuronal Degradation by Microglia Reveals a Role for v0-ATPase a1 in Phagosomal Fusion In Vivo. *Cell*, *133*(5), 916–927. https://doi.org/10.1016/j.cell.2008.04.037

Petsch, D. (2000). Endotoxin removal from protein solutions. *Journal of Biotechnology*, *76*(2–3), 97–119. https://doi.org/10.1016/S0168-1656(99)00185-6

Petsch, D., Deckwer, W.-D., & Anspach, F. B. (1998). Proteinase K Digestion of Proteins Improves Detection of Bacterial Endotoxins by theLimulusAmebocyte Lysate Assay: Application for Endotoxin Removal from Cationic Proteins. *Analytical Biochemistry*, *259*(1), 42–47. https://doi.org/10.1006/abio.1998.2655

Pfeffer, S. R. (2017). Rab GTPases: master regulators that establish the secretory and endocytic pathways. *Molecular Biology of the Cell*, *28*(6), 712–715. https://doi.org/10.1091/mbc.e16-10-0737

Pickett, E. K., Henstridge, C. M., Allison, E., Pitstick, R., Pooler, A., Wegmann, S., Carlson, G., Hyman, B. T., & Spires-Jones, T. L. (2017). Spread of tau down neural circuits precedes synapse and neuronal loss in the rTgTauEC mouse model of early Alzheimer's disease. *Synapse*, *71*(6), e21965. https://doi.org/10.1002/syn.21965

Planel, E., Richter, K. E. G., Nolan, C. E., Finley, J. E., Liu, L., Wen, Y., Krishnamurthy, P., Herman, M., Wang, L., Schachter, J. B., Nelson, R. B., Lau, L.-F., & Duff, K. E. (2007). Anesthesia Leads to Tau Hyperphosphorylation through Inhibition of Phosphatase Activity by Hypothermia. *The Journal of Neuroscience*, *27*(12), 3090–3097. https://doi.org/10.1523/JNEUROSCI.4854-06.2007

Podinovskaia, M., & Russell, D. G. (2015). *Detection and quantification of microbial manipulation of phagosomal function* (pp. 305–329). https://doi.org/10.1016/bs.mcb.2014.10.026

Podinovskaia, M., VanderVen, B. C., Yates, R. M., Glennie, S., Fullerton, D., Mwandumba, H. C., & Russell, D. G. (2013). Dynamic Quantitative Assays of Phagosomal Function. *Current Protocols in Immunology*, *102*(1). https://doi.org/10.1002/0471142735.im1434s102

Podleśny-Drabiniok, A., Marcora, E., & Goate, A. M. (2020). Microglial Phagocytosis: A Disease-Associated Process Emerging from Alzheimer's Disease Genetics. *Trends in Neurosciences*, *43*(12), 965–979. https://doi.org/10.1016/j.tins.2020.10.002

Polanco, J. C., Hand, G. R., Briner, A., Li, C., & Götz, J. (2021). Exosomes induce endolysosomal permeabilization as a gateway by which exosomal tau seeds escape into the cytosol. *Acta Neuropathologica*, *141*(2), 235–256. https://doi.org/10.1007/s00401-020-02254-3

Pooler, A. M., Phillips, E. C., Lau, D. H. W., Noble, W., & Hanger, D. P. (2013). Physiological release of endogenous tau is stimulated by neuronal activity. *EMBO Reports*, *14*(4), 389–394. https://doi.org/10.1038/embor.2013.15

Poorkaj, P., Bird, T. D., Wijsman, E., Nemens, E., Garruto, R. M., Anderson, L., Andreadis, A., Wiederholt, W. C., Raskind, M., & Schellenberg, G. D. (1998). Tau is a candidate gene for chromosome 17 frontotemporal dementia. *Annals of Neurology*, *43*(6), 815–825. https://doi.org/10.1002/ana.410430617

Poorkaj, P., Raskind, W. H., Leverenz, J. B., Matsushita, M., Zabetian, C. P., Samii, A., Kim, S., Gazi, N., Nutt, J. G., Wolff, J., Yearout, D., Greenup, J. L., Steinbart, E. J., & Bird, T. D. (2010). A novel X-linked four-repeat tauopathy with Parkinsonism and spasticity. *Movement Disorders*, *25*(10), 1409–1417. https://doi.org/10.1002/mds.23085

Popova, G., Soliman, S. S., Kim, C. N., Keefe, M. G., Hennick, K. M., Jain, S., Li, T., Tejera, D., Shin, D., Chhun, B. B., McGinnis, C. S., Speir, M., Gartner, Z. J., Mehta, S. B., Haeussler, M., Hengen, K. B., Ransohoff, R. R., Piao, X., & Nowakowski, T. J. (2021). Human microglia states are conserved across experimental models and regulate neural stem cell responses in chimeric organoids. *Cell Stem Cell*, *28*(12), 2153-2166.e6. https://doi.org/10.1016/j.stem.2021.08.015

Poulopoulos, M., Levy, O. A., & Alcalay, R. N. (2012). The neuropathology of genetic Parkinson's disease. *Movement Disorders*, *27*(7), 831–842. https://doi.org/10.1002/mds.24962

Prasad, J. M., Migliorini, M., Galisteo, R., & Strickland, D. K. (2015). Generation of a Potent Low Density Lipoprotein Receptor-related Protein 1 (LRP1) Antagonist by Engineering a Stable Form of the Receptor-associated Protein (RAP) D3 Domain. *Journal of Biological Chemistry*, *290*(28), 17262–17268. https://doi.org/10.1074/jbc.M115.660084

Praschberger, R., Kuenen, S., Schoovaerts, N., Kaempf, N., Singh, J., Janssens, J., Swerts, J., Nachman, E., Calatayud, C., Aerts, S., Poovathingal, S., & Verstreken, P. (2023). Neuronal identity defines α-synuclein and tau toxicity. *Neuron*, *111*(10), 1577-1590.e11. https://doi.org/10.1016/j.neuron.2023.02.033

Prater, K. E., Green, K. J., Mamde, S., Sun, W., Cochoit, A., Smith, C. L., Chiou, K. L., Heath, L., Rose, S. E., Wiley, J., Keene, C. D., Kwon, R. Y., Snyder-Mackler, N., Blue, E. E., Logsdon, B., Young, J. E., Shojaie, A., Garden, G. A., & Jayadev, S. (2023). Human microglia show unique transcriptional changes in Alzheimer's disease. *Nature Aging*, *3*(7), 894–907. https://doi.org/10.1038/s43587-023-00424-y

Prouty, W. F., & Goldberg, A. L. (1972). Effects of Protease Inhibitors on Protein Breakdown in Escherichia coli. *Journal of Biological Chemistry*, *247*(10), 3341–3352. https://doi.org/10.1016/S0021-9258(19)45251-4

Prusiner, S. B. (1982). Novel Proteinaceous Infectious Particles Cause Scrapie. *Science*, *216*(4542), 136–144. https://doi.org/10.1126/science.6801762

Prusiner, S. B. (1998). Prions. *Proceedings of the National Academy of Sciences*, *95*(23), 13363–13383. https://doi.org/10.1073/pnas.95.23.13363

Quinn, J. P., Corbett, N. J., Kellett, K. A. B., & Hooper, N. M. (2018). Tau Proteolysis in the Pathogenesis of Tauopathies: Neurotoxic Fragments and Novel Biomarkers. *Journal of Alzheimer's Disease*, *63*(1), 13–33. https://doi.org/10.3233/JAD-170959

Rabinovitch, M. (1995). Professional and non-professional phagocytes: an introduction. *Trends in Cell Biology*, *5*(3), 85–87. https://doi.org/10.1016/S0962-8924(00)88955-2

Raetz, C. R. H., & Whitfield, C. (2002). Lipopolysaccharide Endotoxins. *Annual Review of Biochemistry*, *71*(1), 635–700. https://doi.org/10.1146/annurev.biochem.71.110601.135414

Ran, F. A., Hsu, P. D., Lin, C.-Y., Gootenberg, J. S., Konermann, S., Trevino, A. E., Scott, D. A., Inoue, A., Matoba, S., Zhang, Y., & Zhang, F. (2013). Double Nicking by RNA-Guided CRISPR Cas9 for Enhanced Genome Editing Specificity. *Cell*, *154*(6), 1380–1389. https://doi.org/10.1016/j.cell.2013.08.021

Ranson, P. A., & Thomas, W. E. (1991). Pinocytosis as a select marker of ramified microglia in vivo and in vitro. *Journal of Histochemistry & Cytochemistry*, *39*(6), 853–858. https://doi.org/10.1177/39.6.2033242

Rauch, J. N., Luna, G., Guzman, E., Audouard, M., Challis, C., Sibih, Y. E., Leshuk, C., Hernandez, I., Wegmann, S., Hyman, B. T., Gradinaru, V., Kampmann, M., & Kosik, K. S. (2020). LRP1 is a master regulator of tau uptake and spread. *Nature*, *580*(7803), 381–385. https://doi.org/10.1038/s41586-020-2156-5

Regan, P., Piers, T., Yi, J.-H., Kim, D.-H., Huh, S., Park, S. J., Ryu, J. H., Whitcomb, D. J., & Cho, K. (2015). Tau Phosphorylation at Serine 396 Residue Is Required for Hippocampal LTD. *The Journal of Neuroscience*, *35*(12), 4804–4812. https://doi.org/10.1523/JNEUROSCI.2842-14.2015

Reichelt, P., Schwarz, C., & Donzeau, M. (2006a). Single step protocol to purify recombinant proteins with low endotoxin contents. *Protein Expression and Purification*, *46*(2), 483–488. https://doi.org/10.1016/j.pep.2005.09.027

Reichelt, P., Schwarz, C., & Donzeau, M. (2006b). Single step protocol to purify recombinant proteins with low endotoxin contents. *Protein Expression and Purification*, *46*(2), 483–488. https://doi.org/10.1016/j.pep.2005.09.027

Ren, Y., Sahara, N., Giasson, B., & Lewis, J. (2015). Tauopathy Mouse Models. In *Movement Disorders* (pp. 849–855). Elsevier. https://doi.org/10.1016/B978-0-12-405195-9.00055-X

Réu, P., Khosravi, A., Bernard, S., Mold, J. E., Salehpour, M., Alkass, K., Perl, S., Tisdale, J., Possnert, G., Druid, H., & Frisén, J. (2017). The Lifespan and Turnover of Microglia in the Human Brain. *Cell Reports*, *20*(4), 779–784. https://doi.org/10.1016/j.celrep.2017.07.004

Rexach, J. E., Polioudakis, D., Yin, A., Swarup, V., Chang, T. S., Nguyen, T., Sarkar, A., Chen, L., Huang, J., Lin, L.-C., Seeley, W., Trojanowski, J. Q., Malhotra, D., & Geschwind, D. H. (2020). Tau Pathology Drives Dementia Risk-Associated Gene Networks toward Chronic Inflammatory States and Immunosuppression. *Cell Reports*, *33*(7), 108398. https://doi.org/10.1016/j.celrep.2020.108398

Rexach, J., & Geschwind, D. (2020). Selective Neuronal Vulnerability in Alzheimer's Disease: A Modern Holy Grail. *Neuron*, *107*(5), 763–765. https://doi.org/10.1016/j.neuron.2020.08.018

Reynolds, E. S. (1963). THE USE OF LEAD CITRATE AT HIGH pH AS AN ELECTRON-OPAQUE STAIN IN ELECTRON MICROSCOPY. *Journal of Cell Biology*, *17*(1), 208–212. https://doi.org/10.1083/jcb.17.1.208

Rezaie, P., Dean, A., Male, D., & Ulfig, N. (2005). Microglia in the Cerebral Wall of the Human Telencephalon at Second Trimester. *Cerebral Cortex*, *15*(7), 938–949. https://doi.org/10.1093/cercor/bhh194

Rock, R. B., Gekker, G., Hu, S., Sheng, W. S., Cheeran, M., Lokensgard, J. R., & Peterson, P. K. (2004). Role of Microglia in Central Nervous System Infections. *Clinical Microbiology Reviews*, *17*(4), 942–964. https://doi.org/10.1128/CMR.17.4.942-964.2004

Rock, R. B., Hu, S., Deshpande, A., Munir, S., May, B. J., Baker, C. A., Peterson, P. K., & Kapur, V. (2005). Transcriptional response of human microglial cells to interferon-γ. *Genes & Immunity*, *6*(8), 712–719. https://doi.org/10.1038/sj.gene.6364246

Rodríguez, A. M., Rodríguez, J., & Giambartolomei, G. H. (2022). Microglia at the Crossroads of Pathogen-Induced Neuroinflammation. *ASN Neuro*, *14*, 175909142211045. https://doi.org/10.1177/17590914221104566

Romero-Molina, C., Garretti, F., Andrews, S. J., Marcora, E., & Goate, A. M. (2022). Microglial efferocytosis: Diving into the Alzheimer's disease gene pool. *Neuron*, *110*(21), 3513–3533. https://doi.org/10.1016/j.neuron.2022.10.015

Rőszer, T. (2015). Understanding the Mysterious M2 Macrophage through Activation Markers and Effector Mechanisms. *Mediators of Inflammation*, *2015*, 1–16. https://doi.org/10.1155/2015/816460

Rozkov, A., & Enfors, S.-O. (2004). *Analysis and Control of Proteolysis of Recombinant Proteins in Escherichia coli* (pp. 163–195). https://doi.org/10.1007/b95567

Russo, I., Bubacco, L., & Greggio, E. (2022). LRRK2 as a target for modulating immune system responses. *Neurobiology of Disease*, *169*, 105724. https://doi.org/10.1016/j.nbd.2022.105724

Ryan, B. J., & Henehan, G. T. (2017). *Avoiding Proteolysis During Protein Purification* (pp. 53–69). https://doi.org/10.1007/978-1-4939-6412-3_4

Saijo, E., Ghetti, B., Zanusso, G., Oblak, A., Furman, J. L., Diamond, M. I., Kraus, A., & Caughey, B. (2017). Ultrasensitive and selective detection of 3-repeat tau seeding activity in Pick disease brain and cerebrospinal fluid. *Acta Neuropathologica*, *133*(5), 751–765. https://doi.org/10.1007/s00401-017-1692-z

Saijo, E., Metrick, M. A., Koga, S., Parchi, P., Litvan, I., Spina, S., Boxer, A., Rojas, J. C., Galasko, D., Kraus, A., Rossi, M., Newell, K., Zanusso, G., Grinberg, L. T., Seeley, W. W., Ghetti, B., Dickson, D. W., & Caughey, B. (2020a). 4-Repeat tau seeds and templating subtypes as brain and CSF biomarkers of frontotemporal lobar degeneration. *Acta Neuropathologica*, *139*(1), 63–77. https://doi.org/10.1007/s00401-019-02080-2

Saijo, E., Metrick, M. A., Koga, S., Parchi, P., Litvan, I., Spina, S., Boxer, A., Rojas, J. C., Galasko, D., Kraus, A., Rossi, M., Newell, K., Zanusso, G., Grinberg, L. T., Seeley, W. W., Ghetti, B., Dickson, D. W., & Caughey, B. (2020b). 4-Repeat tau seeds and templating subtypes as brain and CSF biomarkers of frontotemporal lobar degeneration. *Acta Neuropathologica*, *139*(1), 63–77. https://doi.org/10.1007/s00401-019-02080-2

Saito, Y., Ruberu, N. N., Sawabe, M., Arai, T., Tanaka, N., Kakuta, Y., Yamanouchi, H., & Murayama, S. (2004). Staging of Argyrophilic Grains: An Age-Associated Tauopathy. *Journal of Neuropathology & Experimental Neurology*, *63*(9), 911–918. https://doi.org/10.1093/jnen/63.9.911

Sala Frigerio, C., Wolfs, L., Fattorelli, N., Thrupp, N., Voytyuk, I., Schmidt, I., Mancuso, R., Chen, W.-T., Woodbury, M. E., Srivastava, G., Möller, T., Hudry, E., Das, S., Saido, T., Karran, E., Hyman, B., Perry, V. H., Fiers, M., & De Strooper, B. (2019). The Major Risk Factors for Alzheimer's Disease: Age, Sex, and Genes Modulate the Microglia Response to Aβ Plaques. *Cell Reports*, *27*(4), 1293-1306.e6. https://doi.org/10.1016/j.celrep.2019.03.099

Salter, M. W., & Stevens, B. (2017). Microglia emerge as central players in brain disease. *Nature Medicine*, *23*(9), 1018–1027. https://doi.org/10.1038/nm.4397

Saman, S., Kim, W., Raya, M., Visnick, Y., Miro, S., Saman, S., Jackson, B., McKee, A. C., Alvarez, V. E., Lee, N. C. Y., & Hall, G. F. (2012). Exosome-associated Tau Is

Secreted in Tauopathy Models and Is Selectively Phosphorylated in Cerebrospinal Fluid in Early Alzheimer Disease. *Journal of Biological Chemistry*, *287*(6), 3842–3849. https://doi.org/10.1074/jbc.M111.277061

Sanchez-Contreras, M., Heckman, M. G., Tacik, P., Diehl, N., Brown, P. H., Soto-Ortolaza, A. I., Christopher, E. A., Walton, R. L., Ross, O. A., Golbe, L. I., Graff-Radford, N., Wszolek, Z. K., Dickson, D. W., & Rademakers, R. (2017). Study of *LRRK2* variation in tauopathy: Progressive supranuclear palsy and corticobasal degeneration. *Movement Disorders*, *32*(1), 115–123. https://doi.org/10.1002/mds.26815

Sanchez-Mejias, E., Navarro, V., Jimenez, S., Sanchez-Mico, M., Sanchez-Varo, R., Nuñez-Diaz, C., Trujillo-Estrada, L., Davila, J. C., Vizuete, M., Gutierrez, A., & Vitorica, J. (2016). Soluble phospho-tau from Alzheimer's disease hippocampus drives microglial degeneration. *Acta Neuropathologica*, *132*(6), 897–916. https://doi.org/10.1007/s00401-016-1630-5

Sanders, D. W., Kaufman, S. K., DeVos, S. L., Sharma, A. M., Mirbaha, H., Li, A., Barker, S. J., Foley, A. C., Thorpe, J. R., Serpell, L. C., Miller, T. M., Grinberg, L. T., Seeley, W. W., & Diamond, M. I. (2014). Distinct Tau Prion Strains Propagate in Cells and Mice and Define Different Tauopathies. *Neuron*, *82*(6), 1271–1288. https://doi.org/10.1016/j.neuron.2014.04.047

Santa-Maria, I., Varghese, M., Księżak-Reding, H., Dzhun, A., Wang, J., & Pasinetti, G. M. (2012). Paired Helical Filaments from Alzheimer Disease Brain Induce Intracellular Accumulation of Tau Protein in Aggresomes. *Journal of Biological Chemistry*, *287*(24), 20522–20533. https://doi.org/10.1074/jbc.M111.323279

Sarrazin, S., Lamanna, W. C., & Esko, J. D. (2011). Heparan Sulfate Proteoglycans. *Cold Spring Harbor Perspectives in Biology*, *3*(7), a004952–a004952. https://doi.org/10.1101/cshperspect.a004952

Satoh, J., Kino, Y., Asahina, N., Takitani, M., Miyoshi, J., Ishida, T., & Saito, Y. (2016). TMEM119 marks a subset of microglia in the human brain. *Neuropathology*, *36*(1), 39–49. https://doi.org/10.1111/neup.12235

Sawaya, M. R., Sambashivan, S., Nelson, R., Ivanova, M. I., Sievers, S. A., Apostol, M. I., Thompson, M. J., Balbirnie, M., Wiltzius, J. J. W., McFarlane, H. T., Madsen, A. Ø., Riekel, C., & Eisenberg, D. (2007). Atomic structures of amyloid cross-β spines reveal varied steric zippers. *Nature*, *447*(7143), 453–457. https://doi.org/10.1038/nature05695

Schafer, D. P., Lehrman, E. K., Kautzman, A. G., Koyama, R., Mardinly, A. R., Yamasaki, R., Ransohoff, R. M., Greenberg, M. E., Barres, B. A., & Stevens, B. (2012). Microglia Sculpt Postnatal Neural Circuits in an Activity and Complement-Dependent Manner. *Neuron*, *74*(4), 691–705. https://doi.org/10.1016/j.neuron.2012.03.026

Schafer, D. P., & Stevens, B. (2013). Phagocytic glial cells: sculpting synaptic circuits in the developing nervous system. *Current Opinion in Neurobiology*, *23*(6), 1034–1040. https://doi.org/10.1016/j.conb.2013.09.012

Schafer, S. T., Mansour, A. A., Schlachetzki, J. C. M., Pena, M., Ghassemzadeh, S., Mitchell, L., Mar, A., Quang, D., Stumpf, S., Ortiz, I. S., Lana, A. J., Baek, C., Zaghal, R., Glass, C. K., Nimmerjahn, A., & Gage, F. H. (2023). An in vivo neuroimmune organoid model to study human microglia phenotypes. *Cell*, *186*(10), 2111-2126.e20. https://doi.org/10.1016/j.cell.2023.04.022

Schapansky, J., Nardozzi, J. D., Felizia, F., & LaVoie, M. J. (2014). Membrane recruitment of endogenous LRRK2 precedes its potent regulation of autophagy. *Human Molecular Genetics*, *23*(16), 4201–4214. https://doi.org/10.1093/hmg/ddu138

Scheres, S. H., Zhang, W., Falcon, B., & Goedert, M. (2020). Cryo-EM structures of tau filaments. *Current Opinion in Structural Biology*, *64*, 17–25. https://doi.org/10.1016/j.sbi.2020.05.011

Schlepckow, K., Monroe, K. M., Kleinberger, G., Cantuti-Castelvetri, L., Parhizkar, S., Xia, D., Willem, M., Werner, G., Pettkus, N., Brunner, B., Sülzen, A., Nuscher, B., Hampel, H., Xiang, X., Feederle, R., Tahirovic, S., Park, J. I., Prorok, R., Mahon, C., … Haass, C. (2020). Enhancing protective microglial activities with a dual function <scp>TREM</scp> 2 antibody to the stalk region. *EMBO Molecular Medicine*, *12*(4). https://doi.org/10.15252/emmm.201911227

Schmidt, S. I., Bogetofte, H., Ritter, L., Agergaard, J. B., Hammerich, D., Kabiljagic, A. A., Wlodarczyk, A., Lopez, S. G., Sørensen, M. D., Jørgensen, M. L., Okarmus, J., Serrano, A. M., Kristensen, B. W., Freude, K., Owens, T., & Meyer, M. (2021). Microglia-Secreted Factors Enhance Dopaminergic Differentiation of Tissue- and iPSC-Derived Human Neural Stem Cells. *Stem Cell Reports*, *16*(2), 281–294. https://doi.org/10.1016/j.stemcr.2020.12.011

Schneider, A., Biernat, J., von Bergen, M., Mandelkow, E., & Mandelkow, E.-M. (1999). Phosphorylation that Detaches Tau Protein from Microtubules (Ser262, Ser214) Also Protects It against Aggregation into Alzheimer Paired Helical Filaments. *Biochemistry*, *38*(12), 3549–3558. https://doi.org/10.1021/bi981874p

Schneier, M., Razdan, S., Miller, A. M., Briceno, M. E., & Barua, S. (2020). Current technologies to endotoxin detection and removal for biopharmaceutical purification. *Biotechnology and Bioengineering*, *117*(8), 2588–2609. https://doi.org/10.1002/bit.27362

Schroder, K., Hertzog, P. J., Ravasi, T., & Hume, D. A. (2004). Interferon-γ: an overview of signals, mechanisms and functions. *Journal of Leukocyte Biology*, *75*(2), 163–189. https://doi.org/10.1189/jlb.0603252

Schulz, C., Perdiguero, E. G., Chorro, L., Szabo-Rogers, H., Cagnard, N., Kierdorf, K., Prinz, M., Wu, B., Jacobsen, S. E. W., Pollard, J. W., Frampton, J., Liu, K. J., & Geissmann, F. (2012). A Lineage of Myeloid Cells Independent of Myb and Hematopoietic Stem Cells. *Science*, *336*(6077), 86–90. https://doi.org/10.1126/science.1219179

Schwalbe, M., Ozenne, V., Bibow, S., Jaremko, M., Jaremko, L., Gajda, M., Jensen, M. R., Biernat, J., Becker, S., Mandelkow, E., Zweckstetter, M., & Blackledge, M. (2014). Predictive Atomic Resolution Descriptions of Intrinsically Disordered hTau40 and α-Synuclein in Solution from NMR and Small Angle Scattering. *Structure*, *22*(2), 238–249. https://doi.org/10.1016/j.str.2013.10.020

Schwarz, A. J., Yu, P., Miller, B. B., Shcherbinin, S., Dickson, J., Navitsky, M., Joshi, A. D., Devous, M. D., & Mintun, M. S. (2016). Regional profiles of the candidate tau PET ligand ^{18}F-AV-1451 recapitulate key features of Braak histopathological stages. *Brain*, *139*(5), 1539–1550. https://doi.org/10.1093/brain/aww023

Schweers, O., Schönbrunn-Hanebeck, E., Marx, A., & Mandelkow, E. (1994). Structural studies of tau protein and Alzheimer paired helical filaments show no evidence for beta-structure. *The Journal of Biological Chemistry*, *269*(39), 24290–24297.

Scott, J. D., DeMong, D. E., Greshock, T. J., Basu, K., Dai, X., Harris, J., Hruza, A., Li, S. W., Lin, S.-I., Liu, H., Macala, M. K., Hu, Z., Mei, H., Zhang, H., Walsh, P., Poirier, M., Shi, Z.-C., Xiao, L., Agnihotri, G., … Miller, M. W. (2017). Discovery of a 3-(4-Pyrimidinyl) Indazole (MLi-2), an Orally Available and Selective Leucine-Rich Repeat Kinase 2 (LRRK2) Inhibitor that Reduces Brain Kinase Activity. *Journal of Medicinal Chemistry*, *60*(7), 2983–2992. https://doi.org/10.1021/acs.jmedchem.7b00045

Serdakowski London, A., Kerins, B., Tschantz, W. R., & Mackay, K. (2012). Endotoxin removal and prevention for pre-clinical biologics production. *Biotechnology Journal*, *7*(12), 1509–1516. https://doi.org/10.1002/biot.201200220

Sexton, C., Snyder, H., Beher, D., Boxer, A. L., Brannelly, P., Brion, J., Buée, L., Cacace, A. M., Chételat, G., Citron, M., DeVos, S. L., Diaz, K., Feldman, H. H., Frost, B., Goate, A. M., Gold, M., Hyman, B., Johnson, K., Karch, C. M., … Carrillo, M. C. (2022). Current directions in tau research: Highlights from Tau 2020. *Alzheimer's & Dementia*, *18*(5), 988–1007. https://doi.org/10.1002/alz.12452

Shahnawaz, M., Tokuda, T., Waragai, M., Mendez, N., Ishii, R., Trenkwalder, C., Mollenhauer, B., & Soto, C. (2017). Development of a Biochemical Diagnosis of Parkinson Disease by Detection of α-Synuclein Misfolded Aggregates in Cerebrospinal Fluid. *JAMA Neurology*, *74*(2), 163. https://doi.org/10.1001/jamaneurol.2016.4547

Shen, K., Reichelt, M., Kyauk, R. V., Ngu, H., Shen, Y.-A. A., Foreman, O., Modrusan, Z., Friedman, B. A., Sheng, M., & Yuen, T. J. (2021). Multiple sclerosis risk gene Mertk is required for microglial activation and subsequent remyelination. *Cell Reports*, *34*(10), 108835. https://doi.org/10.1016/j.celrep.2021.108835

Shi, S.-H., Jan, L. Y., & Jan, Y.-N. (2003). Hippocampal Neuronal Polarity Specified by Spatially Localized mPar3/mPar6 and PI 3-Kinase Activity. *Cell*, *112*(1), 63–75. https://doi.org/10.1016/S0092-8674(02)01249-7

Shi, Y., Zhang, W., Yang, Y., Murzin, A. G., Falcon, B., Kotecha, A., van Beers, M., Tarutani, A., Kametani, F., Garringer, H. J., Vidal, R., Hallinan, G. I., Lashley, T., Saito, Y., Murayama, S., Yoshida, M., Tanaka, H., Kakita, A., Ikeuchi, T., … Scheres, S. H. W. (2021). Structure-based classification of tauopathies. *Nature*, *598*(7880), 359–363. https://doi.org/10.1038/s41586-021-03911-7

Shilova, O. N., Shilov, E. S., & Deyev, S. M. (2017). The effect of trypan blue treatment on autofluorescence of fixed cells. *Cytometry Part A*, *91*(9), 917–925. https://doi.org/10.1002/cyto.a.23199

Shinohara, M., Tachibana, M., Kanekiyo, T., & Bu, G. (2017). Role of LRP1 in the pathogenesis of Alzheimer's disease: evidence from clinical and preclinical studies. *Journal of Lipid Research*, *58*(7), 1267–1281. https://doi.org/10.1194/jlr.R075796

Sierra, A., Abiega, O., Shahraz, A., & Neumann, H. (2013). Janus-faced microglia: beneficial and detrimental consequences of microglial phagocytosis. *Frontiers in Cellular Neuroscience*, *7*. https://doi.org/10.3389/fncel.2013.00006

Sierra, A., Encinas, J. M., Deudero, J. J. P., Chancey, J. H., Enikolopov, G., Overstreet-Wadiche, L. S., Tsirka, S. E., & Maletic-Savatic, M. (2010). Microglia Shape Adult Hippocampal Neurogenesis through Apoptosis-Coupled Phagocytosis. *Cell Stem Cell*, *7*(4), 483–495. https://doi.org/10.1016/j.stem.2010.08.014

Sierra, A., Paolicelli, R. C., & Kettenmann, H. (2019). Cien Años de Microglía: Milestones in a Century of Microglial Research. *Trends in Neurosciences*, *42*(11), 778–792. https://doi.org/10.1016/j.tins.2019.09.004

Sillen, A., Leroy, A., Wieruszeski, J.-M., Loyens, A., Beauvillain, J.-C., Buée, L., Landrieu, I., & Lippens, G. (2005). Regions of Tau Implicated in the Paired Helical Fragment Core as Defined by NMR. *ChemBioChem*, *6*(10), 1849–1856. https://doi.org/10.1002/cbic.200400452

Silva, M. C., Cheng, C., Mair, W., Almeida, S., Fong, H., Biswas, M. H. U., Zhang, Z., Huang, Y., Temple, S., Coppola, G., Geschwind, D. H., Karydas, A., Miller, B. L., Kosik, K. S., Gao, F.-B., Steen, J. A., & Haggarty, S. J. (2016). Human iPSC-Derived Neuronal Model of Tau-A152T Frontotemporal Dementia Reveals Tau-Mediated

Mechanisms of Neuronal Vulnerability. *Stem Cell Reports*, *7*(3), 325–340. https://doi.org/10.1016/j.stemcr.2016.08.001

Silvin, A., Uderhardt, S., Piot, C., Da Mesquita, S., Yang, K., Geirsdottir, L., Mulder, K., Eyal, D., Liu, Z., Bridlance, C., Thion, M. S., Zhang, X. M., Kong, W. T., Deloger, M., Fontes, V., Weiner, A., Ee, R., Dress, R., Hang, J. W., … Ginhoux, F. (2022). Dual ontogeny of disease-associated microglia and disease inflammatory macrophages in aging and neurodegeneration. *Immunity*, *55*(8), 1448-1465.e6. https://doi.org/10.1016/j.immuni.2022.07.004

Siman, R., Lin, Y.-G., Malthankar-Phatak, G., & Dong, Y. (2013). A Rapid Gene Delivery-Based Mouse Model for Early-Stage Alzheimer Disease-Type Tauopathy. *Journal of Neuropathology & Experimental Neurology*, *72*(11), 1062–1071. https://doi.org/10.1097/NEN.0000000000000006

Simón-Sánchez, J., Schulte, C., Bras, J. M., Sharma, M., Gibbs, J. R., Berg, D., Paisan-Ruiz, C., Lichtner, P., Scholz, S. W., Hernandez, D. G., Krüger, R., Federoff, M., Klein, C., Goate, A., Perlmutter, J., Bonin, M., Nalls, M. A., Illig, T., Gieger, C., … Gasser, T. (2009). Genome-wide association study reveals genetic risk underlying Parkinson's disease. *Nature Genetics*, *41*(12), 1308–1312. https://doi.org/10.1038/ng.487

Simpson, C., Vinikoor-Imler, L., Nassan, F. L., Shirvan, J., Lally, C., Dam, T., & Maserejian, N. (2022). Prevalence of ten LRRK2 variants in Parkinson's disease: A comprehensive review. *Parkinsonism & Related Disorders*, *98*, 103–113. https://doi.org/10.1016/j.parkreldis.2022.05.012

Smith, A. M., & Dragunow, M. (2014). The human side of microglia. *Trends in Neurosciences*, *37*(3), 125–135. https://doi.org/10.1016/j.tins.2013.12.001

Smith, M. E., van der Maesen, K., & Somera, F. P. (1998). Macrophage and microglial responses to cytokines in vitro: Phagocytic activity, proteolytic enzyme release, and free radical production. *Journal of Neuroscience Research*, *54*(1), 68–78. https://doi.org/10.1002/(SICI)1097-4547(19981001)54:1<68::AID-JNR8>3.0.CO;2-F

Snead, D. M., Matyszewski, M., Dickey, A. M., Lin, Y. X., Leschziner, A. E., & Reck-Peterson, S. L. (2022). Structural basis for Parkinson's disease-linked LRRK2's binding to microtubules. *Nature Structural & Molecular Biology*, *29*(12), 1196–1207. https://doi.org/10.1038/s41594-022-00863-y

Sobue, A., Komine, O., Hara, Y., Endo, F., Mizoguchi, H., Watanabe, S., Murayama, S., Saito, T., Saido, T. C., Sahara, N., Higuchi, M., Ogi, T., & Yamanaka, K. (2021). Microglial gene signature reveals loss of homeostatic microglia associated with neurodegeneration of Alzheimer's disease. *Acta Neuropathologica Communications*, *9*(1), 1. https://doi.org/10.1186/s40478-020-01099-x

Solé-Domènech, S., Cruz, D. L., Capetillo-Zarate, E., & Maxfield, F. R. (2016). The endocytic pathway in microglia during health, aging and Alzheimer's disease. *Ageing Research Reviews*, *32*, 89–103. https://doi.org/10.1016/j.arr.2016.07.002

Speicher, A. M., Wiendl, H., Meuth, S. G., & Pawlowski, M. (2019). Generating microglia from human pluripotent stem cells: novel in vitro models for the study of neurodegeneration. *Molecular Neurodegeneration*, *14*(1), 46. https://doi.org/10.1186/s13024-019-0347-z

Spillantini, M. G., Murrell, J. R., Goedert, M., Farlow, M. R., Klug, A., & Ghetti, B. (1998). Mutation in the tau gene in familial multiple system tauopathy with presenile dementia. *Proceedings of the National Academy of Sciences*, *95*(13), 7737–7741. https://doi.org/10.1073/pnas.95.13.7737

Srinivasan, K., Friedman, B. A., Etxeberria, A., Huntley, M. A., van der Brug, M. P., Foreman, O., Paw, J. S., Modrusan, Z., Beach, T. G., Serrano, G. E., & Hansen, D. V. (2020a). Alzheimer's Patient Microglia Exhibit Enhanced Aging and Unique Transcriptional Activation. *Cell Reports*, *31*(13), 107843. https://doi.org/10.1016/j.celrep.2020.107843

Srinivasan, K., Friedman, B. A., Etxeberria, A., Huntley, M. A., van der Brug, M. P., Foreman, O., Paw, J. S., Modrusan, Z., Beach, T. G., Serrano, G. E., & Hansen, D. V. (2020b). Alzheimer's Patient Microglia Exhibit Enhanced Aging and Unique Transcriptional Activation. *Cell Reports*, *31*(13), 107843. https://doi.org/10.1016/j.celrep.2020.107843

Stancu, I.-C., Cremers, N., Vanrusselt, H., Couturier, J., Vanoosthuyse, A., Kessels, S., Lodder, C., Brône, B., Huaux, F., Octave, J.-N., Terwel, D., & Dewachter, I. (2019). Aggregated Tau activates NLRP3–ASC inflammasome exacerbating exogenously seeded and non-exogenously seeded Tau pathology in vivo. *Acta Neuropathologica*, *137*(4), 599–617. https://doi.org/10.1007/s00401-018-01957-y

Stancu, I.-C., Vasconcelos, B., Ris, L., Wang, P., Villers, A., Peeraer, E., Buist, A., Terwel, D., Baatsen, P., Oyelami, T., Pierrot, N., Casteels, C., Bormans, G., Kienlen-Campard, P., Octave, J.-N., Moechars, D., & Dewachter, I. (2015). Templated misfolding of Tau by prion-like seeding along neuronal connections impairs neuronal network function and associated behavioral outcomes in Tau transgenic mice. *Acta Neuropathologica*, *129*(6), 875–894. https://doi.org/10.1007/s00401-015-1413-4

Steger, M., Diez, F., Dhekne, H. S., Lis, P., Nirujogi, R. S., Karayel, O., Tonelli, F., Martinez, T. N., Lorentzen, E., Pfeffer, S. R., Alessi, D. R., & Mann, M. (2017). Systematic proteomic analysis of LRRK2-mediated Rab GTPase phosphorylation establishes a connection to ciliogenesis. *ELife*, *6*. https://doi.org/10.7554/eLife.31012

Steger, M., Tonelli, F., Ito, G., Davies, P., Trost, M., Vetter, M., Wachter, S., Lorentzen, E., Duddy, G., Wilson, S., Baptista, M. A., Fiske, B. K., Fell, M. J., Morrow, J. A., Reith, A. D., Alessi, D. R., & Mann, M. (2016). Phosphoproteomics reveals that Parkinson's disease kinase LRRK2 regulates a subset of Rab GTPases. *ELife*, *5*. https://doi.org/10.7554/eLife.12813

Stelzmann, R. A., Norman Schnitzlein, H., & Reed Murtagh, F. (1995). An english translation of alzheimer's 1907 paper, ?□ber eine eigenartige erkankung der hirnrinde? *Clinical Anatomy*, *8*(6), 429–431. https://doi.org/10.1002/ca.980080612

Stevens, B., Allen, N. J., Vazquez, L. E., Howell, G. R., Christopherson, K. S., Nouri, N., Micheva, K. D., Mehalow, A. K., Huberman, A. D., Stafford, B., Sher, A., Litke, A. M., Lambris, J. D., Smith, S. J., John, S. W. M., & Barres, B. A. (2007). The Classical Complement Cascade Mediates CNS Synapse Elimination. *Cell*, *131*(6), 1164–1178. https://doi.org/10.1016/j.cell.2007.10.036

Streit, W. J., Braak, H., Xue, Q.-S., & Bechmann, I. (2009). Dystrophic (senescent) rather than activated microglial cells are associated with tau pathology and likely precede neurodegeneration in Alzheimer's disease. *Acta Neuropathologica*, *118*(4), 475–485. https://doi.org/10.1007/s00401-009-0556-6

Suskiewicz, M. J., Sussman, J. L., Silman, I., & Shaul, Y. (2011). Context-dependent resistance to proteolysis of intrinsically disordered proteins. *Protein Science*, *20*(8), 1285–1297. https://doi.org/10.1002/pro.657

Tabata, Y., & Ikada, Y. (1988). Effect of the size and surface charge of polymer microspheres on their phagocytosis by macrophage. *Biomaterials*, *9*(4), 356–362. https://doi.org/10.1016/0142-9612(88)90033-6

Takahashi, K., Tanabe, K., Ohnuki, M., Narita, M., Ichisaka, T., Tomoda, K., & Yamanaka, S. (2007). Induction of Pluripotent Stem Cells from Adult Human Fibroblasts by Defined Factors. *Cell*, *131*(5), 861–872. https://doi.org/10.1016/j.cell.2007.11.019

Takata, K., Kozaki, T., Lee, C. Z. W., Thion, M. S., Otsuka, M., Lim, S., Utami, K. H., Fidan, K., Park, D. S., Malleret, B., Chakarov, S., See, P., Low, D., Low, G., Garcia-Miralles, M., Zeng, R., Zhang, J., Goh, C. C., Gul, A., … Ginhoux, F. (2017). Induced-Pluripotent-Stem-Cell-Derived Primitive Macrophages Provide a Platform for Modeling Tissue-Resident Macrophage Differentiation and Function. *Immunity*, *47*(1), 183-198.e6. https://doi.org/10.1016/j.immuni.2017.06.017

Takeda, S., Wegmann, S., Cho, H., DeVos, S. L., Commins, C., Roe, A. D., Nicholls, S. B., Carlson, G. A., Pitstick, R., Nobuhara, C. K., Costantino, I., Frosch, M. P., Müller, D. J., Irimia, D., & Hyman, B. T. (2015). Neuronal uptake and propagation of a rare phosphorylated high-molecular-weight tau derived from Alzheimer's disease brain. *Nature Communications*, *6*(1), 8490. https://doi.org/10.1038/ncomms9490

Tan, S., & Russell, D. G. (2015). Trans-species communication in the *Mycobacterium tuberculosis*- infected macrophage. *Immunological Reviews*, *264*(1), 233–248. https://doi.org/10.1111/imr.12254

Tardivel, M., Bégard, S., Bousset, L., Dujardin, S., Coens, A., Melki, R., Buée, L., & Colin, M. (2016). Tunneling nanotube (TNT)-mediated neuron-to neuron transfer of pathological Tau protein assemblies. *Acta Neuropathologica Communications*, *4*(1), 117. https://doi.org/10.1186/s40478-016-0386-4

Tay, T. L., Mai, D., Dautzenberg, J., Fernández-Klett, F., Lin, G., Sagar, Datta, M., Drougard, A., Stempfl, T., Ardura-Fabregat, A., Staszewski, O., Margineanu, A., Sporbert, A., Steinmetz, L. M., Pospisilik, J. A., Jung, S., Priller, J., Grün, D., Ronneberger, O., & Prinz, M. (2017). A new fate mapping system reveals context-dependent random or clonal expansion of microglia. *Nature Neuroscience*, *20*(6), 793–803. https://doi.org/10.1038/nn.4547

Taylor, D. R., & Hooper, N. M. (2007). The low-density lipoprotein receptor-related protein 1 (LRP1) mediates the endocytosis of the cellular prion protein. *Biochemical Journal*, *402*(1), 17–23. https://doi.org/10.1042/BJ20061736

Tennant, J. M., Henderson, D. M., Wisniewski, T. M., & Hoover, E. A. (2020). RT-QuIC detection of tauopathies using full-length tau substrates. *Prion*, *14*(1), 249–256. https://doi.org/10.1080/19336896.2020.1832946

Tepper, K., Biernat, J., Kumar, S., Wegmann, S., Timm, T., Hübschmann, S., Redecke, L., Mandelkow, E.-M., Müller, D. J., & Mandelkow, E. (2014). Oligomer Formation of Tau Protein Hyperphosphorylated in Cells. *Journal of Biological Chemistry*, *289*(49), 34389–34407. https://doi.org/10.1074/jbc.M114.611368

Terada, T., Yokokura, M., Obi, T., Bunai, T., Yoshikawa, E., Ando, I., Shimada, H., Suhara, T., Higuchi, M., & Ouchi, Y. (2019). In vivo direct relation of tau pathology with neuroinflammation in early Alzheimer's disease. *Journal of Neurology*, *266*(9), 2186–2196. https://doi.org/10.1007/s00415-019-09400-2

Tian, H., Davidowitz, E., Lopez, P., Emadi, S., Moe, J., & Sierks, M. (2013). Trimeric Tau Is Toxic to Human Neuronal Cells at Low Nanomolar Concentrations. *International Journal of Cell Biology*, *2013*, 1–9. https://doi.org/10.1155/2013/260787

Trabzuni, D., Wray, S., Vandrovcova, J., Ramasamy, A., Walker, R., Smith, C., Luk, C., Gibbs, J. R., Dillman, A., Hernandez, D. G., Arepalli, S., Singleton, A. B., Cookson, M. R., Pittman, A. M., de Silva, R., Weale, M. E., Hardy, J., & Ryten, M. (2012). MAPT expression and splicing is differentially regulated by brain region: relation to genotype and implication for tauopathies. *Human Molecular Genetics*, *21*(18), 4094–4103. https://doi.org/10.1093/hmg/dds238

Tracy, T. E., Madero-Pérez, J., Swaney, D. L., Chang, T. S., Moritz, M., Konrad, C., Ward, M. E., Stevenson, E., Hüttenhain, R., Kauwe, G., Mercedes, M., Sweetland-Martin, L., Chen, X., Mok, S.-A., Wong, M. Y., Telpoukhovskaia, M., Min, S.-W., Wang, C., Sohn, P. D., … Gan, L. (2022). Tau interactome maps synaptic and mitochondrial processes associated with neurodegeneration. *Cell*, *185*(4), 712-728.e14. https://doi.org/10.1016/j.cell.2021.12.041

Tram, T. T. B., Ha, V. T. N., Thu, D. D. A., Dinh, T. D., Vijay, S., Hai, H. T., Hanh, N. T., Phu, N. H., Thwaites, G. E., & Thuong, N. T. T. (2019). Development of ligand-coated beads to measure macrophage antimicrobial activities. *Biology of the Cell*, *111*(10), 262–270. https://doi.org/10.1111/boc.201900042

Tremblay, M.-È., Lowery, R. L., & Majewska, A. K. (2010). Microglial Interactions with Synapses Are Modulated by Visual Experience. *PLoS Biology*, *8*(11), e1000527. https://doi.org/10.1371/journal.pbio.1000527

Tsuchiya, S., Yamabe, M., Yamaguchi, Y., Kobayashi, Y., Konno, T., & Tada, K. (1980). Establishment and characterization of a human acute monocytic leukemia cell line (THP-1). *International Journal of Cancer*, *26*(2), 171–176. https://doi.org/10.1002/ijc.2910260208

Tsvetkov, A. S., Arrasate, M., Barmada, S., Ando, D. M., Sharma, P., Shaby, B. A., & Finkbeiner, S. (2013). Proteostasis of polyglutamine varies among neurons and predicts neurodegeneration. *Nature Chemical Biology*, *9*(9), 586–592. https://doi.org/10.1038/nchembio.1308

Udeochu, J. C., Amin, S., Huang, Y., Fan, L., Torres, E. R. S., Carling, G. K., Liu, B., McGurran, H., Coronas-Samano, G., Kauwe, G., Mousa, G. A., Wong, M. Y., Ye, P., Nagiri, R. K., Lo, I., Holtzman, J., Corona, C., Yarahmady, A., Gill, M. T., … Gan, L. (2023). Tau activation of microglial cGAS–IFN reduces MEF2C-mediated cognitive resilience. *Nature Neuroscience*, *26*(5), 737–750. https://doi.org/10.1038/s41593-023-01315-6

Usenovic, M., Niroomand, S., Drolet, R. E., Yao, L., Gaspar, R. C., Hatcher, N. G., Schachter, J., Renger, J. J., & Parmentier-Batteur, S. (2015). Internalized Tau Oligomers Cause Neurodegeneration by Inducing Accumulation of Pathogenic Tau in Human Neurons Derived from Induced Pluripotent Stem Cells. *The Journal of Neuroscience*, *35*(42), 14234–14250. https://doi.org/10.1523/JNEUROSCI.1523-15.2015

Uversky, V. N. (2002). What does it mean to be natively unfolded? *European Journal of Biochemistry*, *269*(1), 2–12. https://doi.org/10.1046/j.0014-2956.2001.02649.x

Uversky, V. N. (2019). Intrinsically Disordered Proteins and Their “Mysterious” (Meta)Physics. *Frontiers in Physics*, *7*. https://doi.org/10.3389/fphy.2019.00010

Valadez-Barba, V., Cota-Coronado, A., Hernández-Pérez, O. R., Lugo-Fabres, P. H., Padilla-Camberos, E., Díaz, N. F., & Díaz-Martínez, N. E. (2020). iPSC for modeling neurodegenerative disorders. *Regenerative Therapy*, *15*, 332–339. https://doi.org/10.1016/j.reth.2020.11.006

van Furth, R., & Cohn, Z. A. (1968). THE ORIGIN AND KINETICS OF MONONUCLEAR PHAGOCYTES. *The Journal of Experimental Medicine*, *128*(3), 415–435. https://doi.org/10.1084/jem.128.3.415

van Furth, R., Cohn, Z. A., Hirsch, J. G., Humphrey, J. H., Spector, W. G., & Langevoort, H. L. (1972). The mononuclear phagocyte system: a new classification of macrophages, monocytes, and their precursor cells. *Bulletin of the World Health Organization*, *46*(6), 845–852.

van Lengerich, B., Zhan, L., Xia, D., Chan, D., Joy, D., Park, J. I., Tatarakis, D., Calvert, M., Hummel, S., Lianoglou, S., Pizzo, M. E., Prorok, R., Thomsen, E., Bartos, L. M., Beumers, P., Capell, A., Davis, S. S., de Weerd, L., Dugas, J. C., … Monroe, K. M. (2023). A TREM2-activating antibody with a blood–brain barrier transport vehicle enhances microglial metabolism in Alzheimer's disease models. *Nature Neuroscience*. https://doi.org/10.1038/s41593-022-01240-0

van Olst, L., Verhaege, D., Franssen, M., Kamermans, A., Roucourt, B., Carmans, S., Ytebrouck, E., van der Pol, S. M. A., Wever, D., Popovic, M., Vandenbroucke, R. E., Sobrino, T., Schouten, M., & de Vries, H. E. (2020). Microglial activation arises after aggregation of phosphorylated-tau in a neuron-specific P301S tauopathy mouse model. *Neurobiology of Aging*, *89*, 89–98. https://doi.org/10.1016/j.neurobiolaging.2020.01.003

Vanhee, S., De Mulder, K., Van Caeneghem, Y., Verstichel, G., Van Roy, N., Menten, B., Velghe, I., Philippe, J., De Bleser, D., Lambrecht, B. N., Taghon, T., Leclercq, G., Kerre, T., & Vandekerckhove, B. (2015). In vitro human embryonic stem cell hematopoiesis mimics MYB-independent yolk sac hematopoiesis. *Haematologica*, *100*(2), 157–166. https://doi.org/10.3324/haematol.2014.112144

Varshavsky, A. (1996). The N-end rule: functions, mysteries, uses. *Proceedings of the National Academy of Sciences*, *93*(22), 12142–12149. https://doi.org/10.1073/pnas.93.22.12142

Vascellari, S., Orrù, C. D., & Caughey, B. (2022). Real-Time Quaking- Induced Conversion Assays for Prion Diseases, Synucleinopathies, and Tauopathies. *Frontiers in Aging Neuroscience*, *14*. https://doi.org/10.3389/fnagi.2022.853050

Vasek, M. J., Garber, C., Dorsey, D., Durrant, D. M., Bollman, B., Soung, A., Yu, J., Perez-Torres, C., Frouin, A., Wilton, D. K., Funk, K., DeMasters, B. K., Jiang, X., Bowen, J. R., Mennerick, S., Robinson, J. K., Garbow, J. R., Tyler, K. L., Suthar, M. S., … Klein,

R. S. (2016). A complement–microglial axis drives synapse loss during virus-induced memory impairment. *Nature*, *534*(7608), 538–543. https://doi.org/10.1038/nature18283

Vasudevan, S. O., Russo, A. J., Kumari, P., Vanaja, S. K., & Rathinam, V. A. (2022). A TLR4-independent critical role for CD14 in intracellular LPS sensing. *Cell Reports*, *39*(5), 110755. https://doi.org/10.1016/j.celrep.2022.110755

Vaughan-Jackson, A., Stodolak, S., Ebrahimi, K. H., Browne, C., Reardon, P. K., Pires, E., Gilbert-Jaramillo, J., Cowley, S. A., & James, W. S. (2021). Differentiation of human induced pluripotent stem cells to authentic macrophages using a defined, serum-free, open-source medium. *Stem Cell Reports*, *16*(7), 1735–1748. https://doi.org/10.1016/j.stemcr.2021.05.018

Verheyen, A., Diels, A., Dijkmans, J., Oyelami, T., Meneghello, G., Mertens, L., Versweyveld, S., Borgers, M., Buist, A., Peeters, P., & Cik, M. (2015). Using Human iPSC-Derived Neurons to Model TAU Aggregation. *PLOS ONE*, *10*(12), e0146127. https://doi.org/10.1371/journal.pone.0146127

Verney, C., Monier, A., Fallet-Bianco, C., & Gressens, P. (2010). Early microglial colonization of the human forebrain and possible involvement in periventricular white-matter injury of preterm infants. *Journal of Anatomy*, *217*(4), 436–448. https://doi.org/10.1111/j.1469-7580.2010.01245.x

Verny, M., Jellinger, K. A., Hauw, J.-J., Bancher, C., Litvan, I., & Agid, Y. (1996). Progressive supranuclear palsy: a clinicopathological study of 21 cases. *Acta Neuropathologica*, *91*(4), 427–431. https://doi.org/10.1007/s004010050446

Villa, A., Gelosa, P., Castiglioni, L., Cimino, M., Rizzi, N., Pepe, G., Lolli, F., Marcello, E., Sironi, L., Vegeto, E., & Maggi, A. (2018). Sex-Specific Features of Microglia from Adult Mice. *Cell Reports*, *23*(12), 3501–3511. https://doi.org/10.1016/j.celrep.2018.05.048

Violet, M., Delattre, L., Tardivel, M., Sultan, A., Chauderlier, A., Caillierez, R., Talahari, S., Nesslany, F., Lefebvre, B., Bonnefoy, E., BuÃ©e, L., & Galas, M.-C. (2014). A major role for Tau in neuronal DNA and RNA protection in vivo under physiological and hyperthermic conditions. *Frontiers in Cellular Neuroscience*, *8*. https://doi.org/10.3389/fncel.2014.00084

Vogels, T., Leuzy, A., Cicognola, C., Ashton, N. J., Smolek, T., Novak, M., Blennow, K., Zetterberg, H., Hromadka, T., Zilka, N., & Schöll, M. (2020). Propagation of Tau Pathology: Integrating Insights From Postmortem and In Vivo Studies. *Biological Psychiatry*, *87*(9), 808–818. https://doi.org/10.1016/j.biopsych.2019.09.019

von Bergen, M., Barghorn, S., Biernat, J., Mandelkow, E.-M., & Mandelkow, E. (2005). Tau aggregation is driven by a transition from random coil to beta sheet structure.

Biochimica et Biophysica Acta (BBA) - Molecular Basis of Disease, *1739*(2–3), 158–166. https://doi.org/10.1016/j.bbadis.2004.09.010

von Bergen, M., Barghorn, S., Li, L., Marx, A., Biernat, J., Mandelkow, E.-M., & Mandelkow, E. (2001). Mutations of Tau Protein in Frontotemporal Dementia Promote Aggregation of Paired Helical Filaments by Enhancing Local β-Structure. *Journal of Biological Chemistry*, *276*(51), 48165–48174. https://doi.org/10.1074/jbc.M105196200

von Bergen, M., Friedhoff, P., Biernat, J., Heberle, J., Mandelkow, E.-M., & Mandelkow, E. (2000). Assembly of τ protein into Alzheimer paired helical filaments depends on a local sequence motif (^{306} VQIVYK ^{311}) forming β structure. *Proceedings of the National Academy of Sciences*, *97*(10), 5129–5134. https://doi.org/10.1073/pnas.97.10.5129

Waheed, Z., Choudhary, J., Jatala, F. H., Fatimah, Noor, A., Zerr, I., & Zafar, S. (2023). The Role of Tau Proteoforms in Health and Disease. *Molecular Neurobiology*, *60*(9), 5155–5166. https://doi.org/10.1007/s12035-023-03387-8

Wake, H., Moorhouse, A. J., Jinno, S., Kohsaka, S., & Nabekura, J. (2009). Resting Microglia Directly Monitor the Functional State of Synapses *In Vivo* and Determine the Fate of Ischemic Terminals. *The Journal of Neuroscience*, *29*(13), 3974–3980. https://doi.org/10.1523/JNEUROSCI.4363-08.2009

Wallings, R. L., & Tansey, M. G. (2019). LRRK2 regulation of immune-pathways and inflammatory disease. *Biochemical Society Transactions*, *47*(6), 1581–1595. https://doi.org/10.1042/BST20180463

Wang, C., Fan, L., Khawaja, R. R., Liu, B., Zhan, L., Kodama, L., Chin, M., Li, Y., Le, D., Zhou, Y., Condello, C., Grinberg, L. T., Seeley, W. W., Miller, B. L., Mok, S.-A., Gestwicki, J. E., Cuervo, A. M., Luo, W., & Gan, L. (2022). Microglial NF-κB drives tau spreading and toxicity in a mouse model of tauopathy. *Nature Communications*, *13*(1), 1969. https://doi.org/10.1038/s41467-022-29552-6

Wang, H., Li, Y., Ryder, J. W., Hole, J. T., Ebert, P. J., Airey, D. C., Qian, H.-R., Logsdon, B., Fisher, A., Ahmed, Z., Murray, T. K., Cavallini, A., Bose, S., Eastwood, B. J., Collier, D. A., Dage, J. L., Miller, B. B., Merchant, K. M., O'Neill, M. J., & Demattos, R. B. (2018). Genome-wide RNAseq study of the molecular mechanisms underlying microglia activation in response to pathological tau perturbation in the rTg4510 tau transgenic animal model. *Molecular Neurodegeneration*, *13*(1), 65. https://doi.org/10.1186/s13024-018-0296-y

Wang, S., Mustafa, M., Yuede, C. M., Salazar, S. V., Kong, P., Long, H., Ward, M., Siddiqui, O., Paul, R., Gilfillan, S., Ibrahim, A., Rhinn, H., Tassi, I., Rosenthal, A., Schwabe, T., & Colonna, M. (2020). Anti-human TREM2 induces microglia proliferation and

reduces pathology in an Alzheimer's disease model. *Journal of Experimental Medicine*, *217*(9). https://doi.org/10.1084/jem.20200785

Wang, Y., Balaji, V., Kaniyappan, S., Krüger, L., Irsen, S., Tepper, K., Chandupatla, R., Maetzler, W., Schneider, A., Mandelkow, E., & Mandelkow, E.-M. (2017). The release and trans-synaptic transmission of Tau via exosomes. *Molecular Neurodegeneration*, *12*(1), 5. https://doi.org/10.1186/s13024-016-0143-y

Wang, Y., & Mandelkow, E. (2016). Tau in physiology and pathology. *Nature Reviews Neuroscience*, *17*(1), 22–35. https://doi.org/10.1038/nrn.2015.1

Wang, Y., Szretter, K. J., Vermi, W., Gilfillan, S., Rossini, C., Cella, M., Barrow, A. D., Diamond, M. S., & Colonna, M. (2012). IL-34 is a tissue-restricted ligand of CSF1R required for the development of Langerhans cells and microglia. *Nature Immunology*, *13*(8), 753–760. https://doi.org/10.1038/ni.2360

Washer, S. J., Perez-Alcantara, M., Chen, Y., Steer, J., James, W. S., Trynka, G., Bassett, A. R., & Cowley, S. A. (2022). Single-cell transcriptomics defines an improved, validated monoculture protocol for differentiation of human iPSC to microglia. *Scientific Reports*, *12*(1), 19454. https://doi.org/10.1038/s41598-022-23477-2

Wegmann, S., Bennett, R. E., Amaral, A. S., & Hyman, B. T. (2017). *Studying tau protein propagation and pathology in the mouse brain using adeno-associated viruses* (pp. 307–322). https://doi.org/10.1016/bs.mcb.2017.06.014

Wegmann, S., Maury, E. A., Kirk, M. J., Saqran, L., Roe, A., DeVos, S. L., Nicholls, S., Fan, Z., Takeda, S., Cagsal-Getkin, O., William, C. M., Spires-Jones, T. L., Pitstick, R., Carlson, G. A., Pooler, A. M., & Hyman, B. T. (2015). Removing endogenous tau does not prevent tau propagation yet reduces its neurotoxicity. *The EMBO Journal*, *34*(24), 3028–3041. https://doi.org/10.15252/embj.201592748

Weingarten, M. D., Lockwood, A. H., Hwo, S. Y., & Kirschner, M. W. (1975). A protein factor essential for microtubule assembly. *Proceedings of the National Academy of Sciences*, *72*(5), 1858–1862. https://doi.org/10.1073/pnas.72.5.1858

Wesseling, H., Mair, W., Kumar, M., Schlaffner, C. N., Tang, S., Beerepoot, P., Fatou, B., Guise, A. J., Cheng, L., Takeda, S., Muntel, J., Rotunno, M. S., Dujardin, S., Davies, P., Kosik, K. S., Miller, B. L., Berretta, S., Hedreen, J. C., Grinberg, L. T., … Steen, J. A. (2020a). Tau PTM Profiles Identify Patient Heterogeneity and Stages of Alzheimer's Disease. *Cell*, *183*(6), 1699-1713.e13. https://doi.org/10.1016/j.cell.2020.10.029

Wesseling, H., Mair, W., Kumar, M., Schlaffner, C. N., Tang, S., Beerepoot, P., Fatou, B., Guise, A. J., Cheng, L., Takeda, S., Muntel, J., Rotunno, M. S., Dujardin, S., Davies, P., Kosik, K. S., Miller, B. L., Berretta, S., Hedreen, J. C., Grinberg, L. T., … Steen, J. A. (2020b). Tau PTM Profiles Identify Patient Heterogeneity and Stages of

Alzheimer's Disease. *Cell*, *183*(6), 1699-1713.e13. https://doi.org/10.1016/j.cell.2020.10.029

Wijesekara, N., Gonçalves, R. A., Ahrens, R., De Felice, F. G., & Fraser, P. E. (2018). Tau ablation in mice leads to pancreatic β cell dysfunction and glucose intolerance. *The FASEB Journal*, *32*(6), 3166–3173. https://doi.org/10.1096/fj.201701352

Wilgenburg, B. van, Browne, C., Vowles, J., & Cowley, S. A. (2013). Efficient, Long Term Production of Monocyte-Derived Macrophages from Human Pluripotent Stem Cells under Partly-Defined and Fully-Defined Conditions. *PLoS ONE*, *8*(8), e71098. https://doi.org/10.1371/journal.pone.0071098

Wilham, J. M., Orrú, C. D., Bessen, R. A., Atarashi, R., Sano, K., Race, B., Meade-White, K. D., Taubner, L. M., Timmes, A., & Caughey, B. (2010). Rapid End-Point Quantitation of Prion Seeding Activity with Sensitivity Comparable to Bioassays. *PLoS Pathogens*, *6*(12), e1001217. https://doi.org/10.1371/journal.ppat.1001217

Wille, H., Drewes, G., Biernat, J., Mandelkow, E. M., & Mandelkow, E. (1992). Alzheimer-like paired helical filaments and antiparallel dimers formed from microtubule-associated protein tau in vitro. *Journal of Cell Biology*, *118*(3), 573–584. https://doi.org/10.1083/jcb.118.3.573

Williams, D. R., Holton, J. L., Strand, C., Pittman, A., de Silva, R., Lees, A. J., & Revesz, T. (2007). Pathological tau burden and distribution distinguishes progressive supranuclear palsy-parkinsonism from Richardson's syndrome. *Brain*, *130*(6), 1566–1576. https://doi.org/10.1093/brain/awm104

Willnow, T. E., Armstrong, S. A., Hammer, R. E., & Herz, J. (1995). Functional expression of low density lipoprotein receptor-related protein is controlled by receptor-associated protein in vivo. *Proceedings of the National Academy of Sciences*, *92*(10), 4537–4541. https://doi.org/10.1073/pnas.92.10.4537

Willnow, T. E., Rohlmann, A., Horton, J., Otani, H., Braun, J. R., Hammer, R. E., & Herz, J. (1996). RAP, a specialized chaperone, prevents ligand-induced ER retention and degradation of LDL receptor-related endocytic receptors. *The EMBO Journal*, *15*(11), 2632–2639. https://doi.org/10.1002/j.1460-2075.1996.tb00623.x

Wilsie, L. C., & Orlando, R. A. (2003). The Low Density Lipoprotein Receptor-related Protein Complexes with Cell Surface Heparan Sulfate Proteoglycans to Regulate Proteoglycan-mediated Lipoprotein Catabolism. *Journal of Biological Chemistry*, *278*(18), 15758–15764. https://doi.org/10.1074/jbc.M208786200

Wilson, D. M., & Binder, L. I. (1997). Free fatty acids stimulate the polymerization of tau and amyloid beta peptides. In vitro evidence for a common effector of pathogenesis in Alzheimer's disease. *The American Journal of Pathology*, *150*(6), 2181–2195.

Wilson, M., Blum, R., Dandona, P., & Mousa, S. (2001). Effects In Humans Of Intravenously Administered Endotoxin On Soluble Cell-Adhesion Molecule And Inflammatory Markers: A Model Of Human Diseases. *Clinical and Experimental Pharmacology and Physiology*, *28*(5–6), 376–380. https://doi.org/10.1046/j.1440-1681.2001.03463.x

Wischik, C. M., Novak, M., Edwards, P. C., Klug, A., Tichelaar, W., & Crowther, R. A. (1988). Structural characterization of the core of the paired helical filament of Alzheimer disease. *Proceedings of the National Academy of Sciences*, *85*(13), 4884–4888. https://doi.org/10.1073/pnas.85.13.4884

Wischik, C. M., Novak, M., Thøgersen, H. C., Edwards, P. C., Runswick, M. J., Jakes, R., Walker, J. E., Milstein, C., Roth, M., & Klug, A. (1988). Isolation of a fragment of tau derived from the core of the paired helical filament of Alzheimer disease. *Proceedings of the National Academy of Sciences*, *85*(12), 4506–4510. https://doi.org/10.1073/pnas.85.12.4506

Wlodarczyk, A., Holtman, I. R., Krueger, M., Yogev, N., Bruttger, J., Khorooshi, R., Benmamar-Badel, A., de Boer-Bergsma, J. J., Martin, N. A., Karram, K., Kramer, I., Boddeke, E. W., Waisman, A., Eggen, B. J., & Owens, T. (2017). A novel microglial subset plays a key role in myelinogenesis in developing brain. *The EMBO Journal*, *36*(22), 3292–3308. https://doi.org/10.15252/embj.201696056

Woerman, A. L., Aoyagi, A., Patel, S., Kazmi, S. A., Lobach, I., Grinberg, L. T., McKee, A. C., Seeley, W. W., Olson, S. H., & Prusiner, S. B. (2016). Tau prions from Alzheimer's disease and chronic traumatic encephalopathy patients propagate in cultured cells. *Proceedings of the National Academy of Sciences*, *113*(50). https://doi.org/10.1073/pnas.1616344113

Wong, C.-O., Gregory, S., Hu, H., Chao, Y., Sepúlveda, V. E., He, Y., Li-Kroeger, D., Goldman, W. E., Bellen, H. J., & Venkatachalam, K. (2017a). Lysosomal Degradation Is Required for Sustained Phagocytosis of Bacteria by Macrophages. *Cell Host & Microbe*, *21*(6), 719-730.e6. https://doi.org/10.1016/j.chom.2017.05.002

Wong, C.-O., Gregory, S., Hu, H., Chao, Y., Sepúlveda, V. E., He, Y., Li-Kroeger, D., Goldman, W. E., Bellen, H. J., & Venkatachalam, K. (2017b). Lysosomal Degradation Is Required for Sustained Phagocytosis of Bacteria by Macrophages. *Cell Host & Microbe*, *21*(6), 719-730.e6. https://doi.org/10.1016/j.chom.2017.05.002

Wu, J. W., Herman, M., Liu, L., Simoes, S., Acker, C. M., Figueroa, H., Steinberg, J. I., Margittai, M., Kayed, R., Zurzolo, C., Di Paolo, G., & Duff, K. E. (2013). Small Misfolded Tau Species Are Internalized via Bulk Endocytosis and Anterogradely and Retrogradely Transported in Neurons. *Journal of Biological Chemistry*, *288*(3), 1856–1870. https://doi.org/10.1074/jbc.M112.394528

Wu, J. W., Hussaini, S. A., Bastille, I. M., Rodriguez, G. A., Mrejeru, A., Rilett, K., Sanders, D. W., Cook, C., Fu, H., Boonen, R. A. C. M., Herman, M., Nahmani, E., Emrani, S., Figueroa, Y. H., Diamond, M. I., Clelland, C. L., Wray, S., & Duff, K. E. (2016). Neuronal activity enhances tau propagation and tau pathology in vivo. *Nature Neuroscience*, *19*(8), 1085–1092. https://doi.org/10.1038/nn.4328

Wulf, M.-A., Senatore, A., & Aguzzi, A. (2017). The biological function of the cellular prion protein: an update. *BMC Biology*, *15*(1), 34. https://doi.org/10.1186/s12915-017-0375-5

Yadavalli, N., & Ferguson, SM. (2022). LRRK2 Suppresses Lysosome Degradative Activity in Macrophages and Microglia via Transcription Factor E3 Inhibition. *BioRxiv*.

Yamada, K., Cirrito, J. R., Stewart, F. R., Jiang, H., Finn, M. B., Holmes, B. B., Binder, L. I., Mandelkow, E.-M., Diamond, M. I., Lee, V. M.-Y., & Holtzman, D. M. (2011). *In Vivo* Microdialysis Reveals Age-Dependent Decrease of Brain Interstitial Fluid Tau Levels in P301S Human Tau Transgenic Mice. *The Journal of Neuroscience*, *31*(37), 13110–13117. https://doi.org/10.1523/JNEUROSCI.2569-11.2011

Yamada, K., Holth, J. K., Liao, F., Stewart, F. R., Mahan, T. E., Jiang, H., Cirrito, J. R., Patel, T. K., Hochgräfe, K., Mandelkow, E.-M., & Holtzman, D. M. (2014). Neuronal activity regulates extracellular tau in vivo. *Journal of Experimental Medicine*, *211*(3), 387–393. https://doi.org/10.1084/jem.20131685

Yamamoto, M., & Akira, S. (2009). *Lipid A Receptor TLR4-Mediated Signaling Pathways* (pp. 59–68). https://doi.org/10.1007/978-1-4419-1603-7_6

Yan, M. H., Wang, X., & Zhu, X. (2013). Mitochondrial defects and oxidative stress in Alzheimer disease and Parkinson disease. *Free Radical Biology and Medicine*, *62*, 90–101. https://doi.org/10.1016/j.freeradbiomed.2012.11.014

Yates, R. M., & Russell, D. G. (2008). *Real-Time Spectrofluorometric Assays for the Lumenal Environment of the Maturing Phagosome* (pp. 311–325). https://doi.org/10.1007/978-1-59745-157-4_20

Yeh, F. L., Wang, Y., Tom, I., Gonzalez, L. C., & Sheng, M. (2016). TREM2 Binds to Apolipoproteins, Including APOE and CLU/APOJ, and Thereby Facilitates Uptake of Amyloid-Beta by Microglia. *Neuron*, *91*(2), 328–340. https://doi.org/10.1016/j.neuron.2016.06.015

Yoshiyama, Y., Higuchi, M., Zhang, B., Huang, S.-M., Iwata, N., Saido, T. C., Maeda, J., Suhara, T., Trojanowski, J. Q., & Lee, V. M.-Y. (2007). Synapse Loss and Microglial Activation Precede Tangles in a P301S Tauopathy Mouse Model. *Neuron*, *53*(3), 337–351. https://doi.org/10.1016/j.neuron.2007.01.010

Yu, J., Vodyanik, M. A., Smuga-Otto, K., Antosiewicz-Bourget, J., Frane, J. L., Tian, S., Nie, J., Jonsdottir, G. A., Ruotti, V., Stewart, R., Slukvin, I. I., & Thomson, J. A. (2007).

Induced Pluripotent Stem Cell Lines Derived from Human Somatic Cells. *Science*, *318*(5858), 1917–1920. https://doi.org/10.1126/science.1151526

Yu, Y., Zhang, Z., Walpole, G. F. W., & Yu, Y. (2022). Kinetics of phagosome maturation is coupled to their intracellular motility. *Communications Biology*, *5*(1), 1014. https://doi.org/10.1038/s42003-022-03988-4

Zettel, K., Korff, S., Zamora, R., Morelli, A. E., Darwiche, S., Loughran, P. A., Elson, G., Shang, L., Salgado-Pires, S., Scott, M. J., Vodovotz, Y., & Billiar, T. R. (2017). Toll-Like Receptor 4 on both Myeloid Cells and Dendritic Cells Is Required for Systemic Inflammation and Organ Damage after Hemorrhagic Shock with Tissue Trauma in Mice. *Frontiers in Immunology*, *8*. https://doi.org/10.3389/fimmu.2017.01672

Zhang, J., Jin, J., Su, D., Feng, T., & Zhao, H. (2023). Tau-PET imaging in Parkinson's disease: a systematic review and meta-analysis. *Frontiers in Neurology*, *14*. https://doi.org/10.3389/fneur.2023.1145939

Zhang, W., Tarutani, A., Newell, K. L., Murzin, A. G., Matsubara, T., Falcon, B., Vidal, R., Garringer, H. J., Shi, Y., Ikeuchi, T., Murayama, S., Ghetti, B., Hasegawa, M., Goedert, M., & Scheres, S. H. W. (2020). Novel tau filament fold in corticobasal degeneration. *Nature*, *580*(7802), 283–287. https://doi.org/10.1038/s41586-020-2043-0

Zhang, X., Gao, F., Wang, D., Li, C., Fu, Y., He, W., & Zhang, J. (2018). Tau Pathology in Parkinson's Disease. *Frontiers in Neurology*, *9*. https://doi.org/10.3389/fneur.2018.00809

Zhang, Y., Wu, K.-M., Yang, L., Dong, Q., & Yu, J.-T. (2022). Tauopathies: new perspectives and challenges. *Molecular Neurodegeneration*, *17*(1), 28. https://doi.org/10.1186/s13024-022-00533-z

Zhang, Z., Song, M., Liu, X., Kang, S. S., Kwon, I.-S., Duong, D. M., Seyfried, N. T., Hu, W. T., Liu, Z., Wang, J.-Z., Cheng, L., Sun, Y. E., Yu, S. P., Levey, A. I., & Ye, K. (2014). Cleavage of tau by asparagine endopeptidase mediates the neurofibrillary pathology in Alzheimer's disease. *Nature Medicine*, *20*(11), 1254–1262. https://doi.org/10.1038/nm.3700

Zhao, Y., Wu, X., Li, X., Jiang, L.-L., Gui, X., Liu, Y., Sun, Y., Zhu, B., Piña-Crespo, J. C., Zhang, M., Zhang, N., Chen, X., Bu, G., An, Z., Huang, T. Y., & Xu, H. (2018). TREM2 Is a Receptor for β-Amyloid that Mediates Microglial Function. *Neuron*, *97*(5), 1023-1031.e7. https://doi.org/10.1016/j.neuron.2018.01.031

Zhong, Q., Congdon, E. E., Nagaraja, H. N., & Kuret, J. (2012). Tau Isoform Composition Influences Rate and Extent of Filament Formation. *Journal of Biological Chemistry*, *287*(24), 20711–20719. https://doi.org/10.1074/jbc.M112.364067

Zhou, Y., Song, W. M., Andhey, P. S., Swain, A., Levy, T., Miller, K. R., Poliani, P. L., Cominelli, M., Grover, S., Gilfillan, S., Cella, M., Ulland, T. K., Zaitsev, K., Miyashita, A., Ikeuchi, T., Sainouchi, M., Kakita, A., Bennett, D. A., Schneider, J. A., … Colonna, M. (2020). Author Correction: Human and mouse single-nucleus transcriptomics reveal TREM2-dependent and TREM2-independent cellular responses in Alzheimer's disease. *Nature Medicine*, *26*(6), 981–981. https://doi.org/10.1038/s41591-020-0922-4

Zhu, B., Liu, Y., Hwang, S., Archuleta, K., Huang, H., Campos, A., Murad, R., Piña-Crespo, J., Xu, H., & Huang, T. Y. (2022). Trem2 deletion enhances tau dispersion and pathology through microglia exosomes. *Molecular Neurodegeneration*, *17*(1), 58. https://doi.org/10.1186/s13024-022-00562-8

Zhu, C., Kros, J. M., van der Weiden, M., Zheng, P., Cheng, C., & Mustafa, D. A. M. (2017). Expression site of P2RY12 in residential microglial cells in astrocytomas correlates with M1 and M2 marker expression and tumor grade. *Acta Neuropathologica Communications*, *5*(1), 4. https://doi.org/10.1186/s40478-016-0405-5

Zilka, N., Filipcik, P., Koson, P., Fialova, L., Skrabana, R., Zilkova, M., Rolkova, G., Kontsekova, E., & Novak, M. (2006). Truncated tau from sporadic Alzheimer's disease suffices to drive neurofibrillary degeneration in vivo. *FEBS Letters*, *580*(15), 3582–3588. https://doi.org/10.1016/j.febslet.2006.05.029

Zilkova, M., Nolle, A., Kovacech, B., Kontsekova, E., Weisova, P., Filipcik, P., Skrabana, R., Prcina, M., Hromadka, T., Cehlar, O., Rolkova, G. P., Maderova, D., Novak, M., Zilka, N., & Hoozemans, J. J. M. (2020). Humanized tau antibodies promote tau uptake by human microglia without any increase of inflammation. *Acta Neuropathologica Communications*, *8*(1), 74. https://doi.org/10.1186/s40478-020-00948-z

Zimprich, A., Biskup, S., Leitner, P., Lichtner, P., Farrer, M., Lincoln, S., Kachergus, J., Hulihan, M., Uitti, R. J., Calne, D. B., Stoessl, A. J., Pfeiffer, R. F., Patenge, N., Carbajal, I. C., Vieregge, P., Asmus, F., Müller-Myhsok, B., Dickson, D. W., Meitinger, T., … Gasser, T. (2004). Mutations in LRRK2 Cause Autosomal-Dominant Parkinsonism with Pleomorphic Pathology. *Neuron*, *44*(4), 601–607. https://doi.org/10.1016/j.neuron.2004.11.005